

Populations of the Middle Nile: Using Bioarchaeological and Paleogenetic Analyses to Understand Nubian Ancestry

by

Abigail M. Breidenstein

A dissertation submitted in partial fulfillment
of the requirements for the degree of
Doctor of Philosophy
(Anthropology)
in The University of Michigan
2019

Doctoral Committee:

Associate Professor Abigail W. Bigham, Chair
Associate Professor Maureen Devlin
Associate Research Scientist Geoff Emberling
Associate Professor John Kingston
Professor Janet Richards

Abigail M. Breidenstein

abstein@umich.edu

ORCID iD 0000-0002-1675-8399

© Abigail M. Breidenstein 2019

Dedication

For my parents

Acknowledgements

I would like to thank the various funding sources which supported this dissertation. This includes the Rackham Graduate Program through fellowships, conference support, and research funds, various UM institutes (International Institute, African Studies Center, Mary Sue Coleman Scholarship Fund, Weiser Center for Emerging Democracies), the Anthropology Department through teaching fellowships, departmental funding, and research support for field and lab research, and the UROP program at UM. Lastly, thank you to the National Geographic Society for their continuing support of my project.

This project spanned five countries, four labs, and countless collaborations that I am incredibly grateful for their invaluable contributions. To begin, a very special thanks to the villagers of El-Kurru and officials at the National Corporation for the Antiquities and Museums in Khartoum, Sudan, including Fakhri Hassan Abdallah Hassan and Dr. Abdelrahman Ali for their permission and help exporting skeletal remains as well as your continuing trust with such important objects of their heritage. Additionally, I would like to thank Mohamed Saad for opening the NCAM collection to my project and more notably, helping me so much when I lived in Khartoum for two weeks. I am grateful to my International Kurru Archaeological Project Team members, especially Tim, Martin, Jalina, Jack, and Nacho, who helped in the field and packed up remains when time was running short. Thank you to my collaborators abroad: Robert Stark (McMaster University), Robert Mahler, Magna Srienc, and Dr. Mahmoud El-Tayeb (PCMA) for taking a chance on a piloted paleogenomics project. I am so grateful for the donation of samples and look forward to our work in the future.

To the three different labs that I have worked in throughout my paleogenomics training, I am so grateful for your generosity and time. Firstly, I am especially grateful to Verena Schuenemann and Frank Rühli for supporting my project, being immensely open to collaborations, and our future work together. Thank you to the Archaeogenetics Group at the University of Tübingen and Ella Reiter for teaching me enrichment techniques. And a big thank you to Bastiaan Starr at the University of Oslo for introducing me to the Bone Crusher, then to Agata Gondek and Giada Ferrari for our marathon lab sessions in Blindern. Then, many thanks to Milford Wolpoff for letting me take over his Paleoanthropology lab at UM for a year to analyze

the Nubian remains. And thank you to the students over than years that helped at various stages of this project: Renee, Julian, Serena, and especially Zenta and Abby for their hard work and enthusiasm for my project through UROP.

A special thank you to my mentor Geoff. We met so many years ago when I was a docent at the Kelsey Museum, before I even started graduate school, and I never imagined I would be able to do archaeological field work as part of my dissertation project. I am so honored you brought me on your team to El-Kurru, supported me through two field seasons, showed me the ropes, and laid the foundation for work beyond El-Kurru. Your research implementing community engagement is inspiring and I hope to draw on your example for the Nuri Project. I sincerely look forward to our work in the future.

Thank you to the Ancient Biomolecules Group at UZH, both times I was part of this team. Round one including Giada, Claudia, Sabrina, and Abi for their training, guidance, side-jobs at cheese shops, and being so open to have a new member of their team. You truly made Zürich feel like home. Then round two: Gül, Judith, Enrique, and Christian. I would not have made it to the finish line without your invaluable help, from finishing my sequencing lanes to drilling petrous bones to running bioinformatic pipelines. I am excited we have the opportunity to continue working together in Zürich.

A sincere thanks to my dissertation committee members for their advice, scientific or otherwise, on navigating the graduate program and most importantly, becoming a better instructor and scientist. A special thank you to my chair advisor, Abby, for years of support before and during graduate school. I am grateful for the environment you cultivated to provide me the freedom to explore my own project and grow as a scientist, gaining a multitude of skills and independence along the way, and weathering the troubles with a level-head I still attempt to emulate.

To my Michigan friends, Ann Arbor has been my home for well over a decade. The friends I have made are more than friends, you are family. My sincere and heartfelt thanks to Amanda and family, Jessie, Celia, Sylvia, Jack, Julian, Danielle, Emma & Henry, Liz, Vince, Elspeth, Bree, Máire, Andrew, Obed, Greg, Ainash, Jordan, and Rachna. I would not have made it here without you; I cherish our memories from Ann Arbor, Detroit, the lake house, and conferences, and I look forward to new adventures.

Finally, to my family – Mom, Dad, Kurt, Jillian, Harrison, Lulu and Fiona. Thank you for your unwavering support and immense patience. Your enthusiasm for my work has been the backbone of my success. You never achieve anything alone and I am so happy to have you on my team. Thank you.

TABLE OF CONTENTS

Dedication	ii
Acknowledgements	iii
List of Figures	vi
List of Tables	ix
List of Appendices	xi
Abstract	xii
CHAPTER 1: Introduction	1
CHAPTER 2: Life and Death at the End of Christian Nubia: Bioarchaeological Analyses of the Medieval Population from El-Kurru, Sudan	22
CHAPTER 3: Method Optimization of aDNA Extraction from Ancient Nubian Archaeological Materials ...	50
CHAPTER 4: Ancient Mitochondrial Genomes from Middle Nile Region of Sudan: A New Perspective of Nubian Ancestry	91
CHAPTER 5: Conclusion	129
Appendices	132
References	134

List of Figures

Figure 1.1. Map of Ancient Nile River Valley	3
Figure 1.2. Modern Political Map of Nile River Valley with ethnic groups referenced in cited studies	8
Figure 1.3. Mitochondrion in a human somatic cell	11
Figure 1.4. Human mitochondrial DNA	12
Figure 1.5. Lineage of Major Material Haplogroups for Mitochondrial DNA	13
Figure 1.6. General workflow for NGS methodology (for archaeological samples)	15
Figure 1.7. European bias of paleogenomic work around the world, as of 2017.....	17
Figure 1.8. Published African mitochondrial and nuclear genomes, through August 2019	18
Figure 2.1. Modern Map of Africa and ancient Nile Valley with close up of 4 th Cataract region.	23
Figure 2.2. El-Kurru Royal Cemetery plateau with Napatan Pyramid, temple in foreground.	23
Figure 2.3. Excavation map of El-Kurru, including royal cemetery, medieval wall, and Napatan structures.	24
Figure 2.4. Satellite view of El-Kurru excavations in relation to modern day agricultural and domestic land.	25
Figure 2.5. Excavation of Medieval Christian structures at El-Kurru.	26
Figure 2.6. Excavations centered on Medieval Christian settlement and cemetery.	26
Figure 2.7. Mortality Distribution of 27 Christian Individuals from El-Kurru cemetery.	32
Figure 2.8. Artifacts uncovered within grave fill for El-Kurru burials.	34
Figure 2.9. El-Kurru Ind. 203 showing extended and supine burial.	35
Figure 2.10. Burial treatment and body treatment of El-Kurru individuals	36
Figure 2.11. Cribra orbitalia severity and stages of healing observed in El-Kurru population.....	38
Figure 2.12. Stages of severity observed in cribra orbitalia lesions in El-Kurru population.....	39
Figure 2.13. Healed lesions observed in El-Kurru population.....	39
Figure 2.14. Porotic Hyperostosis in El-Kurru population.	40
Figure 2.15. Linear Enamel Hypoplasias found in El-Kurru population.	41

Figure 2.16. Two instances of endocranial lesions observed in El-Kurru population.	42
Figure 2.17. Cribra femoralis found in the El-Kurru population.....	43
Figure 2.18. Cribra humeralis found in El-Kurru population.....	43
Figure 2.19. Four instances of trauma found in El-Kurru population.	44
Figure 3.1. Geographic locations of Nubian populations included in this study.	52
Figure 3.2. Excavations centered on Medieval Christian settlement and cemetery.	55
Figure 3.3. Map of Ghazali monastery complex, including surrounding cemeteries and settlement area.	57
Figure 3.4. Topographical Map of Berber Meroitic Cemetery with dating (Bashir & David 2015).	61
Figure 3.5. Laboratory facilities used for ancient DNA work at the University of Zürich.....	65
Figure 3.6. Examples of teeth with dental calculus build up requiring sampling.	66
Figure 3.7. Processing of tooth samples in clean lab.	67
Figure 3.8. Set up for processing teeth within sampling hood in clean lab.....	68
Figure 3.9. Crushing of root dentine using steel mortar and pestle.	69
Figure 3.10. Anatomical parts of temporal bone.	70
Figure 3.11. Visual of how the petrous portion of temporal bone is sectioned for processing.	71
Figure 3.12. Preparation of bone samples from petrous portion using stainless steel mortar and pestle with sleeve.....	72
Figure 3.13. Flowchart for all trialed extraction methodologies.	73
Figure 3.14. Library preparation of ancient DNA extractions and subsequent sequencing.	75
Figure 3.15. Sequencing and post-sequencing analysis.	77
Figure 3.16. Mapped ancient reads listed by method.....	79
Figure 3.17. Impact of bleach on contaminating bacteria in extracts.....	81
Figure 3.18. Endogenous Content (%) comparison by method.....	82
Figure 3.19. Cluster Factor value comparison by method.	83
Figure 3.20. Comparison of tissue type to successfully obtain aDNA.....	84
Figure 3.21. Comparison of burial context to successfully obtain aDNA.....	85
Figure 4.1. Map of Berber Meroitic Cemetery.....	94
Figure 4.2. Burial context of Individual BMC 6a and tooth sample.....	94
Figure 4.3. Ghazali complex located near 4 th Cataract, Sudan.	95

Figure 4.4. Burial context of Ghazali-4-008.2/GHZ 2.....	96
Figure 4.5. Burial context and sampling of GHZ-1-010/GHZ 5.....	97
Figure 4.6. Aerial view of the site of Kwieka near the 5 th Cataract region.	97
Figure 4.7. Burial context of KWC T2, associated finds, and sampling material.	98
Figure 4.8. Burial context of KWC T6 and sampling material.	99
Figure 4.9. Right temporal bone from TARP T9.	99
Figure 4.10. Coverage of the Mitochondrial Genome of Nubian Individuals.	107
Figure 4.11. Example of Coverage Plot of KWC 2 on the circular human mitogenome.....	108
Figure 4.12. Map Damage Profiles of Mapped Mitochondrial Reads from merged library samples.	109
Figure 4.13. Read Fragmentation Plots of Mapped MT reads from merged library samples.....	110
Figure 4.14. Haplotype Diversity of Northeast Africa region coordinated with geographic locations	115
Figure 4.15. Haplotype Frequencies of modern Northeast African populations and Sudanese subpopulations	116
Figure 4.16. Principle Component Analysis based on haplotype frequencies, whole MT genomes.....	118
Figure 4.17. Principle Component Analysis based on haplotype frequencies, ancient groups only	119
Figure 4.18. Multi-Dimensional Scaling Plot mapping F_{ST} pairwise differences among Ancient and Modern African and Eurasian populations	122
Figure S1. Sequence counts histogram of Negative Blank libraries with more than zero reads.....	133

List of Tables

Table 2.1. Results from AMS Radiocarbon dating performed at ETH Zürich.....	31
Table 2.2. List of El-Kurru Individuals and demographic data.....	37
Table 2.3. Summary Table of Health Status observations.....	45
Table 3.1. Archaeological information and sampling of Nubian populations included in this study.....	53
Table 3.2. List of El-Kurru individuals, including demographic data, archaeological context, and samples collected.....	55
Table 3.3. List of Ghazali Individuals, including demographic data, archaeological context, and samples collected.....	57
Table 3.4. List of Kwieka Individuals, including archaeological context and samples collected.....	58
Table 3.5. List of TARP Individuals, including demographic data, archaeological context, and samples collected.....	59
Table 3.6. List of BMC individuals, including archaeological context, contextual dating, and samples collected.....	61
Table 3.7. List of El-Zuma individuals, including demographic data, archaeological context, and samples collected.....	62
Table 3.8. List of el-Detti individual, including demographic data and samples collected.....	63
Table 3.9. List of Tanqasi individuals, including demographic data and samples collected.....	64
Table 3.10. Four samples selected for bleach pretreatment and results.....	80
Table 4.1. Sources and group counts for haplotype frequencies data for dataset assembly.....	102
Table 4.2. Libraries enriched and analyzed with Schmutzi.....	105
Table 4.3. Sequence Quality Analysis Summary - from EAGER analysis of enriched reads.....	107
Table 4.4. Demographic and Archaeological information of Nubian individuals (ordered by date).....	111
Table 4.5. Results of Molecular Sexing.....	112
Table 4.6. Summary of consensus mitochondrial sequence information and haplogroup assignments..	112
Table 4.7. Haplogroup Frequencies Grouped by Population or Subpopulations (in percentages).....	113

Table 4.8. F_{ST} Values for comparisons to Ancient Nubians 120

List of Appendices

Appendix A - Supplementary information relating to methods:.....	132
Appendix B - Analysis / MultiFastQC of negative control samples	133

Abstract

This work investigated a new means to explore Nubian ancestry using ancient DNA retrieved from archaeological skeletal material and marrying this perspective with bioarchaeological and other data sources. The focus of this project is centered on sites within the Middle Nile region of Sudan dated to before the Islamic conquest, where no paleogenomic work has recently taken place, but there is a wealth of bioarchaeological research. To begin, a sample population of 27 individuals was excavated from a cemetery, El-Kurru, northern Sudan, (near the 4th Cataract). Burial traditions and body treatment identify these individuals as Christian and their remains were bioarchaeologically analyzed for demographics (estimations of sex and age) and physiological markers of stress and disease (orbital lesions and cranial lesions, dental hypoplasias, non-specific lesions, trauma). The cemetery was contextually dated to post-14th century CE, meaning these people were living on the brink of a cultural transition, from Christian to Islamic dominance in the Upper Nubian region. Their remains showed high frequencies of dental hypoplasias and non-specific lesions, especially in subadults, indicating a heavy disease load and other stressors before adulthood; however, many adults lived to an older age with little signs of trauma. The frequencies of stress signals were interpreted within the context of Nubian contemporaneous populations and found to be consistent with other reported ranges. Christian burial treatments and “normal” stress markers of this population indicated the cultural transition had likely not arrived or did not have adverse consequences on this Medieval community along the Nile.

To explore the genetic structure of Nubian ancestry in the Middle Nile region, a new dataset needed to be built from archaeological materials and new protocols were trialed to establish the most successful method to extract ancient DNA from human bone and tooth samples. Trials included the use of bleach and/or a predigestion treatment prior to extraction to increase the endogenous genetic content, leading to higher numbers of ancient sequence reads without compromising the uniqueness of reads obtained. Next-generation sequencing techniques were used to sequence these samples with a 40 percent success rate. Various burial contexts, states of preservation, and tissue types used were compared across the skeletal sample collection. These trials established that aDNA can be retrieved from material from the

Middle Nile region of Sudan with extensive pretreatments of the tissue prior to extraction of the DNA.

Mitochondrial genomes of six ancient Nubians were constructed using a hybridization enrichment method, which was vital to obtain sufficient 10X coverage of the genome. As a uniparental marker, mitochondrial DNA can reconstruct maternal heritage of individuals through common ancestors with genetic similarities. Two individuals showed African lineage, while the other four showed non-African ancestry. While limited, these results showed Nubians had a strong African component with evidence of gene flow from Eurasia dating back to at least Meroitic (4th century BCE) through Christian times. Through two dimension-reduction analyses, ancient Nubians show most genetic affinity with modern Egyptians, Middle Easterners, and East Africans, while less so to modern Sudanese. Although these individuals encompass varying archaeological contexts and span well over one thousand years, these initial results hint at a complexity of the genetic makeup and begin to reconstruct the impact of human migrations from outside Africa. This would be expected given the dynamic history of this powerful kingdom centered in the Middle Nile Valley.

CHAPTER 1: Introduction

A distinguishing trait of our species is our demonstrated adaptability and flexibility to occupy almost every niche of this planet. As our ancestors explored and inhabited new landscapes, their genomes kept a record of past demographic events, environmental changes, and cultural shifts. While archaeological, anthropological, and historic data can provide a temporal aspect and context of external factors – that is political, social, environmental, health-related forces, human genetic data serves as a significant source of information for understanding the patterns of human variation and reconstruction of the past. A considerable amount of work seeks to understand the movement of humans out of Africa and modern discoveries rewrite the history of our species every year. In fact, recent findings lend unexpected evidence suggesting *H. sapiens* migrations occurred much earlier (ca. 200,000 ya) than previously thought (Wade, et al. 2019, Harvati, et al. 2019).

We are also beginning to understand human population movements within Africa. These movements have shaped the incredible amount of biological diversity seen on this continent. One particular place of interest is the Nile River Valley in northeast Africa. Positioned at the corridor between Sub-Saharan Africa and Eurasia, this region has a long history of human occupation and has served as an important migration corridor, especially the Middle Nile Basin or Ancient Nubia (modern-day southern Egypt and northern Sudan). Centuries of archaeological expeditions in this area have uncovered ancient cities, temples, and settlements as well as the skeletal remains of their inhabitants.

Investigating human history in the Nile River Valley is a complex topic which requires a multidisciplinary approach integrating genetic and bioarchaeological components. Genetic data allows us to explore an individual's traits and ancestry, then on a population level, adaptation and migration can be explored. Skeletal data provide snapshots of past people's lives. When used in conjunction with genetic data, they are a valuable means to study population history. The usefulness of this mixed methods strategy has been demonstrated in modern publications (i.e. Prendergast, et al. 2019, Aronsen, et al. 2019, Amorim, et al. 2018) and is well-exemplified in work elucidating the Neolithic Transition in Europe (or the change from foraging to farming subsistence strategies). The driving force of this transition was debated as either the spread of

people (demic diffusion) or the spread of ideas (cultural diffusion) or the process occurring regionally (Childe 1968, Clark 1965, Ammerman & Cavalli-Sforza 1971, Menozzi, et al. 1978). Archaeological data alone were unable to discern the driving force behind this major event in population prehistory. With the inclusion of genetic data, the demic diffusion hypothesis was supported (Sokal, et al. 1991). This multifaceted approach provides a template for analysis and demonstrates the value of such a strategy.

Modeling this method, this dissertation research uses a two-pronged approach combining bioarchaeological and paleogenomic analyses (both fields outlined below) to address questions about the population history of Nubians in context of external forces shaping these individuals. Such strategies have been implemented in the Nile Valley in the past. For example the combination of archaeological, paleopathological, and paleodemographical data to study people during cultural transitions and demographic shifts in Nubian history (Armelagos 1969, Van Gerven, et al. 1995). However, these works did not utilize genetic evidence because it was not yet available. Therefore, this is the first study in ancient Nubia to integrate these lines of evidence to produce a more holistic view of these individuals and better address the complexity of population dynamics in the Middle Nile Valley.

Ancient Nubia and Nubian Archaeology

For more than three centuries, explorers and archaeologists have been traversing the Nile Valley uncovering a complex ancient history. Most of this endeavor has overlooked the Nubian kingdoms in the south, in modern Sudan. Still, considerable progress has been made during the past half-century, shedding light on this important chapter of African history. Known as “the land between Cataracts”, Nubia occupies the region of the middle Nile basin, positioned at an important corridor for human interactions along the Nile River (Figure 1.1). The successive kingdoms of Nubia were influential in the development of humanity in Africa – they amassed power and wealth while being masters of building, trade, and war.

Figure 1.1. Map of Ancient Nile River Valley.



Lower Nubia spanned from the 1st to the 3rd Cataract. Upper Nubia spanned from 3rd Cataract to Khartoum. Major archaeological sites in Nubia and Egypt marked with black dots. Archaeological sites where samples were obtained for this project marked with blue dots. El-Zuma marks the sites of El-Detti and Tanqasi, which are all in close proximity of El-Kurru. Map from *Nubia: Ancient Kingdoms of Africa* (Emberling, 2011, p.3, Institute for the Study of the Ancient World, New York University).

The Nile River Valley was occupied before the modern Holocene (ca. 10,000 BCE) as evidenced by the presence of lithics and human burials (e.g. Wadi Kubbania) (Wendorf, et al. 1976, Leplongeon 2017, Wendorf, et al. 1988). Climatic and environmental changes greatly impacted the development of human societies in this region. Specifically, the appearance of

more hospitable conditions around 8,000 years ago was pivotal (Edwards 2004). During the early Holocene, inhabitants most likely subsisted by hunting, fishing, and gathering as seasonally or semi-nomadic groups, centered around stable water sources outside the Nile Valley (Edwards 2004). Evidence of the first permanent settlements dates to around 7,000 BCE and the advent of pottery in this region appeared between the 10th and 9th millenniums BP (ca. 8,000-7,000 years ago) (Edwards 2004, Close 1995, Jesse 2010). Aridification of the Sahara around 5,000 BCE changed the environment drastically, forcing settlements to closely hug the Nile (deMenocal, et al. 2000, Claussen, et al. 1999). Around this time, people shifted away from the hunter-gatherer lifestyle first with the domestication of animals then closely followed by crop domestication (Edwards 2004). Shortly before 3,000 BCE, evidence of trade and more advanced social structures were present (e.g. presence of foreign materials from the Red Sea associated with burials) (Edwards 2004). The oldest distinguishable kingdoms of Nubia formed in the region of Lower Nubia by 3,000 BCE, known as the Terminal A-Group (Edwards 2004). Elite and royal burials with fine goods associated with this group demonstrated social stratification, labor specialization, and wealth. Raids from neighboring cultures disturbed and likely dispersed the A-Group and the area was not resettled for more than a half century by a new population known as the C-Group (so-called “B-Group” culture was reclassified as early A-Group due to work by Smith (1966)) (Edwards 2004, Gatto 2006). The origins of these individuals are still debated, but they are characterized by distinct so-called “pan grave” burials, and may have been related to eastern desert nomads, the Medjay (Bietak 1987, Emberling 2011). Others argue similarities to the later Kushites suggest a migration of people from the south (Edwards 2004).

Around 2,500 BCE, the Kerma culture emerges among other political units in the 3rd Cataract area (Figure 1.1) and develops into a sprawling urban center with palatial structures, massive temples, and royal tombs, which still stand today (Bonnet 1986, Bonnet 1990). Here, the “Kingdom of Kush” began. These powerful kings built an imposing military force, primarily known for their superior skills in archery, who often undertook raids to the north in Egypt. The Kermans appear to have maintained independence, although regularly engaging with the ancient Egyptian civilization to the north, until 1,550 BC when Egyptian pharaohs of the New Kingdom established direct control over Nubia (W. Adams 1984). When incorporating Nubia within the Egyptian empire, this was a time of intensive intermingling of these populations. Following the fall of the Egyptian New Kingdom (1550–1069 BCE), the Nile River Valley saw the rise of the second Kingdom of Kushite, now centered in Napata near the 4th Cataract (Figure 1.1). This period was a revival of both Kushite and Egyptian beliefs, under the dominion of the

Napatan kings. During the 8th century BCE, the Napatan kings ruled all of Egypt and Nubia as pharaoh for approximately a century. After losing control of Egypt, Napatan Kush flourished in Nubia for nearly four more centuries (ca. 700–300 BCE).

The second Kingdom of Kush underwent a still poorly understood transition, when the capitol was moved upriver to Meroe, ushering in the Meroitic period (ca. 300 BCE – 300 CE). The kingdom continued to prosper during this time with far reaching control of the Middle Nile and expansive trade networks. The fall of the Kingdom of Kush at the end of the Meroitic period is also poorly documented but may be attributed to encroachment of the Kingdom of Aksum from Ethiopia or the Nuba people from the Western Desert (Hintze 1967). For the next few centuries, Persians pushed into North Africa and occupied both Egypt and Nubia. At this time, Lower Nubia was occupied by smaller agrarian communities of the X-Group or the Ballana culture, which later made up a new independent state known as Nobadia. The state of Makuria rose to power in Upper Nubia at this time. By the 6th century, the region had largely converted to Christianity. The Islamic conquest began in the north in the 7th century, itself taking centuries to complete (Welsby 2002) and having a major impact the genetic structure of the entire Northeast region as Arabic influence spread through the Nile Valley (Hollfelder, et al. 2017, Dobon, et al. 2015). During Medieval times, the Middle Nile was controlled by three Christian kingdoms with regional capitols along the Nile River. Generally existing autonomously, these polities prospered for eight centuries and were set amongst many other powerful African kingdoms, for example in Mali (Canós-Donnay 2019), Chad, Darfur, Ghana, and Ethiopia (Edwards 2004). The Christian kingdoms pushed back multiple attempts by Islamic invaders from the north to control the Nubian heartland while also expanding the economy, keeping peace in Lower Nubia, and maintaining robust trade networks moving through the Nile corridor. By the 14th century the medieval Nubian Kingdoms came under Arab control and new polities arose, including the Funj Sultanate of Sinnar (south of Khartoum) and the Sultanate of Darfur (in the west).

In order to understand ancient Nubian history from the site of El-Kurru and across time, we implemented a paleogenomic approach that focused on mitochondrial DNA – an important marker in understanding prehistory. Background information on mitochondrial DNA and its usefulness in anthropological research are detailed below.

Bioarchaeological Research in Sudan and Nubia

The informative value of human remains is extensive, despite the small archaeological footprint. Skeletal material serves as a direct way to study human populations and reconstruct the lives of past individuals and is the primary material for bioarchaeological research. The Nile

River Valley has a long tradition of exploratory work with human remains tightly paired with centuries of archaeological research in the Valley and was pivotal to the birth and advancement of such fields as paleopathology and bioarchaeology (Baker & Judd 2012). Arid conditions and cultural burial practices preserved substantial skeletal collections from this region. This is particularly the case for Nubia, whose skeletal collections make up some of the world's largest and most expansive in time (Binder 2019). Like the collections from which the DNA samples derive, the remains and burial context of these individuals provides an important means to understand lived experiences and stressors, diet and nutrition, social identity, health and disease, and demographic data to reconstruct population dynamics, social and biological identity, and disease in antiquity. Understanding who these individuals were, is of paramount importance to explore.

While the prehistory of Sudan has been the subject of exploration from outside scholars since the early 19th century, Nubia was perhaps best characterized during large archaeological campaigns in the 20th century (Baker 2016). The First Archaeological Survey of Nubia, from 1907-1911, explored hundreds of sites and unearthed thousands of individuals from all time periods of Sudan's history (Adams 1977). Excavators and medical professionals recognized the value of studying the people themselves, who built the towns they excavated or crafted the goods they were shipping home to museums (Smith & Jones 1910). This survey mostly focused on demographic typologies, but soon grew to include the vast number of pathologies observed (Waldron 2000). Many of the more curious or diagnostic examples were shipped out of Sudan to contribute to or begin medical collections around the world (Baker & Judd 2012). The Second Archeological Survey of Nubia, conducted from 1929 to 1934, was launched as a salvage campaign with the raising of the Aswan Dam. Again, thousands of bodies were excavated and the focus of studying these remains was mostly descriptive of racial affinities and included observations of pathologies (Admas 1977, Waldron 2000).

The next surge of excavations came in the 1960s with another salvage campaign when the Aswan Dam was raised again, putting over a thousand sites underwater as far as the 2nd Cataract (Adams 1977). This time, biological anthropologists were employed alongside archaeologists to excavate burials, which gave rise to a new paradigm in the field of anthropology – the biocultural approach, as named by Borthwell (1967), then most notably implemented by Armelagos (1969). Such an approach contextualized variation in human biology observed in the skeletal remains within a cultural and environmental framework discerned from the accompanying archaeological data (Baker 2016). This shift from descriptive to biocultural studies gave rise to the “bridging” field of bioarchaeology, a broad reaching discipline which

describes methods for extracting biological and cultural data from archaeological skeletal materials (Larsen 2015, Baker 2016).

As the field shifted, so did the location of work moving further south into Sudan to include Dongola and Meroe as Lower Nubia was flooded (Binder 2019). Then in the 1990s, another dam project threatened the region near the 4th Cataract at Meroe, prompting thousands of salvage excavations and providing more skeletal remains to be studied (Emberling 2012). Undoubtedly supported by such an abundance of material, further expansion of archaeological projects for the next few decades, and most importantly, the ability to export these materials for more extensive investigations beyond the field (collections summarized in Binder 2019), bioarchaeology in Nubia developed as a discipline unto itself and continues to be a staple of investigation to elucidate the history and inhabitants of Nubia.

Modern Genetic Landscape of Sudan and Northeast Africa

Studies using genetic data, even from ancient sources, are not a new strategy to understand Nubian history. Located in the Middle Nile Basin, ancient Nubians were positioned at a corridor connecting Sub-Saharan Africa to North Africa that ultimately lead to Europe and Asia. The Nile River served as a means to carry natural resources and other riches from the interior of Africa to Egypt and beyond, turning Nubia into a strategic economic power (Adams 1977). This also meant the flow of people and ideas passed through this region, influencing the population seen today as a unique blend of African and Mediterranean (Adams 1967). To verify this observation, ancient DNA from Meroitic Lower Nubia and modern genetic data has been used to show the Nile Valley was a genetic corridor for the bi-directional migration of people since ancient times (Lalueza Fox 1997, Krings, et al. 1999). These works set the stage to further understand the genetics of Nubia, this ancient group at a strategic place along the Nile River, as well as demonstrate the viability of paleogenetic work with archaeological materials from this region.

The past decade or more has seen a continued interest in the genetics of the Nile River Valley, specifically Sudan and South Sudan, while also including Egypt and Ethiopia. Modern studies utilize uniparental markers from the maternal lineage including mitochondrial (mtDNA) (outlined below) and the paternal lineage including the non-recombining region of the Y Chromosome (NRY), microsatellites or short tandem repeats (STRs), as well as autosomal DNA including single nucleotide polymorphism (SNP) arrays and whole genome sequencing data. Such studies follow a similar research design to genetically survey ethnic groups across region. These include Nubians in the north, central groups of Arab descent further up the Nile River, the

eastern Beja near the Red Sea, the pastoral Nilotes in South Sudan, the Nuba near the mountains, the Darfurian groups in the western desert, and some nomadic groups, like the Fulani and the Meseria, with more expansive occupation areas across the country (Figure 1.2).

Figure 1.2. Modern Political Map of Nile River Valley with ethnic groups referenced in cited studies.



Modern map of the Nile River Valley and surrounding counties. Orange labels represent ethnic groups included in various genetic studies and their general locales; pastoral groups not included (Doban, et al. 2015, Babiker, et al. 2011, Hollfelder, et al. 2017, Hassan, et al. 2008, Hassan 2009). CAR – Central African Republic, DRC – Democratic Republic of Congo. Map obtained from d-maps.com and modified by author.

While some of these datasets are more robust than others, what is published converges on the uniqueness of Nubians among other ethnic groups and shows interesting signals of complexity that were influenced by past demographic events, namely the Arab expansion from the North. However, a new dataset from ancient individuals is required to fill in gaps in knowledge to fully understand this complexity while also addressing new questions. For example, what ancient groups contributed to the high diversity found in modern populations? What is the genetic profile of Nubians before the Arabic expansion? And how can these data

augment anthropological, historical, and archaeological hypotheses and notions of the Nubian past?

Nubians are unique compared to other ethnic groups in the Northeast region of Africa and other Sudanese groups. They are characterized by higher intrapopulation variation, meaning the most genetic diversity exists among individuals of this group, rather than diversity between Nubians and another outside group. This had been observed with mtDNA (Alfonso, et al. 2008, Hassan 2009) and nuclear SNP data (Hollfelder, et al. 2017). Autosomal (nuclear) markers show Nubians are highly admixed through various measures of genetic diversity (e.g. high allelic richness, an abundance of private alleles and shared private alleles, and short runs of homozygosity) (Hollfelder, et al. 2017). The origin of this diversity has been the focus of several recent studies using autosomal data that aim to understand the underlying genetic structure in the Sudanese region. Such genetic variation is shaped by demographic forces, including migration and admixture, as well as biological factors like genetic drift and natural selection (Li, et al. 2008). While not mutually exclusive, the diversity present in Nubians is likely to be the outcome of demographic events – namely gene flow (or the movement of genetic material from one population to another) – which introduced material from Eurasia and East Africa. Both uniparental, single locus markers add to this same narrative: haplogroup frequencies indicate past gene flow or migration events, especially from outside Africa (Hassan, et al. 2008, Hassan 2009, Lalueza Fox 1997, Krings, et al. 1999). Nubians have a significant Eurasian component (roughly half) as part of their genetic makeup, with the remaining part quantified as a “Nilo-Saharan” component that is distinct from Sub-Saharan or North African signatures (Hollfelder, et al. 2017). Other ethnic groups in the surrounding region, the Beja, central Arabic groups, and even modern Ethiopians, have this same two-part signature. The Nilo-Saharan component is unique to East Africa and is hypothesized to characterize the ancestral genetic state of this region (Hollfelder, et al. 2017). Archaeological samples can directly test this hypothesis. South Sudanese Nilotes have this makeup almost exclusively and it closely resembles the 4,500-year-old individual from Ethiopia with no Eurasian admixture (Gallego Llorente, et al. 2015).

However, it remains unclear from which group these gene flow signals originate. Genetic data from extant Nubians show a particularly close connection with Egyptian populations (Krings, et al. 1999, Babiker, et al. 2011, Lalueza Fox 1997). This would be expected from their geographic proximity to each other and from archaeological and historical records that document interactions between these two groups for millennia, especially during Egypt’s colonial period in Sudan and subsequent “Egyptianization” and also during the rise of the

Napatan state during the 25th Dynasty. Both uniparental markers also attest to this narrative as amounts of variance between the populations are low (Hassan, et al. 2008, Alfonso, et al. 2008). This suggests there was no sex bias in the intermingling of these two populations, at least the recent past. Paleogenomic data would test if this closeness was the result of these known events of their affinity being more basal.

Several genetic surveys of Africa support the idea that the genetic landscape of this continent is profoundly shaped by geography (Scheinfeldt, et al. 2010, Tishkoff, et al. 2009) and the Sudanese region keeps to this pattern. Based on autosomal data, Sudan and South Sudan can be divided geographically into groups of the northeast (including Nubians, the Beja, Copts, and central Arabs) and the southwest (including the Nuba, western desert groups, and Nilotes) (Hollfelder, et al. 2017, Dobon, et al. 2015, Babiker, et al. 2011) (Figure 1.2). These two regional groups were differentiated as a result of the presence of Eurasian and/or Middle Eastern genetic signals in the northeast and general absence in the southwest. This shared Eurasian component is the signature of the Arab expansion, which began in the 7th century in Egypt, but did not reach the Middle Nile region until much later in the 14th century. Reconstructive analyses showed successive admixture events moving southward along the Nile. However, the Nubians are again distinct, even among the northeast ethnic groups, when concerning linguistic affiliations. Nubians may be genetically close to those groups in geographic proximity, but they speak Eastern-Sudanic languages while all others speak Afro-Asiatic ones (Hollfelder, et al. 2017, Dobon, et al. 2015). Eastern-Sudanic languages belong to the Nilo-Saharan language family that are more commonly spoken among the southern Nilotes and other ethnic groups in the southwest region. This would suggest population integration on a genetic level (i.e. exchange of genetic material between people) but not all cultural transitions occurred as happened with Arabic groups which adopted Afro-Asiatic languages (Hollfelder, et al. 2017).

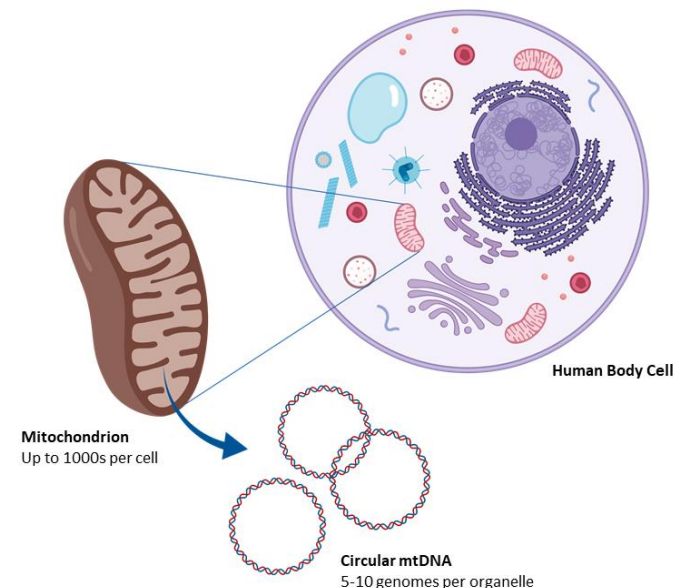
Outlined here, the complexity of Nubian genetics is likely defined by East African ancestry and was significantly impacted by recent migratory events. This begs the question of what was the genetic landscape of Nubians predating the Arab expansion and was this the source of diversity that is unique to Nubians in this region. DNA from the ancient from ancient and historic populations in Sudan can refine the timing of admixture events and directly survey the genetic landscape before the Arab expansion and characterize the basal state for Northeastern Africans. Ancient DNA would also lend more data to help elucidate the linguistic connection between Nubians and their southern neighbors.

Mitochondrial DNA

Mitogenomic data are an important means of reconstructing and detecting signatures of human migrations with cross-disciplinary reaches. Human mitochondrial DNA (mtDNA) has been pivotal to understanding the origins and evolution of our species (Cann, et al. 1987, Krings, et al. 1997), human migrations and peopling events (e.g. Mulligan & Szathmary 2017), and the reconstruction of historical events, especially when biological sexes are differently affected (Bamshad et al 1998).

Mitochondrial DNA is circular, double-stranded extranuclear genetic material that is found in the energy-producing organelles of all somatic cells (save red blood cells) (Figure 1.3). The 16,569 base pair genome is organized into 37 genes encoding proteins, rRNAs, or tRNAs involved with cellular respiration or energy production (Stoneking 2017, p.111) (Figure 1.4). While these molecules mutate at a rate 5-10x faster than nuclear DNA, they are inherited uniparentally from an individual's mother and thus do not undergo recombination with each generation. Without recombination, mutation is the only source of variation. This makes mtDNA ideal for tracing ancestral lineages, which can be used for constructing phylogenetic trees of relatedness, even for closely related populations (Kaestle 2010). Especially advantageous for forensic and paleogenomic applications, mtDNA is found at a high copy number per cell (i.e. up to few thousand mitochondria per cell, 5-10 genomes per mitochondrion), in comparison to nuclear DNA (Giles, et al. 1980, Paabo and Wilson 1988) (Figure 1.3).

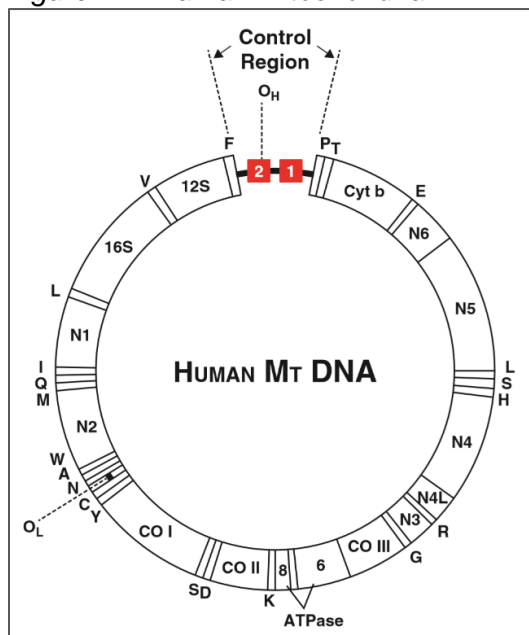
Figure 1.3. Mitochondrion in a human somatic cell.



(Created with BioRender.com by author)

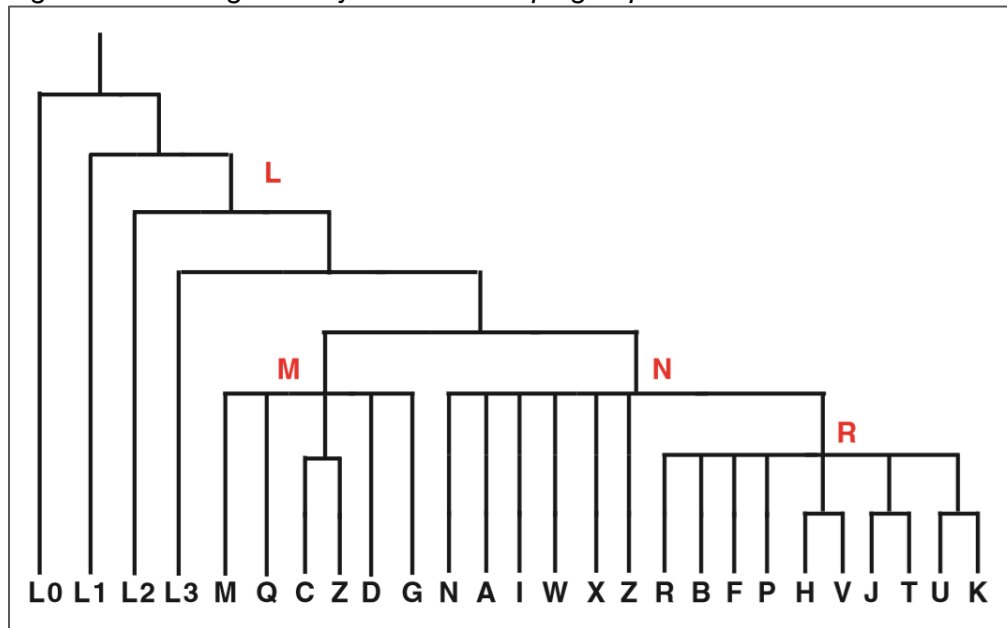
Mitochondrial (MT) genetic variation is a valuable tool to observe the impact of historical events on genetic makeup and can reconstruct demographic history through the lens of maternal ancestors (Cann, et al. 1987, Vigilant, et al. 1991). Analyses track mutations to create unique sequence profiles that differ from the human reference sequence, including the Cambridge Reference Sequence (CRS), first proposed in 1981 by Anderson, et al., the Revised Cambridge Reference Sequence (rCRS) (Anderson, et al. 1999), or the most recent iteration, the Reconstructed Sapiens Reference Sequence (RSRS) (Behar, et al. 2012). Specifically, most mutations accumulate at two hypervariable regions (HVRI and HVRII), therefore sequence data from these regions are the most helpful to infer genetic relationships among individuals and populations (Figure 1.5). Individuals with genetic variants that share a common ancestor will cluster together in clades as a result of shared common mutations; these clusters are defined as haplogroups (groups of related sequences defined with nomenclature) (Stoneking 2018). Main groups are named with letters (e.g. L, M, N) and subhaplogroups with numbers and letters (e.g. L0a1a). L lineages originated in Africa, while M and N (and all those that derive from these two lineages) – are found mostly outside of Africa (Stoneking 2018, Cerezo, et al. 2012). Typically, research designs target HVRs for haplogroup assignment, rather than the whole mitogenome. However, dropping costs and the implementation of massively parallel sequencing techniques (next generation methods) have made whole mitogenomes more accessible and common for projects.

Figure 1.4. Human mitochondrial DNA.



Genetic map of human mitochondrial DNA, spans 16,569 base pairs; inset shows the control region where the Hypervariable Regions I and II are located (numbered, in red). (Figure 9.2 from Stoneking, et al. 2016, *An Introduction to Molecular Anthropology*, p. 113)

Figure 1.5. Lineage of Major Material Haplogroups for Mitochondrial DNA.



Phylogenetic tree illustrating the relationships of the major mtDNA haplogroups. Macrohaplogroups L, M, N, and R are indicated. Note that branch lengths are not proportional to mutational difference. (Figure 9.4 from: Stoneking, et al. 2017, *An Introduction to Molecular Anthropology*, p. 118)

Despite the utility of mtDNA in population genetic analyses, there are some disadvantages that should be considered here. First, it is a single genetic locus that tracks the maternal lineage. Therefore, no information on paternal lineage history, sex-biased behaviors, or cultural practices (e.g. marriage traditions or those with a sex-bias) can be obtained from this locus. Illustrating this, MT haplogroup assignment has been found to provide limited information concerning an individual's continental region of origin or ancestry (Emery et al. 2015). This indicates that identifying the mtDNA haplogroup for an ancient individual, then reconstructing ancestry or even country of origin may not be as specific as it would seem. Furthermore, mtDNA may be less informative of overall population history if it experienced locus specific genetic drift or selection (Stoneking 2018). Second, the MT genome, only 16K base pairs, is a small fraction of the human genome and is much less discriminatory than 2.9 base pairs found in nuclear DNA. Third, new data show that heteroplasmy is possible, meaning the inherent assumption that this marker is indicative of maternal heritage is currently under debate (Luo et al. 2018). Despite these drawbacks, mtDNA is and continues to be an informative workhorse in evolutionary studies (DeSalle et al. 2017).

As is related to this dissertation research, this locus, among others, has been utilized to characterize the genetic landscape of the modern Sudanese people as well as some ancient populations. However, a largescale paleogenomics project has yet to be conducted in ancient Nubia.

Paleogenomics and Ancient DNA Methodologies

More than 30 years ago, the field of paleogenomics (or the analysis of genetic information of extinct living things) was developed. Since then, the scope of the field and the number of projects undertaken have increased due to advances in sampling methods and the implementation of NGS techniques (Hagelberg, et al. 2015). As research designs have moved past the use of PCR products to NGS techniques, the fundamentals have remained the same (Cooper & Poinar 2000, Fulton & Shapiro 2019). Today, ancient DNA studies are a useful tool in various disciplines, including conservation genomics of endangered wildlife, evolutionary genetics, and archaeological analysis (Leonard 2008, Green, et al. 2006, Amorim, et al. 2018). In human population genetics, aDNA contributes to the exploration of population dynamics over time and the timing of demographic shifts. Importantly, this genomic view into the past has demonstrated that present-day population structure is the product of migrations and dynamic admixture events, most ancestors likely originated from somewhere else, and unfortunately, this complexity may not be reflected in the genetics of extant populations (Pickrell & Reich 2014).

Most commonly, aDNA is retrieved from bones or teeth, however other non-traditional mediums are currently in use, including soft tissues, dental calculus, coprolites, and soil. Regardless of the source material, successful extraction of aDNA faces the same hurdles. ADNA is short, heavily damaged, found in low quantities, and contaminated. To address these limitations, NGS methods are particularly well suited to handle the short, degraded molecules (Figure 1.6). Briefly, DNA is extracted from a tissue sample, most commonly a powder. An enzymatic treatment pulls the DNA into solution, and it is then purified and concentrated. These short fragments of DNA are built into “libraries” by attaching adaptors and unique barcodes, which are then massively sequenced in parallel on a sequencing platform (e.g. an Illumina) (Dabney et al. 2013, Meyer and Kircher 2010, Kircher, et al. 2012) (Figure 1.6). Sequencing products are processed bioinformatically, including assessment of damage, contamination estimation, and consensus assembly.

Figure 1.6. General workflow for NGS methodology (for archaeological samples).

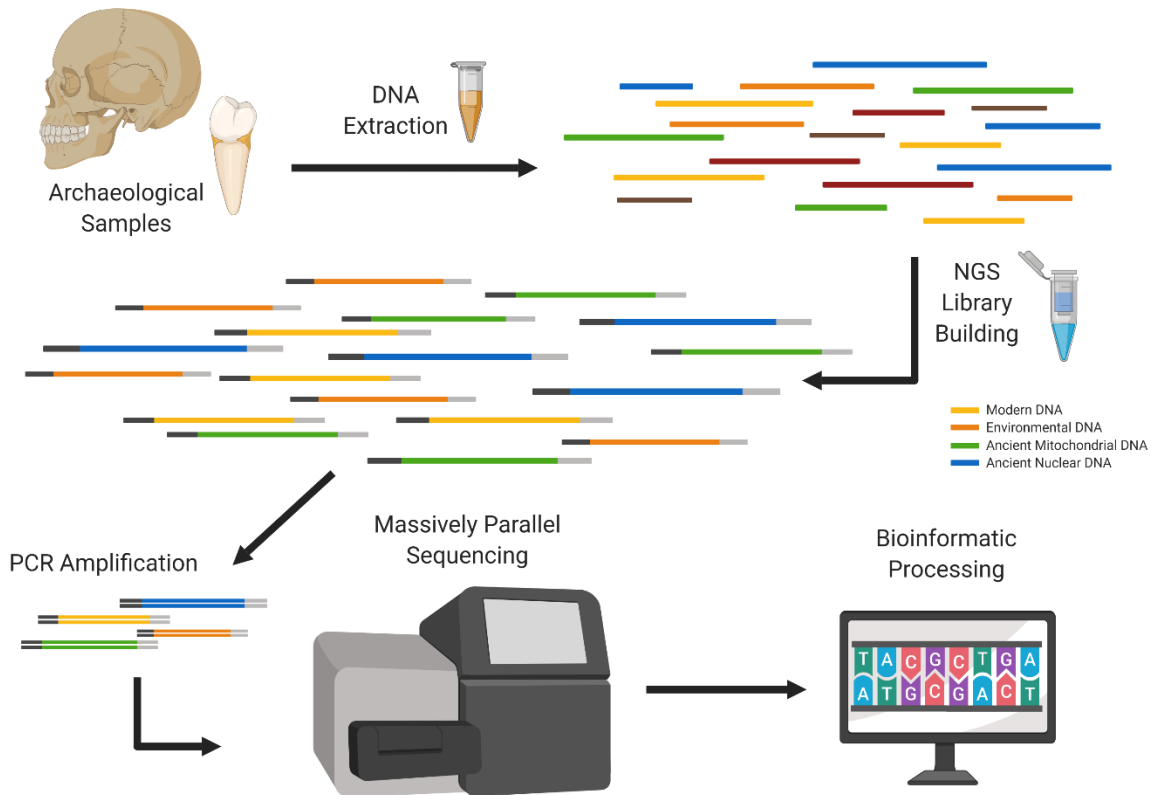


Figure created with BioRender by author.

Post-mortem damage is also a limitation to working with aDNA. While unavoidable, the typical, chemically damaged profile is instead used as an authentication criterion to differentiate ancient from modern sequences. Molecular degradation begins immediately after cellular death when DNA repair mechanisms cease to function. In a burial context, decaying body tissues damage genetic material as do environmental factors, including bacterial and chemical changes in the surrounding soil (Allentoft, et al. 2012). This damage only increases with time, resulting in fragmented (less than 100bp, usually 35-55bp) and chemically modified genetic material (Briggs, et al. 2007, Poinar et al 2006). Hydrolysis is also a major problem causing strand breakage and miscoding lesions, where the deamination of cytosine to uracil later causes C to T transitions within the genetic code (Lindahl 1993). These C to T transitions are the most common signature of damage and are used for authentication analysis by distinguishing contaminating (those without extensive damage) sequences from ancient ones (Skoglund, et al. 2014, Fulton & Shapiro 2019).

Contamination from modern sources has plagued the field since its inception (e.g. Wall & Kim 2007). From the start, the sample (bone, tooth, etc.) itself is at risk of contamination due

to the porousness of biological tissues. Environmental conditions and microorganisms may further compromise the integrity of the tissue, allowing exogenous DNA to be absorbed. Handling of the sample by archaeologists or paleogeneticists also may introduce contamination. Both methodological and sampling strategies (i.e. petrous bone) have been implemented to combat this problem. Sample processing and aDNA extraction occurs in clean-room facilities with strict contamination-reducing protocols, including UV radiation, bleach, personal protection equipment, and filtered air systems (Fulton & Shapiro 2019). Negative controls are implemented during extraction, library construction, and PCRs to monitor any contamination. Additionally, during the library-building step, unique tags are attached to sequences extracted in the clean room to identify likely ancient material, while contaminating sequences acquired later will be untagged (Henneberger, et al. 2019, Dabney, et al. 2013). Untagged modern DNA sequences can be filtered out during computational processing steps later. Furthermore, there are several bioinformatic tools or pipelines to quantify and remove contaminating reads (e.g. Schmutzi, ContamMix).

Sampling is also a means to mitigate contamination. The success of petrous portion sampling of the temporal bone in the skull, first described by Gamba, et al. (2014), was revolutionary for the field. Previously, teeth were (and still are) used for tissue sampling. Teeth allow for easy implementation of sampling strategies, they typically exhibit better preservation than the rest of the skeleton as a result of higher mineralization, and DNA binds to these minerals leading to higher endogenous contents, or the amount of human genetic material compared to the amount of exogenous DNA (i.e. bacterial, fungal, environmental, unclassified material, etc.) in a sample (Damgaard, et al. 2015, Hansen, et al. 2017). However, because the petrous portion encases the cochlea and inner ear bones, it is extremely dense and fortified. This protection helps to fend off contamination, leading to higher endogenous contents; thus, often outperforming teeth as a useful sampling material. While destructive, obtaining bone powder from this part of the skull is now the gold standard and continues to be optimized to be less invasive and more efficient at obtaining the highest amount of aDNA (Sirak, et al. 2017, Hansen, et al. 2017, Pinhasi, et al. 2015, Pinhasi, et al. 2019). For ancient samples, this amount is typically less than 1% due to the conditions described above (Der Sarkissian, et al. 2015). It is therefore crucial for all projects to assess if this small percentage can be utilized from samples before proceeding with further testing and/or destruction of sample material.

Sample preservation can be assessed on a case-by-case basis and is highly dependent on the depositional environment (Hoss, et al. 1996). Ideal conditions for DNA preservation include low, stable temperatures and low humidity, like those in caves (e.g. Noonan, et al.

2005). Material from temperate and arctic regions have produced better yields for aDNA compared to material from more hot or humid locations (Pinhasi, et al. 2015). This preservation bias in addition to the abundance of preserved archaeological material in Europe has led to a European bias in paleogenomics (Figure 1.7). Armed with new methodologies, the field of paleogenomics has expanded its scope to include Africa which was previously inaccessible (Pääbo 1985, Pääbo & Wilson 1988). Work in this continent was hindered for decades due to extensive thermal degradation of genetic material found to be common with the archaeological samples from extremely arid environments of Africa (e.g. the Nile River Valley). Early work with African samples showed significantly lower DNA preservation with which to start, let alone retrieve. However, the combination of NGS and sampling of the petrous portion has been a successful combination to bring the genomic revolution to Africa. In 2014, the first ancient African genome of a male individual from Mota Cave in Ethiopia was published by Gallego Llorente, et al. (2014). In the five short years since this first success, the genomes of 230 African individuals have been fully sequenced for mitochondrial (230) or nuclear genomes (101) (or both) encompassing more than 15,000 years of genetic history from the Canary Islands to South Africa (Figure 1.8). Within the Nile Valley, the first project exploring the genetics of Ancient Egyptian individuals was published by Schuenemann, et al. (2017). However, projects using Ancient Nubian remains are scarce or forthcoming (e.g. Jugert, et al. 2018, Sirak, K., personal communication).

Figure 1.7. European bias of paleogenomic work around the world, as of 2017.

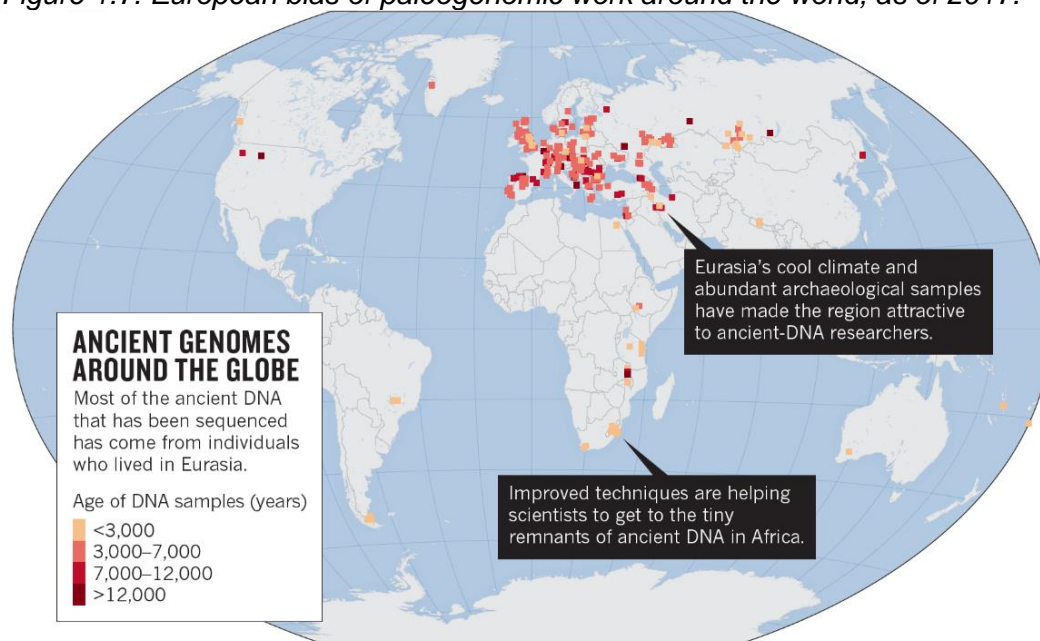
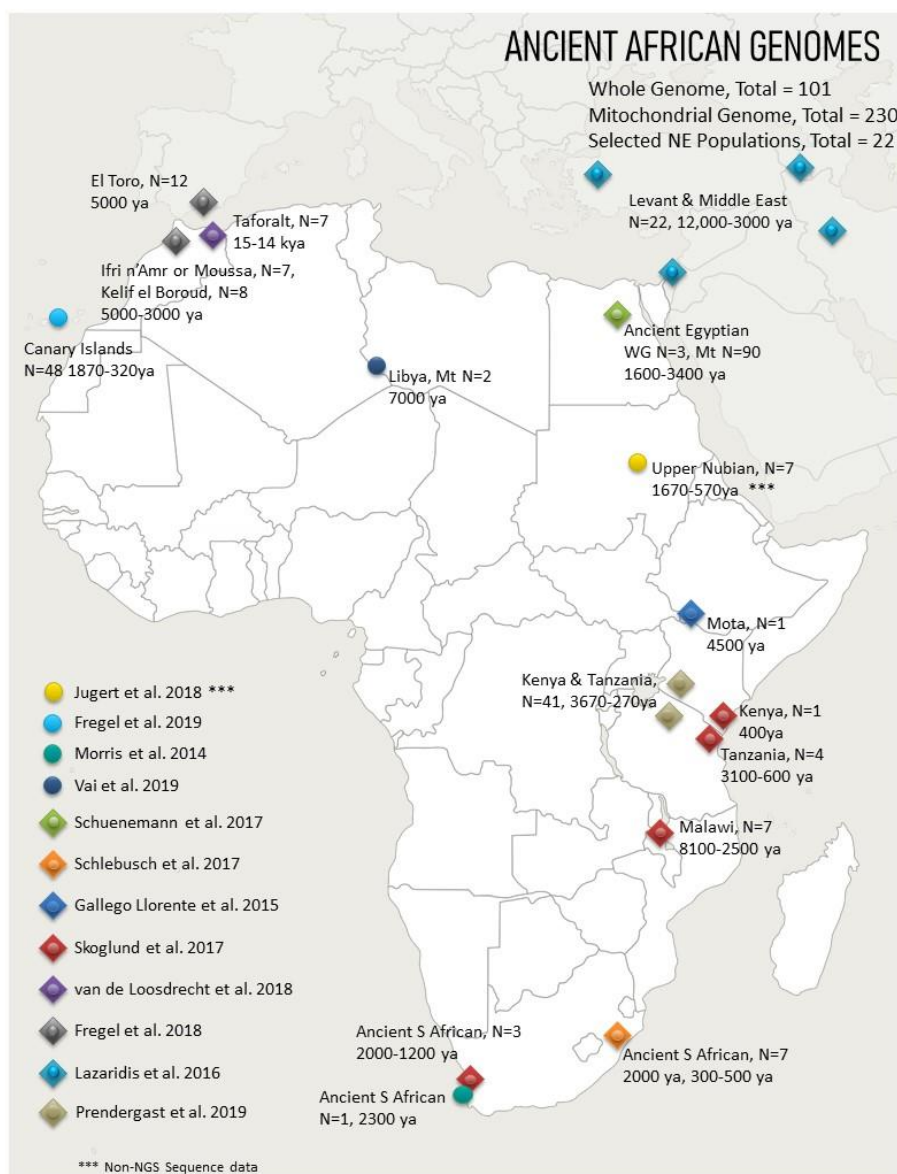


Figure obtained from Callaway (2017), *Nature*.

Figure 1.8. Published African mitochondrial and nuclear genomes, through August 2019.



Geolocations of published genomes in Africa with estimated dating of individuals. Grouped by archaeological site, or publication, archaeological name from publications or (modern) country. Legend at left, circles denote mitochondrial sequence data only, diamonds with dots represent whole genome and mitochondrial sequence data. WG - Whole genome, Mt - mitochondrial, NE - Near Eastern, N - number of individuals, ya - years ago, *** designates non-NGS protocols used. Some individuals from Lazaridis et al. 2016 publication mapped because were included in analyses.

Chapter Outline

For this dissertation research, I excavated and collected a Nubian sample population from El-Kurru, Sudan (Figure 1.1), conducted bioarchaeological analysis of the remains, and performed paleogenomic analyses. The goal was to join all lines of evidence for an interdisciplinary approach, marrying archaeological, bioarchaeological, and genetic data, to reconstruct the identity of Nubians near the 4th Cataract region (MacEachern 2013). Chapters of

this dissertation research are organized temporally and reflect a logical progression of the project (i.e. collection of samples, protocol optimization, implementation). First, Nubian remains were analyzed using a bioarchaeological approach (Chapter 2) to collect data on demographics and indicators of health and trauma. In addition, the mortuary and archaeological context of this population was investigated to understand cultural affiliations (e.g. Christian or Muslim) and the use of the space (e.g. domestic, administrative, palatial). These bioarchaeological analyses shed light onto our understanding of life along the Nile in this Late Christian town during a time of transition to Islam as a state religion, following the Arab conquest.

In Chapter 3, ancient DNA (aDNA) extraction methods were trialed using various standard and non-standard methodologies in order to maximize aDNA yields. Some methodologies were new developments in the field (i.e. extraction from petrous bone), while others have been implemented for a longer time (i.e. bleach treatment). Unfortunately, paleogenomic analyses using the El-Kurru samples analyzed in Chapter 2 were unsuccessful (i.e. no aDNA was obtained). However, these skeletal materials provided a valuable means to pilot paleogenomic work, trial new methodologies, and ultimately led to the successful extractions of other samples from the Middle Nile region (Chapters 3 and 4). aDNA extraction from tooth and bone samples (mostly teeth) from the El-Kurru collection was attempted using a PCR-based procedure. The results of this pilot work showed high contamination and poor preservation of the tissue, which ultimately pushed the research design to move onto more advanced extraction methods. These included a new sampling technique using bone tissue instead of teeth, employing only NGS techniques, and including an enrichment step. Furthermore, since this was one of the only paleogenomic projects in the ancient Nile River Valley to date, there was a lack of comparative ancient sequence data. Only three studies have been conducted on material from the Middle Nile region. However, none of the data from these studies were able to be incorporated into this analysis as the data was generated using outdated methodologies or the dataset was not comparable (i.e. different genetic markers including Y-chromosomal or nuclear polymorphisms) (Lalueza Fox 1997, Jugert, et al. 2018, and Hassan 2009). Due to this dearth of comparable datasets, an expanded sample set was collected through various collaborations in Sudan and abroad. In total, seven additional populations of at least four individuals each were obtained and sampled for comparison to the El-Kurru group and each other (Figure 1.1). These populations spanned multiple archaeological sites from the 3rd to past the 5th Cataract. This extensive geographic sampling is the first to include remains from regions never previously analyzed using NGS techniques.

The focus of this project was to obtain full mitogenomes of Nubian individuals from varying archaeological contexts, creating a time transect, to understand the genetic landscape of Nubia before the Arab conquest and trace population continuity through time (Buzon 2008, Buzon, et al. 2016, Irish & Joel 2005). The goal was to address ways paleogenomic data can help understand the demography of this region in context of archaeological, historical, and anthropological records. In Chapter 4, the mitochondrial genomes were reconstructed for six individuals. Two individuals had African ancestry, while four showed ties to the Near East. These genomes were compared to publicly available ancient and modern mitochondrial genomes from Africa, the Middle East, and Europe. We found that Ancient Nubians have close affinities to modern Egyptians, Middle Easterners, and East Africans, and less affinity to modern Sudanese and Ancient Egyptians.

Significance

There are few bioarchaeological studies from the Upper Nubia region. Those that do exist are concentrated at the same archaeological sites providing a narrow perspective of the region. The Christian population from El-Kurru will serve as a new dataset for comparison with other contemporaneous groups, like other Christian groups in the Upper Nubia region or those living further north in Lower Nubia. Similarly, it can be used to understand temporal changes in the region by comparison to groups that vary in time. The El-Kurru population is as an example of a group of individuals in transition. This collection may be a useful example for other bioarchaeological investigations of groups or communities facing cultural transitions around the globe. Although a small number of people, the skeletal remains help to build a narrative of life along the Nile during an important cultural transition in this region.

Second, paleogenomic research using samples from arid environments is an important advancement in the field but possesses new hurdles to overcome. Compared to Europe, where most of the paleogenomic research was developed and is currently taking place, studies analyzing skeletal remains from Africa are rare. Furthermore, the paleogenomics of the Nile River Valley of Africa is particularly understudied. There is no standard protocol for aDNA methodology using material from this region and no study to date has trialed different methods to optimize aDNA extraction techniques. With more enthusiasm for African paleogenomic work, it is critical to understand which methods should be employed to obtain ancient genetic material. In addition, this will better inform sampling strategies for future work.

Third, to date, no aDNA study using NGS techniques has been conducted on populations of the Middle Nile Basin. Paleogenomics can be used to reconstruct Nubian

demographic history to further understand the dynamics of this region. While drawing upon the growing knowledge from archaeological work, archaeological samples provide glimpses of various eras to reconstruct population dynamics (e.g. admixture, integration, displacement/replacement events) and understand the mobility and interactions of these groups across the landscape. ADNA can contribute a new line of evidence to complement those from other disciplines, which can in turn address larger questions requiring a more multi-dimensional approach.

CHAPTER 2: Life and Death at the End of Christian Nubia: Bioarchaeological Analyses of the Medieval Population from El-Kurru, Sudan

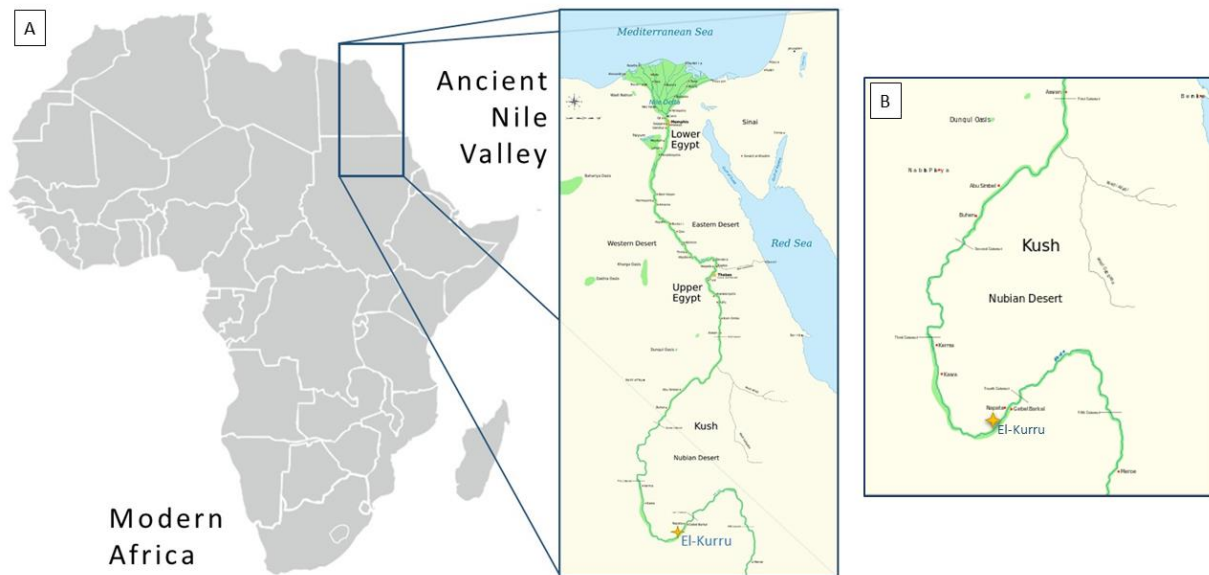
INTRODUCTION

The 4th cataract region of Sudan, the S-bend of the Nile (Figure 1.1), has been the subject of recent salvage archaeological investigations due to the construction of a dam at Merowe (Emberling 2012). This area is characterized by fast moving water, dangerous rapids, and land not as suitable for agricultural practices. Long thought to be less ideal for settling, the salvage projects from 1991-2008 revealed the opposite conclusion. Several thousand sites are estimated to dot the Nile region here, dating from the Paleolithic through the Islamic era. Furthermore, several significant monumental sites are located here, for example the royal pyramids at Nuri, temples and palaces of Gebel Barkal, and the putative location of Napata's capital, all of which have provided a wealth of information to deepen our knowledge of Nubian occupation and history (Figure 1.1). In this region, the first kingdom of Sub-Saharan Africa arose at Kerma around 2500 BCE (see Chapter 1, Figure 1.1), then further upstream the Napatan (ca. 800 BCE) and Meroitic kingdoms through the 4th century CE. To inform the period following, Scores of Post-Meroitic burials and a few settlements have been investigated downriver of the Cataract (e.g. El-Zuma). During Medieval times, churches and fortified towns were built along the Nile and were part of the Makurian kingdom. At its center was the capital of Old Dongola where excavations have revealed extensive settlements, citadels, churches, tombs as well as evidence of large-scale industry during this time of stability (Godlewski 2014).

Another of these 4th Cataract sites has multiple cultural horizons and the focus of this chapter. Deep in the ancient Napatan heartland, the archaeological site of El-Kurru (18.406569, 31.773974) is located in northern Sudan (Figure 2.1A) on the west side of the Nile River, near the 4th cataract (Figure 2.1B). This site is well known as the burial place for Napatan (25th dynasty BCE) kings and queens beneath pyramids and the presumed first capital of the powerful kingdom of Kush (Figure 2.2, 2.3) (Welsby 1996). Deeper excavation at this site has revealed another cultural horizon beyond the Kushite one. Facing the Nile River, a fortified town was uncovered dating to Medieval times, close to 2,000 years after the pyramids were built nearby. Within the defensive perimeter, a complex of housing and other domestic structures

was built of mudbrick (Kendall 1992, Dann & Emberling, et al. 2016). Ceramic and midden evidence indicated multiple phases of use from the 9th through the 14th century (Dann & Emberling, et al. 2016). Currently, the modern town of Alkuro lies northwest of the defensive wall and surrounds the plateau where the royal cemetery was built. These villagers trace their ancestry to the Arabic kingdoms of the 14th century but may also have ties with the Medieval Makurian kingdom which preceded it.

Figure 2.1. Modern Map of Africa and ancient Nile Valley with close up of 4th Cataract region.



A) Geographic location of Nile River Valley with ancient regions spanning modern Egypt and Sudan. B) Location of archaeological field site El-Kurru (yellow star); map insert of 4th Cataract and surrounding Upper Nubia region.

Figure 2.2. El-Kurru Royal Cemetery plateau with Napatan Pyramid, temple in foreground.



El-Kurru was first excavated by George Reisner of Harvard University early in the 20th century to explore the royal pyramids and burial tombs of the Kushite kings who ruled over Egypt during the 25th Dynasty (747-646 BCE) (Figure 2.3, left). This royal cemetery offers a

unique opportunity to observe the development of the mortuary landscape of the Kingdom of Kush (ca. 750-300 BCE). Here, a sequence of tombs become sequentially more elaborate while appropriating themes from elite Egyptian culture: Nubian tumuli (large burial mounds), rectangular structures with chapels, and steep-sided pyramids with underground tombs, which was a uniquely Nubian feature (while Egyptians tombs were constructed inside pyramids). Reisner excavated most of these burial structures including the central pyramid, a large rock-cut funerary temple to the east (Figure 2.2), and exported the artifacts back to Boston. On the periphery, he and his team also explored to some extent the areas surrounding the rocky plateau. There, he uncovered what he postulated (incorrectly) to be an expansive Napatan palace, which is known to be a fortified Medieval settlement (Figure 2.3, right lower).

Figure 2.3. Excavation map of El-Kurru, including royal cemetery, medieval wall, and Napatan structures.

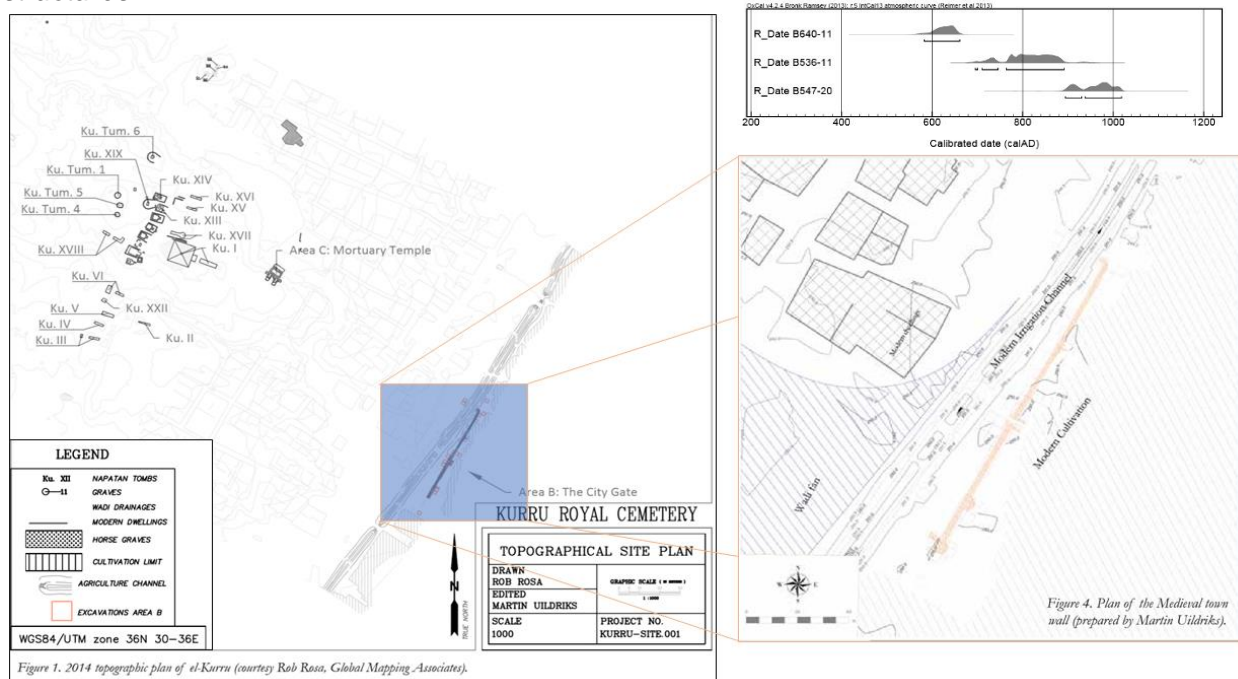


Figure 1. 2014 topographic plan of el-Kurru (courtesy Rob Rosa, Global Mapping Associates).

Left: Excavation plan of El-Kurru with pop-out (right) showing a close up of the defensive wall (in orange) and modern features in this area (i.e. irrigation channels, etc.). Kurru cemetery map from Emberling & Dann, et al. (2013) with modifications by author. Top: Radio carbon dating of samples from along the excavated city wall. Approximate date range: ca. 600-1000 CE (Emberling & Dann, et al. 2013).

Very little work was conducted on the pyramids or the features in the periphery after the exploratory excavations by Reisner, until the International Kurru Archaeological Project (IKAP) was launched in 2013. Co-directed by Dr. Geoff Emberling (University of Michigan), Dr. Rachel Dann (University of Copenhagen), and Dr. Abbas Sidahmed Mohammed Ali (University of Dongola, Karima, Sudan), IKAP began new research initiatives at this site. This team of international scholars has conducted archaeological excavation of the pyramid, its burial

chambers, and the settlement closer to the Nile River (Figure 2.3, Figure 2.4) as well as projects on various topics including geophysical survey, cultural heritage, restoration and conservation of art and architectural structures on site. This project sought to understand the multi-phase use of this space and the significance of El-Kurru during the Kushite Kingdom, as well as engage the local community who have become the stewards of their ancestral past.

Figure 2.4. Satellite view of El-Kurru excavations in relation to modern day agricultural and domestic land.



Google map (2019) showing satellite view of the modern landscape, shaded blue area shows Medieval excavation site in relation to agricultural land and a modern village. To the north, Royal pyramids on plateau labeled with a map marker. Map obtained from Google (2019).

Recent work identified and completed excavation of structures from Reisner's field notes, including the stone block wall near the edge of the modern village (Figure 2.4). During excavations, associated finds dated this settlement as Medieval Christian (ca. 600-1400 CE) and it was later dated via AMS to be ca. 600-1000 CE (Figure 2.3 right upper), much later than the Kushite pyramids. More than two meters thick, the wall ran parallel with the Nile in a defensive manner facing the river and had multiple bastions along its 138-meter length, including at the corners (Figure 2.3, Figure 2.5 left). The entrance was marked with a large petrified log from the forest several kilometers away (Figure 2.5 left). The wall was built around the 9th-10th century CE, followed by mudbrick domestic structures shortly after. These housing structures within the wall had at least two phases of occupation and the presence of storage jars, cooking pots, and grinding tools provide more evidence of a domestic use (Figure 2.5 right). Middens (trash/refuse piles) and ceramics from multiple Christian time periods suggested

an extended occupation (Emberling & Dann, et al. 2016). Following the second phase of the domestic structures, the space within the wall was used for refuse dumping during the 12th-14th centuries (Emberling & Dann, et al. 2016). The last phase of this space was the cemetery, where at least 27 individuals were interred in approximate rows, stratigraphically on top of the domestic layers, while avoiding the stone block wall (Figure 2.6). Given these graves cut into this refuse area in this space, this cemetery is stratigraphically dated to post-14th century.

Figure 2.5. Excavation of Medieval Christian structures at El-Kurru.



Left: Entrance to defensive wall; threshold is a log of petrified wood (between the parallel walls). Right: Mudbrick domestic spaces near wall entrance. Images from Dann & Emberling, et al. 2016.

Figure 2.6. Excavations centered on Medieval Christian settlement and cemetery.



Left: Map of settlement excavations, wall in orange (Emberling & Dann, et al. 2013). Blue box zooms in on cemetery, wall entrance (east), and modern irrigation channel (west). Right: Expanded view of cemetery, graves outlined within excavation squares. Courtesy of M. Uildriks.

The focus of this project concerns the skeletal remains excavated from the cemetery within the town wall (Figure 2.6). As the probable inhabitants of this settlement, the skeletal remains from this cemetery offered an unexplored perspective to understand more about those who lived at El-Kurru. Anthropological analyses of these remains provide data about their demography (i.e. age and biological sex), cultural practices and identities (i.e. burial treatments), and life experiences (i.e. indicators of health status). Given the likely contextual date of post-14th century and that Islam was officially instated in the southern most Christian Kingdom of Soba by 1493 CE with the establishment of the Funj Sultanate, this skeletal population may offer important insights in to the increasing Arab influence on Nubian Kingdoms in the Middle Nile region and impact of the transition to Islam (Hillelson 1930).

MATERIALS & METHODS

Excavation of El-Kurru Sample Population

Archaeological excavation of the Medieval cemetery found near the town wall and anthropological evaluations of the human remains began in 2014 and continued through 2016 by various personnel associated with IKAP. Skeletal remains were excavated by Mohamad Saad (National Corporation of Antiquities and Museums, Khartoum, Sudan), Tim Skuldbøl (University of Copenhagen), Gretchen Emma Zoeller (Indiana University Purdue University, Indianapolis), and Abigail Breidenstein (University of Michigan). The burials were uncovered during the course of normal excavation of settlement architecture and domestic spaces. Within the burials excavated, skeletal remains were exposed, photo-planned, and lifted. To limit the risk of looting during excavation, each individual was excavated in one day. Outside the field, remains were cleaned, sorted, and cataloged. Bone and teeth samples were collected for ancient DNA analysis and exported from Khartoum, Sudan, to the University of Zürich, Switzerland. All other remains were packed and exported from Khartoum to the University of Michigan for detailed anthropological evaluation.

Age & Sex Estimation and Health Status Indicators

Age-at-death was estimated using as many features as possible, including degree of epiphyseal fusion (Cunningham, et al. 2016), tooth formation (Thoma & Goldman 1960, Smith 1991) and dental eruption sequences (Buikstra & Ubelaker 1994, AlQahtani 2008) as well as (to

a lesser degree) occlusal wear or dental attrition (Gilmore & Grote 2012), the auricular surface (Lovejoy 1984, Brooks & Suchey 1990), and the pubic symphyseal face (Buikstra & Ubelaker 1994). Dental attrition was observed or noted but not utilized to age an individual since standards for this method are not calibrated for comparison with African populations in desert environments. Biological sex was estimated with reference to non-metric cranial traits (Buikstra & Ubelaker 1994), the morphology of the pubis (Phenice 1969), and the morphology of the greater sciatic notch (Buikstra & Ubelaker 1994). Lastly, all pathological or traumatic features were recorded and scored using standard reference texts and their methods as prompted on the data collection sheets (Ortner 2003, Waldron 2009, Aufderheide & Rodriguez-Martin 1998, Buikstra & Ubelaker 1994) or specialized methodologies specified below. These estimations and observations were recorded following field data sheets “Human Remains Recording Sheet” by Antione (2018).

Health Status Evaluation

To understand the life experiences of the El-Kurru individuals, the skeletal remains offer a glimpse into these lives, especially those experiences which affected their health. In general, the skeletal remains – cranial, dentition, and post-cranial – were examined to determine the health status of every individual. Using a bioarchaeological approach, multiple tests are conducted with this sampling to understand the stress response on a population level. These tests record porotic hyperostosis, cribra orbitalia, linear enamel hypoplasias, and non-specific lesions or periostitis (e.g. endocranial lesions, joint porosity/cribra). Skeletal tissue and enamel formation are sensitive to insults that may increase or arrest these processes, such as nutritional deficiencies, disease, or other hardships (Larsen 2015). The tests include evaluating the presence or absence of health signals and usually a score for severity and/or status of active or healing. Additionally, the presence of trauma was noted for all individuals with enough preservation.

Cribra orbitalia (CO) (pitting lesions in the upper eye sockets) and porotic hyperostosis (PH) (porous lesions on ectocranium) are both commonly assessed in skeletal remains from archaeological contexts (Walker, et al. 2009, Ortner 2003). Currently, the exact etiology of these lesions is hotly debated with possible causes including genetic anemias (any of the thalassemias, G6PD deficiency, sickle-cell etc.), deficiency-related anemias including malnutrition (rickets, scurvy, iron, B₁₂ etc.), or those related to infectious disease (e.g. malaria, hookworm infections) (Moseley 1974, Steinbock 1976, Walker, et al. 2009). The presence of CO and/or PH is likely multifactorial, meaning these lesions are non-diagnostic and should be

considered with other stress indicators (Brickley 2018, McIlvaine 2013). Both conditions are evaluated as per Rinaldo, et al. (2019). Briefly, individuals were included in the analysis if at least one eye orbit was intact for inspection. One or both orbits were evaluated for the presence or absence of lesions and the stage of severity and/or healing were both judged according to the published chart and accompanying description of the lesions (Rinaldo, et al. 2019).

Next, when available, all dentition was checked for the presence of linear enamel hypoplasias (Buikstra & Ubelaker 1994). Individuals were included in this test if at least one anterior tooth (incisor and/or canine) was present for observations. Hypoplasias were noted as present or absent and graded in severity and structure (i.e. pits or line) as per Buikstra and Ubelaker (1994). LEHs present as lines, grooves, or a grouping of pits which encircle the crown and can be macroscopically detected with a fingernail test (i.e. deep enough to catch when running a fingernail over the surface of the tooth crown) (Buzon 2006). These defects are a response to interruptions in the deposition of enamel during the formation of the tooth crown, which varies from before birth to roughly 19 years old (Hillson 1996, White & Folkens 2005). Disruptions in enamel formation can be caused by bouts of illness, malnutrition or diet deficiencies, or local trauma (Goodman & Rose 1991, Goodman, et al. 1980). But differentiating between causes is difficult, therefore the presence of these hypoplasias is seen as a general marker for physiological stress (Larsen 2015, Goodman & Rose 1991).

Lastly, the presence of non-specific lesions is an important indicator of variable health. Lesions are deposits of woven bone tissue as a response to inflammation (Larsen 2015, Buikstra 2019, Waldron 2008). These lesions are judged as “non-specific” as most have a long list of etiologies from infectious disease, genetics, environmental hazards, trauma, behaviors, nutrition, etc., but are informative of an unhealthy environment and whether adaptation is required to survive this hardship (Buzon 2006, Goodman & Armelagos 1988).

Dating of Skeletal Remains

Two individuals with good preservation from different depths and excavation squares were chosen for AMS carbon dating. Bone and tooth samples from Ind. 206 (from area B249) and Ind. 214 (from area B451) were sent to ETH Zürich (Department of Physics, Zürich, Switzerland) for collagen extraction and c14 dating. When results were unsuccessful (See Results), additional samples were sent to the University of California, Irvine (UCI), to the ESS KECK/AMS Facility for troubleshooting with knowledge of the low collagen levels. Samples from Ind. 212 (cranial fragments), Ind. 214 (mandible fragment), and Ind. 206 (mandible fragment) were trialed for radiocarbon dating, but were again unsuccessful, likely due to poor preservation.

RESULTS

Excavation and preservation

The skeletal remains from the El-Kurru settlement were excavated over three consecutive field seasons: two in 2014, ten in 2015, and fifteen in 2016. Over the course of three excavation seasons, squares B350, B450, B249, B349, and B449 were excavated to bedrock. Squares B351 (half opened) and B451 were not exposed to bedrock and are expected to contain more individuals (Figure 2.6). *In situ* burials in the northwest balk of B350 confirms that the cemetery extends further in the southwest and northwest directions and contains other individuals. Due to time constraints and the proximity of the modern irrigation channel, these squares remain unexcavated. The Reisner trench (within B348 and B448) may have contained burials and still does, as indicated by the *in situ* burials remaining within the northeast corner of B448 and another burial in B447. In general, the bodies were not buried in the vicinity of other obvious structures, except the fortification wall. However, two individuals were excavated in close proximity to mudbrick structures (i.e. Ind. 216 was between a mudbrick wall and door jamb, Ind. 210 underneath a partial wall collapse), but these instances did not invalidate the dating of the cemetery as ca. post-14th century.

In general, the skeletal remains found in the El-Kurru settlement were in various states of preservation with most skeletal remains weathered, brittle, and mostly fragmented. Remains from 2014 and 2015 were in fair to poor preservation, while those from 2016 were better preserved. In contrast, the teeth were in better condition than the skeletal remains for most individuals, allowing for a thorough evaluation of dental health and disease as well as sampling for molecular analyses, (e.g. stable isotopes and ancient DNA). Preservation of the remains was compromised by the cemetery's location near several water hazards – namely a large wadi (seasonally active water drainage route) to the west, active agricultural fields to the east, and a modern irrigation channel northwest of the cemetery (Figures 2.3 & 2.5). There was evidence of several other hazards impacting the taphonomy of these remains, including but not limited to a palm grove to the south (lateral roots systems damaged the skeletal remains), animal scavenging, and heavy weathering from the arid climate. Lastly, there was no evidence of looting or disturbance of burials.

Dating of Skeletal Remains

Despite being tested at two highly-reputable facilities and using the (perceivably) best preserved biotissues, AMS dating was unsuccessful. Results from the testing at ETH are listed

in Table 2.1. Specifically, C/N ratios should be lower and collagen extraction by weight was not enough. Results from UCI were reported as unsuccessful due to poor preservation which led to insufficient collagen extraction. Therefore, the individuals interred in the cemetery will remain to be contextually dated to ca. post-14th century.

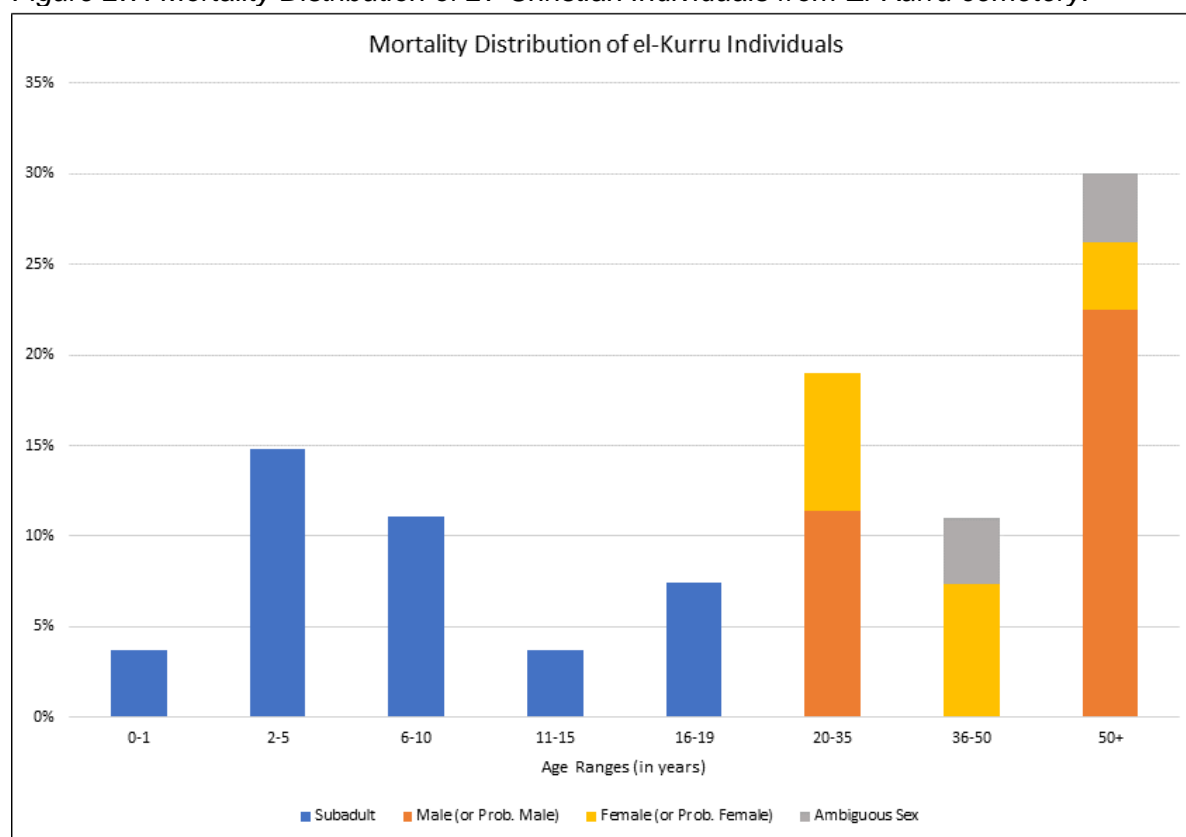
Table 2.1. Results from AMS Radiocarbon dating performed at ETH Zürich.

Sample	Tissue Type	Nitrogen Content (%)	Carbon Content (%)	C/N Ratio	Total Collagen Weight
IND. 206 (B249)	Bone (Mandible)	0.56	2.33	4.1572	241.4 mg
	Tooth	0.38	0.79	2.1007	--
IND. 214 (B451)	Bone (Mandible)	0.39	2.43	6.2510	184.5mg
	Tooth	0.41	1.45	3.5251	--

Anthropological Profiles of El-Kurru individuals

The El-Kurru skeletal sample is composed of 11 subadults (40.7%) (aged less than 20 years of age) and 16 adults (59.3%) (aged 20+ years), as summarized in Figure 2.7, with an approximate mean age-at-death of 25 years. For biological sex, the adult group consists of nine males (or probable males), five females (or probable females), and two of ambiguous or indeterminate sex (Figure 2.7). Subadults were divided into five categories: Infants (0-1 year), Early Child (2-5 years), Late Child (6-10), Adolescent (11-15 years), and Pubescent (16-19 years). Adults were divided into three age ranges: young adults (20-35 years old), middle adults (35-50 years old), and older adults (50 years or older). No fetal or prenatal remains were found. During excavation, it was found that preliminary assessment of biological sex was easier to determine with *in situ* remains than after lifting the bones, especially with the pelvis. For an unknown reason, the remains of male individuals were better preserved overall compared the females and may present a bias for later analyses. Sub-adults were not assessed for biological sex since puberty has not been reached. For adults, cranial features seemed to be misleading while the pelvis seemed to be much more reliable. From experience of the author, the population tended to have more gracile features, especially of the skull, and less robusticity overall; therefore, features of the pelvis were weighted more than cranial ones for final estimations of biological sex.

Figure 2.7. Mortality Distribution of 27 Christian Individuals from El-Kurru cemetery.



Age and sex distribution for El-Kurru sample population, N = 27. The y-axis is the number of individuals classified in each age category. Colored bars represent estimated sex of each individual: blue – subadults, not assessed, orange – male or probable male, yellow – female or probable female, grey – ambiguous sex, could not be determined due to preservation or intermediate scores). X-axis lists age range (in years): Infant, Early Child, Late Child, Adolescent, Pubescent, Young Adult, Middle Adult, Older Adult (respectively).

Within this sample of 27 individuals from El-Kurru, all age classes were present as well as both sexes within the adult categories. The demographic data from this population showed a typical “U-shaped” mortality curve, with some notable exceptions. In a “normal” graph, those experiencing the most risk are the young and old (represented as larger groups for age-at-death, or taller columns, at the far left and right, respectively), while the robusticity of the older subadults and young adults are less at risk, thus creating a U-shaped graph when counts are tallied from a skeletal population (Jackes 2011). Exceptions to this pattern seen in Figure 2.7 were a lack of infants or neonates (0-1 years) and middle adult males (36-50 years). The missing infants from this sample may suggest these individuals are buried elsewhere (e.g. in the home or a separate cemetery) (Pinhasi & Bourou 2007). The absence of males in the middle adult category suggested either better survivorship that could be evidenced with the abundance of older male adults (>50 years), or these individuals were dying elsewhere, which could be expected given their proper age for military contribution. More broadly speaking of the 16 adults,

males and females were not equally dispersed (Figure 2.7), with a sex ratio of 180 (expressed as the number of males per females). Additionally, given this mortality distribution of this sample, more than 40% of the population did not reach adulthood. Eleven individuals were categorized as subadults ranging from less than one year of age to 17.5 years old. The first three categories (N = 8) suggested a mortality of nearly 30% for individuals under the age of ten for the subpopulation represented at this cemetery. This is well within the range of premodern populations and this death curve is typical of ancient populations: on average, in the past two millennia youth (less than 15 years of age) mortality is 46.2% and infant mortality is 26.9% (Volk & Atkinson 2013). Figure 2.7 shows an abundance of individuals dying young – half of which are under the age of five – then a typical drop off in the middle phases, speaking to the robusticity and survivorship of the juveniles making it to adulthood. The timing of this life stage relates to surviving weaning after early childhood, known to be a challenging stage for infants and young children (Lewis 2007). The risk of death then steadily increases as individuals enter phases of reproduction and more adult activity. For this population, however, the distribution of those dying in adulthood is atypical, with more dying younger than those in the middle adult range. This is possibly due to unequal or higher risk of death for females. However, it is more likely the result of a small sample size. Lastly, the category with the most adults is the older adults, representing individuals that died after the estimated age of 50. For the adults, the sex distribution is not equal after the young adult category – suggesting a high risk of death for women dying younger and males surviving longer to over 50 years. This could indicate females had a hard life in this Medieval community. Overall, mortality peaks for older adults may actually indicate a well-adapted population for this region. These two peaks – high mortality in the first few years (approx. 19%) and later in adulthood (approx. 30%) – are typical; however, it seems more atypical that adults were living to an advanced age in an ancient population. While it was not unheard of, it is rare for people in ancient times to live past their early sixties. For example, Roman working-class commoners had a mean age at death of 30 (Caldarini et al. 2015), while those from various Nubian time periods is between 26 and 36 years (Armelagos 1969).

Mortuary Archaeology of El-Kurru Cemetery

A total of 27 individuals were excavated from the cemetery. Unmarked graves were roughly organized into three or more rows running northeast to southwest, which were parallel to the fortified wall and the bank of the Nile (Figure 2.6). Fully extended bodies were arranged perpendicular to the town wall, head to the northwest and feet to the southeast. Graves were dug as simple pit inhumations with a thin oblong shape, which were adapted to the size of the

individual with no evidence of coffins, boxes, or beds. Burials were typically single occupation, with the exception of one double burial with an adult and a child (Ind. 106 and Ind. 113). Bodies were buried about 1.5 feet (half a meter) from the modern surface up until a depth of 4 feet (1.2 meters) at the bedrock. Adult individuals were not buried with grave goods (e.g. vessels, jewelry, etc.), but some children or infants had small tokens. Small beads of ostrich egg shell or faience were found near the neck or wrists for two subadults suggesting they were likely buried with simple jewelry. The burial style and lack of grave goods is consistent with typical Christian burial treatments.

Some grave markers were thought to be associated with burial pits, although these stones could also have been deposited serendipitously with a body. For example, a carved sandstone block was in context with burial 206, indicating that it could possibly be a headstone. During excavation, the stratigraphy of the bodies (ie. overlapping, varying depth) indicated multiple phases of use. For example, burials 206 and 209 overlap in such a way that Ind. 209's grave cuts Ind. 206's, which was excavated first. This could be explained by those maintaining the cemetery forgetting where the first body was buried without the use of grave markers.

Organics from the wall date the fortification to ca. 600-1000 CE (Figure 2.3). The burials were located at a higher elevation than the threshold of the fortified wall. Furthermore, stratigraphy and the arrangement of the burials to the wall suggested that the burials post-date the wall and were interred later than the 14th century. Given that the treatment of the bodies exhibited typical Christian characteristics, it is estimated the group of individuals date to after the upper limit of the wall's contextual dating. Other finds associated with the graves included decorated pottery sherds in the grave fill that are not considered grave goods, but likely refuse mixed with the dirt used to fill graves. Sherds were dated to Classic Christian (ca. 800-1100 CE) or Late Christian (ca. 1100 – 1450 CE) periods based on painted motifs (e.g. "twisted rope motif") and fine ware symbols (Figure 2.8A & C) (Klimaszewska-Drabot 2008, Phillips 2003).

Figure 2.8. Artifacts uncovered within grave fill for El-Kurru burials.



Examples of contextual finds from the grave fill used for dating. A) Example of pottery sherds in context with skeletal remains used to date burials; white fabric with “twisted rope motif” are Classic Christian (ca. 800-1100 CE) and used a finer fabric than red or black course ware. B) River “prayer” pebbles. C) White fine ware with cross symbol.

Another observation of note for those buried at El-Kurru was the ubiquitous presence of colorful river pebbles found in the top layers of the grave fill (Figure 2.8B). Found on the banks of the Nile, river pebbles were prayers or tokens of affection for the dead. This tradition has a deep history in this region of Sudan as far back as the Meroitic period (Cavendish 1966). It is common during the Christian period (e.g. El-Ar (early Christian 6th cent.) and Nuri (ca. early Christian)) and has continued into the present (e.g. Manasir) (Cavendish 1966, Zurawski 2007).

Burial Treatment

Most graves did not have a super structure. A few individuals had a rough mud cap over the grave, shallowly constructed 0.5m above the body (e.g. Ind. 201). There was no evidence of coffins or box graves within the pit (structure made of flat rocks outlining the body). Although it was expected to find traces of a burial shroud, as is typical of Christian style treatments (Welsby 2016), no organics or fabrics were preserved. However, for those buried supine, features of the articulated body suggested that burial shrouds or some materials were possibly used for binding. For example, the clavicles had a characteristic verticalization arrangement (Harris & Tayles 2012, Nilsson Stutz, 2003) (Figure 9, blue arrow) *in situ* caused by the arms being drawn tightly to the body in a close bind and for some individuals, hands were very closely clasped together (Figure 2.10C). This suggests that burial shrouds could have been in use and likely decomposed as a result of the inundation of the area since antiquity.

Figure 2.9. El-Kurru Ind. 203 showing extended and supine burial.



Close-up photograph of Ind. 203 within the grave before lifting. Blues arrows point to clavicles, *in situ*.

Each individual shared three characteristics of how the body was arranged during burial: clasped hands, fully extended, and supine (body facing upwards) or side-facing placement (Figure 2.10A-C). The bodies of all individuals were fully extended, never flexed. Sometimes, bodies were turned to fit into tight spaces for burials. Most bodies were facing to either side but not in a uniform way, specifically 15 to the right (65%) and eight to the left (35%), while four were supine. Body position may have shifted during decomposition as indicated by twisted, but still articulated legs (Figure 2.10B). This suggested that the body started in a supine position then may have turned after burial (e.g. Ind 207). All burials had clasped hands positioned over the pelvis, regardless of the body arrangement. This also indicated the use of binds at the time of burial and during the decomposition or skeletonization of the body (Welsby 2016). All bodies were oriented with the head to the northwest (west when aligned to Nile) and feet to the southeast (east when aligned to the Nile) (Figure 2.5). All individuals were found in anatomical position with little to no disruption of the skeletal remains post-deposition. The only exception was Ind. 209, where the left arm and hand was found cutting the grave cut of Ind. 206; additionally, a few epiphyses of 209's hand bones were found inside the mouth of 206.

Little variability was identified in the El-Kurru cemetery population. All individuals appear to be uniformly treated. There was no apparent relationship between body positioning or burial orientation with relation to sex or age of the individuals (Table 2.2). The treatment of the body (i.e. extended, bound) was uniform with no variation based on the age or sex. Lastly, interment position within the whole cemetery does not show a pattern based on age or sex; for example, children and infants were buried among adults, instead of being buried elsewhere.

Figure 2.10. Burial treatment and body treatment of El-Kurru individuals.



Examples of body treatment of individuals buried at El-Kurru. A) Fully extended body positioning, e.g. Ind. 104. B) Body placed in a supine or side-facing position, e.g. Ind. 207. C) Hands probably bound by cloth or a shroud, without preservation of textiles or organics, e.g. close up of Ind. 210.

Table 2.2. List of El-Kurru Individuals and demographic data.

Ind. No.	Season	Age at Death (in years)^α	Sex ^β	Body Position	Burial Orientation
004	2014	3-5	SA	Extended, right side	W-E, facing S
005	2014	20-35	M	Extended, supine	W-E, facing up
104	2015	20-35	M	Extended, right side	W-E, facing S
105	2015	20-35	F	Extended, left side	W-E, facing N
106	2015	36-50	I	Extended, left side	W-E, facing N
107	2015	16	F	Extended, right side	W-E, facing S
108	2015	50+	M	Extended, right side	W-E, facing S
109	2015	7-9	SA	Extended, left side	W-E, facing N
110	2015	36-50	F	Extended, left side	W-E, facing N
111	2015	36-50	F	Extended, supine	W-E, facing S
113	2015	12.5-15.5	SA	Extended, right side	W-E, facing S
115	2015	< 1	SA	Extended, right side	W-E, facing S
201	2016	50+	M	Extended, right side	W-E, facing down
202	2016	7.5	SA	Extended, left side	W-E, facing N
203	2016	20-35	M	Extended, supine	W-E, facing S
204	2016	50+	I	Extended, right side	W-E, facing S
205	2016	50+	F	Extended, left side	W-E, facing down
206	2016	20-35	F	Extended, supine	W-E, facing up
207	2016	50+	M	Extended, right side	W-E, facing S
209	2016	17.5	SA	Extended, left side	W-E, facing N
210	2016	50+	M	Extended, right side	W-E, facing S
211	2016	4.5	SA	Extended, right side	W-E, facing up
212	2016	3.5	SA	Extended, right side	W-E, facing S
213	2016	5.5	SA	Extended, right side	W-E, facing S
214	2016	5.5-6.5	SA	Extended, left side	W-E, facing N
215	2016	50+	M	Extended, right side	W-E, facing S
216	2016	50+	M	Extended, right side	W-E, facing S

^α Cunningham et al 2016, Thoma & Goldman 1960, Smith 1991, Buikstra & Ubelaker 1994, AlQahtani 2008, Gilmore & Grote 2012, Lovejoy 1984, Brooks & Suchey 1990

^β Buikstra & Ubelaker 1994, Phenice 1969

+ = more than

< = less than

F = Female or probable female

M = Male or probable male

I = Indeterminate sex or could not be determined as male or female

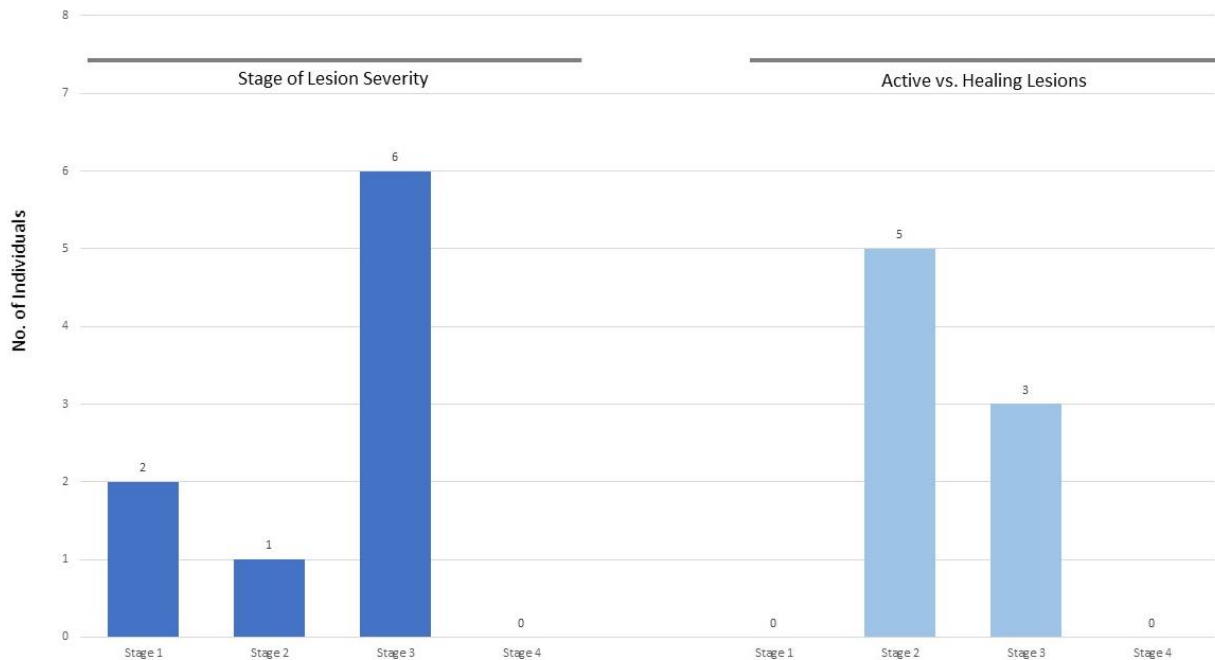
SA = Subadult, no sex estimate

W-E = skull at west end, feet at east end; directions not cardinal, oriented toward the river

Health Status Evaluation

Cranial remains were evaluated for cribra orbitalia (CO) as per Rinaldo, et al. (2019). Fifteen of the 27 individuals (ten adults and five subadults) were able to be evaluated and those not included had poor preservation. Of the ten adults, two females and two males were affected or 40% of the sample. These results show no bias for sex, although this is a small sample. For the five subadults evaluated, four or 80% exhibit CO. Age estimates range from 3.5 – 17 years old. The lesions judged were most commonly at stage 3, or “presence of holes that join within inner bone tissue” (Rinaldo, et al. 2019) (Figure 2.11, Figure 2.12). In general, all lesions were in some stage of healing, none were judged as active. The most common stage observed was stage 2 (Figure 2.11, Figure 2.13). Taken together, 40% of the population was estimated to have moderate signs of CO, but the lesions were in remission. This would suggest these individuals were vulnerable to stress, but adapted enough to live through the hardship.

Figure 2.11. Cribra orbitalia severity and stages of healing observed in El-Kurru population.



Left: Counts for stages of severity observed in those individuals with orbit lesions or cribra orbitalia (dark blue). Lower stages refer to small area affected and small pores, while higher stages have a large affected area with deep, joining pores. Right: Counts for stages of healing observed in those individuals with orbit lesions or cribra orbitalia (light blue). Lower scores describe no signs of healing, while higher stages are for healing or healed lesions. Counts above bars. Y-axis= count of individuals.

Figure 2.12. Stages of severity observed in cribra orbitalia lesions in El-Kurru population.



Individuals used as examples: Stage 1 = Ind. 205 (left orbit), Stage 2 = Ind. 212 (right orbit), Stage 3 = Ind. 203 (right orbit).

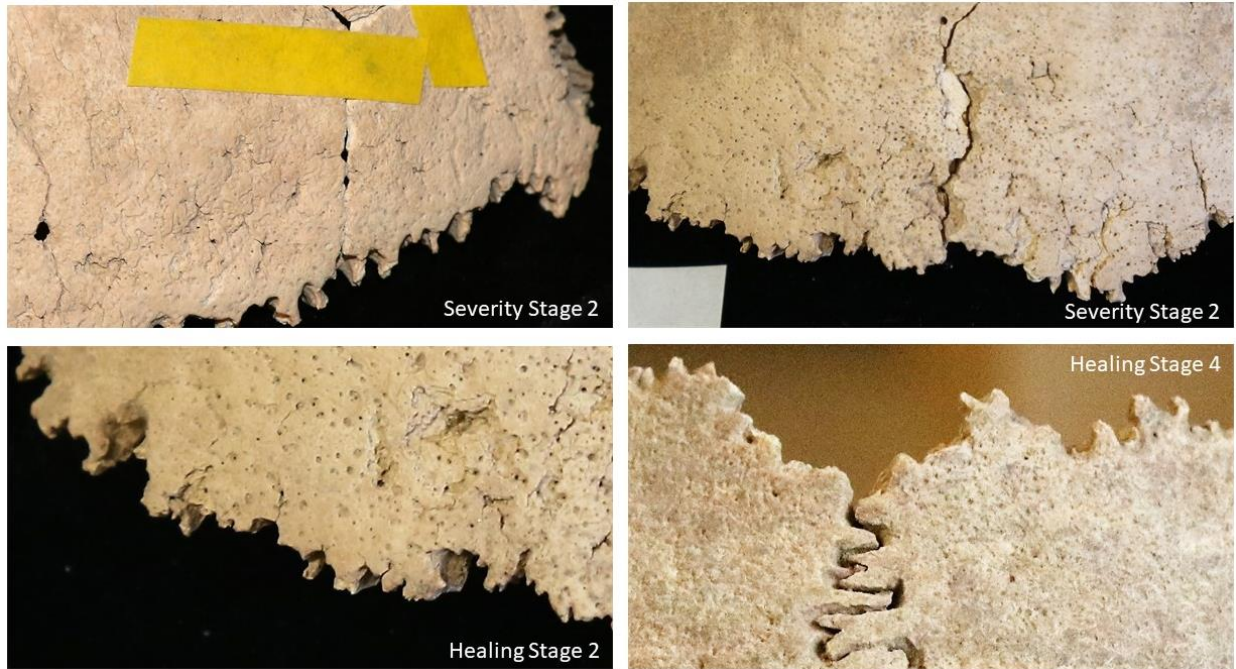
Figure 2.13. Healed lesions observed in El-Kurru population.



Individuals used as examples. Stage 2 healed = Ind. 105 (right orbit), Stage 3 healed = Ind. 214 (left orbit). Of note are the rounded margins of the pores within the lesions.

Porotic hyperostosis (PH) could be evaluated in 16 of the 27 individuals (i.e. more than 50% cranial surface observable). Those not included were due to poor preservation of the crania. The severity and healing stages were scored as per Rinaldo, et al. (2019) and Stuart-Macadam (1989). Of the 19 evaluated, only three were affected: Ind. 203, a young male adult, Ind. 205, an older probable female adult, and Ind. 216, an older male adult. Thus, PH is observed in roughly 19% of the population. All individuals were at stage 2 severity, and were either stage 2 or stage 4 healing (Figure 2.14).

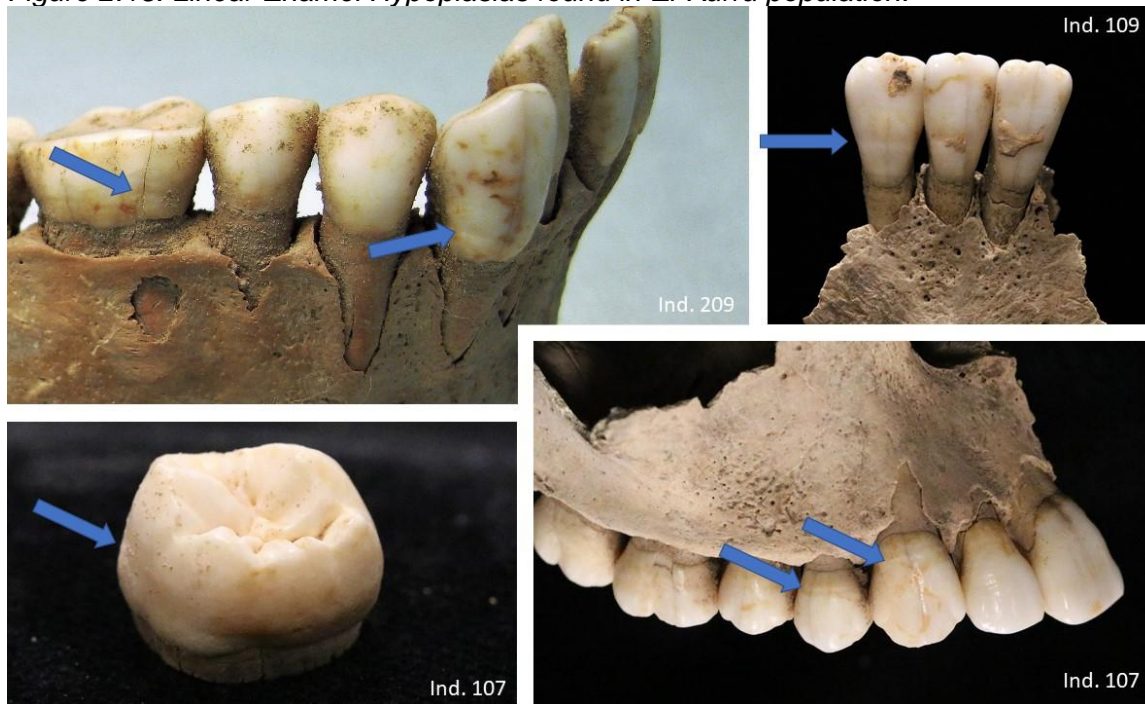
Figure 2.14. Porotic Hyperostosis in El-Kurru population.



Examples of Porotic Hyperostosis (PH) found in El-Kurru population. Top: Ind. 203 right parietal and frontal bones. Bottom: Ind. 203 frontal bone and Ind. 216 parietal bones.

For the evaluation of linear enamel hypoplasias (LEH), 22 individuals from El-Kurru could be included in this test (Figure 2.15). Five were not included due to poor preservation of the teeth or attrition (tooth wear) was so severe that enamel could not be viewed. Of these 22 individuals, 16 (73%) had at least one tooth with an LEH and 6 (27%) had none. Those affected included all ages and both sexes: 7 subadults ranging in age from 3 – 17 years and 9 adults, including 2 females, 2 of indeterminate sex, and 5 males. This sex bias may indicate males were more susceptible to hardships, but the sample size is very small. Despite heavy attrition, LEHs were very common among adults and subadults.

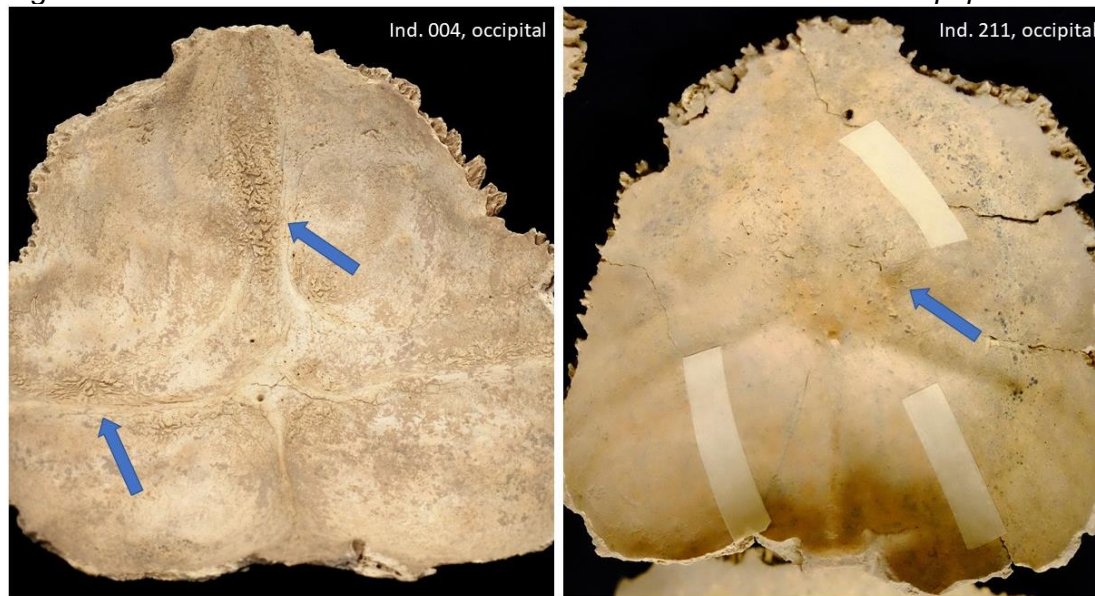
Figure 2.15. Linear Enamel Hypoplasias found in El-Kurru population.



Blue arrows point to linear grooves or lines where enamel production was arrested. Ind. 209: right mandible. Ind. 109: mandibular incisors (and some calculus build up). Ind. 107 left: unerupted third molar. Ind. 107 right: right maxillary teeth. Ind. = individual

Endocranial lesions were observed in 2 of 18 individuals able to be evaluated, (i.e. preservation of more than 50% of the cranium). The other individuals had crania too fragmentary to observe the inner table of the skull or for which reconstruction was impossible. Ind. 004 (child 4.5 years old) had extensive, active (i.e. “hair-on-end”) lesions within the endocranium, while those found within the skull of Ind. 211 (child 4.5 years old) were already well healed (Lewis 2017) (Figure 2.16). The etiology of such lesions, especially found in children, is still debated; from non-pathological to vitamin deficiency to infectious disease (Lewis 2004, Wolbach & Bessey 1941, Mitchell 2006).

Figure 2.16. Two instances of endocranial lesions observed in El-Kurru population.



Both examples found on occipital bones of skull. Blue arrows show areas of where the lesions are located. Ind. = individual

Porous lesions found on the humerus (*cribra humeralis*) and of the femur (*cribra femoralis*) were quite common, but only among the younger individuals. Eighteen individuals had adequate preservation of the post-cranial skeleton to observe the joints where these lesions appear. Seven out of 18 (39%) showed porotic lesions at the proximal metaphysis of the femur and/or the distal metaphysis of the humerus (Figure 2.17, Figure 2.18). These lesions are often associated with each other (Smith-Guzmán 2015b). All instances were bilateral, occurring in both the arms and leg bones, and characterized by deep pores penetrating the cortical bone. One individual (Ind. 005) was a young adult (20-35 years old) while the six others were aged between approx. 4 - 17 years old. The etiology of these lesions is poorly understood and not clinically linked with anemia or a deficiency in the way CO or PH is (Lewis 2017). For those individuals that could be evaluated for CO (i.e. preservation of at least one orbital roof), all (N=4) also had CO. Together, this is known as the “cribrous syndrome” and is the result of red bone marrow expansion during red blood cell proliferation, the subsequent thinning of the cortical bone superficial to marrow, and the substitution of the trabecular bone underneath (Miquel-Feucht, et al. 1999a,b, Djuric, et al. 2008). Furthermore, the association of these types of lesions with malaria has also been examined by Smith-Guzmán (2015b). Using the lesion presence or absence algorithm, two individuals can be diagnosed with malaria: Ind. 206 and Ind. 212. The lesions are in variable states of activity; those present in Ind. 209 seemed quite sharp or active, while those present in Ind. 212 have more rounded edges and have signs of

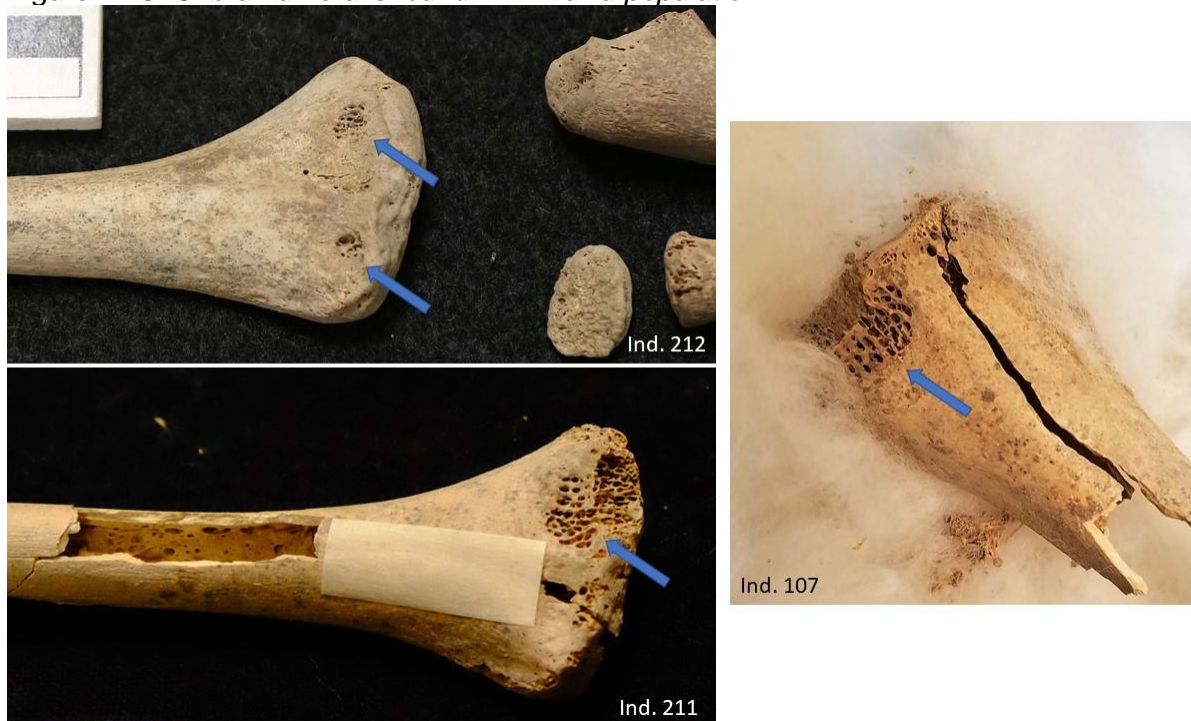
healing (Mensforth, et al. 1978) (Figure 2.17). Erosion and taphonomic damage made it difficult to judge these lesions consistently.

Figure 2.17. *Cribra femoralis* found in the El-Kurru population.



All proximal ends of femora. Blue arrows point to lesions on cortical bone. Ind. = Individual

Figure 2.18. *Cribra humeralis* found in El-Kurru population.



All distal ends of humeri. Blue arrows point to lesions on cortical bone. Ind. = Individual

Four instances of trauma were observed in the entire El-Kurru population (15%) (Figure 2.19). All were well-healed fractures as evidenced by the boney callus and subsequent resorption of lamellar bone. All fractures occurred in quite mundane locations of the skeleton, specifically a right second toe (Ind. 216), a left upper arm (Ind. 205), and a right clavicle (Ind. 210), and all to older (50+ years or older) adults of both sexes. All of these injuries are extremely common, especially the right clavicle that is the most commonly broken bone in the human body (Arizona Science Center). The healed fracture in Ind. 204 (indeterminate sex) is classified as a “parry fracture,” or an injury associated with a defensive wound from a frontal (likely right-handed) attack (Judd 2000). This was a left ulna (forearm bone) and the fracture only involved this bone, not the adjacent radius, and was located at the distal (closer to hand) end (Figure 2.19, Ind. 204). These criteria fit the definition of a “parry fracture” exactly and the fracture was well healed indicating the individual likely sustained the injury early in life.

Figure 2.19. Four instances of trauma found in El-Kurru population.



Ind. 204 “parry fracture” of left ulna. Ind. 205 healed left humerus. Ind. 210 (poorly) healed right clavicle. Ind. 216 right second proximal metatarsal. Blue arrows show the boney callus, all healed fractures. Ind. = Individual

Table 2.3. Summary Table of Health Status observations.

Test	No. evaluated	No. Afflicted	Percentage
Porotic Hyperostosis	16	3	19 %
Cribra Orbitalia	15	8	40 %
Linear Enamel Hypoplasias	22	16	73 %
Endocranial Lesions	18	2	11 %
Joint Cribra	18	7	39 %

No. – number of individuals

DISCUSSION

Archaeological records of late Medieval Nubia in the 4th cataract region in Upper Nubia are sparse (Edwards 2013). The excavation of the cemetery at El-Kurru and its subsequent bioarchaeological analyses offers a perspective of the climate at the end of the Christian time period in the Middle Nile Region. Political constructs began to weaken after the first Muslim king was put in place up river at Dongola in the early 13th century (Welsby 2002). There is also a possibility that plague, which spread through Egypt and Ethiopia, played a part in the instability at this time (Borsch 2005). Contextually dated to post-14th century, the cemetery at El-Kurru contained at least 27 individuals culturally associated to Christians as per associated pottery sherds, grave constructions, and body treatment (i.e. extended position, arms at the pelvis, supine or side-facing). Using bioarchaeological evaluations, the presence of stress signals were detected in this skeletal population that can identify if these individuals were living in unhealthy environments. Since the etiologies of these disruptions are not easy to discern and health itself is influenced by a multitude of factors, stress markers were taken together to portray a more general view on stressors in the population, which can originate from biological, environmental, social-political, etc. causes (Goodman & Martin 2002, Larsen 2015). In the El-Kurru population, high frequencies of LEHs indicate stressors during developmental years (< 20 years) and the presence of distinctive lesions suggest parasitic infections were common among the subadult population with two probable cases of malaria.

In general, the percentages of stress signals (CO, PH, LEH, other lesions) detected in the El-Kurru population (Table 2.3) were consistent with those reported from this region and time. The appearance of porotic hyperostosis (19%) was well within the context of other data reported on the presence of these lesions. From Lower Nubia, PH was present in 4% - 68% of Christian individuals, while for subadults the frequency range was 40 - 80 % (Van Gerven, et al. 1981, Carlson, et al. 1974, Hurst 2014, Soler 2012). The presence of PH begins to build an overall narrative of a stress response and can be an indicator of anemias, metabolic disorders (e.g. scurvy), chronic infectious disease, or malnutrition (Buikstra 2019, Brickley 2018). Next, the presence of CO was also within the range of reported populations in the Northeast Africa.

CO was recorded in 40% of the individuals at El-Kurru, with 80% of those being subadults. Among past Nile River Valley populations, instances of CO range ca. 30 – 60 % and malaria has been suggested as the causative agent being present at endemic levels from prehistoric to Christian time periods (summarized by Smith-Guzmán 2015a). Specifically, rates from Upper Nubia were on the lower side at some sites, e.g. 11% all individuals, 43% subadults from Tombos, 21% all individuals, 32% subadults from Wadi Halfa (Carlson, et al. 1974, Buzon 2006), but higher in others, e.g. over 60% at Amarna West or 45% from Kulubnarti (Mittler & Van Gerven 1994, Binder 2014, Hummert & Van Gerven 1994). The cause of these lesions was speculated to be from nutritional deficiencies, namely iron, from a millet and wheat-centered diet (Carleson, et al. 1974). However, a heavy disease burden should not be discounted, as malaria, hookworm, and schistosomiasis are also endemic in the region presently and likely present in the past (Hibbs, et al. 2011, Larsen 2015). In Upper Nubia, Christians from Mis Island show 49% prevalence, with more than 80% of those affected being subadults (Soler 2012, Hurst 2014). The prevalence of CO from El-Kurru and the higher rates in subadults is consistent with other populations close in space and time. Given the lesions are all in healing states (non-active), this suggests stressors likely occurred in the early years of life and individuals lived through the stressful conditions, for example iron deficiency anemia triggered by poor nutrition, weaning, or bouts of infectious disease.

The high frequency of LEHs (73%) present in the El-Kurru population is consistent with other prevalence data reported from Christian Nubia. At Kulubnarti, (300-1400 CE) in Lower Nubia, every individual examined had at least one hypoplasia event recorded, while at Mis Island roughly 50% were affected (Van Gerven, et al. 1990, Soler 2012, Hurst 2014). While methodologies may be responsible for this difference, sampling of Nubian groups deeper in time showed similar variation in values. Two surveys conducted during the New Kingdom period and after (ca. 1400-800 BCE) show that 21% of individuals at Tombos displayed LEHs, while 69% of individuals from Amarna West showed these lesions (Buzon 2006, Binder 2014). While each of these frequencies were interpreted within the context of these sites, especially varying political or cultural situations, the etiology of these lesions can be attributed to high chronic stress during childhood when the teeth are forming (Goodman & Rose 1990, Hillson 2008). These stressors may be a consequence of an iron-deficient diet, a heavy disease load, or weaning. Thus, the high frequency found in the Late Christians from El-Kurru would indicate a majority of those living at this fortified town experienced hardships when growing up, but given the abundance of older individuals, these Nubians were surviving to old age. Lastly, other lesions present (joint cribra and endocranial lesions) in the El-Kurru population have not been evaluated in other

Nubian populations for comparison. However, another dataset from Medieval Serbia attributed high frequencies of the “cribrous syndrome” in subadults to parasitic infections, causing hemolytic anemia and/or diarrhea (Djuric, et al. 2008). Given that these non-specific lesions occurred in the subadult population from El-Kurru, their occurrence speaks to a heavy disease burden on the youngest individuals of the population.

Four instances of healed, non-lethal trauma (14%) implies the El-Kurru population was one not likely in conflict (Figure 2.19). The fractures observed in this selection of individuals are mundane injuries or accidents. The clavicle is the most broken bone in the human body, and this fracture in Ind. 210 (Figure 2.19) is the right side no less; it is evidence of a fall, where the man stuck out his right hand to brace the fall, shattering his collarbone as the force radiated up his arm. It was poorly set and the lack of woven bone indicated the callus has been smoothed away by many years, even decades, of healing. Another example, Ind. 216’s right foot with a broken second metatarsal. One can imagine this man dropping something on the top of his foot, breaking only that one bone. Again, this break has a smooth callus speaking to years of healing. A few of these foot bone injuries also have been recorded in other New Kingdom individuals (Binder 2014). The other two instances, the broken humerus of the older woman and the parry fracture for Ind. 204 (indeterminate sex) possibly suggest interpersonal violence. The arm fracture was well healed and there are myriad scenarios, with and without aggression, to reconstruct this injury. However, the “parry fracture” observed on Ind. 204’s left ulna is a more convincing signal of violence (Judd 2000). However, no other signs of interpersonal violence were recorded, for example head lesions. From Lower Nubia, 14% of individuals display head lesions from Meroitic through Christian time periods (Armelagos 1969). On the other hand, post-cranial lesions of violence are low (ca. 4%) in the earlier periods and increase to 11% in Christian times, indicating a possible uptick in aggression (Armelagos 1969). These are both much lower than occurrences recorded in the Kerma period (ca. 2500-1500 BCE) which ranged from 40-80% with at least one injury (Judd 2002). Taken together, the frequency of trauma at El-Kurru was low, suggesting that this sample of the population was not experiencing intra-group or inter-group violence.

The limitations of this study include the sample size, the preservation of remains, and the inability to radiocarbon date these remains. The cemetery was not completely excavated and therefore more individuals could have been included. However, even with only 27 individuals, demographically all categories were covered with two notable exceptions (infants and middle adults), implying that this was approximately a representative sample (Jackes 2011). Moreover, the preservation of these skeletal remains impacted the post-field analyses and

molecular analyses. The heavy weathering and severe water damage made these bones chalky, brittle, and diagenetically compromised. Several individuals were excluded from post-cranial analyses due to poor preservation. This impacted the bioarchaeological recordings (e.g. difficult to judge the severity of lesions due to erosion, etc.), the molecular extraction of DNA, and both attempts at radiocarbon dating. These previous two failures likely indicate collagen levels were damaged to the point of no recovery, likely from the heat, but perhaps more so from the constant or seasonal presence of water that leached the protein out of the bone tissue matrix.

Future directions of this work would include fitting these individuals within the context of more Medieval Nubian sample populations in the Middle Nile region when these data become publicly available. This could include more bioarchaeological studies or those which explore the identity of these Nubians expressed through their mortuary archaeology. Another perspective would be to pilot stable isotopic analysis (i.e. carbon and nitrogen) of the El-Kurru individuals to further contextualize signals of the childhood stress and the presence of lesions. From previous work, Nubians generally had a mixed diet between C₃ and C₄ plants (i.e. wheat and barley, fruits and vegetables; sorghum and millet, respectively) and had little contribution of protein from land animals (not aquatic ones) (Basha, et al. 2016, White & Schwarcz 1994). Modern villagers in the region, including those living in Alkuro, subsist as sedentary agriculturalists and it is likely that little has changed since Christian times. Specifically, a stable isotopic study could shed further light on their means of subsistence and test if malnutrition was a challenge. Lastly, since there is so little knowledge, the plague hypothesis could be tested using pathogen screening of the remains (reviewed in Spyrou, et al. 2019). This would be limited in scope (i.e. small number of individuals) and likely not viable given the little success with other molecular analyses due to poor preservation. However, any vascularized tissue may be used to screen for the *Yersinia pestis* genome (Spyrou, et al. 2019). Plague would explain the many deaths of younger individuals but there are no indications of special body treatment (e.g. encased in lye), which would lend credence to this hypothesis.

CONCLUSION

Recently, a small Christian cemetery at El-Kurru, Sudan, was excavated in context of a fortified, Medieval town close to the Nile River. Mortuary treatment of the bodies was consistent with Christian traditions, as were the pit graves and a general lack of burial goods. Demographic analysis revealed both sexes and all age categories were buried here, from infants to older adults. A slight sex bias was observed where younger females were dying sooner than older

males and subadult mortality was normal, less than 20%. Bioarchaeological analysis of these individuals recorded markers of stress, including high levels of childhood hardship or malnutrition and likely exposure to parasitic infections, which affected the subadult population the most. The lesions found in two subadults were likely from malaria. Additionally, only one case of trauma which can be attributed to interpersonal violence suggesting this population was not exposed to interpersonal violence or those who did were buried elsewhere.

This sample population from El-Kurru represents a group of individuals living at a time of transition, the end of Christianity and the rise of Islam in the Middle Nile region. There does not seem to be an over-abundance of hardships or deaths, as all the frequencies of stress markers are mostly congruent with those from this time period. This fact ultimately hints that transition to Arab rule and the Islamitization at this location did not impact their well-being, but certainly warrants further investigation.

CHAPTER 3: Method Optimization of aDNA Extraction from Ancient Nubian Archaeological Materials

INTRODUCTION

When ancient DNA sampling is performed using skeletal material of our past ancestors, it is destructive of some tissue which cannot be used for future work. Therefore, increasing the endogenous human DNA to start with is paramount when utilizing precious archaeological materials. In addition to advancements in sampling (outlined in Chapter 1), other strategies that were previously developed may also be used on samples with very low endogenous levels, including those from arid regions of Africa. These strategies include additional treatments during the sample processing step to boost the endogenous content prior to DNA extraction. A bleach pre-treatment, first introduced by Kemp and Smith (2005), has been used to decontaminate ancient samples and is standard procedure of those samples with high contamination (Barta, et al. 2013, Korlević, et al. 2018, Korlević & Meyer 2019). This mild pre-treatment uses low percentage sodium hypochlorite (NaClO or bleach) to decrease the amount of exogenous DNA that has been absorbed by the tissue. This step has been shown to increase the amount of target DNA by almost five-fold and decreases the amount of contaminating DNA. However, the impact of bleach on library complexity, or the uniqueness of DNA reads, is debated (Korlević & Meyer 2019, Boessenkool, et al. 2017). In addition to a bleach pretreatment, the use of a mild enzymatic digest before the DNA extraction has also shown to be useful in removing contamination and subsequently increase the endogenous content (Schroeder, et al. 2019). Also known as a “double digest,” the sample is subjected to an enzymatic solution for a short time (15 min to 1 hour), this solution is removed, and the sample is ready for an overnight, full digestion followed by extraction the next day. Like the bleach pre-treatment, this method removes exogenous DNA from the sample powder to increase the endogenous content prior to DNA extraction (Damgaard, et al. 2015). Both of these pre-treatments can be used in combination (i.e. Boessenkool, et al. 2017) or separately (e.g. Damgaard, et al. 2015) depending on the extent of contamination or sample fragility.

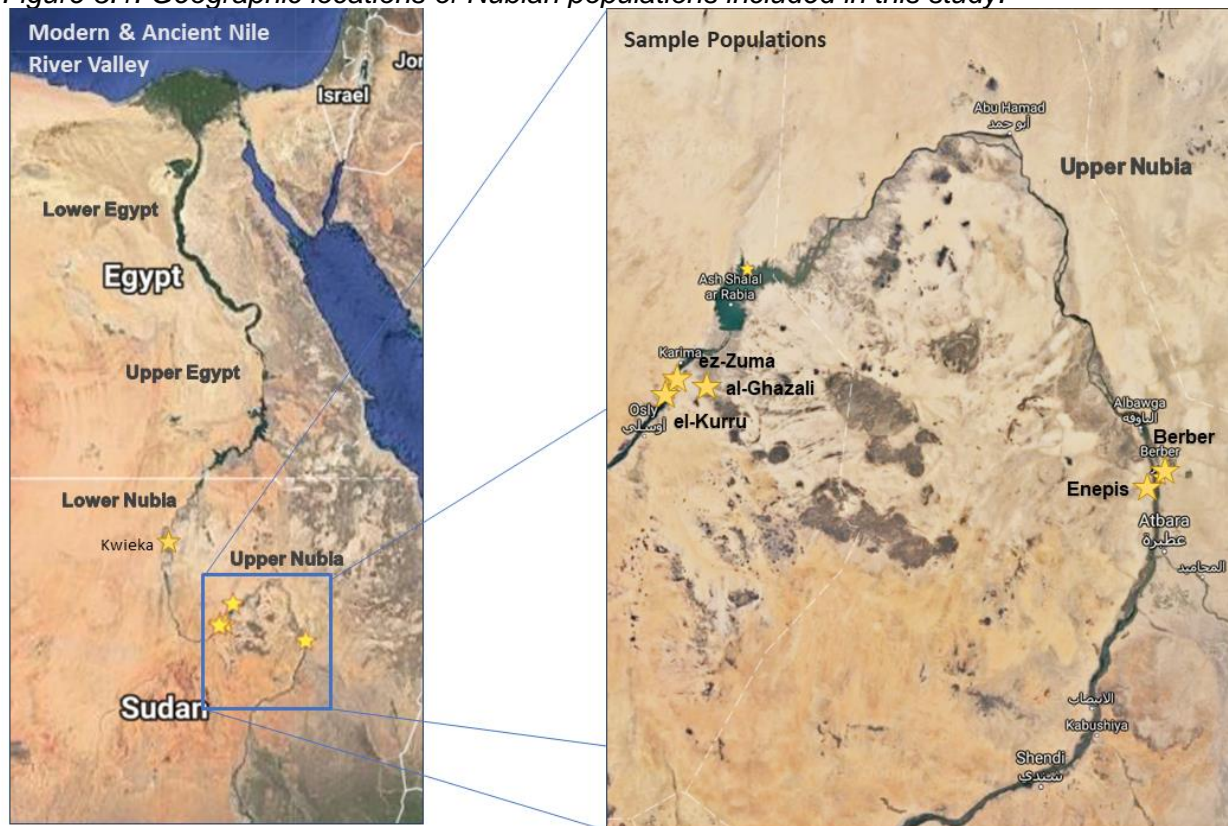
Samples from Africa are particularly difficult to work with due to thermal degradation and low DNA preservation, thus alternative methods must be considered to retrieve any DNA that

remains in the tissue. For these reasons, and the fact that only one protocol has been recently published outlining successful DNA extraction using material from Sudan and none from the Middle Nile region, for this study it was necessary to optimize a new protocol. In the present work, multiple combinations of the steps described above were piloted to assess the extent of DNA viability in Ancient Nubian samples from the Middle Nile region. Furthermore, it was investigated which pretreatments were most helpful to retrieve aDNA, quantify differences between material used (bone versus tooth dentine and if certain environments or burial contexts impact the survival of DNA. These trials and the optimized procedure may be used for current paleogenomic work with archaeological materials from Sudan and will better inform sampling strategies in the future.

MATERIALS

Samples were collected from eight archaeological collections of the Middle Nile Basin representing nearly 3,000 years of history in this region (Figure 3.1, Table 3.1). Field sites span nearly 1000 kilometers (km) along the Nile River, from the 5th Cataract at Berber to past the 3rd near Abri, Sudan. With well over 200 tooth or bone samples, 89 individuals represent five cultural horizons in Nubian history, from the Napatan period of the Kushite Kingdom to Medieval Nubian times at the end of the Christian Kingdoms (Table 3.1). The archaeological and anthropological contexts of all sites and samples are briefly described here to present the variables introduced from different burial treatments and environments. Samples listed in Table 3.1 were shipped from collaborators or collected by the author for aDNA extraction at the Institute of Evolutionary Medicine, University of Zürich, Zürich, Switzerland. Any remaining tissue after processing, including enamel, tissue powder, or bone fragments, was returned to the collaborators.

Figure 3.1. Geographic locations of Nubian populations included in this study.



Left: Satellite map of modern Nile River Valley with labels of approximate regions in the ancient world. Kwieka is located in Lower Nubia, near the between the 2nd and 3rd Cataract. Blue box zooms in on Upper Nubia. Right: Expanded view of Upper Nubian sites near the 4th and 5th Cataracts. Maps obtained from Google (2019), edited by author. Note: ez-Zuma is another version of El-Zuma, both are used in the literature.

Table 3.1. Archaeological information and sampling of Nubian populations included in this study.

Nubian Group	Location/Site	Date(s)	N	Sample Material	Excavated by (year(s)):
Napatan, Meroitic	Enepis	800 – 350 BCE, 350 BCE – 350 CE	10	27 bone and tooth samples	NCAM, Tinga Archaeological Rescue Project (2017)
Meroitic	Kwieka	350 BCE – 350 CE	4	8 bone and tooth samples	NCAM, Kwieka Archaeological Rescue Project (2018)
Meroitic	Berber	350 BCE – 350 CE	12	28 bone and tooth samples	NCAM, Berber Meroitic Cemetery (2009 - 18)
Post-Meroitic	El-Zuma	450-550 CE (2 nd phase Early Makurian period)	16	26 bone and tooth samples	Polish Centre for Mediterranean Archaeology, Early Makuria Project (2015-17)
Post-Meroitic	El-Detti	450-550 CE (2 nd phase Early Makurian period)	4	10 bone and tooth samples	Polish Centre for Mediterranean Archaeology, Early Makuria Project (2015-17)
Post-Meroitic	Tanqasi	350-600 CE	4	9 bone or tooth samples	Polish Centre for Mediterranean Archaeology, Early Makuria Project (2015-17)
Early Christians	Al-Ghazali	650-1000 CE	12	12 tooth samples	Polish Centre for Mediterranean Archaeology (2016)
Medieval Christians	El-Kurru	900-1400 CE	27	40+ bone samples, 80+ tooth samples, post-cranial remains	International Kurru Archaeological Project (2016)

N = Number of individuals

BCE = Before Common Era

CE = Current Era

NCAM = National Committee for Antiquities and Museums, Khartoum, Sudan

El-Kurru

Known for its royal pyramids, tombs, and mortuary temple dating to the Napatan time period, El-Kurru was an important site in Upper Nubia since the Kingdoms of Kush. It is located on the east bank of the Nile, near the 4th Cataract, and has been the focus of the International Archaeological Kurru Project since 2013 (Figure 3.1, 3.2). Recent archaeological work has concentrated on further exploration of the pyramids and burial tombs on the plateau as well as exploration of the unfinished excavations by George Reisner (from the 1910s) closer to the Nile (Emberling & Dann, et al. 2015). This work has uncovered a fortified Medieval settlement and an associated cemetery located within the town walls. This cemetery contained at least 27 individuals and was excavated over three seasons (2014-2016) (Figure 3.2). Anthropological analysis of these remains was conducted, including sex and age estimations in addition to evaluations of stress markers and health status. All age groups were represented by at least one individual, ranging from infant to older adult (50+ years) (mean of 26 years), and there was a slight abundance of males from this group. Mortality distributions peak during first years of life and at the end, demonstrating survival conditions typical of ancient populations. Material remains, including ceramics and cookware, typical of Middle to Classic Christian periods were found near burials and were associated with the surrounding domestic spaces. Radiocarbon dating of organics from the wall date the fortification to 600-1000 CE; the Christian burials are likely dated after this phase to around the arrival of Islam in Nubia, ca. 1450 CE (Skuldbøl, et al. 2016, Welsby 2016). Preservation of the remains was generally fair (likely due to proximity to the Nile, the natural hydrology of the site, and modern irrigation strategies (Figure 2.4)), but still provided many opportunities for tissue samples; specifically, the temporal bones seemed in better condition, while tooth dentine was chalky and demineralized. A summary of individuals, including excavation season, demographics, burial observations, and sampling materials for ancient DNA extraction, are summarized in the table below. More than 200 teeth and temporal bones were exported to Zürich for piloting methods for extracting DNA (Table 3.2).

Figure 3.2. Excavations centered on Medieval Christian settlement and cemetery.



Left: Map of settlement excavations, wall in orange (Emberling & Dann, et al. 2013). Blue box zooms in on cemetery, wall entrance (east), and modern irrigation channel (west). Right: Expanded view of cemetery, graves outlined within excavation squares. Courtesy of M. Uildriks.

Table 3.2. List of El-Kurru individuals, including demographic data, archaeological context, and samples collected.

Ind No.	Season	Age at Death (in years) ^a	Sex ^b	Body Position	Burial Orientation	Tooth	Bone
004	2014	3-5	SA	Extended, right side	W-E, facing S		✓
005	2014	20-35	M	Extended, supine	W-E, facing up	✓	
104	2015	20-35	M	Extended, right side	W-E, facing S	✓	✓
105	2015	20-35	F	Extended, left side	W-E, facing N	✓	
106	2015	36-50	I	Extended, left side	W-E, facing N	✓	
107	2015	16	F	Extended, right side	W-E, facing S	✓	✓
108	2015	50 +	M	Extended, right side	W-E, facing S		
109	2015	7-9	SA	Extended, left side	W-E, facing N	✓	✓
110	2015	36-50	F	Extended, left side	W-E, facing N	✓	✓
111	2015	36-50	F	Extended, supine	W-E, facing S		✓
113	2015	12.5-15.5	SA	Extended, right side	W-E, facing S	✓	✓
115	2015	< 1	SA	Extended, right side	W-E, facing S		✓

201	2016	50 +	M	Extended, right side	W-E, facing down	✓	✓
202	2016	7.5	SA	Extended, left side	W-E, facing N	✓	✓
203	2016	20-35	M	Extended, supine	W-E, facing S	✓	✓
204	2016	50 +	I	Extended, right side	W-E, facing S	✓	✓
205	2016	50 +	F	Extended, left side	W-E, facing down	✓	
206	2016	20-35	F	Extended, supine	W-E, facing up	✓	✓
207	2016	50 +	M	Extended, right side	W-E, facing S	✓	✓
209	2016	17.5	SA	Extended, left side	W-E, facing N	✓	✓
210	2016	50 +	M	Extended, right side	W-E, facing S	✓	✓
211	2016	4.5	SA	Extended, right side	W-E, facing up	✓	✓
212	2016	3.5	SA	Extended, right side	W-E, facing S	✓	✓
213	2016	5.5	SA	Extended, right side	W-E, facing S	✓	✓
214	2016	5.5-6.5	SA	Extended, left side	W-E, facing N	✓	✓
215	2016	50 +	M	Extended, right side	W-E, facing S	✓	✓
216	2016	50 +	M	Extended, right side	W-E, facing S	✓	✓

^a Cunningham 2016, Thoma & Goldman 1960, Smith 1991, Buikstra & Ubelaker 1994, AlQahtani 2008, Lovejoy, et al. 1985, Brooks & Suchey 1990

^b Buikstra & Ubelaker 1994, Phenice 1969

+ = more than

< = less than

F = Female or probable female

M = Male or probable male

I = Indeterminate sex or could not be determined as male or female

SA = Subadult, no sex estimate

W-E = skull at west end, feet at east end; directions not cardinal, oriented toward the river

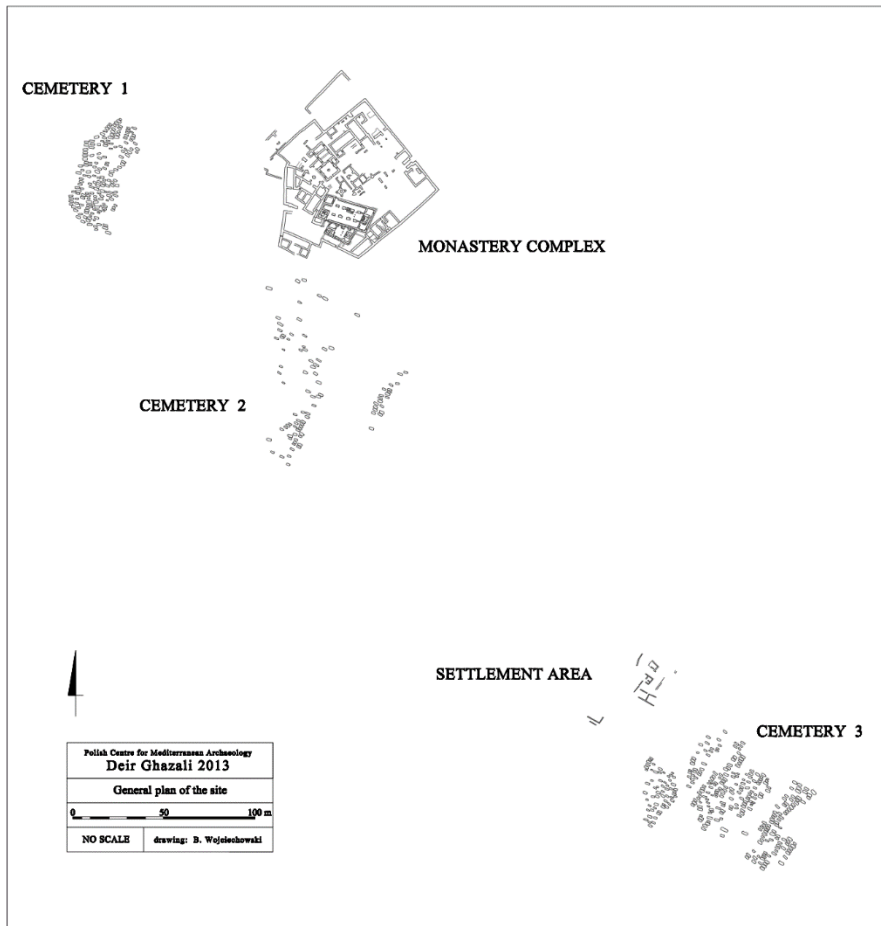
✓ = at least one available

Ghazali Monastery Complex

Ghazali is a medieval monastery complex dated to the 7th-13th century CE and is located in the 4th Cataract region, northwest of the Bayuda desert (Figure 3.1, Figure 3.3). This site has been excavated since 2012 by the Polish-Sudanese Ghazali Archaeological Site Preservation Project (Obłuski, et al. 2015). In addition to the monastery, four cemeteries have been excavated with variable mortuary architecture— for example, simple rock cut pits with stone cairns or mud-brick mastabas with double vaulted chamber tombs (Obłuski 2014). Cemetery 2 contains the graves of monastic monks; here, all the interred are male, burials were located in close vicinity to the church, and associated goods indicated the individuals' religious status. While cemeteries 1-3 are likely associated with the religious complex, Cemetery 4 is more isolated and had an unknown function (Figure 3.3, Cemetery 4 not pictured). Here, 15 box graves were excavated demonstrating typical Christian burial style, but atypical body treatments (Welsby 2016). Due to the great preservation of the skeletal remains, samples were requested

for ancient DNA extraction. Currently, human remains are stored at the team field house in Karima or at McMaster University (Ontario, Canada). Intact tooth samples from 12 individuals were selected by the project anthropologist (Robert Stark) for ancient DNA analysis. At least one individual from each of the four cemeteries was selected for comparison of genetic makeup, but also to evaluate tissue preservation at this site for future analyses. Demographic data of these 12 individuals were evaluated by Stark and are summarized in the table below (Table 3.3).

Figure 3.3. Map of Ghazali monastery complex, including surrounding cemeteries and settlement area.



Obtained from Stark & Ciesielska (2019).

Table 3.3. List of Ghazali Individuals, including demographic data, archaeological context, and samples collected.

Ind No.	Site Cemetery	Sampling No.	Age-at-death (in years) ^α	Sex ^β	Tooth Sample
4-010	Ghazali 4	(none)	~ 40	M	3 rd M (?)
4-008.2	Ghazali 4	(none)	~ 35	F	RM ²
3-002	Ghazali 3	(none)	50 +	F	RM ¹
3-009	Ghazali 3	(none)	~ 40	M	RM ¹

1-010	Ghazali 1	(none)	~ 45	M	LM ²
1-004.1	Ghazali 1	4.22.1	~ 25	M	RM ₂
2-009	Ghazali 2	3.03.1	~ 45	M	LM ³
2-010	Ghazali 2	3.30.2	~ 45	M	RM ¹
2-011	Ghazali 2	3.12.1	50 +	M	RM ³
2-004.2	Ghazali 2	4.23.1	~ 50	M	RM ²
2-004.1	Ghazali 2	3.06.1	~ 40	M	RM ³
2-013.2	Ghazali 2	3.14.1	~ 40	M	LM ³

^a Buikstra and Ubelaker 1994

^b Schaefer 2009, AlQahtani, et al. 2010

~ = approximately

+ = more than

M = Male

F = Female

R or L = Right or Left, M = Molar, (superscript) = Maxillary (upper), (subscript) = Mandibular (lower), numbers reference which molar (i.e. 1 = first, etc.)

(?) = unknown assignment, likely third molar based on morphology of crown and roots

Sampling No. = refers to internal numbering for the Ghazali excavation project

Kwieka Cemetery

The archaeological site of Kwieka is located on the east bank of the Nile, near the modern town of Abri and Sai Island (Figure 3.1). More than 200 mound graves were identified in the area between the highway and settlement areas in proximity to the Nile River. To date, 17 graves have been excavated over two rescue seasons in 2016 and 2018 by National Corporation for Antiquities and Museums (NCAM, Khartoum, Sudan) officials. Mortuary excavations suggest multiple phases of occupation, spanning from Late Meroitic to Christian periods. Various types of graves and burial architecture were categorized by a suite of features, including super- and subterranean structures, which were useful for contextual dating when compared to other 4th Cataract burials (Abdallah 2018). Most burials showed evidence of looting in antiquity, but still contained fine grave goods (decorated ceramics, beads, metal objects), indicating more elite social status of these individuals (Abdallah 2018). Samples representing four individuals were collected from storage at NCAM and transported to Zürich for processing. Of the four collected, only one (T5) was contextually (i.e. from artifacts) dated to the late Meroitic period (3rd - mid 4th century CE). For each individual, at least one sample was collected (mostly two per individual, Table 3.4), including teeth and the petrous portion of the temporal bone. A total of eight samples were exported to Zürich (Table 3.4).

Table 3.4. List of Kwieka Individuals, including archaeological context and samples collected.

Ind No.	Site	Burial Type (Abdallah 2018)	Samples	Sample Details
Tomb 1	KWC	Type B - small mound, rectangular pit, oval rock-cut burial chamber	2 teeth	RPM ₁ , M2

Tomb 2	KWC	Type F - rounded rock superstructure, rectangular pit, oval burial chamber	2 bone, 1 tooth	L & R Petrous, Molar
Tomb 5	KWC	Type C - circular superstructure, trapezoid descendary, oval burial chamber	1 bone	L Petrous
Tomb 6	KWC	Type D - rounded super structure, rectangular shaft, rectangular burial chamber	2 bone	L & R Petrous

R or L = Right or Left

PM = Premolar

M = Molar

(subscript) = Mandibular

No sub- or superscript = Unknown assignment

Numbers reference which molar (i.e. 1 = first, etc.)

Enepis Cemetery - Tinga Archaeological Rescue Project (TARP)

The Tinga Archaeological Rescue Project (named for the modern canal in the vicinity) began in July 2017 by NCAM officials as a salvage project to excavate 34 graves (containing 32 individuals) discovered during the expansion of modern agriculture projects. The TARP cemetery site is located in the Berber region, south of the modern town of Enepis and on the east side of the Nile River (Figure 3.1). The site has a large cemetery of grouped tumuli. Tombs were dug into the alluvium layer, sometimes down to the bedrock layer, with 6 types of superstructures: 1) circular mound of large pebbles with stone slab substructure, 2) rectangular grave with EW orientation with variable shapes, 3) oval-shaped grave with EW orientation with variable skeleton positioning, 4) rounded grave pit with a diameter of nearly one meter, 5) cylindrical (long and rounded) with EW orientation, 6) Meroitic shape extending EW with burial niche to the west (Bushara et al 2017). Various body positions and orientations were observed: flexed, contracted, crouched, extended – which are possibly indicative of various cultural occupations at this site. Grave goods were discovered, with preservation of ochre, metal goods, and leather items in some cases. Overall good preservation of the skeletal remains allowed for preliminary analyses of demographics, paleopathology, and stature. Twenty-six samples from ten individuals were sampled from those excavated in 2017 for genetic analysis, including two from a double burial. Samples include temporal bones and/or single rooted permanent or deciduous teeth (Table 3.5). Of those individuals collected, only G18 was dated to the Medieval period.

Table 3.5. List of TARP Individuals, including demographic data, archaeological context, and samples collected.

Grave No.	Ind. No.	Season	Age Estimation ^α	Sex ^β	Grave Type & Body Position	Samples	Sample Details
G06	T6 D3	2017	Young Adult	F	Rectangular, flexed	1 bone, 2 teeth	L Petrous, RC ¹ , RI ²
G07	C3	2017	Mature Adult	M	Circular, crouched	2 bone, 2 teeth	L & R Petrous, 2 PM
G09	C4	2017	Child	SA	Rectangular, flexed	1 bone	R Petrous

G17	-	2017	Mature Adult	F	Rectangular, flexed	2 teeth	LC ₁ , RC ₁
G18	D4	2017	Infant	SA	Oval, extended	1 tooth	LC ₁ , RC ₁
G21	-	2017	Adolescent	F	Oval, crouched	2 bone, 1 tooth	L & R Petrous, RC ¹
G22	T3	2017	Child	SA	Circular, crouched	2 bone	L & R Petrous
G23	E3	2017	Child	SA	Circular, contracted	2 bone, 1 tooth	L & R Petrous, I ₂
G27	T4	2017	Mature Adult	F	Oval, extended	3 teeth	RI ¹ , RI ² , RC ₁
G28	T5	2017	Child	SA	Circular, crouched	2 bone, 2 teeth	L & R Petrous, deciduous teeth

^α Buikstra & Ubelaker 1994, Lovejoy, et al. 1985, Brooks & Suchey 1990, Walker, et al. 1991

^β Buikstra & Ubelaker 1994

F = Female or probable female

M = Male or probable male

SA = Subadult, no sex estimation

Samples: R or L = Right or Left, I = Incisor, C = Canine, PM = Premolar, M = Molar, (superscript) = Maxillary (upper), (subscript) = Mandibular (lower), numbers reference which tooth in series (i.e. 1 = first, etc.)

Berber Meroitic Cemetery

In 2009, a cemetery was discovered on the East bank of the Nile south of the 5th Cataract while construction crews were digging foundations for the construction of a factory (Figure 3.1). A rescue project was launched by NCAM to excavate burial structures, human remains, and associated funerary objects at this archaeological site - The Berber Meroitic Cemetery (BMC). Contextual finds date this cemetery to the Meroitic Kingdom (350 BC – 350 CE) and the necropolis contained more than 57 individuals of good preservation, despite the disturbance from foundation trenches and ancient or modern looting (Figure 3.4). Burials yielded large caches of wooden objects, decorated ceramics, and finer items associated with the skeletons as evidence of good preservation. The burial formations include those typical of a Meroitic tradition common in central Sudan (i.e. slope to burial niche, blocking wall) and likely represent an elite community, especially with the fine grave goods (Bashir 2010, 2013). Variation in burial practices, representative ceramics, and selective c14 dating of organic material have constructed a finer chronology of the burials on site (Figure 3.4) (Bashir & David 2015).

Skeletal remains from the six seasons of excavation at BMC are currently housed at NCAM in Khartoum. After assessing individuals with good preservation, samples from twelve individuals were selected for ancient DNA analysis. Samples from these remains were catalogued, photographed, and packaged for exportation in 2018 and transported to Zürich for processing. For each individual, at least one sample was collected (mostly two per individual), including teeth and the petrous portion of the temporal bone. At least one individual was selected from each occupation phase of the site (Bashir & David 2015), totaling 22 samples from twelve individuals. The table below summarizes these samples, including tissue type and

excavation data of the graves and is also color-coded to match the internal chronology of the publication (Table 3.6, Figure 3.4) (Bashir & David 2015, Bashir 2010).

Figure 3.4. Topographical Map of Berber Meroitic Cemetery with dating (Bashir & David 2015).

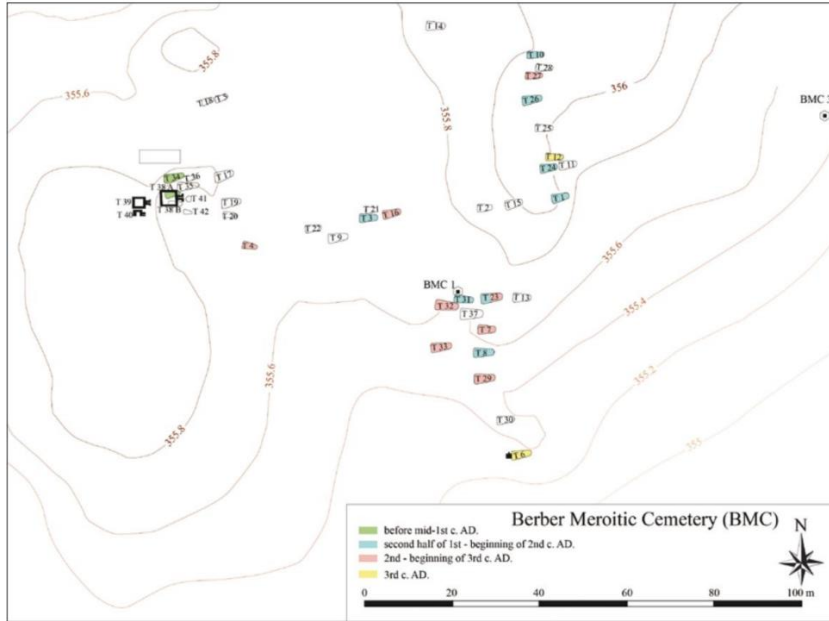


Table 3.6. List of BMC individuals, including archaeological context, contextual dating, and samples collected.

Tomb No.	Ind. No.	Season	Demographic &/or Archaeological Notes	Sample Type	Sample Details
T34	-	2012	Extended, wooden bed	2 teeth	LC ₁ , LPM (Lower)
T26	SK1	2012	Semi flexed; double burial	1 bone, 1 tooth	R Petrous, LPM (Lower)
T3	SKA	2009	Double burial; fine grave goods	1 bone, 1 tooth	R Petrous, PM
T3	SKB A-45	2009	Double burial	2 bone	L & R Petrous
T33A	-	2012	Flexed; fine grave goods	1 bone	L & R Petrous
T16	SKB	2012	Double burial, semi-flexed, male and female adults	1 bone	L & R Petrous
T32	-	2012	Multiple burials (adult, two children)	1 bone	L & R Petrous
T6	63-6(A)	2009	Meroitic script on finds	3 teeth	RPM ₁ , lower Incisor, RC ₁
T57	-	2016	Bone lesions	1 bone, 2 teeth	R Petrous, PM ² (L?), C ¹ (R?)
T53	SKB	2016	Double burial	2 teeth	2 x C
T53	SKA	2016	Double burial	3 teeth	LI ² , LC ¹ , RPM ₁
T49	SKB	2016	(none)	2 teeth	RC ¹ , LC ₁

Green – before mid-1st century CE

Blue – second half of 1st – beginning of 2nd century CE

Red – 2nd – beginning of 3rd century CE

Yellow – 3rd century CE

Grey – no date available, recent excavation

SK - skeleton

Samples: R or L = Right or Left, I = Incisor, C = Canine, PM = Premolar, M = Molar, (superscript) = Maxillary (upper), (subscript) = Mandibular (lower), numbers reference which tooth in series (i.e. 1 = first, etc.), (?) = questionable assignment

El-Zuma

Excavations of the Early Makuria Research Project at El-Zuma are directed by Dr. Mahmoud El-Tayeb of the Polish Centre of Mediterranean Archaeology (PCMA) (University of Warsaw). Explorations of this site began in 2005 and excavation seasons take place every year (El-Tayeb 2007). El-Zuma is located in the northern province between the 3rd and 4th Cataract on the right side of the bank (Figure 3.1). Finds date the site to the second phase of the Makuria period (mid-4th to mid-6th century CE). More than 30 tumuli (some up to 50m in diameter and 10m in height) are the subject of intense research and varying burial practices suggest different social status of those interred, all from the Meroitic period. The tumuli have been classified into three types by the archaeologists: Type 1 – large superstructure made of sand and stone with rock cut tunnel and burial chambers with additional rooms, presence of pillars; Type 2 – flat top superstructure, smaller in diameter than Type 1, shaft that leads to a main burial chamber with additional rooms but no tunnels, presence of pillars, closed off with stones or bricks, dating to Meroitic period; Type 3 – have the smallest superstructures with a stone ring around the base, one rock-cut shaft with a bench and one burial chamber located on the West, indicating Meroitic traditions (El-Tayeb & Czyżewska 2011, El-Tayeb, et al. 2016a). Most of these burials were looted in antiquity, suggesting the large amount of wealth buried with these individuals.

After remains were assessed for preservation, i.e. some were glued or bone tissue was excessively moldy or chalky, 16 individuals were selected for sampling. For each individual, at least one sample was collected (mostly two per individual), including intact teeth with no glue or cracks, and temporal bones with complete petrous portions or areas which were able to still be sampled, totaling 26 samples (Table 3.7). Summary table constructed from El-Tayeb, et al. (2014) and personal communication with anthropologist Robert Mahler (PCMA).

Table 3.7. List of El-Zuma individuals, including demographic data, archaeological context, and samples collected.

Ind. No.	Age-at-death (in years)	Sex	Burial Type	Sample Type	Sample Details
T.8	35-45	F	I	1 bone	R Petrous
T.10	30-40	M	III	2 bone	L & R Petrous
T.11	16-18	SA	II	2 bone	L & R Petrous
T.14	20-30	F	II	1 bone	R Petrous
T.15	21-24	F	II	1 bone, 2 teeth	L Petrous, LPM ² , LC ₁

T.16	16-24	M	II	1 bone	R Petrous
T.17	30-40	M	III	1 bone	L Petrous
T.18	50+	F	III	2 bone	L & R Petrous
T.19	35-45	M	III	1 bone	R Petrous
T.20	50+	M	III	2 bone	L & R Petrous
T.22	35-45	M	III	1 bone	L Petrous
T.24	15-18	F	II	1 bone	R Petrous
T.25	24-35	F	II	2 bones, 2 teeth	L & R Petrous, RPM ¹ , RPM ²
T.26	45-55+	F	II	1 bone	L Petrous
T.27	35-45	M	III	1 tooth	LPM ² , RPM ²
T.28	40-55	F	III	1 bone	R Petrous

+ = more than

F = Female or probable female

M = Male or probable male

SA = Subadult, no sex estimation

Samples: R or L = Right or Left, I = Incisor, C = Canine, PM = Premolar, M = Molar, (superscript) = Maxillary (upper), (subscript) = Mandibular (lower), numbers reference which tooth in series (i.e. 1 = first, etc.), (?) = questionable assignment

El-Detti

The archaeological site of El-Detti is located on the right bank of the Nile River between the 3rd and 4th cataracts (Figure 3.1). Excavation work has been on-going since 2014 and is most notable for over 50 tumuli for comparison with other burial architecture in the region – namely Tanqasi and El-Zuma (El-Tayeb, et al. 2016b). Tumuli from this site are categorized as type II (multi-chambered) and type III (single-chambered), much like those found in El-Zuma. Skeletal remains from the tumuli have been recovered by the Early Makuria Research Project. This site is dated to the Meroitic Period, specifically Early Vistur period, phase II or mid-4th to the end of 6th century CE (El-Tayeb, et al. 2016b). The remains from four individuals were selected for sampling for ancient DNA analysis. For each, at least one sample was collected (up to four for one individual), including teeth and/or the petrous portions of the temporal bone. A total of 10 samples were brought to Zürich for aDNA extraction. Samples for these four individuals are summarized in Table 3.8, including demographics (personal communication, Magda Srienc).

Table 3.8. List of el-Detti individual, including demographic data and samples collected.

Ind. No.	Age-at-death (in years)	Sex	Sample Type	Sample Details
T.2	45-55	M	2 bone, 2 teeth	L & R Petrous, LPM ² , LI ¹
T.4	45-55	M	1 bone, 2 teeth	L Petrous, RI ₁ , LPM ₂
T.5	40-50	M	1 bone	R Petrous
T.7	40-50	M	2 bone	L & R Petrous

M = Male or probable male

Samples: R or L = Right or Left, I = Incisor, PM = Premolar, M = Molar, (superscript) = Maxillary (upper), (subscript) = Mandibular (lower), numbers reference which tooth in series (i.e. 1 = first, etc.), (?) = questionable assignment

Tanqasi

The Tanqasi archaeological site is located in the vicinity of El-Zuma and El-Detti, near the 4th Cataract (Figure 3.1). This site has been part of the Early Makuria Research Project since 2005, directed by the PCMA. Skeletal remains have been recovered from inside tumuli and likely represent a cultural group from the Post-Meroitic time period. Due to preservation issues, only four individuals were selected for sampling. For each, at least one sample was collected (up to five per individual), including teeth and the petrous portion of the temporal bone. A total of nine samples were brought to Zürich, as summarized in Table 3.9, including demographics (personal communication, Magda Srienc).

Table 3.9. List of Tanqasi individuals, including demographic data and samples collected.

Ind. No.	Age-at-death (in years)	Sex	Sample Type	Sample
T.16	30-35	F	bone	R Petrous
T.23	25-35	M	2 bone, 3 teeth	L & R Petrous, LI ₁ , RPM ₁ , LC ₁
T.46	35-45	M	tooth	LPM ₁
T.179	45-55	F	tooth	RI ¹ , RPM ²

F = Female or probable female

M = Male or probable male

Samples: R or L = Right or Left, I = Incisor, PM = Premolar, M = Molar, (superscript) = Maxillary (upper), (subscript) = Mandibular (lower), numbers reference which tooth in series (i.e. 1 = first, etc.), (?) = questionable assignment

METHODS

Clean Lab facilities

All DNA extractions were performed at the Ancient DNA Laboratory at the Institute for Evolutionary Medicine (IEM) at the University of Zürich, Switzerland (Figure 3.5). This facility is dedicated solely to aDNA research and has four self-contained rooms with independent HEPA air filtration systems where researchers adhere to strict contamination control protocols including uni-directional workflows, regular decontamination of work surfaces with UV irradiation, DNase treatment, and/or bleach solution. The ancient lab is located in a separate building from the modern genomics labs to avoid cross-contamination of stable PCR products. All researchers wear full Tyvek suits, filtered masks, goggles, shoe covers, sleeve covers, hair nets, and double disposable gloves during lab work. All reagents, solutions, tools, and consumables were decontaminated before use with UV radiation (i.e. at least 30 minutes in UV crosslinker) or DNase treatment, whenever possible. Additionally, all tools, surfaces, hoods, and some elements of PPE (i.e. gloves and sleeves) are bleached, UV-sterilized, treated with

DNase, and/or changed between individuals to prevent cross contamination (Appendix A). The lab is equipped with separate air-filtered laminar fume hoods for dedicated sample extraction and PCR preparation. For these experiments, no positive controls were used, as these could be a possible source of contamination. Instead, negative controls were processed in parallel with all samples, continuously monitored for contamination, and carried through final sequencing steps.

Figure 3.5. Laboratory facilities used for ancient DNA work at the University of Zürich.



Left) View from entry room to Ancient Laboratory at the Institute of Evolutionary Medicine, University of Zürich, Zürich, Switzerland. Right) Bone cellar accessible to IEM members; bone and tooth samples not stored in the clean room are stored here, which is in the same building as the clean lab, but not modern PCR labs on campus to prevent contamination of stable PCR products.

General sample preparation and clean lab protocols

Sampling materials from the archaeological collections were intact rooted teeth or temporal bones – the petrous is known to contain more authentic DNA, even in hot climates - or both, as specified in previous Materials section (Gamba, et al. 2014, Pinhasi, et al. 2015, Gallego Llorente, et al. 2015). Prior to processing tissue samples, some samples were cleaned in a non-PCR wet lab at the IEM to remove external sand and dirt. Digital photographs were taken of teeth or temporal bones before processing. All data required for sex or age estimations or notable/pathological characteristics were recorded and photographed (e.g. dental eruption patterns, the mastoid process, dental disease, presence of bone lesions). In the clean lab, tooth and bone samples were UV-decontaminated for at least 10 minutes on each side before

processing with additional treatments. However, for tooth specimens with dental calculus build-up, this calculus was sampled prior to this step (see below for steps followed) (Figure 3.6).

Figure 3.6. Examples of teeth with dental calculus build up requiring sampling.



A) Tanqasi T.179, right second maxillary premolar. B) Berber Meroitic Cemetery T6 63-6a, right first mandibular premolar. C) Ghazali-3-002, right first maxillary molar.

Processing of teeth samples for Ancient DNA Extraction

Tooth calculus sampling technique follows Warinner “Dental Calculus, Sampling Protocol v.4, 2016” (personal communication). Working in the sampling laminar hood, calculus build up was removed/scraped off from outer enamel or dentine surfaces with a sterile dental scaler, collected, and weighed in a UV-treated tube. Samples were stored in the clean lab at 4°C and protected from decontamination UV light, i.e. in carton sample boxes or covered with aluminum foil. Sterile calculus samples were taken whenever possible for proteomic or additional genetic analyses in the future (Figure 3.6A-C).

Sterile samples of dentine tissue were processed via drilling with a dental drill (Nakanishi (Hoffman Estates, IL) Emax EVolution electric micro grinder (Model No. EV410-120, Cat No. 8233)) as per standard lab protocols outlined in Damgaard, et al. (2015) or crushed with a stainless-steel mortar and pestle as per Gondek, et al. (2018). Each sample was assessed for the most optimal method for dentine tissue extraction – including friability, taphonomic damage, rooted or unrooted tooth, and size of root or crown. Generally, samples that showed signs of weathering or were quite friable or chalky were known from experience to be difficult to drill or obtain a sterile sample. Such samples were chosen for crushing after extensive UV treatment, ablation of outer surfaces along dentine tissue, including the cementum when necessary, and mechanical removal of enamel, as per personal communication with researchers who developed techniques using the steel mortar and pestle (Gondek, et al. 2018). Removal of these layers is important to increase the endogenous content of the samples. This method has proved beneficial for teeth that were especially friable, would not withstand drilling, or were broken during handling within the clean lab. With this method, sterile tissue was isolated and crushed, where drilling would have been impossible. Tissue samples of at least 200 mg were extracted

for processing; unused powder was stored at 4°C. For subadults with small roots, dentine powder was pooled from multiple teeth to reach 100mg. Unused enamel was stored at room temperature in the clean lab for future analyses or returned to collaborators.

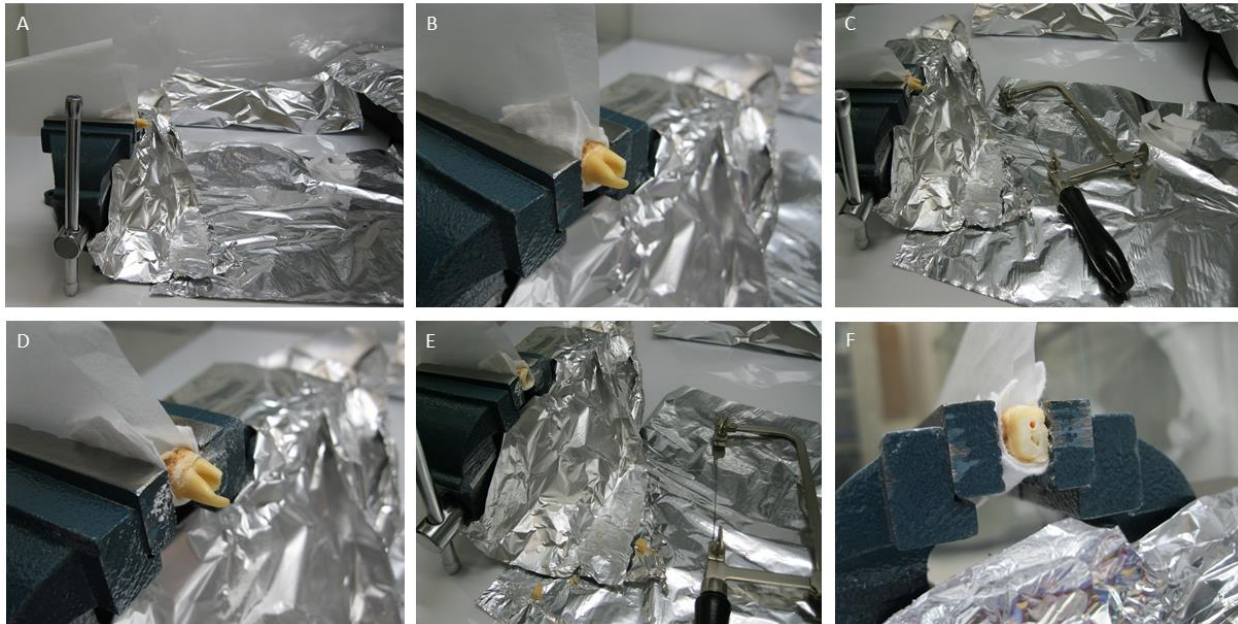
Dentine powder can be collected from within the crown using a dental drill. First, using a dental drill and a sterile spherical cutter bit drill bit, a generous layer of the outer surface was removed and discarded (Figure 3.7B). This outer layer typically consisted of remaining calculus, residual dirt, and degraded cementum. Following this cleaning step, the root tissue then looked polished (Figure 3.7C). Dust was wiped away using a damp lab tissue and the sample was UV treated for 10 min per side. Next, the vise and jaws were lined with wax paper and the tooth was firmly loaded into the vise (crown clasped horizontally within the jaws, roots pointing to the side) within the sample hood (Figure 3.8A, B). The roots were removed from the crown with a coping saw equipped with a sterilized fine-tooth blade (Figure 3.8C-E). Roots were retained for crushing, as detailed below. For each tooth, crown dentine was drilled with a new spherical cutter drill bit and collected into a tube using a sterilized glass funnel (6cm diameter) placed below the crown (Figure 3.8F). Powder was weighed and stored at 4°C until extraction.

Figure 3.7. Processing of tooth samples in clean lab.



Cleaning of external surface, before drilling of crown dentine or crushing root dentine, to decrease contamination during extraction step. Ghazali individual 4, GHZ-3-009, right first maxillary molar. A) Tooth sample before calculus sampling or cleaning in the clean lab. B) Removal of outer layer using electric dental drill with a spherical cutter drill bit. C) Tooth sample after cleaning showing a polished surface, inferior to the cementum-enamel junction (CEJ).

Figure 3.8. Set up for processing teeth within sampling hood in clean lab.



A) Cleaned tooth is loaded into a vise. B) Roots are positioned as such to leave crown in the vise to later drill the dentine from beneath the enamel; sterile padding is used to keep the crown from cracking. C) Roots are cut from the crown using a coping saw with new blade per sample. D) Cut is using made just inferior to the cementum-enamel junction (CEJ). E) Root dentine is collected for crushing later; crown is left in the vise for drilling. F) Crown dentine ready for drilling.

Following collection of crown dentine, the roots were wiped of dust then UV treated again for 10 minutes per side before crushing in the stainless-steel mortar and pestle as per Gondek, et al. (2018). Dentine tissue was loaded in the mortar with sleeve and crushed using the pestle and a rubber mallet (Figure 3.9A). Several rounds of crushing (Figure 3.9B-E) were necessary depending on how mineralized the tissue was and degree of preservation. Between rounds, a sterilized spatula was used to move larger chunks around or scape powder back into the well of the mortar. Powder should be a consistency finer than cornmeal (Figure 3.9E). Powder was collected into a tube, weighed, and stored at 4°C until extraction.

Figure 3.9. Crushing of root dentine using steel mortar and pestle.



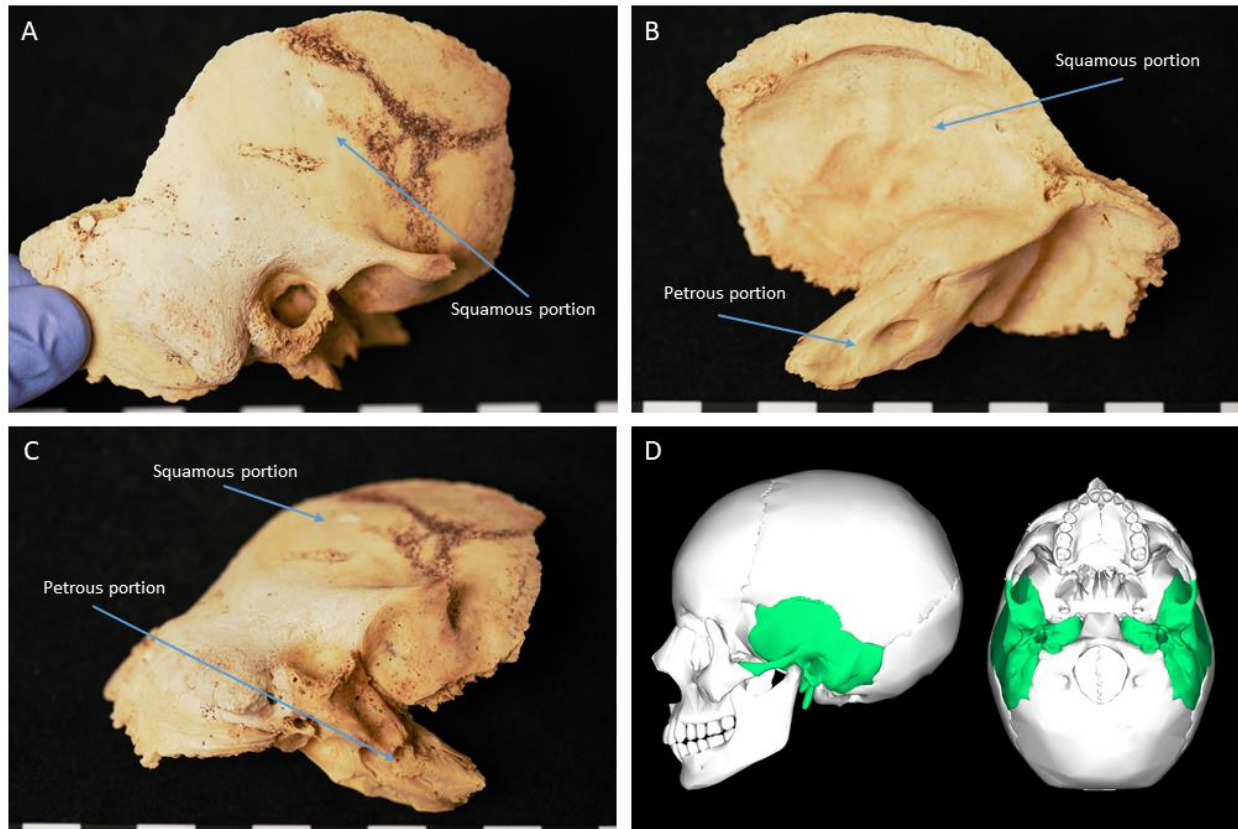
A) Set up of stainless-steel mortar and pestle with sleeve (inside dish to contain loose powder). B) Root dentine after first round of crushing using mallet. C) Root dentine after second round of crushing. D) Root dentine after third round of crushing. E) Root dentine after fourth round of crushing. F) Weighing of final amount of powder produced.

Processing temporal bone samples for Ancient DNA Extraction

Samples of petrosal bone tissue were obtained by opening the pyramidal/petrous portion of the temporal bone to access sterile tissue for drilling with an electric dental drill (Nakanishi (Hoffman Estates, IL) Emax EVOLution electric micro grinder (Model No. EV410-120, Cat No. 8233)) as per published protocols (Gamba, et al. 2014, Pinhasi, et al. 2015) or the petrous portion was removed, cleaned, and crushed with a stainless-steel mortar and pestle as per Gondek, et al. (2018) (Figure 3.10A-D). Samples were individually assessed for the most optimal method for bone tissue processing – including degree of friability, taphonomic damage, and size or morphology of petrous portion – to isolate the inner ear canals and surrounding dense bone tissue for sterile sampling (Figure 3.11). Generally, samples with heavy weathering or those that were friable or chalky were known from experience to be difficult to drill (i.e. tissue does not stand up well to the mechanical force) to obtain a sterile sample (Hansen, et al. 2017). Such samples were chosen for crushing after extensive UV treatment, manual ablation of outer surfaces, and mechanical removal of less dense tissue surrounding the densest portion of the pyramidal part. In general, outer tissue is heavily contaminated by environmental and modern DNA. Removal of these layers is important to increase the endogenous content of the samples. This method has proved beneficial for petrous bones with weathering (Gondek, et al. 2018). Samples that were selected for drilling were processed according to published protocols

(Gamba, et al. 2014, Pinhasi, et al. 2015, Hansen, et al. 2017, Gallego Llorente, et al. 2015). Tissue samples of at least 200 mg were extracted for processing; powder is stored at 4°C until extraction step.

Figure 3.10. Anatomical parts of temporal bone.

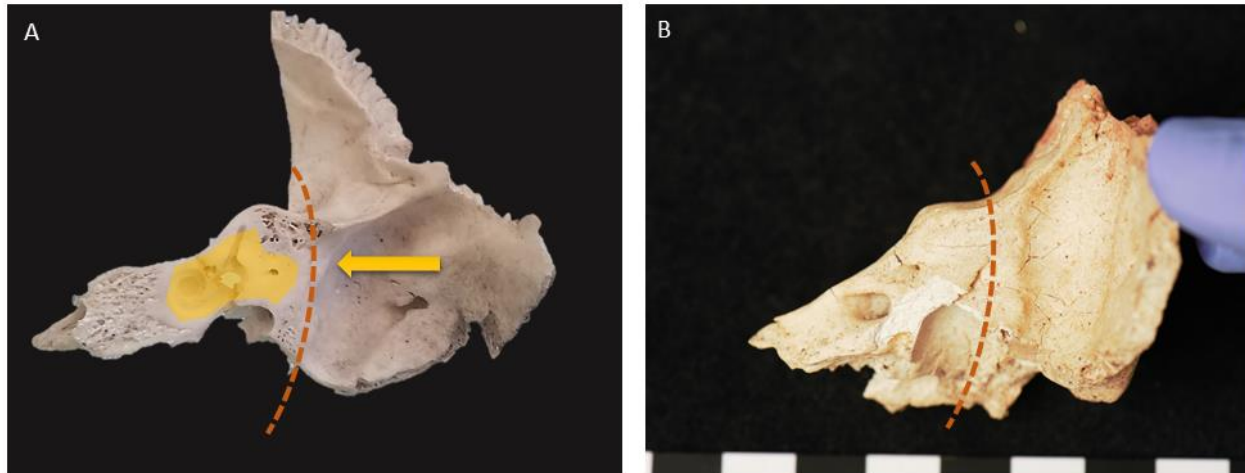


Example of temporal bone from current archaeological collection, right temporal bone of TARP 2017 G9. A) External view of temporal bone, showing external auditory meatus, zygomatic process, mastoid process, and squamous portion. B) Internal view of temporal bone, showing squamous and petrous or pyramidal portion. C) Inferior view of same bone. D) Anatomical location of temporal bone (in green), showing lateral view and superior view of skull.

The procedure to drill petrous portions of temporal bone was adapted from various published protocols utilizing especially degraded samples (i.e. hot, dry) and the researcher's experience with skeletal remains (Pinhasi, et al. 2015, Gamba, et al. 2014, Hansen, et al. 2017, Gallego Llorente, et al. 2015). Following cleaning steps and UV decontamination, a diamond dust-encrusted circular blade attached to a dental drill was used to remove the petrous portion of the temporal bone from the squamous portion to expose the inner ear labyrinth (Figure 3.10A-C, Figure 3.11A-C). Another layer from the freshly cut surface and surrounding area was then removed with a new spherical cutter bit. The sample was wiped with a lab tissue and UV irradiated for 10 minutes per side. Using a new spherical cutter bit, the dense bone of the cochlea and surrounding tissue was drilled and collected using a 6cm funnel inside a 2mL tube.

Care was taken to not overheat the tissue by using short scraping movements with the drill bit and using the lowest speed possible with the dental drill. Powder was weighed and stored at 4°C until extraction. Remaining portions of the petrous were wrapped in sterile aluminum foil and stored in the clean lab for additional sampling, when necessary.

Figure 3.11. Visual of how the petrous portion of temporal bone is sectioned for processing.



A) Coronal (anterior/posterior) cross section of petrous portion to reveal cochlea and dense bone surrounding the labyrinth; orange dotted line shows where a cut is made to separate the petrous portion from the squamous portion; shaded area (yellow) is targeted for drilling to collect the most sterile sample for extraction; yellow arrow shows the orientation of the drill bit during drilling. Specimen from Anatomy Collection, University of Zürich, Zürich, Switzerland. B) Example of right petrous portion TARP 2017 G28 T5; orange dotted line shows approximately where the cut is made, lateral to the flat ridge, to expose the target area for drilling.

To prepare a temporal sample for crushing, the petrous portion was removed from the squamous portion of the temporal bone as specified above (Figure 3.11). Next, the petrous portion was manually trimmed (including trabecular and/or cortical bone) to be small enough to fit into the steel sleeve (Figure 3.12A). Using an electric dental drill with a sterile spherical or conical cutter drill bit (New Technology Instruments, Kahla, DE), the outer surface of the sample was removed and discarded. Bone dust was wiped away with damp lab tissue (KimWipe with purified Milli-Q Water). The sample was UV treated again for 10 min each side before being crushed. As per Gondek, et al. (2018) and personal communications, samples were loaded into the mortar with the sleeve in place and crushed lightly with one or two blows with a mallet and pestle to separate the less dense tissue from denser portions being targeted. Less dense bone was flakey, darker in color, while denser pieces were irregular and chunky after crushing (Figure 3.12B). These dense chunks were manually separated with sterile tweezers for another round of crushing, while the less dense pieces were removed from the mortar (and stored/labeled separately.) Shattered bone was swept away first using a dry lab tissue, taking care to especially remove powder from the mortar, pestle, and sleeve. The dense pieces were reloaded

into the mortar with sleeve for mallet crushing. Between uses of the mallet, a sterile metal spatula was occasionally used to move around uncrushed or overly crushed parts within the mortar. The goal was to create an evenly mixed powder with both small and large chunks of tissue, rather than perfectly homogenous (Figure 3.12C). Sample powder was collected by placing a 50mL Falcon tube over the mortar well and carefully flipping the powder into the tube. Lastly, powder was weighed and stored in the clean room until extraction.

Figure 3.12. Preparation of bone samples from petrous portion using stainless steel mortar and pestle with sleeve.

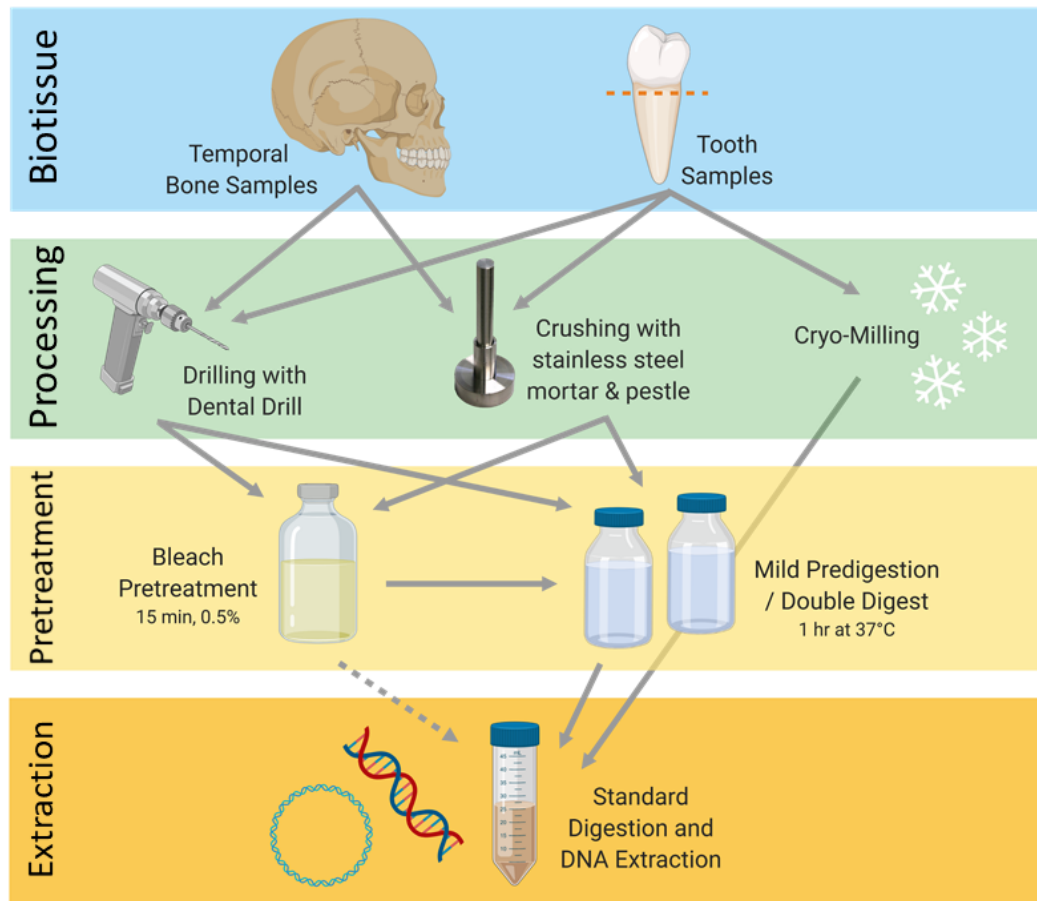


A) Set up with sleeve loaded in the mortar (left), pestle at the side. B) Petrous portion after first few strikes to separate less dense bone from more dense bone of the inner ear channels and surrounding tissue. C) Final result is a fine powder, which will be weighed and divided into 100mg or 200mg aliquots for DNA extraction.

Extraction of ancient DNA from prepared dentine or bone powder

To release DNA from the powder generated during the processing steps, bone or dentine samples were subjected to three different extraction methods to optimize and boost endogenous DNA content: 1) single digest method, as per Schuenemann and Peltzer, et al. (2017) with modification from Dabney et al. (2013), 2) double digest method, as per Damgaard, et al. (2015) and “Orlando Lab June 2015 protocol, with Viking lab modifications,” (used in Ancient DNA Lab in Blindern, Oslo) and 3) double digest with bleach pretreatment, as per Kemp & Smith (2005) and Bossenkool, et al. (2017) (Figure 3.13). Additionally, the amount of powder used for these extraction methods varies between 50mg and 200mg. Cryo-milling, where whole chunks of teeth or bone are powdered while being chilled by liquid nitrogen (Figure 3.13). This technique is no longer used because other methods (i.e. drilling) are more sterile.

Figure 3.13. Flowchart for all trialed extraction methodologies.



Methodologies are depicted in this flowchart; a total of ten different methods were trialed. Solid grey lines show methods piloted; dotted lines have not been trialed. For more details, see Chapter 3. (Image created with BioRender.com by author)

For the single digest method, for each individual, approximately 50-100mg of powder (dentine or bone tissue) was digested with a lysis solution of 0.45M EDTA and 0.25mg/mL proteinase K overnight with rotation at 37°C (Figure 3.13). Following centrifugation, DNA was isolated from the supernatant using binding buffer and a QIAGEN (Hilden, Germany) silica column with centrifugation (as per Gamba, et al. 2015 or Dabney & Meyer 2019), followed by purification steps with in-house modifications (binding centrifugation speed 1500 rpm, washing 14,000 rpm, and eluted in 50uL of TET buffer twice). Final volume for DNA was 100uL in TET for library preparation.

For the double digest method (Figure 3.13), also referred to as mild digestion pretreatment, approximately 200mg of powder (dentine or bone tissue) for each individual was digested in duplicate (pooled later) with a lysis solution of 0.45M EDTA, 0.25mg/mL proteinase K, and 0.5% N-lauryl-Sarcosyl for 1 hour at 37°C with nutation. Following centrifugation, the first digest supernatant was removed, stored in a labeled tube, and pellet was resuspended in fresh

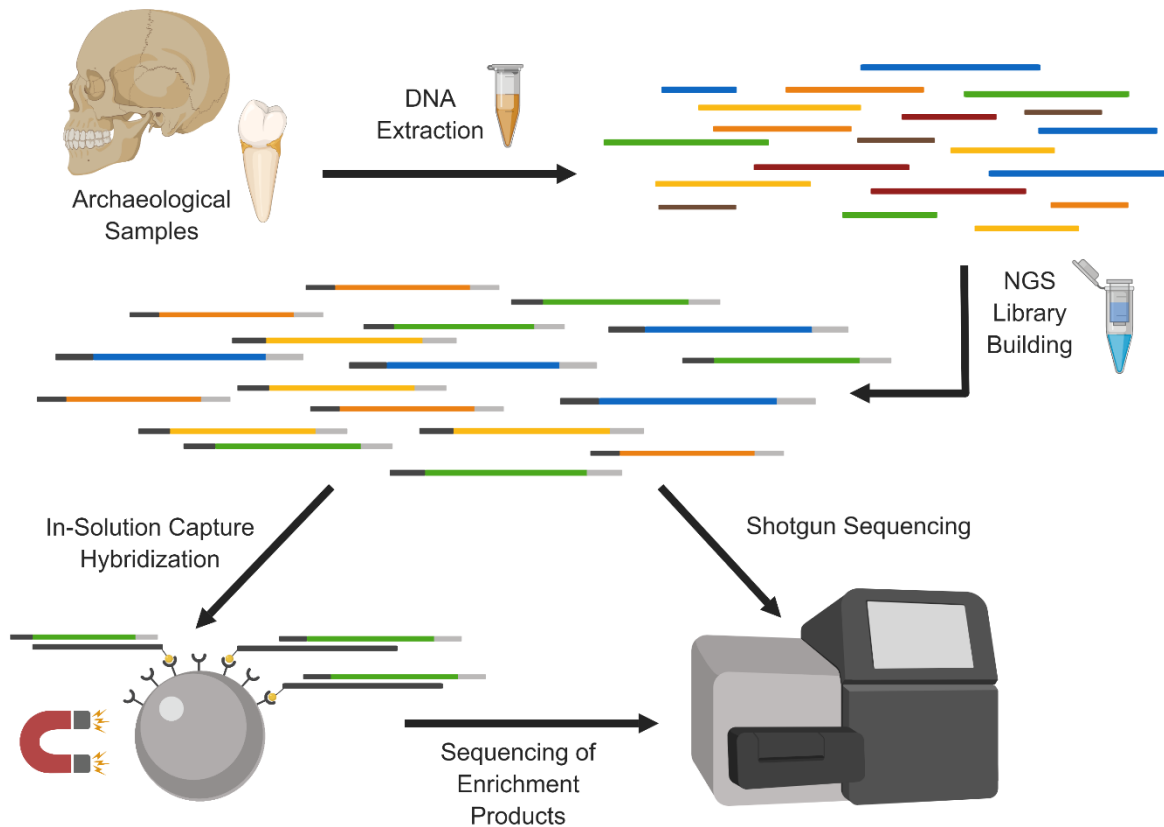
lysis solution for overnight incubation at 37°C with nutation. Following centrifugation, DNA was isolated from supernatant using a binding buffer and a QIAGEN silica column with a Manifold vacuum system, followed by purification steps using MinElute PCR Purification reagents and protocols (QIAGEN, Hilden, Germany). DNA was eluted in 65uL of elution buffer for library preparation.

Some samples were selected for bleach pretreatment, namely those with visible mold and heavy weathering. For these samples, approximately 200mg of powder (dentine or bone tissue) was incubated with 0.5% bleach solution for up to 15min at RT with nutation (Figure 3.13). Following centrifugation, the pellet was washed three times with purified Milli-Q water. Then, the protocol proceeds with a double digestion, as outlined in the section above.

Library Preparation

From this step forward, all samples were treated the same. In the clean lab, double-stranded Illumina libraries were prepared with 20uL of sample extract (or extraction blanks) as outlined in Meyer and Kircher (2010) (Figure 3.14). Briefly, libraries of sample DNA were blunt-end repaired, adaptors ligated to the fragments, and gaps filled in with silica-column purifications (QIAGEN) between each step to remove interfering molecules (i.e. hairpin fragments with identical adaptors or dimers) (Meyer & Kircher, 2010). Before indexing, the quantity of molecules was measured by qPCR on a LightCycler (Roche Life Science, Basel, Switzerland) for quality control and to monitor the process. Next, libraries were dual indexed (i.e. indexing or 'barcoding' both adaptors) as described in Kircher, et al. (2012) to decrease the chances of downstream misidentification. The quantity was measured again via qPCR and libraries were reamplified with Herculase II Fusion Polymerase (Agilent, Santa Clara, CA, USA) according to the qPCR measurement to reach a copy number of 10^{13} ; concentrations and fragment length of libraries were quantified on an Agilent 2200 TapeStation (Agilent, Santa Clara, CA, USA). Libraries were then ready for shotgun sequencing for screening or a targeted enrichment step, followed by sequencing (Figure 3.14).

Figure 3.14. Library preparation of ancient DNA extractions and subsequent sequencing.



Genetic material from original extraction is depicted with various colors: green – human mitochondrial DNA, blue – human nuclear DNA, yellow – modern contaminating DNA, orange – environmental DNA. Purification steps are depicted as the tube with silica column. Library material is sequenced for shotgun sequencing or is enriched for mitochondrial DNA with in-solution capture step with magnetic beads, then sequenced. (Image created with BioRender.com by author)

Shotgun Sequencing Screening and Processing

Pooled DNA libraries were screened for human DNA through shotgun sequencing on the Illumina HiSeq 4000 platform (San Diego, CA, USA), with 2x150bp read lengths, at the Functional Genomics Center Zürich (UZH) or the Genomics Core Facilities at the Oslo University Hospital. Sequencing data were analyzed with the pipeline EAGER v1.92 (Efficient Ancient Genome Reconstruction) as it is tailored for ancient DNA obtained via NGS (Peltzer, et al. 2106). This tool uses FastQ files generated by the Illumina platform Reporter that are demultiplexed and sent as raw files for analysis. Raw reads were analyzed by EAGER to map to the human reference sequence and the mtDNA revised Cambridge Reference Sequence (rCRS; NC012920), as well as assess endogenous content, average coverage, damage, and average fragment length (Fu, et al. 2013). Data authenticity was established by examining the molecular damage patterns and characteristic fragment distribution using mapDamage2.0

(Ginolhac, et al. 2011, Jónsson, et al. 2013). Samples not demonstrating typical molecular behaviors were excluded from the following enrichment step. Those libraries with authentically ancient human reads (nuclear or mtDNA) were selected for an mtDNA capture step for enrichment of human mitochondrial DNA. For comparison among processing methodologies, libraries were also analyzed with MALT (MEGAN Alignment Tool) to categorize the contaminating sequencing DNA not mapping to the human genome (Herbig, et al. 2016).

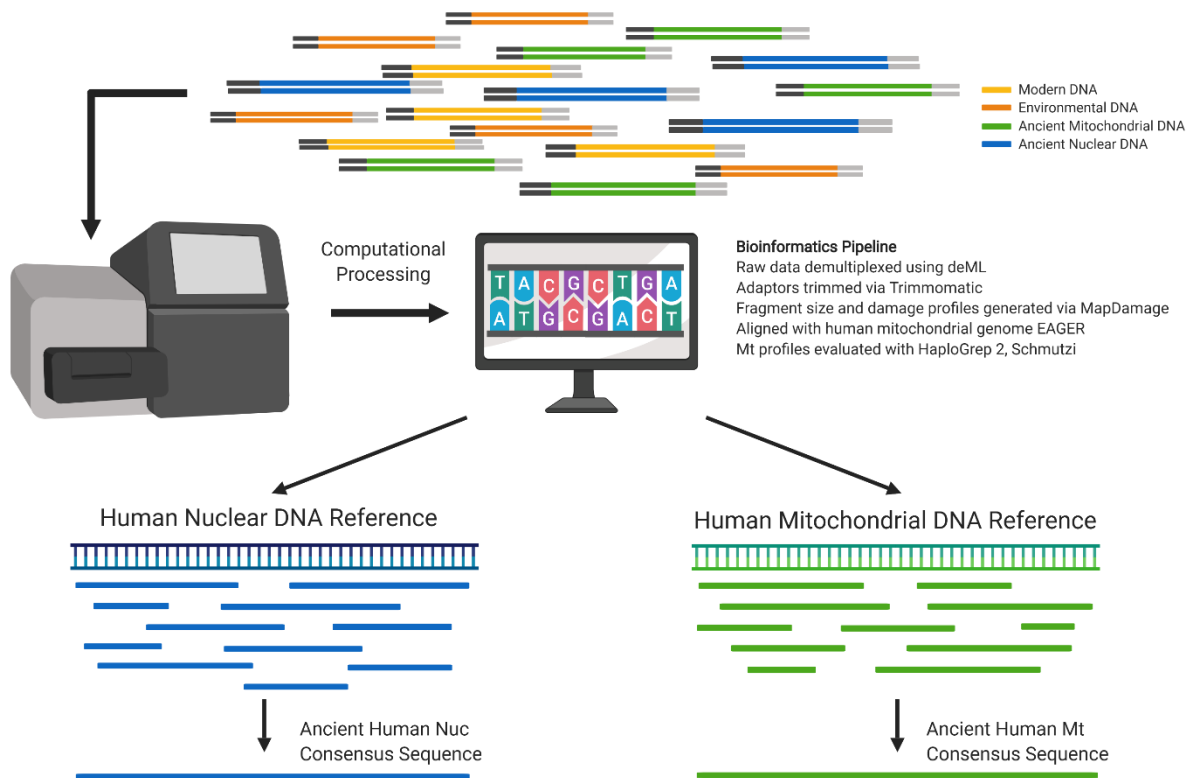
mtDNA Capture and Sequencing

Those libraries selected in the previous step were enriched for human mtDNA using bead capture hybridization as outlined in Maricic, et al. 2010 (Figure 3.14). Subsequent steps for enriched library amplification follow Schuenemann & Peltzer, et al. 2017, with sequencing performed on an Illumina MiSeq or NexSeq (Mid-output) (San Diego, CA, USA) at the Functional Genomics Center Zürich (UZH). Results relating to the enrichment step are detailed in Chapter 4.

mtDNA Processing, Alignment, and Analysis

For read processing, EAGER again was used on sequenced libraries (Peltzer, et al. 2106). As outlined in Schuenemann & Peltzer, et al. (2017), options like CircleMapper, DeDup, and other included features of the EAGER pipeline were utilized as they are optimized for NGS datasets from mitochondrial aDNA. To measure contamination from modern human mtDNA, Variant Called Files (VCF) were analyzed using the statistical program Schmutzi (Renaud, et al. 2015) with strict criteria settings to identify contamination and to estimate the percentage of endogenous DNA for each sample and its quality. Samples with more than 5% contamination were excluded from further analysis. For those under this threshold, consensus sequence files for each library were generated by this tool (Figure 3.15) and libraries were then merged if they were from the same individual (e.g. KWC_2 single digest library + KWC_2 double digest library). Samples with a mapping quality score of over 30, high coverage of the mitochondrial genome (roughly 10X or more), and low contamination were retained for haplogroup analysis. Negative controls were processed through this step and analyzed to identify DNA introduced during lab work. More detailed analysis of the results from the enrichment part of this research design are detailed in Chapter 4.

Figure 3.15. Sequencing and post-sequencing analysis.



Following amplification, libraries are demultiplexed, removing adaptors and barcodes, using various bioinformatic pipelines for the assembly of a consensus sequence for individuals (using either mitochondrial (green) or nuclear DNA (blue) (not performed)). (Image created with BioRender.com by author)

RESULTS

Results presented here are comparisons with shotgun sequencing data, not results from enrichment (see Chapter 4). Read counts refer to mapped reads to the human genome, not necessarily the human mitochondrial genome. Shotgun sequencing is a screening step performed to assess the viability of ancient genetic material and can be used for mitochondrial or autosomal screening. Mitochondrial reads are expected to be higher given the high quantity of mitochondria in each cell (few thousand mitochondrial genomes compared to one nuclear genome per cell (Giles, et al. 1980)). Three metrics were compiled to measure the effectiveness of the methodologies trialed: number of ancient mapped reads (human genome as reference), percent of endogenous content (the amount of aDNA in a sample), and library complexity measured by “cluster factor” (uniqueness of reads).

In total, 43 individuals were trialed, most with two or more extracts processed in three different ways including bleach pretreatment with double digestion, double digestion, or single digestion (Figure 3.13). Given the low endogenous content typical of Nubian samples recovered

from harsh environments, the goal of these pretreatments (i.e. bleach or double digestion or both) was to increase the endogenous content prior to extraction to obtain more ancient reads while not compromising library complexity. Seventy-five NGS libraries from 43 individuals were built using these extraction methods. Twenty-five libraries (33% success rate), from 17 unique individuals were successful in obtaining ancient human DNA, a 40% success rate.

To compare methodologies, pairs of libraries – where a single library pair consisted of two libraries constructed from different extracts from the same individual – were compared with the metrics outlined above. Twenty-seven bone or tooth powder samples were trialed in Zürich with a double digest and were compared to 27 parallel extracts using the single digestion method. These trials included samples from all eight archaeological contexts (Table 3.1). Eight libraries from the double digest method were successful in obtaining ancient reads and eight were successful for the single digest method. From these successful trials, seven library pairs for both methods were compared for analysis.

Mild bleach treatment can increase an extract's endogenous content while also removing contaminating genetic material introduced as the result of taphonomic factors (Damgaard, et al. 2015). Therefore, in addition to comparing samples processed with a double digest to the single digest, samples prepared with a mild bleach treatment followed by a double digest were compared to samples processed with only a double digest. For this analysis, four bone samples were trialed at the Ancient DNA Laboratory (Centre for Ecological and Evolutionary Synthesis) in the Department of Biosciences at the University of Oslo. Samples of different preservation were selected – two graded as good (TARP 9, KWC 6) and two graded as poor (ZUM 18, KU 210) – to test if macroscopic tissue integrity impacted our ability to obtain aDNA. Two aliquots were extracted at the same time during tissue processing; one aliquot first was treated with bleach, then both were treated with a double digest, totaling eight trials. Four extracts were successful in obtaining aDNA, while four were not. Of the successful trials, only one library pair was generated for method comparison (KWC 6). Furthermore, samples extracted at Oslo were shotgun sequenced twice, at two facilities (i.e. Oslo and Zürich), resulting in a duplicate library pair from KWC 6 for analysis. For the unsuccessful library pairs, one of the two extracts failed to produce aDNA, and were thus removed from downstream analysis.

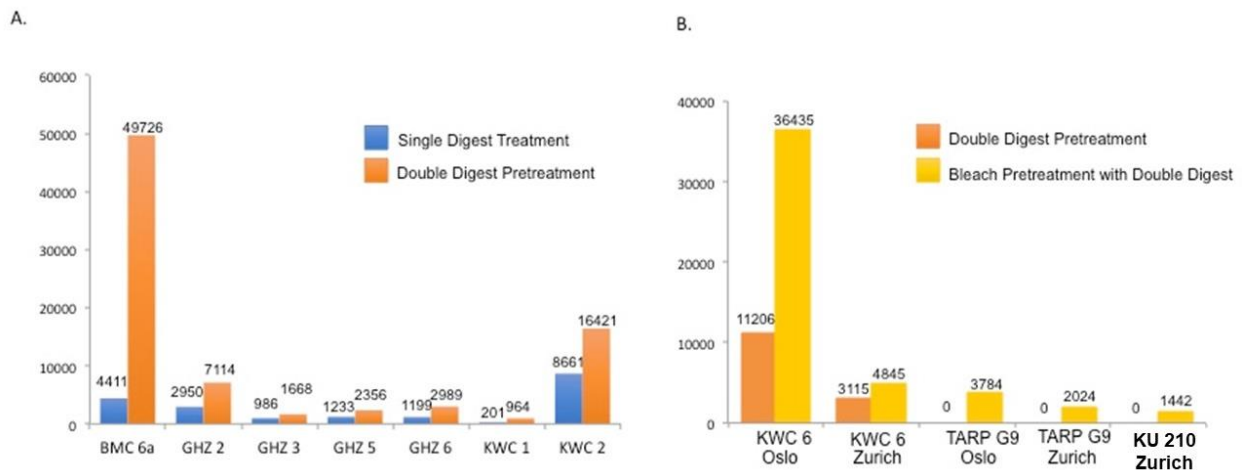
Ancient Mapped Reads

Counts of mapped ancient reads showed an increase with both pretreatments compared to the single digest method (Figure 3.16A, B). First, the double digest method increased the

number of ancient reads by 278% on average when compared to the single digest method. A paired *t*-test was performed to determine significance of the reads increase. For all trials, the double digest method increased the number of ancient reads retrieved over the single digest method, but this increase was not significant ($t = 1.3014$, $df = 12$, $p\text{-value} = 0.2176$).

For the samples extracted at Oslo, aDNA was obtained for three of the four samples: TARP 9B, KWC 6B, KU 210B (Table 3.10, Figure 3.16B). For KWC 6, we obtained aDNA for both aliquots, with and without bleach. However, the bleach treatment resulted in a 56% increase in reads. For TARP 9B and KU 210B, the double digestion method retrieved no ancient reads while the bleach pretreatment facilitated aDNA extraction. These samples had 2024 and 1442 reads mapping to the human genome, respectively. We failed to obtain aDNA from ZUM 18. For this sample, 8,181 reads were reported, however damage pattern analyses indicated the reads were not ancient. Overall, the mild bleach pretreatment increased the aDNA yield of the ‘good’ tissue samples. However, it is unclear if bleach pretreatment would aid in aDNA recovery for ‘poor’ samples as it was successful for one poor sample, but unsuccessful the other.

Figure 3.16. Mapped ancient reads listed by method.



A) Single vs. double digest comparison B) Double digest vs. bleach pretreatment. Counts of ancient mapped reads are listed above columns for each library. TARP G9 and KU 210 did not have ancient human mapped reads for the double digest method and were listed as zero without bars. Ancient mapped reads were not significantly different for either method comparison based on student's *t*-test. Oslo and Zurich below the sample IDs in (B) designate the lab where the sequencing was performed. BMC = Berber Meroitic Cemetery, GHZ = Ghazali, KWC = Kwieka Cemetery, TARP = Tinga Archaeological Rescue Project.

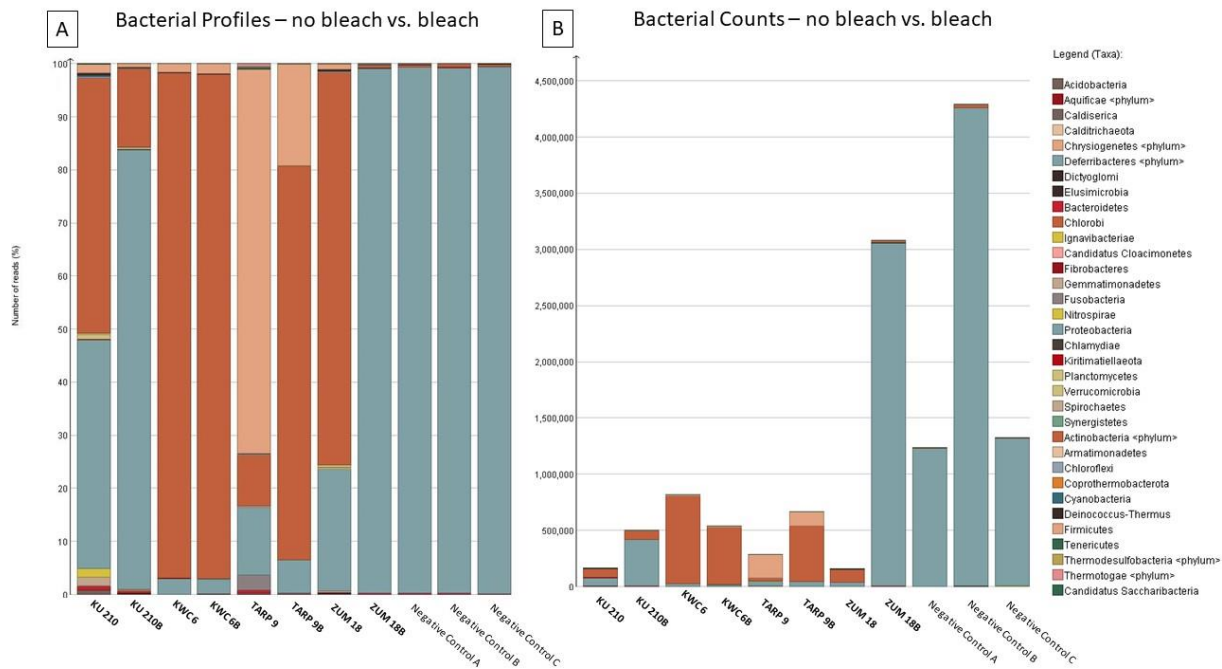
Table 3.10. Four samples selected for bleach pretreatment and results.

Sample Picture	Sample ID & Bone Type	Preservation Notes	Read Count No Bleach	Read Count With Bleach	Conclusion
	El-Kurru 2016 Ind. 210 (KU 210) Right Temporal bone	Poor preservation; covered in silty dirt, moldy throughout cortical bone, extensive weathering	78 reads NO ANCIENT DNA	1442 reads ANCIENT DNA	Ancient DNA obtained
	Kwieka 2016 Tomb 6 (KWC 6) Left Temporal bone	Good preservation, subadult, good bone integrity	3115 reads ANCIENT DNA	4845 reads ANCIENT DNA	Ancient DNA obtained 55.5% increase ↑
	TARP 2017 Area G, Tomb 9 (TARP 9) Right Temporal bone	Good preservation, high bone integrity, hard compact bone, subadult	456 reads NO ANCIENT DNA	2024 reads ANCIENT DNA	Ancient DNA obtained
	El-Zuma Tomb 18 (ZUM 18) Right Temporal bone	Moldy, chalky, soft bone tissue; much of external surface removed for sampling	106 reads NO ANCIENT DNA	8181 reads NO ANCIENT DNA	Failed

Read counts include all mapped reads, both ancient and those determined to be from modern contamination.

To examine the impact of bleach on these tissues, bacterial profiles for each extract were constructed and examined with MALT (Herbig, et al. 2016). This tool classifies and counts bacterial reads from shotgun sequence data. Data from the bleach trials were selected to organize the bacterial reads by phylum (Figure 3.17). The most prominent phyla across the extracts were: Actinobacteria phylum (approx. 10-95%) (highly diverse terrestrial and aquatic bacteria), Proteobacteria (approx. 4-82%) (nitrogen fixing bacteria in soil, some are pathogenic), Firmicutes (approx. 2-72%) (abundant cell wall bacteria or fermenters, some are pathogenic), and Nitrospirae (up to 4%) (common aquatic or nonaquatic bacteria involved in nitrogen cycle) (Figure 3.17).

Figure 3.17. Impact of bleach on contaminating bacteria in extracts.



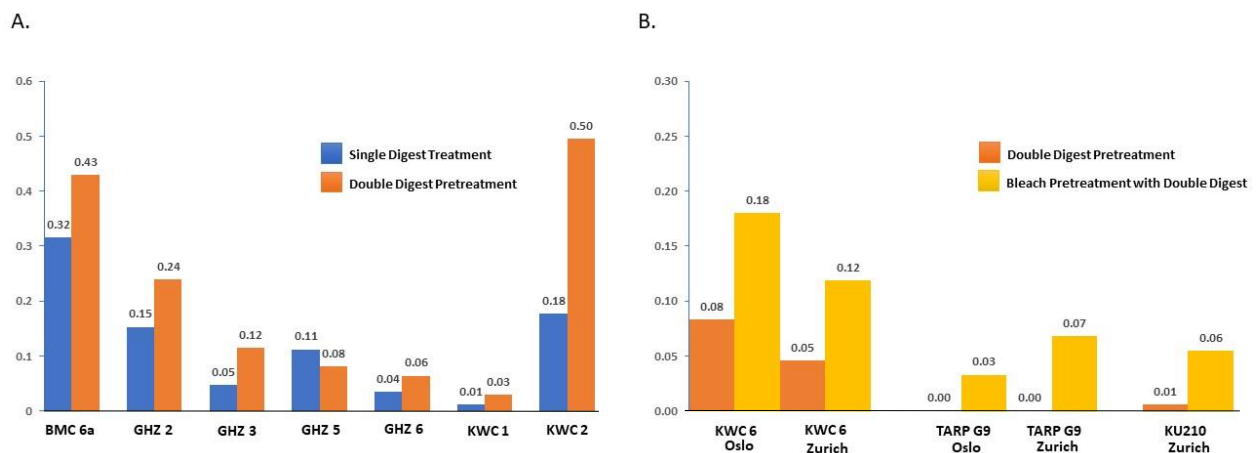
Graphs generated by MALT, legend of bacterial phyla detected at far right. Both graphs organized per individual, listed as without bleach treatment then with bleach treatment where B following the sample ID indicates bleach, followed by negative controls from the Oslo Ancient Lab. A) Bacterial profiles, scaled to 100 percent (y-axis – number of reads %). B) Reads of bacterial DNA from each trial sample (y-axis – number of reads).

Bacterial read counts increased with bleach treatment for three of the four trials, (KWC 6 decreased), but were not statistically different ($t=1.18$, $df=3$, $p\text{-value}=0.32$). This suggested that the bleach treatment does not have a decontaminating effect. However, upon visual inspection, the bacterial profiles did change for three of the four individuals. Again, KWC 6 differed from the pattern of the other four samples, mostly remaining the same. Following the bleach treatment, KU 210 showed an increase in Proteobacteria and a decrease in Actinobacteria. The TARP 9 profile was dominated by Actinobacteria, not Firmicutes, and the ZUM 18 sample lost all of the Actinobacteria signal. The negative controls (i.e. water) contained Proteobacteria only. This indicated that these Proteobacteria were likely contaminating bacteria introduced during the laboratory processing of the extracts. Previously, these bacteria phyla have been tagged as lab contaminants found in the reagents used during library construction that should be ignored (Salter, et al. 2014). Proteobacteria also dominated the ZUM 18 sample that was treated with bleach, likely showing a two-step process where pretreatment removed most of the bacteria, then lab processes introduced contaminant bacterial reads since the profile is identical to negative controls. This comparison lends more support that this phylum of bacteria was introduced by lab processes.

Endogenous Content

Endogenous content showed the same positive results as mapped reads where its proportion increased with pretreatments, either bleach treatment or double digest (Figure 3.18A, B). First, when comparing single to double digest methods, the endogenous content increased an average of 89%. Only GHZ 5 showed a 28% decrease with a double digestion. If we remove GHZ 5 from the comparison, endogenous content increased 109%. When the values for all library pairs were compared via a paired *t*-test, the difference between the endogenous content obtained from the single digest method versus the double digest was not significant ($t = 2.01$, $df = 6$, $p\text{-value} = 0.091$). Bleach treatment increased the endogenous content for all library pairs (percent increase 117% to over 800%). However, the difference was not statistically significant ($t = 2.6885$, $df = 4$, $p\text{-value} = 0.05$).

Figure 3.18. Endogenous Content (%) comparison by method.



A) Single vs. double digest comparison B) Double digest vs. bleach pretreatment. Percentages are listed above columns for each library. TARP G9 had zero endogenous content for the double digest method and were listed as zero without bars y-axis is Endogenous content (%). Ancient mapped reads were not significantly different for either method comparison based on student's *t*-test. Oslo and Zurich below the sample IDs in (B) designate the lab where the sequencing was performed. BMC - Berber Meroitic Cemetery, GHZ - Ghazali, KWC - Kwieka Cemetery, TARP - Tinga Archaeological Rescue Project.

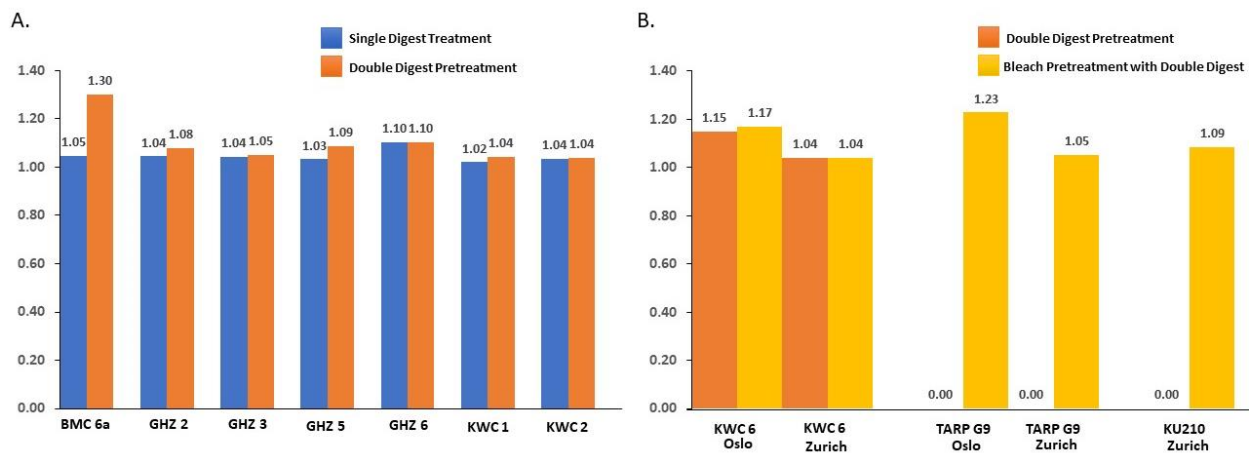
Library Complexity

Library complexity is an important metric that judges the impact of pretreatments on the uniqueness of reads which are built into libraries. Overall, libraries with low complexity are less informative for genetic projects as they provide less distinct reads and more duplicates.

Therefore, to observe if pretreatments decrease the number of unique reads, we compared library complexity across extraction methodologies. The EAGER pipeline produces a metric called a "cluster factor" as a measure of complexity; it is defined as the number of duplicates divided by the number of mapped reads. Duplicates are removed during bioinformatic

processing, are not helpful for constructing genomes, and do not contribute to higher coverage. Thus, a higher cluster factor indicates more duplicates and therefore less complexity. A cluster factor of 1 is an ideal complexity. Cluster results of all pretreatment trials (bleach and/or double digest) were relatively the same when compared to the single digest method (Figure 3.19A, B). When these values were compared via a paired *t*-test, the results were not significant, supporting the idea that digestion method did not impact library complexity ($t = 2.306$, $df = 8$, $p\text{-value} = 0.070$). This analysis established that pretreatments do not impact read uniqueness and therefore do not lead to poor quality libraries.

Figure 3.19. Cluster Factor value comparison by method.

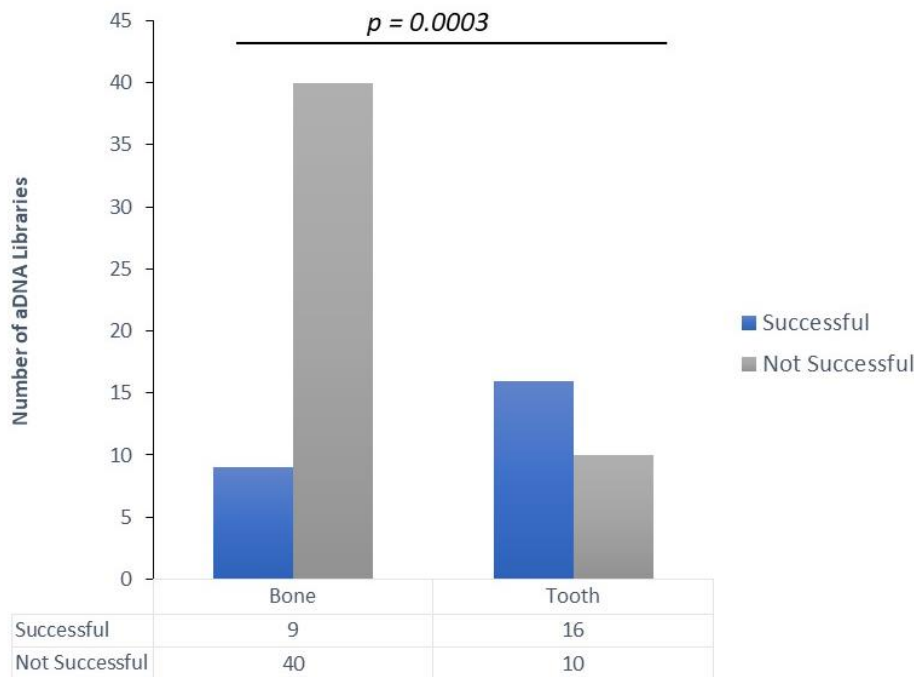


A) Single vs. double digest comparison B) Double digest vs. bleach pretreatment. Cluster factors are listed above columns for each library. BMC = Berber Meroitic Cemetery, GHZ = Ghazali, KWC = Kwieka Cemetery, TARP = Tinga Archaeological Rescue Project.

Tissue Comparison

Two tissue types were collected for sampling which allowed us to compare the performance of tooth dentine and petrous bone tissue when obtaining aDNA. For this analysis, processing was not taken into account, therefore tooth tissue was drilled or crushed dentine and bone tissue was drilled or crushed petrous portions of the temporal bone. Extraction method also was not considered as a cofactor. Thus, a trial was successful if aDNA was obtained and not successful if no aDNA was obtained regardless of extraction methodology. The total number of libraries was 75. Nine out of 49 libraries were successful using bone tissue, while 16 out of 26 trials libraries were successful using teeth (Figure 3.20). Extractions from teeth yielded significantly more successful extractions compared to bone extractions from the petrous portion (Fisher's Exact test, $p\text{-value} = 0.0003$).

Figure 3.20. Comparison of tissue type to successfully obtain aDNA.



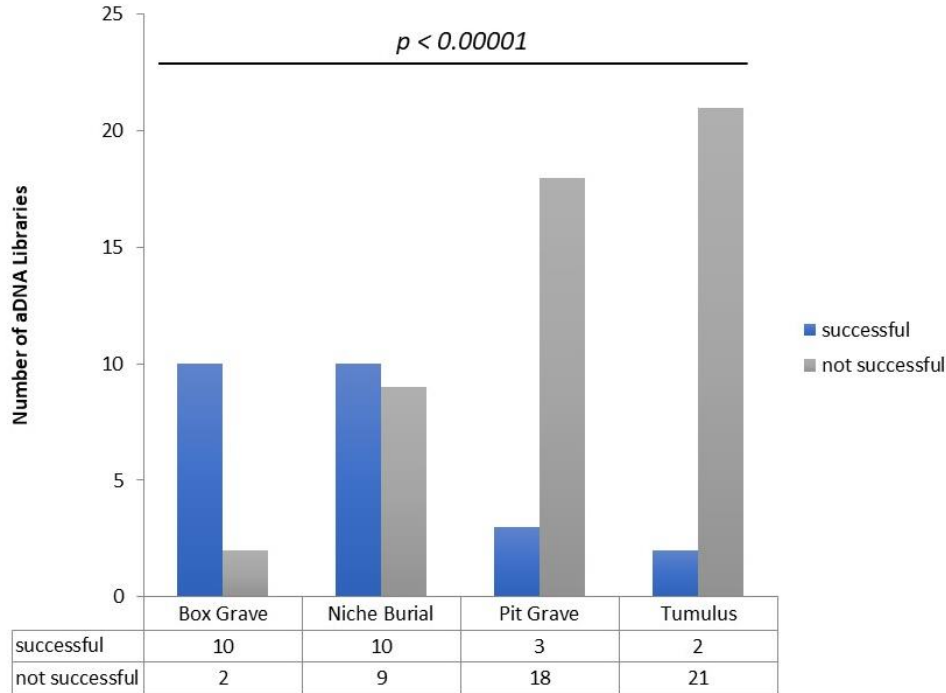
Trial outcomes are listed in the 2x2 contingency table below columns. The Fisher's Exact test statistic value is 0.0003. The result is significant at $p < 0.05$. X-axis is tissue type. Y-axis is number of aDNA libraries obtained.

Burial Context Comparison

Varying archaeological contexts were represented in the eight populations included in the full collection of skeletal samples (listed in Table 3.1). The burial conditions in which the skeletons were interred were compared to understand if grave type had an impact on the ability to retrieve aDNA from the sample material. Four material contexts were designated: box grave (skeleton encased within stone-slab structure, e.g. Ghazali individuals), niche burial (skeleton placed within an undercut or underneath a blocking wall, e.g. BMC individuals), pit grave (skeleton placed at the bottom of a shaft, e.g. El-Kurru individuals), and tumulus (large, multi-chambered, open tomb, e.g. El-Zuma individuals). Tissue type and extraction method were not designated for this analysis. Successful trials produced libraries with aDNA and unsuccessful trials did not; again, 75 trials were counted. Successful trials included 10 of 12 box graves burials, 10 of 19 niche burials, 3 of 21 pit inhumations, and 2 of 23 tumuli burials (Figure 3.21). A Chi-squared test for independence was applied to these data and results showed burial context was significantly associated successful aDNA recovery ($\chi^2 = 26.40$, $p\text{-value} = 0.00001$, significant at the 0.05 level). Samples from tumuli or pit graves did not perform well, while those

from niche burials and box graves did better to retrieve aDNA. These results are illustrated in Figure 3.21.

Figure 3.21. Comparison of burial context to successfully obtain aDNA.



Trial outcomes are listed in the 2x4 contingency table below columns of four burial types. The Chi-squared statistic is significant at the 0.05 level. X-axis is grave type. Y-axis is number of aDNA libraries obtained.

DISCUSSION

Paleogenomic research in Africa lags behind equivalent research in other regions of the world, particularly Europe. High heat and variable preservation have been barriers to aDNA recovery from samples excavated from this region of the world (Pinhasi, et al. 2015). Methodologies that were successful with samples from cold, temperate regions with adequate endogenous DNA preservation (i.e. Europe) have not been suitable for samples from arid or humid environments. These environmental conditions expose tissues to destructive processes, resulting in samples with very low endogenous contents. To utilize these small amounts of aDNA and successfully assemble ancient African genomes, we trialed new method combinations for optimal aDNA extraction that produced high quality libraries for NGS techniques. This included a digest with an enzymatic solution prior to an overnight digestion (i.e. double digest) or bone or tooth powder pretreated with a bleach solution before performing the double digest. Here, we tested whether tissue pretreatment increased mapped ancient reads and endogenous content and impacted library complexity. These results serve as a “best

practice” suggestion for sampling of ancient Nubian materials and may be extended to other human remains preserved in similar conditions.

At this time, it is critical to optimize methods to prevent over- or unnecessary sampling of tissues as paleogenomic work extends to additional African archaeological sites and more samples are collected from museum assemblages. In the future, sensitive techniques for difficult samples may be developed. Strategic sampling schemes should strive to preserve tissue samples for future developments while also maximizing aDNA output from the tissues consumed now.

We compared the performance of three extraction methods including the standard single digestion, a bleach pretreatment, and double digestion on ancient Nubian tooth or bone samples. We found that both bleach pretreatment and double digestion increased the endogenous content and number of ancient mapped reads over the single digest method. Furthermore, these two pretreatment methods maintained library complexity, an important feature for downstream NGS applications. Similar results were obtained in other methodological evaluations including Boessenkool, et al. (2017) and Damgaard, et al. (2015). However, *t*-tests comparing the extraction techniques did not yield significant differences. This is likely explained by our limited sample size, and we would expect our findings to reach significance thresholds with increased sampling. In particular, we found that the bleach pretreatment was particularly robust to rescue samples that would have otherwise had unsuccessful extractions of aDNA. Differences in read counts of bleached vs. non-bleached samples with double digest was approaching significance ($p=0.05$). Nevertheless, we suggest that these pretreatments should be implemented in all future work.

Successful paleogenomic studies in Africa have utilized multiple types of skeletal tissue. For example, Skoglund, et al. (2017) used teeth, petrosal bones, and long bone samples from South and East Africa. In this trial, the type of tissue used for sampling was found to be significantly associated with the ability to obtain aDNA libraries. In fact, teeth outperformed bone tissue by producing more aDNA libraries. This result may have been driven by the many successful trials from Ghazali (6 of 7 trialed). However, the biological composition of dentine tissue also may explain better preservation of DNA. While bone and teeth are both composed of two materials, specifically inorganic minerals (mostly hydroxyapatite) and organic protein (collagen), the degree of mineralization differs. Tooth dentine has a mineral content of roughly 70%, while bone tissue is approximately 60% (Berkovitz, et al. 2017). This differentiation speaks to the tissue’s biological functions within the human body: bone tissue is more flexible, dynamic, and adaptable to stressors, while teeth are mostly unchanging (dentine may remodel, but not

enamel) and fortified for heavy load-bearing activities including mastication. A commonly held theory is that DNA is preserved within the organic portion of the tissue; however, the biochemical particulars are currently being explored. Previous studies have demonstrated that the mineral component is as important, or more, to binding and preserving DNA than collagen and this component is enriched with small-length genetic molecules as a result of tissue degradation and cellular death (Campos, et al. 2012, Schwarz, et al. 2009). These findings may explain why teeth outperformed bone samples when retrieving aDNA from these tissues. Furthermore, when devising a sampling strategy, using teeth samples is less invasive given there are up to 32 potential tooth samples compared to two temporal bones per individual. Therefore, our findings encourage sampling of teeth rather than first harvesting petrous bones. This is a key finding given that the currently recommended method for African materials is the sampling of petrous portions, which is far more invasive than sampling from teeth.

The viability of genetic material also may be impacted by the burial context. We found that interment method was significantly associated with successful extraction of aDNA ($p=0.00001$). Skeletal remains from tumuli and pit inhumations performed poorly, indicating the interment conditions likely destroyed DNA beyond recovery. The populations that performed the worst were those from El-Detti (individuals T.2, T.4, T.5, T.7) and El-Zuma (individuals T.10, T.11, T.15, T.17, T.18, T.28); none of these individuals were successful. These individuals were interred in large rock-cut burial chambers or underneath tumuli. The humidity here seems to be the likely problem and many samples were externally moldy, overly porous, and had a chalky texture. Thus, we suggest that skeletal remains in these contexts may be trialed (e.g. teeth may work better due to higher mineralization of tissue), but should not be intensively sampled if they do not first yield any endogenous content.

Additionally, the El-Kurru population samples did not perform well or were highly contaminated. These skeletal remains were inundated for hundreds of years and were in close proximity to agricultural land. Furthermore, these remains were interred directly into the ground with no physical barriers, like a box-grave constructed from slabs of rocks (i.e. Ghazali monastic site), to protect the remains. This preservation difference has been corroborated with another aDNA study conducted in the 4th Cataract region at Wadi Abu Dom. While this study was PCR-based, the preservation of aDNA was poor with tumuli and best with box graves (Jugert, et al. 2018). Additionally, the successes from Sirak, et al. (2016) are notable, however the remains from Kulubnarti (near modern Sudan's north border and Aswan) had impeccable preservation due to more extreme dryness in northern Sudan or Lower Nubia. In many cases, flesh and organics were perfectly preserved by natural mummification (Armelagos & Van Gerven 2017,

Van Gerven, et al. 1995). In the Middle Nile region, the area is (relatively) wetter and archaeological sites closer to the Nile River are more at risk. Therefore, the sample processing should be specific to those remains from the Middle Nile basin. Lastly, in general, the populations that performed the best were individuals from Ghazali (70% success rate) and Kwieka (100%). The preservation of the tissues may have been better due to the site locations in the desert, further from the Nile River bank, and/or not in proximity to wadis or irrigation that would cause water level fluctuations. Including BMC and TARP, all field sites which produced successful samples were located on the east bank of the Nile with no apparent (modern) wadis or other water sources in the vicinity (with the exception of Ghazali which is somewhat near seasonal wadis). The exception to this rule is El-Kurru, which was less than 400m from the west bank and between two artificial water sources described above. While distance from the Nile likely has an influence, no pattern was apparent. For example, the Ghazali, BMC, TARP, Tanqasi are located far from the banks, around ca. 14km, 2.5km, 5.5km, and 4km, respectively, while Kwieka and El-Kurru were less than a kilometer from the bank and all sites had at least one successful ancient library produced. Those sites with no recovery of aDNA, El-Zuma and El-Detti, range from 2.5km to 800m from the Nile and are in close proximity to other modern sources of water, including irrigation channels or wadis, which may be responsible for water fluctuations. Thus, these eight sites suggest distance from the river may not be a driving factor for preservation; instead, seasonal or flooding water may affect the preservation of skeletal tissue. In conclusion, the burial context and the resulting preservation of biological tissues of the skeletal remains as well as the geographic location with proximity to water sources (that are not the Nile River) should be considered when implementing an invasive sampling strategy for future work in this region.

One of the major limitations of this study was the small sample size of library pairs that were evaluated for number of mapped reads, endogenous content, and library complexity. Forty-three individuals were trialed with at least two different methods. With a 40% success rate, the final number of individuals compared was small. Additional trials may increase this success rate and produce more pairs of libraries to compare. Next, we did not trial a single digestion with bleach treatment. In the context of the results from the other trials, this method would assess the necessity for a double digestion following the bleach pretreatment. Given that the single digestion method produced viable libraries with aDNA with appropriate cluster factors (Figure 3.19), it would be worthwhile to trial this extraction strategy as it would lead to decreased reagent consumption as well as subject the sample to less treatment and thus may reduce contamination.

Future directions of this work will include the implementation of both pretreatments for all processing of samples from the Middle Nile region to verify these results. In addition, future studies whose aim is to extract aDNA from the Middle Nile region should employ a strict sampling strategy wherein sampling of remains from burial contexts that have been shown to be problematic are excluded. Here, the impact of burial context and taphonomy has been shown to impact the success of paleogenomic work and these factors should be considered when sampling in the field. The impact of external factors on tissue preservation, such as aridity and water fluctuation, requires further investigation and the geography of each archaeological site should be observed to discern a pattern in the future. Considerations of burial context and geography will encourage a more conservative strategy for collecting samples that will leave material for future paleogenomic work (or other fields like paleoproteomics). Furthermore, the comparison of sampling tissues also should be pursued to a larger extent. While less invasive techniques have been developed (e.g. Sirak, et al. 2017), harvesting bone powder from the petrous portion of the temporal bone remains destructive. If teeth are available and they produce high-quality libraries, these tissues should be used in place of temporal bones. Moreover, the use of dental calculus should also be piloted for human aDNA retrieval because it has been successful with other Nile Valley samples (Neukamm, *in prep*) and is the least invasive sampling technique (e.g. Ziesemer, et al. 2018). Again, this will conserve material for future work and is typically all that is allowed for sampling of skeletal remains, especially where museum collections are concerned.

As the field of paleogenomics expands across the globe, it is important to utilize the materials we choose to sample in the most impactful way. As the first NGS study using skeletal samples from the Middle Nile, this study demonstrated the viability of ancient DNA research in region of Sudan and trialed a combination of methods to be implemented for further work. These methodologies are recommended to other researchers performing aDNA extracts from bone or teeth samples from Sudan.

CONCLUSION

Skeletal remains from archaeological excavations in the Middle Nile basin of Sudan was used to extract ancient DNA from Nubian individuals. Forty percent of samples were successful for NGS. Multiple methodologies were trialed to compare the amount of human DNA able to be obtained. Two pretreatments, bleach and a double digestion, of the bone or tooth powder were piloted separately and in combination before a standard overnight digestion. Except for one trial, both pretreatments resulted in the increase of endogenous contents and amount of mapped

ancient human DNA reads. Additionally, these treatments did not impact the complexity of the libraries built from these extracts. Tooth samples outperformed bone samples for obtaining aDNA. Additionally, bone or tooth samples from protected burials (e.g. box grave construction) performed the best, while those recovered from tumuli contexts did not. Moving forward, both pretreatments should be used for future work involving skeletal materials from the Middle Nile region. In order to include paleogenomics in research projects in Africa, especially those from the Nile River Valley, viable access to these molecules using precious materials was a critical hurdle to overcome. Now, DNA analysis from archaeological remains may be added to current or future projects in this region as a valuable line of evidence, such as the research designed employed here to join bioarchaeological data with paleogenomic while in context with the archaeological settings.

CHAPTER 4: Ancient Mitochondrial Genomes from Middle Nile Region of Sudan: A New Perspective of Nubian Ancestry

INTRODUCTION

Decades of archaeological, ethnographic, and linguistic work attest to the vast diversity found in North East (NE) Africa, the region that encompasses the Nile River Valley including Egypt, Sudan, South Sudan, and Ethiopia (Figure 1.2). The occupational history of this region is one of the deepest known to humanity – from the origin of our species through developed civilizations that flourished here for millennia. Furthermore, modern genomic studies show that this region houses some of the greatest diversity on the African continent, which itself has the most genetic variation on the planet (Tishkoff, et al. 2009).

Within the Valley, the Sudanese region (Sudan and South Sudan) is of particular interest given its own extensive diversity and the presence of a historically underrepresented group of inhabitants, the Nubians. Ancient Nubia spanned from modern-day Aswan in southern Egypt to Khartoum in Northern Sudan (Figure 1.1). Past populations in this region were mobile with broad trade contacts since prehistoric times, through the empire of Kush, the Medieval Christian kingdoms, and the arrival of Islam in the 14th century CE. Nubians had a dynamic history with their neighbors to the north – robust trade, conquest, colonialism – all of which may have contributed to their genetic ancestry (as outlined in Chapter 1). Despite this entangled relationship, the modern profile of Nubians is unique and has been the subject of ongoing genetic projects during the past three decades, summarized in Chapter 1 (Alfonso, et al. 2008, Krings, et al. 1999, Lalueza Fox 1997, Hassan 2009, Hassan, et al. 2008, Dobon, et al. 2015, Hollfelder, et al. 2017). However, the lens of modern population data has only described the genetic landscape up until the Islamic conquest, while ancient demographic trends before this large migratory event remain speculative or unknown. Sampling from archaeological populations provides an opportunity address these unknowns by directly characterizing genomic structure in the past. Such data will contribute to our understanding of human prehistory in the region and reconstruct the multifaceted history of Nubians.

When the field of paleogenomics appeared, samples from the Nile Valley were some of the first to be trialed (Pääbo 1985). Unfortunately, serious complications with contamination sidelined the exploration of this resource for ancient molecular studies (Hofreiter, et al. 2014, Pääbo & Wilson 1985). Paleogenomic work was simply unsuccessful when using archaeological material from such a hot, dry environment which degrades ancient DNA to the point of no recovery. However, recent advances in biotechnology and optimization of methodologies have opened an exciting opportunity to scientific work. This includes the use of parallel sequencing platforms or next-generation sequencing techniques, specialized extraction treatments (e.g. bleach pre-treatment), and use of petrous portions of the temporal bone for sampling, which is known to contain more authentic DNA, even from hot, dry climates (Hansen, et al. 2017, Gamba, et al. 2014, Pinhasi, et al. 2015, Gallego Llorente, et al. 2015, Dabney, et al. 2013, Kircher, et al. 2011). These advances now open the Middle Nile, and likely much more of Africa, to the genomic revolution and will continue to expand our knowledge about this continent's populations and human migrations (Hofreiter, et al. 2015, e.g. Schlebusch, et al. 2017, Skoglund, et al. 2017).

While most knowledge about this region of the world is informed by historical, anthropological, and archaeological data, a paleogenetic study using complete mtDNA has yet to be published, making the present study the first. Furthermore, it includes an unprecedented time-series of samples from underrepresented African groups. The samples elucidate the demographic history of this region dating to the time of Kushite power along the entire Nile (around 8th century BCE), the later invasion of foreign rulers, followed by restructuring of the Kingdom of Kush at Meroe (3rd century BCE), the rise of Christian Kingdoms (7th century CE), and ending with the Arab expansion (14th century CE). Such events (e.g. invasions, migrations, entanglement) affect the genetic ancestry of the individuals, which in turn can be analyzed to reconstruct past demographic events (Kriings, et al. 1999, Hollfelder, et al. 2017). This sample set, which varies in time and space (Table 3.1), was uniquely powered to observe the dynamics of population structure in real-time while simultaneously contributing to the growing interest centered on the genetic past of indigenous African populations.

The primary aim was to genetically characterize the inhabitants of Nubia by extracting DNA from archaeologically excavated human remains and using these data for population genetic analyses. Sequence data from these ancient individuals allowed us to describe variation within the Nubian populations and begin to reconstruct ancestry of each individual to understand the diversity that exists between and within the ancient groups. Due to the lack of ancient comparative data, extant Sudanese are used for comparison. Additionally, metapopulations of

modern Sudanese are grouped by region from previous datasets (e.g. Hassan 2009, Babiker, et al. 2011). Specifically of interest was the genetic makeup of Nubians before the arrival of Islam, which can be used to more accurately time the major influx of Eurasian component in the Middle Nile basin. These data stand to test hypotheses of population continuity as well as how ancient Nubians have contributed to the genetic diversity of modern inhabitants of the Nile Valley by comparing them to extant Sudanese and regional neighbors, given geography plays such an influencing role. Lastly, these data may characterize a distinct genetic signature present in the Middle Nile region which may be differentiated from other areas, i.e. Lower Nubia, Egyptians, or other ancient populations.

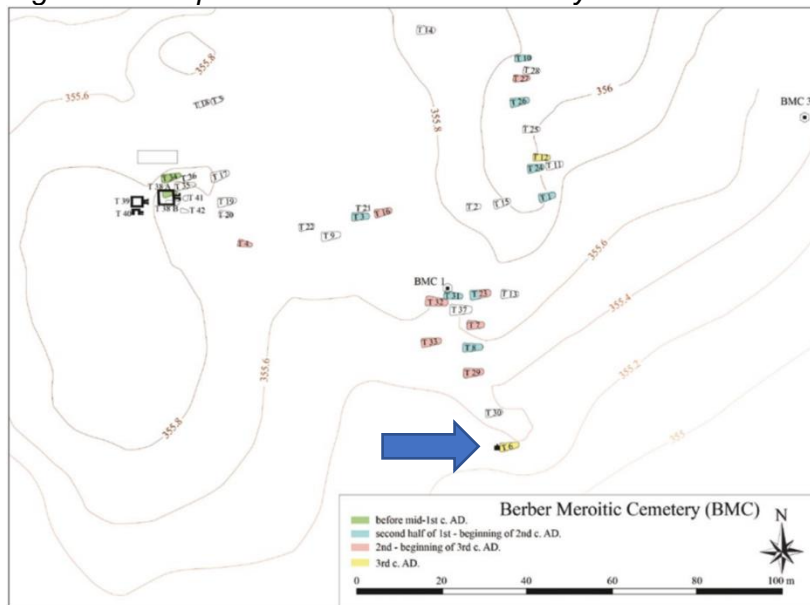
MATERIALS

Of the eight sample populations and 43 unique individuals, six individuals from four sample populations had aDNA successfully extracted from skeletal materials. Outlined below are the specific archaeological contexts for each individual in addition to a few details on the sites and the sampling tissue.

Berber Meroitic Cemetery Individual 6 / BMC 6a

Near the 5th Cataract, the Berber Meroitic Cemetery has been excavated by NCAM for several seasons since 2009 after building foundation trenches disturbed these burials (Figure 1.1). This site was occupied during the Meroitic period ca. 50-350 CE, has 38 tombs, and three mudbrick pyramids (Bashir & David 2015) (Figure 4.1). Body positioning was related to the burial chambers found at this site. Oval graves had contracted or semi-flexed skeletons, while east-west burials had extended body positioning within a box grave.

Figure 4.1. Map of Berber Meroitic Cemetery.



Dating estimations based on radiocarbon dating, pottery types, and decorations found in context with the burials (Bashir & David 2015). Tomb 6 is dated to the 3rd Century CE (arrow).

Located in the southern part of the cemetery, the burial niche for BMC 6 was disturbed by a foundation trench, but excavations revealed it contained intact pottery, kohl pots of ebony and ivory, and preserved wood (Figure 4.1) (Bashir & David 2015). Regardless of robber disturbances, a sandstone offering table with cursive Meroitic writing naming the deceased, *Sobt*, was found in the grave (Figure 4.2A). This artifact dates the grave to mid-3rd century CE (ca. 250 BCE) (Bashir & David 2015). Skeletal data is unavailable at this time. The right mandibular 1st premolar was extracted from the mandible for aDNA sampling (Figure 4.2B).

Figure 4.2. Burial context of Individual BMC 6a and tooth sample.

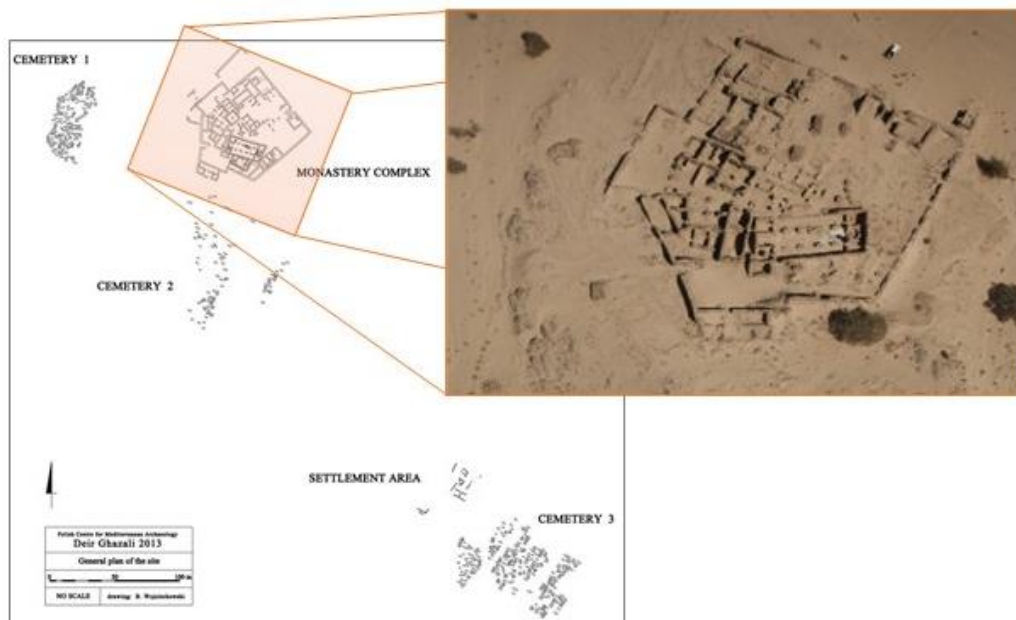


A) Sand stone offering table artifact with cursive Meroitic writing discovered in context with BMC 6a. B) Right mandibular 1st premolar for Individual BMC 6a.

Ghazali Individual 4-008.2 / GHZ 2

Ghazali 4-008.2/GHZ 2 Individual was interred in Cemetery 4 within the Early Christian monastery complex at Ghazali in the 4th Cataract region (Figure 4.3). The main church has been radiocarbon dated to 670-770 CE. This cemetery was somewhat isolated on site and those buried here have inconsistent burial treatments, as opposed to those in the other larger cemeteries at Ghazali, and remains show evidence of interpersonal violence (Stark & Ciesielska 2019). Project archaeologists suggest this cemetery has a different, but unknown function compared to the other three in the vicinity (Stark & Ciesielska 2019).

Figure 4.3. Ghazali complex located near 4th Cataract, Sudan.



Line map drawing (left) of cemeteries, settlement area and monastery complex at Ghazali. Aerial kite photograph (right) of the monastery. Cemetery 1 visible to the west of the monastery where GHZ 5 was interred, Cemetery 4 (where GHZ 2 is buried) is not mapped. Map obtained from Stark & Ciesielska (2019).

Excavated in 2016, GHZ 2 was buried beneath a superstructure consisting of vertically arranged rocks from the local landscape that outlined the grave (Figure 4.4A). The body treatment shows typical Christian burial traditions, including a fully extended body, arms extended at the side, head is encased with flat rocks (two framing the skull and one over the face). Also, some traces of a burial shroud still remain *in situ* (Figure 4.4B). Anthropologists estimated GHZ 2 as a female, aged 30-40 years old. The right 2nd maxillary molar was obtained for aDNA extraction (Figure 4.4C).

Figure 4.4. Burial context of Ghazali-4-008.2/GHZ 2.

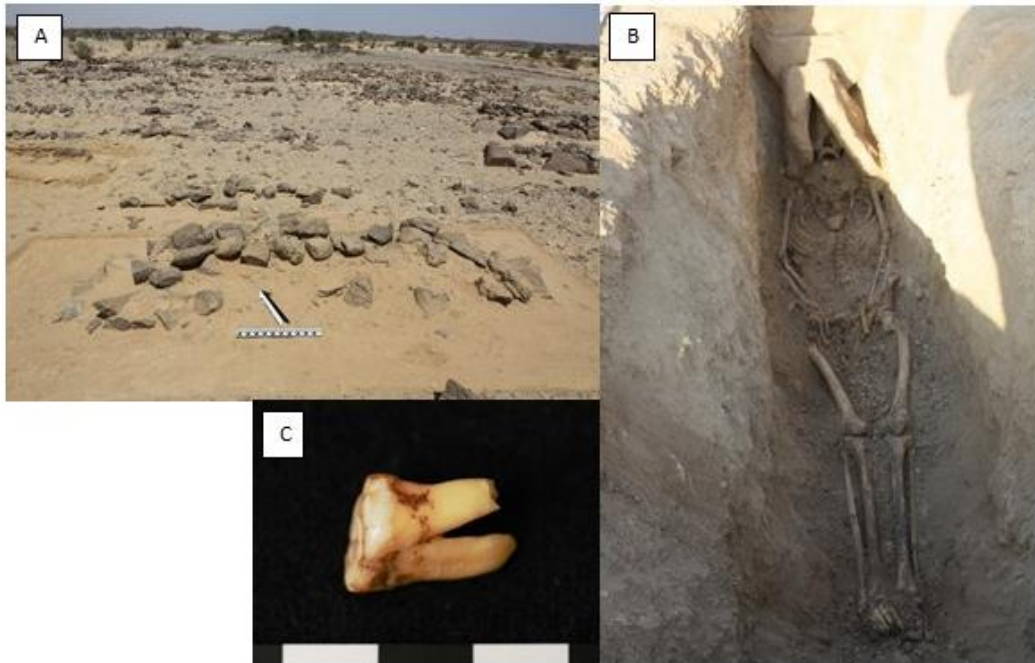


Ghazali individual 4-008.2 from cemetery 4. A) Superstructure covering the grave of this individual. B) Skeletal remains of GHZ 2 *in situ*. C) Right 2nd maxillary molar, before cleaning.

Ghazali Individual 1-010 / GHZ 5

GHZ 5 was buried in Cemetery 1, west of the Early Christian monastery complex at Ghazali. The main church has been radiocarbon dated to the Early Christian period (670-770 CE) (Figure 4.3). This cemetery was reserved for *ad sanctos* burials for people in the surrounding areas wishing to be interred near a holy place, i.e. the monastery. The skeletal remains of GHZ 5 were contained within a stone box-grave, oriented Northwest-Southeast, with a large stone superstructure (Figure 4.5A). The grave was constructed in typical Nubian Christian traditions with regards to the superstructure (like GHZ 2). The body was fully extended and supine with the arms extended at the sides and hands clasped over the pelvis (Figure 4.5B). Evidence of a burial shroud were discovered. The left upper 2nd molar was sampled for aDNA extraction (Figure 4.5C).

Figure 4.5. Burial context and sampling of GHZ-1-010/GHZ 5.



A) Exposed rocky super structure of burial for GHZ-1-010 / GHZ 5. B) *In situ* skeletal remains of GHZ 5 at the bottom of the burial pit. C) Left Maxillary 2nd molar, before cleaning.

Kwieka T2 Individual / KWC 2

The cemetery at Kwieka was likely occupied during Meroitic (350 BCE – 350 CE), Post-Meroitic (350 – 550 CE), and Christian periods (550 – 1450 CE) as per the burial traditions observed during excavations (Abdallah 2018). This site was excavated in 2016 by NCAM officials and its archaeological context is described by Abdallah (2018) (Figure 4.6).

Figure 4.6. Aerial view of the site of Kwieka near the 5th Cataract region.



Kwieka T2 individual was interred near the eastern edge of the excavated area of the cemetery, dated contextually to the Meroitic period based on grave construction, approximately 350 BCE-350 CE (Figure 4.6, Figure 4.7A). The burial had a rounded superstructure of quartz stones (Type F), a rectangular tomb shaft, and an oval chamber cut into the sandstone (Figure 4.7A, B) (Abdallah 2018). The skeletal remains were found within this grave cut, along with a clay storage bin (or *quseiba*), and a broken beer cup (Figure 4.7A). NCAM archaeologists determined the skeleton was completely disturbed by robbers, thus its original positional cannot be determined. Kwieka T2 was estimated to be an adult and the intact right temporal bone was used for aDNA sampling (Figure 4.7C).

Figure 4.7. Burial context of KWC T2, associated finds, and sampling material.



A) Circular superstructure of KWC T2 (upper) and rectangular substructure (lower), with associated finds (inset) (Saad 2018). B) Adult skeletal remains of KWC 2 with evidence of disturbance. C) Right temporal bone for sampling.

Kwieka T6 Individual / KWC 6

The grave of individual KWC T6 was discovered by local villagers when mining gravel used for local building projects. The grave had a rounded, flat-topped gravel superstructure, up to 7m in diameter and half a meter high (Classified as a Type D tumulus) (Abdallah 2018). The underground substructure was a 1.3m-deep rectangular shaft with a sub-rectangular burial chamber and mud-brick blockage wall that showed signs of robber activity (Figure 4.8A). Within the burial chamber, the skeletal remains were found to be disturbed and some ceramic sherds were found within the fill (Figure 4.8A). The skeleton was that of a child and thus, no skeletal sex estimation was conducted. The intact left temporal bone was used for sampling to extract aDNA (Figure 4.8B).

Figure 4.8. Burial context of KWC T6 and sampling material.



A) Disturbed skeletal remains of KWC T6, immature long bones seen without distal epiphyses. B) Left temporal bone used for aDNA sampling.

TARP G9 individual / TARP 9

The Tinga Archaeological Rescue Project took place near the 5th Cataract and in close geographic proximity to the Berber Meroitic Cemetery. Excavations were conducted in 2017 by NCAM officials. The archaeological context of burials exhumed were described by Bushara, et al. (2018). TARP individual G9 was interred in a rectangular grave, oriented East-West, with a traditional wooden bed. This grave type is similar to Napatan style burials found down river in Meroe and at Berber, another 5th Cataract site north of TARP. The skeleton was found in a typical flexed position on a wooden bed, head towards the west end of the grave and facing south. The remains belong to a child and were not assessed for biological sex. The right temporal bone was used for aDNA sampling (Figure 4.9).

Figure 4.9. Right temporal bone from TARP T9.



TARP = Tinga Archaeological Rescue Project, T = tomb number

METHODS

Ancient DNA Extraction, Library Assembly, and Sequence Data Processing

A full description of the processing, pretreatment, and extraction of DNA is outlined in the Chapter 3. All samples are approved for destructive analysis as per agreements with the directors of the archaeological excavations and/or the National Committee for Antiquities and Museums from Sudan. In brief, all work was performed in a designated clean lab at the Institute of Evolutionary Medicine at the University of Zürich or the Ancient Laboratories at the University of Oslo in Blindern, Norway. Bone and teeth samples were externally decontaminated with UV irradiation treatments in a crosslinker. Sterile powder was collected from the petrous portion of the temporal bone or the inner dentine of intact teeth using methods optimized for the tissue type and integrity (i.e. crushing or drilling). Powder (100-200mg) was subjected to a pretreatment of bleach or a mild pre-digestion step or both as per Korlevic & Meyer (2019) and Schroeder, et al. (2019). DNA was extracted following Gamba, et al. (2014) with modifications from Dabney & Meyer (2019). DNA extracts were converted into paired-end Illumina libraries as outlined in Meyer & Kircher (2010), indexed for sequencing as per Kircher, et al. (2012). All libraries were shotgun sequenced on an Illumina HiSeq4000 to screen for libraries containing DNA displaying typical molecular characteristics of degraded genetic material and estimate endogenous content. Those libraries selected for further analysis (i.e. low contamination, endogenous DNA present, typical damage profiles) were enriched for human mitochondrial DNA using in-solution hybridization capture (Maricic, et al. 2010). These libraries were sequenced at a high percentage on an Illumina NexSeq sequencing platform and negative control samples on an Illumina MiSeq Micro.

A more in-depth description of the processing of sequence data, is found in the previous chapter. Generally, raw reads from the ancient Nubians and negative controls were processed with the bioinformatic pipeline EAGER (v1.92) to assess mapped reads to the human mitochondrial genome and again estimate criteria for authenticity (Peltzer, et al. 2016). Those libraries demonstrating typical molecular behavior of genetic material consistent with age and degradation were analyzed with the tool Schmutzi to estimate modern contamination and build endogenous consensus sequences (Renaud, et al. 2015). Libraries with low contamination (< 5%) were merged when necessary for each individual and consensus sequences were used for haplogroup assignment. Coverage plots were generated for each individual used in the haplogroup analysis with an in-house R script.

Samples later included in the haplogroup analysis were molecularly sexed by utilizing a bioinformatic pipeline and shotgun read data from the first screening of viable genetic material (Mittnik, et al. 2016). This pipeline used the reads which mapped to the sex chromosomes and measured the ratio of the X and Y chromosomes to estimate a male or female karyotype (Mittnik, et al. 2016). Values classified individuals as being “assigned” with a certain karyotype or “consistent” with one karyotype but not the other. These data were compared to those estimations of sex (and age) done by archaeologists (listed above or Chapter 3, Materials) using standard bioarchaeological methods, characterizing discrete traits of the skull and post-crania to estimate age-at-death and degree of sexual dimorphism (Buikstra & Ubelaker 1994). Sex estimation was not performed on subadult individuals.

Haplogroup Assignment

Using the consensus sequence files generated from the previous step, haplogroups were assigned using HaploGrep 2 (<https://haplogrep.uibk.ac.at/>) (Weissensteiner et al 2016). Consensus sequences used for this analysis was chosen by balancing the highest rank achieved and highest quality data (i.e. lower quality (Q20) may have less ‘no calls’ or N’s, but rank or confidence of haplotype assignment may not increase with more nucleotide calls; therefore, a higher quality sequence would be selected for assignment).

Comparative Dataset Assembly and Alignment

Two comparative datasets – haplogroup frequencies and a whole MT genome dataset – were assembled from publicly available sources and databases: HmtDB (Clima, et al. 2016), National Center for Biotechnology Information Nucleotide Database (Benson et al 2018), European Molecular Biology Laboratory (EMBL) Nucleotide Sequence Database (Baker, et al. 2000), other collaborations, and other published manuscripts outlined below.

For haplogroup frequencies, there is a dearth of mitochondrial genomic data for the country of Sudan; however, there are two data sources with limited availability and coverage of the mitogenome that are useful for context of Sudan. One is Krings, et al. (1999) sequenced the HVRI of 68 Egyptians, 80 Nubians, and 76 Southern Nilotes. The other is Hassan (2009, Table 4.1) that provides haplotype frequencies for six geographic groups that include 15 ethnic groups for comparison. These frequencies were derived from sequence data from the HVRI region, but these sequences are no longer accessible. These frequencies and others from the Northeast region of Africa provided by Abu-Amero, et al. (2008) (Nile River Valley countries) and Fadhlouzi-Zid, et al. (2011) (Libya) were merged into one dataset (Table 4.1).

Table 4.1. Sources and group counts for haplotype frequencies data for dataset assembly.

Population or Subpopulation	N	Published source
Libyans	268	Fadhlaoui-Zid, et al. 2008
Egyptians	68	Krings, et al. 1999
	58	Stevanovitch, et al. 2003
	118	Rowold, et al. 2007
Nubians (Northern Sudan)	79	Krings, et al. 1999
	29	Hassan 2009
Beja (East)	48	Hassan 2009
Central Sudanese (Arab) – Arakein, Copts, Gaalien, Hausa	103	Hassan 2009
Western Sudanese – Borgu, Masalit, Fur	87	Hassan 2009
Southern Nilotes – Dinka, Shilluk, Nuer, Nuba	94	Hassan 2009
Pastoralists – Fulani, Meseria	43	Hassan 2009
Ethiopians	74	Thomas, et al. 2002
	270	Kivisild et al 2004
Kenyans	99	Brandstätter, et al. 2004
	42	Rowold, et al. 2007

Geographic groups in bold typeface and the subpopulations included in macrogroup listed underneath.

N = number of individuals, count.

For whole MT genome analyses, both modern and ancient whole mitogenomes were obtained for 2,006 individuals from all of Africa, northern, western, and central Europe, and the Middle East, dating as far back as 15,000 years ago to as recent as the past few centuries. While a large part of this dataset is from extant human populations (i.e. 1,740 individuals), a significant amount are ancient genomes. Two hundred sixty-six ancient individuals cover North Africa, from the Canary Islands to Egypt (Schuenemann, et al. 2017, van de Loosdrecht, et al. 2018, Vai, et al. 2019, Fregel, et al. 2019, Fregel, et al. 2018), East Africa, including Kenya and Ethiopia (Prendergast, et al. 2019, Gallego Llorente, et al. 2015), then continuing southward to Tanzania, Malawi, & South Africa (Skoglund, et al. 2017, Schlebusch, et al. 2017, Morris, et al. 2014) (Figure 1.8). Those outside the African continent include 22 individuals from the Levant area – namely ancient Natufians, Anatolians, and other Near Eastern farmers (Lazardis, et al. 2016) (Figure 1.8) – and five ancient individuals from Europe (Fu, et al. 2013, not pictured in Figure 1.8).

For those ancient individuals with no publicly accessible mitogenomes, raw files were obtained from databases mentioned above, mapped to the human mitochondrial reference sequence, and VCF files were created to be uploaded in Haplogrep 2 to generate a FASTA file

containing the mitogenome for each individual (Weissensteiner et al 2016). For those publications with published polymorphism files for ancient individuals, these data were formatted and uploaded into Haplogrep 2 to generate FASTA files containing the mitogenome for each individual (Weissensteiner et al 2016). Haplogroup assignments were checked for each generated FASTA file with those in the published works. Additionally, those with low overall ranks (< 75%) from Haplogrep 2 were not included.

All MT sequence data, including those of the six ancient Nubians, were aligned using AliView v1.26 (Lasson 2014). For whole MT analyses, populations groups were collapsed into “macrogroups” for haplogroup frequency PCA analysis and pairwise difference analyses (e.g. PCA, F_{ST} , MDS). Table 4.2 outlines the countries of origin which characterized these collapsed groups. MitoBench v1.1 beta (Neukamm & Peltzer 2019) was used to compile and generate files to be used in Arlequin (Excoffier & Lischer 2010) for F_{ST} calculations.

Table 4.2. Macrogroups used for analyses and which populations are included within each one.

Macrogroup	N	Countries or Population Groups Included in Macrogroup
AncientEuropean	5	Czech Republic, Germany, France, Luxemburg
AncientNearEastFarmers	43	Turkey, Armenia, Jordan, Israel, Iran
AncientNorthAfrican	67	Libya, Morocco, Canary Islands
AncientEgyptiansPPP	60	Northern Egypt (Abusir el-Mepeq)
AncientEgyptiansPtoP	16	Northern Egypt (Abusir el-Mepeq)
AncientEgyptiansRoman	14	Northern Egypt (Abusir el-Mepeq)
AncientNubians	6	Sudan (Upper Nubia)
AncientEastAfrican	50	Kenya, Malawi, Tanzania, Ethiopia
AncientSouthAfricans	11	South Africa
WesternEuropeModern	81	Spain, Portugal, France
NorthernEuropeModern	17	United Kingdom, Ireland, England, Scotland, Finland
CentralEuropeModern	21	Netherlands, Poland, Germany, Czech Republic
SouthernEuropeModern	90	Italy, Sicily, Bulgaria, Romania, Greece
SardiniaModern	6	Sardinia
MiddleEastModern	301	Saudi Arabia, Kuwait, Oman, Yemen, United Arab Emirates, Iraq, Syria, Lebanon, Cyprus, Israel, Jordan, Palestine, Georgia, Iran, Pakistan, Armenia, Turkey, Azerbaijan
NorthAfricaModern	165	Algeria, Canary Islands, Libya, Morocco, Tunisia
EgyptModern	70	Egypt
SudanModern	68	Sudan
EthiopiaModern	56	Ethiopia
EastAfricaModern	147	Eritrea, Ethiopia, Kenya, Rwanda, Somalia, Tanzania, Uganda
CentralAfricaModern	74	Chad, Equatorial Guinea, Cameroon, Central African Republic, Democratic Republic of Congo, Sao Tome and Principe, Lake Chad
SouthernAfricaModern	592	Angola, Botswana, Mozambique, Namibia, South Africa, Zambia

WestAfricaModern	52	Guinea-Bissau, Gambia, Ghana, Ivory Coast, Mali, Mauritania, Nigeria, Senegal, Niger, Burkina Faso
-------------------------	----	----------------------------------------------------------------------------------------------------

PPP, Pre-Ptolemaic Period; PtoP, Ptolemaic Period

"Ancient" populations refer to where samples were excavated within modern political boundaries.

N = number of individuals, count

Haplogroup Profile Construction

To visualize the varying genetic components that describe the ancestry of a defined population, haplogroup profiles were compiled from published data or calculated from haplogroup frequency counts found in published data. Since mitochondrial DNA is a single marker, each individual contributes one data point as a haplogroup assignment. Therefore, a large number of individuals, or a large sample number, was required to create an accurate profile of the population. Raw counts of individuals were tallied and frequencies of haplogroups were calculated as percentages, then subgroups were collapsed into macro-haplogroups to simplify the profile (e.g. L0a1a grouped as L0). Profiles were constructed based on these percentages and were visualized as stacked columns or pie charts (both equal to 100%), then were color-coded to correspond to informational groupings of these haplogroups (e.g. all African L lineages are warm colors).

Population Comparison Analyses

Using the Haplogroup frequencies dataset, a Principle Component Analysis plot was constructed in MitoBench v1.1 beta (Neukamm & Peltzer 2019). MitoBench was also used to construct Arelquin files for F_{ST} values calculations to estimate between population differences. F_{ST} values were generated in Arelquin 3.5 (Excoffier & Lischer 2010). The MDS plot to visualize the genetic distances was created with an in-house R script and implemented in R Studio.

RESULTS

Contamination Estimation Analysis

Bone and teeth samples from 43 Nubian individuals were piloted using various extraction methods to obtain ancient genetic material. With the first screening step of shotgun sequencing, these methods were successful in yielding authentically ancient DNA – either mitochondrial or nuclear – from 17 of these individuals, a 40% recovery rate. Given low reads mapping to the human mitochondrial genome, a capture step was performed using baits and in-solution beads to enrich for the mitogenome. Twenty-two libraries (and all negative controls) were enriched for human mitochondrial DNA (Table 4.2). (Some libraries with ancient reads were not included due to over lapping indexes and time constraints). Negative controls

established no cross contamination of ancient material and a negligible amount of modern contamination throughout the process; these results are detailed in Appendix B. Of these enriched libraries, seven failed, five were successful, but were estimated to be heavily contaminated, and 10 were successful enrichments with low contamination (Table 4.2). For those libraries from the same individual, raw files were merged and run through Schmutzi (“_merged”, listed at the end of table, green). All merged files had less contamination and the consensus sequence built from the merged reads was used for all analyses following this. For sample BMC 6a, merging the reads decreased the overall contamination rate, despite being constructed from the double digest library having a moderate contamination estimation.

Table 4.2. Libraries enriched and analyzed with Schmutzi.

Archaeological Site	Sample Name	Final contamination estimation (%)	Low (%)	High (%)	Comment
Berber Meroitic Cemetery	BMC 6a_DD	0.12	0.11	0.13	Switching
	BMC 6a_SD	0.01	0.0	0.02	Stable
	BMC 6a_merged	0.02	0.01	0.03	Stable
	GHZ 2_merged	0.01	0.0	0.02	Stable
	GHZ 5_merged	0.01	0.0	0.02	Stable
	KWC 2_merged	0.01	0.0	0.02	Stable
	KWC 6_merged	0.01	0.0	0.02	Stable
El-Detti	DET 7_oslo	NR	-	-	-
Ghazali	GHZ 1_DD	NR	-	-	-
	GHZ 2_DD	0.01	0.0	0.02	Switching
	GHZ 2_SD	0.01	0.0	0.02	Stable
	GHZ 3_SD	0.99	0.98	0.99	Stable
	GHZ 5_DD	0.01	0.0	0.02	Stable
	GHZ 5_SD	0.01	0.0	0.02	Stable
	GHZ 6_SD	0.99	0.98	0.99	Stable
El-Kurru	KU 210B_oslo	NR	-	-	-
	KU 212_oslo	0.99	0.98	0.99	Stable
Kwieka Cemetery	KWC 2_DD	0.02	0.01	0.03	Stable
	KWC 2_SD	0.01	0.0	0.02	Stable
	KWC 6_oslo	0.01	0.0	0.02	Stable
	KWC 6B_oslo	0.01	0.0	0.02	Stable
	TAQ 179_oslo	0.0	0.0	0.005	Stable
Tinga Archaeological Rescue Project	TAR 22_DD	NR	-	-	-
	TAR 9B_oslo	0.01	0	0.02	Stable
El-Zuma	ZUM 18B_oslo	NR	-	-	-

ZUM 28_DD	NR	-	-	-
ZUM 28_SD	NR	-	-	-

Reads were run through the Schmutzi pipeline to build a consensus mitochondrial sequence using endogenous (i.e. ancient) reads. The contamination estimation (%) of modern human contamination is reported (“Final”) as is the average between the “High” and “Low” values reported from the multiple iterations of the pipeline. Comments about the contamination estimation are noted in that last column; “stable” refers to consensus, calling, and contamination estimations run iteratively that reached a stable estimation value, “switching” indicates inconsistent values were reached during iterative runs, suggesting that the results should not be necessarily trusted. Samples with “NR” as the final estimation have too few reads for this tool.

BMC - Berber Meroitic Cemetery, DET - El-Detti, GHZ – Ghazali, KU - El-Kurru, KWC - Kwieka Cemetery, TAQ – Tanqasi, TAR - Tinga Archaeological Rescue Project, ZUM - El-Zuma, DD - double digestion method, SD - single digestion, oslo – Oslo method used (i.e. double digestion) and prepped at the University of Oslo, B - bleach pretreatment, NR - Not Reported.

Green – enrichment successful, not contaminated

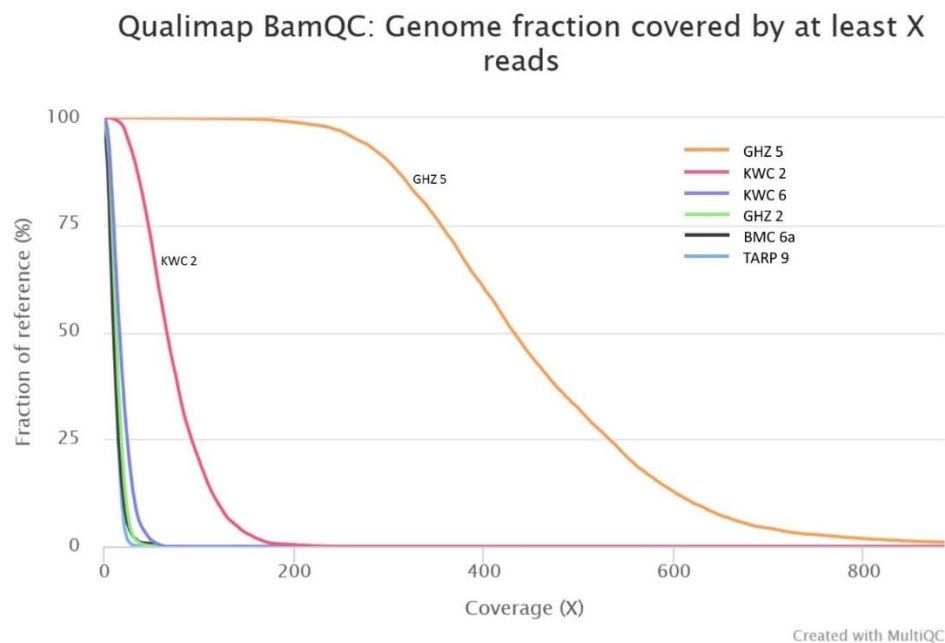
Yellow – enrichment successful, contaminated

White – enrichment failed

Sequence Quality Analysis

Six individuals had a viable number of endogenous reads for consensus sequence reconstruction of the entire mitogenome (with contamination estimations of 2% or less): BMC T6a (BMC 6a_SD/BMC 6a_DD/BMC 6_merged), Ghazali 4-008.2 (GHZ 2/GHZ 2_SD/GHZ 2_DD), Ghazali 1-010 (GHZ 5/GHZ_SD/GHZ_DD), KWC T2 (KWC 2/KWC 2_SD/KWC 2_DD/KWC_merged), KWC T6 (KWC 6B_oslo/KWC 6_oslo/KWC 6_merged), and TARP G9 (TAR9B_oslo). TAQ179_oslo was not contaminated, but read count and endogenous content were low. These six individuals had reads mapping to human mitochondrial reference genome ranging from 3,356 to 146,987 (Table 4.3). Samples had a mean coverage ranging from 3X to 450X with some individuals (i.e. GHZ 5 and KWC 2) up to 100% of bases covered at least fivefold or more (Table 4.3, Figure 4.10). Two individuals, GHZ 5 and KWC 2, had immensely high coverage resulting in very confident reconstructions of their respective full mitogenomes (an example, KWC 2 depicted in Figure 4.11). Some individuals had two libraries built from their sample extracts. For these individuals, raw data was merged for analysis. For example, libraries for individual KWC T6 (KWC6) were obtained from two separate bone powder samples, “KWC6_oslo” and “KWC6B_oslo”, obtained using different methods (see Chapter 3 for more details), and were merged into the file “KWC6_merged” for analysis. Sequence quality (read count, damage, etc.) was determined for all libraries, merged or unmerged.

Figure 4.10. Coverage of the Mitochondrial Genome of Nubian Individuals.



Graph of six Nubian individuals with full genome coverage. The x-axis depicts the extent of coverage as a function of the entire mitochondrial genome, shown on the y-axis up to 100%. KWC - Kwieka Cemetery, GHZ – Ghazali, BMC - Berber Meroitic Cemetery, TARP - Tinga Archaeological Rescue Project. Coverage graph was generated using Qualimap BamQC.

Table 4.3. Sequence Quality Analysis Summary - from EAGER analysis of enriched reads.

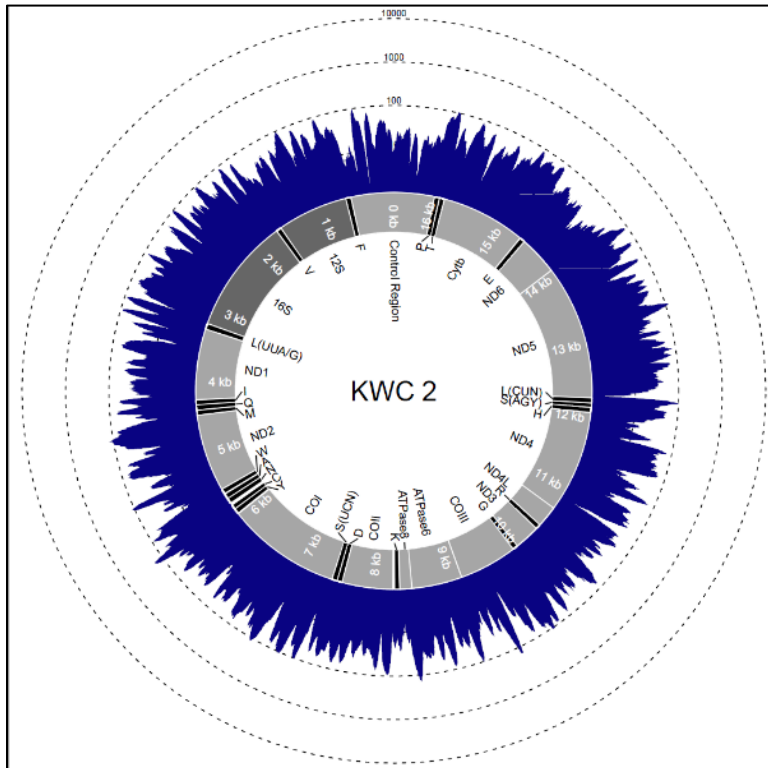
Sample Name	Number of Mito Reads	Endogenous DNA (%)	Mean MtDNA Coverage	Coverage(%)		Damage at 1st Base 5' (%)	Damage at 1st Base 3' (%)	Average Fragment Length (bp)
				1X	5X			
BMC 6a_SD	2,112	0.84	5.9	95.74	59.63	0.199	0.246	46.39
BMC 6a_DD	1,071	1.34	3.4	42.81	29.11	0.201	0.160	53.00
BMC 6a_merged*	3,641	1.23	10.6	96.98	79.95	0.202	0.218	48.04
GHZ 2_SD	2,756	0.80	7.8	98.71	79.09	0.216	0.236	47.06
GHZ 2_DD	673	1.01	2.12	38.27	18.31	0.210	0.310	52.37
GHZ 2_merged*	4,443	0.91	13.0	99.04	90.73	0.218	0.239	48.60
GHZ 5_SD	29,647	11.96	116.2	100	100	0.247	0.256	64.96
GHZ 5_DD	8,927	16.05	27.4	99.72	97.54	0.224	0.222	50.80
GHZ 5_merged*	146,987	12.84	450.6	100	100	0.258	0.269	50.82
KWC 2_SD	4,296	0.10	11.5	99.77	88.29	0.456	0.542	44.53
KWC 2_DD	14,171	0.50	38.2	100	99.93	0.489	0.546	44.65
KWC 2_merged*	27,465	0.44	71.3	100	99.99	0.486	0.526	43.03
KWC 6_oslo	3,609	0.07	10.3	98.42	79.35	0.497	0.494	47.16
KWC 6B_oslo	2,808	0.11	7.2	97.08	65.84	0.475	0.493	42.69
KWC 6_merged*	6,356	0.09	17.4	99.32	93.18	0.490	0.498	45.27
TARP 9B_oslo*	3,691	1.36	11.1	99.83	91.22	0.244	0.250	49.87

Results obtained from EAGER pipeline (Peltzer, et al. 2016). Output includes number of reads mapped to mitochondrial reference sequence. Endogenous content was calculated by the number of reads obtained/reads mapped to the human reference. Coverage was calculated from the number of unique reads that included a given nucleotide in a reconstructed sequence. Percentages reported for coverage at 1X to 5X coverage. Percent damage (misincorporations/lesions) recorded for both ends of reads. Naming example: “KWC 6_merged” combined reads from “KWC 6_oslo” and “KWC 6B_oslo.”

*** Libraries used for haplogroup analysis**

GHZ - Ghazali, KWC - Kwieka Cemetery, TARP - Tinga Archaeological Rescue Project, BMC - Berber Meroitic Cemetery; bp - base pair

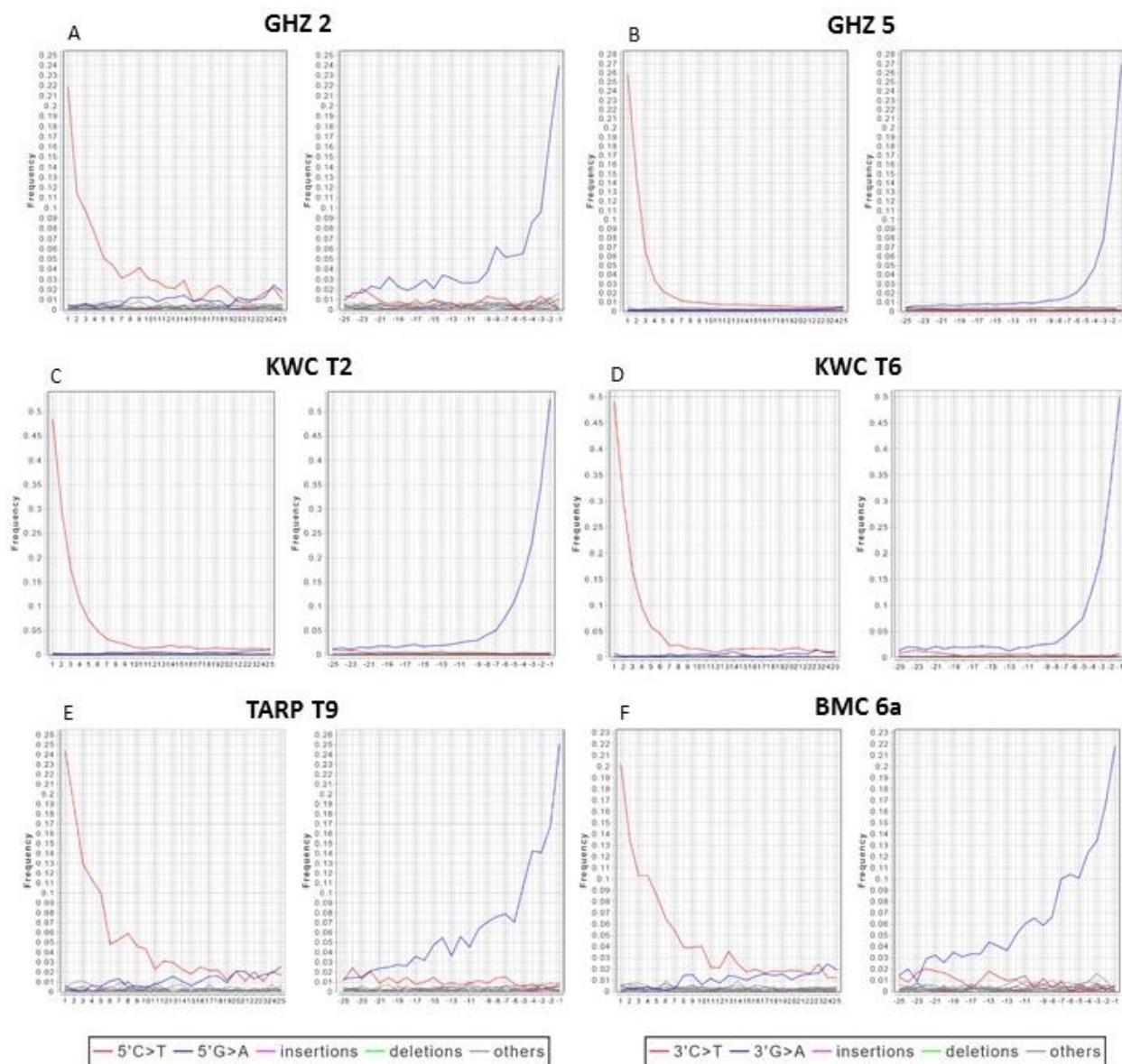
Figure 4.11. Example of Coverage Plot of KWC 2 on the circular human mitogenome.



Logarithmic scale for coverage amount (X). KWC 2 (Ind. Kwieka Cemetery 2) averaged 71X.

To authenticate the mapped reads as ancient, nucleotide misincorporation patterns were observed to be consistent with typical ancient genetic material. Percent damage at the first base on either the 5' or 3' end ranged from 20% to 53% (Table 4.3, Figure 4.12). Further authenticating these reads, the average fragment length of the six individuals varied from 43 to 51 base pairs (Table 4.3, Figure 4.13).

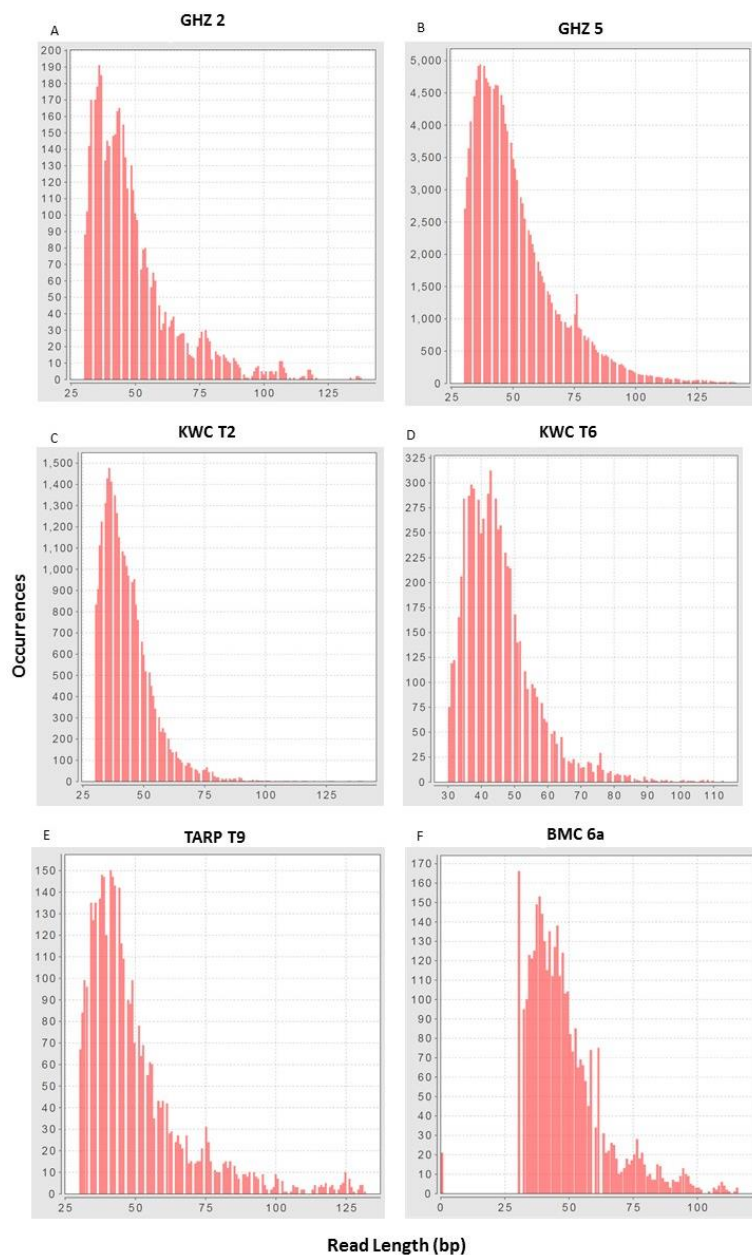
Figure 4.12. Map Damage Profiles of Mapped Mitochondrial Reads from merged library samples.



Misincorporation patterns observed for mapped sequences to the human mitochondrial genome following enrichment steps. Reads used totals: A) GHZ 2 (4,443 reads) B) GHZ 5 (146,987 reads) C) KWC T2 (27,465 reads) D) KWC T6 (6,356 reads) E) TARP T9 (3,691 reads) F) BMC 6a (3,641 reads). X-axis maps the position from the end of the sequence. Y-axis is the frequency of misincorporations of the mapped reads, in percentage. The cytosine to thymine (C>T) deamination rate at the 5' end is labeled in red (left graph). Guanine to adenosine (G>A) deamination rate at the 3' end is labeled in blue (right graph). Fuchsia indicates insertions, green indicates deletions, grey indicates other misincorporations. Scales are not identical for each individual. Map Damage Profiles, generated by mapDamage 2.0

(Jonsson, et al. 2013). GHZ - Ghazali, KWC - Kwieka Cemetery, TARP - Tinga Archaeological Rescue Project, BMC - Berber Meroitic Cemetery.

Figure 4.13. Read Fragmentation Plots of Mapped MT reads from merged library samples.



Read length distributions for samples mapping to human mitochondrial reference, generated by mapDamage2.0 (Jonsson, et al. 2013). Reads used totals: A) GHZ 2 (4,443 reads) B) GHZ 5 (146,987 reads) C) KWC T2 (27,465 reads) D) KWC T6 (6,356 reads) E) TARP T9 (3,691 reads) F) BMC 6a (3,641 reads). X-Axis displays Read Length, as measured in base pairs; ranges are not equal for all graphs. Y-axis measures all reads mapped by abundance including positive and negative strands, ranges different for all graphs. EAGER pipeline removes all sequences below

30bp that are likely contamination or too damaged and are typically not included in analysis. This parameter can be changed/extended, however sequences less than 30bp were not observed to be mapped for these samples. Scales are not identical for each individual. Map Damage Profiles, generated by mapDamage 2.0 (Jonsson, et al. 2013). GHZ - Ghazali, KWC - Kwieka Cemetery, TARP - Tinga Archaeological Rescue Project, BMC - Berber Meroitic Cemetery.

Molecular Sexing, Archaeological Context, and Haplotype Assignment

These six individuals span a wide breadth in time (Napatan (ca. 800-300 BCE) to Christian periods (ca. 600-1450 CE)) and space (3rd to 5th Cataracts). Additionally, various methodologies were utilized to obtain full coverage of the mitogenomes (Table 4.4). The archaeological context, sample material, and specifics of molecular sexing are individually outlined below in Table 4.4 and Table 4.5. Results of haplotype assignments with confidence percentages and specifics of the consensus sequence used (including contamination rates) are outlined in Table 4.6.

Two individuals were assigned to L lineage haplogroups, GHZ 2 – L2a1 and TARP 9B – L0a1a. Both of these haplogroups are common in modern Sudanese, 7.7% for L2a1 and 10.2% for L0a. However, haplogroup L0a is only common today within Southern Nilotes (Nuba, Dinka) (Hassan 2009). The other four Ancient Nubians were assigned non-Africa haplogroups (Figure 1.5). H2a was assigned to two individuals, GHZ 5 and KWC 2. Lineage N was assigned to KWC 6 (N1a1a3). Lastly, the Berber individual (BMC 6a) from the 5th Cataract was assigned to haplogroup T1. Taken together, all haplogroup assignments were superficially plausible and very broadly speak to a blend of African and Near Eastern descent (Table 4.6). In later haplogroup frequency surveys, all haplogroups were present in modern groups of Northeast Africa in various proportions, with the exception of Near Eastern haplogroups (N, T, H) in the southern Nilotic groups, Western Sudanese groups, and Pastoralists (Figures 4.14 and 4.15).

Table 4.4. Demographic and Archaeological information of Nubian individuals (ordered by date).

Sample Name	Excavation ID	Age Est.^α	Sex Est.^α	Sample Material	Extraction Method	Molecular Sexing^μ	Dating
GHZ 2	GHZ-4-008.2	30-40 years	Female	Tooth RM ²	SD, DD (UZH)	Female	Cemetery 4 670-770 CE
GHZ 5	GHZ-1-010	~45 years	Male	Tooth LM ²	SD, DD (UZH)	Likely Male	Cemetery 1 670-770 CE
BMC 6a	BMC 2009 63-6a (T6)	n/a	NA	Tooth RPM ₁	SD, DD (UZH)	Female	Meroitic ca. 3 rd Century CE
KWC 2	KWC T2	Adult	None	Bone R Petrous	SD, DD (UZH)	Male	Meroitic 350 BCE-350 CE
KWC 6	KWC T6	Child	NA	Bone L Petrous	DD, B+DD (Oslo)	Female	Meroitic 350 BCE-350 CE

TARP 9	TARP G9	Child	NA	Bone R Petrous	B+DD (Oslo)	Likely Female	Napatan 800-350 BCE
--------	---------	-------	----	-------------------	----------------	------------------	------------------------

^aMethods compiled by Buikstra & Ubelaker 1994, performed by archaeologists and/or anthropologists

[#]Mittnik, et al. 2016

SD - Single Digest, DD - Double Digest, B+DD - Bleach pretreatment + Double Digest;

UZH - University of Zürich; Oslo - University of Oslo

CE - Current Era, BCE - Before Common Era;

R/L - Right, Left; M - Molar; PM - Premolar;

GHZ – Ghazali, BMC - Berber Meroitic Cemetery, KWC - Kwieka Cemetery, TARP - Tinga Archaeological Rescue Project; T - tomb; NA - data not available because individual was a subadult, not performed, or data not available; Est - Estimation.

Table 4.5. Results of Molecular Sexing.

Sample Name	R-Squared Value, confidence intervals (CI - 95%)	Pipeline output/assessment	Outcome
GHZ 2	Rx = 0.970, 95% CI: 0.904, 1.036	Sample should be assigned as Female	Female
GHZ 5	Rx = 0.615, 95% CI: 0.564, 0.667	Sample consistent with an XY karyotype, but not XX	Likely Male
BMC 6a	Rx = 0.910, 95% CI: 0.872, 0.9488	Sample should be assigned as Female	Female
KWC 2	Rx = 0.509, 95% CI: 0.470, 0.549	Sample should be assigned as Male	Male
KWC 6	Rx = 1.035, 95% CI: 0.953, 1.117	Sample should be assigned as Female	Female
TARP 9	Rx = 0.822, 95% CI: 0.766, 0.877	Sample is consistent with an XX karyotype, but not XY	Likely Female

Table 4.6. Summary of consensus mitochondrial sequence information and haplogroup assignments.

Sample Name	Quality	Number of N's	% No Call	Haplogroup	Overall Rank (Quality)	Mean Coverage	Contamination
GHZ 2_merged	Q20	462	2.8	L2a1+143	91.81%	13X	1.0%
GHZ 5_merged	Q80	0	0.0	H2a	83.51%	450X	1.0%
BMC 6a_merged	Q30	1813	10.9	T1	76.83	11X	2.0%
KWC 2_merged	Q30	3	0.0	H2a	88.34%	71X	1.0%
KWC_6_merged	Q30	519	3.1	N1a1a3	89.62%	17X	1.0%
TARP9B_oslo	Q20	176	1.1	L0a1a	94.38%	11X	1.0%

Results of haplogroup assignments from Haplogrep 2 (Weissensteiner, et al. 2016), quality of consensus sequence used, number of missing nucleotides (counts and as a percentage of whole human mitogenome). Overall quality rank output from Haplogrep 2 as a confidence measure of the assignment, contamination percentages from Schmutzi (Renaud, et al. 2015).

N indicates “no call” or “missing data” at nucleotide position

Haplogroup Frequencies Dataset Analysis

To put the mitogenomes of Ancient Nubians within context of the Nile Valley and the wider Northeast region, the haplogroup frequencies dataset was assembled from published

sources outlined in Methods (Table 4.7). These data were visualized via two different means (Figure 4.14, 4.15).

Table 4.7. Haplogroup Frequencies Grouped by Population or Subpopulations (in percentages).

Haplogroup	Libyans	Egyptians	Nubians	Beja	Central	Western	S. Nilotes	Pastoralists	Ethiopians	Kenyans
L0	1.5	2.9	15.7	6.3	1.9	20.7	19.2	4.7	7.3	19.9
L1	3.4	1.6	5.6	8.3	7.8	14.9	11.7	23.3	2.9	4.2
L5	0.0	2.4	4.6	2.1	2.9	2.3	18.1	0.0	2.9	2.8
L2	8.6	6.1	11.1	16.7	20.4	25.3	26.6	23.3	14.2	9.2
L4	1.1	0.0	2.8	2.1	0.0	8.1	7.5	0.0	0.0	0.0
L3	12.7	5.2	17.6	35.4	34.0	28.7	17.0	39.5	8.1	30.4
L/N/M*	0.4	7.4	7.4	0.0	0.0	0.0	0.0	0.0	17.7	23.4
M	3.4	7.3	8.3	4.2	3.9	0.0	0.0	0.0	15.4	4.2
D	0.0	0.0	0.9	0.0	0.0	0.0	0.0	0.0	0.0	0.0
N	1.9	4.9	0.9	0.0	1.0	0.0	0.0	0.0	2.3	0.7
I	0.0	1.6	0.0	0.0	0.0	0.0	0.0	0.0	0.6	0.0
W	0.0	1.2	0.0	0.0	0.0	0.0	0.0	0.0	0.9	0.7
X	2.2	1.2	0.9	0.0	0.0	0.0	0.0	0.0	0.6	0.0
RO	6.3	0.0	0.0	0.0	0.0	0.0	0.0	0.0	0.0	0.0
HV	8.6	6.5	9.3	0.0	6.8	0.0	0.0	0.0	12.5	2.1
H	17.2	9.9	5.6	8.3	0.0	0.0	0.0	0.0	2.0	0.0
J	9.7	9.0	2.8	0.0	7.8	0.0	0.0	9.3	2.1	0.7
T	6.0	13.1	2.8	2.1	4.9	0.0	0.0	0.0	3.8	0.0
U	11.9	8.8	2.8	2.1	8.7	0.0	0.0	0.0	5.3	0.7
K	5.2	3.7	0.9	12.5	0.0	0.0	0.0	0.0	1.5	0.7
Other	0.0	6.6	0.0	0.0	0.0	0.0	0.0	0.0	0.0	0.0
Total N	268	244	108	48	103	87	94	43	344	141

Haplogroup frequencies expressed as percentages for populations and subpopulations in the Northeast Africa region, see Table 6 for ethnic groups included in geographic groups. Major Haplogroups (column 1) are collapsed for simplicity. Individual totals are listed at the end of the table. L/N/M* refers to undifferentiated individuals with not enough diagnostic variation sites to classify further. Grouping breakdown and references listed in Table 4.2. S; Southern.

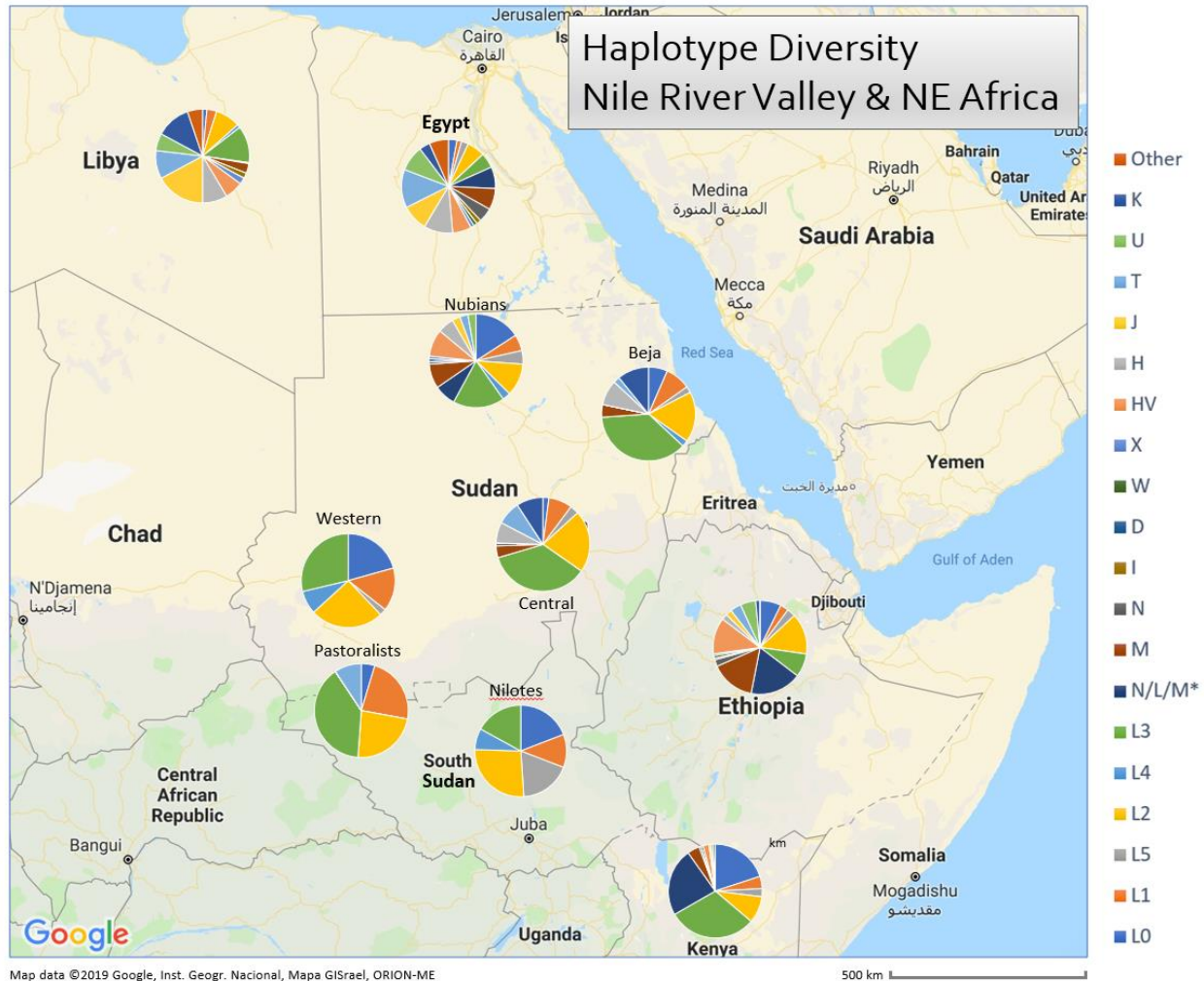
Analysis of Mitochondrial Genomes: Haplotype Profiles

Haplotype profiles are a useful way to visualize and quantify genetic differentiation and homogeneity among populations (Brandt, et al. 2013, Schuenemann, et al. 2017). From these haplogroup profiles, we observed highly similar signatures for southwestern ethnic groups of Sudan that showed less diversity than those in the north-east part of the country. Western,

Pastoralists, and Nilotes shared similar compositions of the Africa-specific L lineages, in slightly different proportions. Other subpopulations within Sudan showed much more haplotypic variation, including lineages outside of the L macrogroup. In general, the L3 lineage was the greatest proportion for a majority of populations or subpopulations of the Sudanese region, followed by L2 (Table 4.7, Figure 4.14).

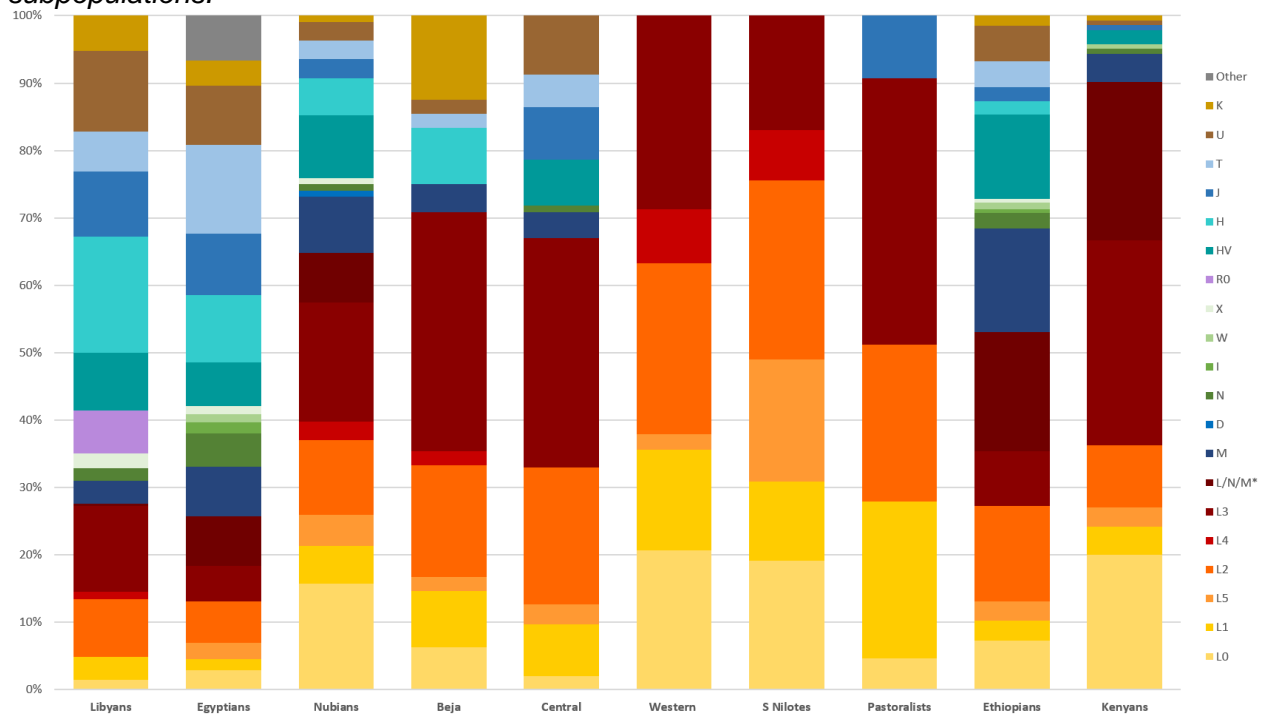
Haplotype frequencies were visualized as stacked columns to observe homogeneity between populations in this region (Figure 4.15). Arranged roughly geographically, the African signature increased in a step-wise fashion, with the other part of the profile being a Eurasia-originating component. The African ancestry of Libyans and Egyptians was less than 30%. Northern Sudanese, including the Nubian, Beja, and Central Arab ethnic groups have roughly 70% African ancestry. To be expected, the southern and south western Sudanese groups had none or very little Eurasian gene flow. Ethiopians also had a large non-African component like Egyptians and Libyans (ca. 70%), but this component was more intermediate (ca. 50%) when compared to the northern Sudanese groups (ca. 30%). Kenyans had an approximately 10% non-African component; however, 20% of this profile was not diagnostic to discern more specific haplogroups (i.e. classified as L/N/M*). While the six Nubians did not constitute a population and cannot be directly compared, these profiles placed the Ancient Nubians in context of the northeast region.

Figure 4.14. Haplotype Diversity of Northeast Africa region coordinated with geographic locations.



MtDNA haplogroup frequencies for modern populations of the Nile Valley and Eastern Africa, including Libya for comparison. A total of 1480 individuals are represented in these charts. Sample sizes for the populations are as follows: Libyans (n=268), Egyptians (n=244), Nubians (n=108), Beja (n=48), Central Sudanese (n=103), Western Sudanese (n=87), South Nilotes (n=94), Sudanese Pastoralists (n=43), Ethiopians (n=344), Kenyans (n=141). Haplogroup profiles for populations and subpopulations are depicted as pie charts coordinated with geographic locations; pastoralist groups do not have a set geographic location and instead occupy a larger expanse due to nomadic lifestyles. Sudanese subpopulations total 483 Individuals that is encompassed in the simplified pie chart to the left to emphasize the abundance of macrohaplogroups (legend right).

Figure 4.15. Haplotype Frequencies of modern Northeast African populations and Sudanese subpopulations.



MtDNA haplogroup frequencies for modern populations of the Nile Valley and Eastern Africa, including Libya, for comparison (N=1480). Sample sizes for the populations are as follows: Libyans (N=268), Egyptians (N=244), Nubians (N=108), Beja (N=48), Central Sudanese (N=103), Western Sudanese (N=87), South Nilotes (N=94), Sudanese Pastoralists (N=43), Ethiopians (N=344), Kenyans (N=141). All populations combined: individuals representing the North East African region around the Nile River Valley. Legend at right. Warm colors (red, orange, yellow) describe Sub-Saharan content of populations and subpopulations. Cool colors describe other lineages: back to Africa (M, N) and Eurasian lineages (H, etc.). N - number of individuals, counts.

Analysis of Mitochondrial Genomes: Haplotype PCA and Pairwise Differences

To further test genetic affinities and shared ancestry with extant African and Eurasian populations, a Principle Component Analysis (PCA) based on haplogroup frequencies and Multi-dimensional Scaling (MDS) of pairwise genetic distances using the F_{ST} statistic were performed. This dataset includes the six whole mitogenomes of the Ancient Nubians captured here, eight ancient groups, and 14 modern populations spanning Africa, the Middle East, and Europe (Table 4.1). For PCA analysis, mitogenomes were transformed into macrohaplotype frequencies and collapsed into large haplogroups based on geography given the role of geography in genetic structure (Hassan 2009, Babiker, et al. 2011, Hollfelder, et al. 2017, Dobon, et al. 2015). For F_{ST} or pairwise distance calculations, groups are specified in Table 4.1.

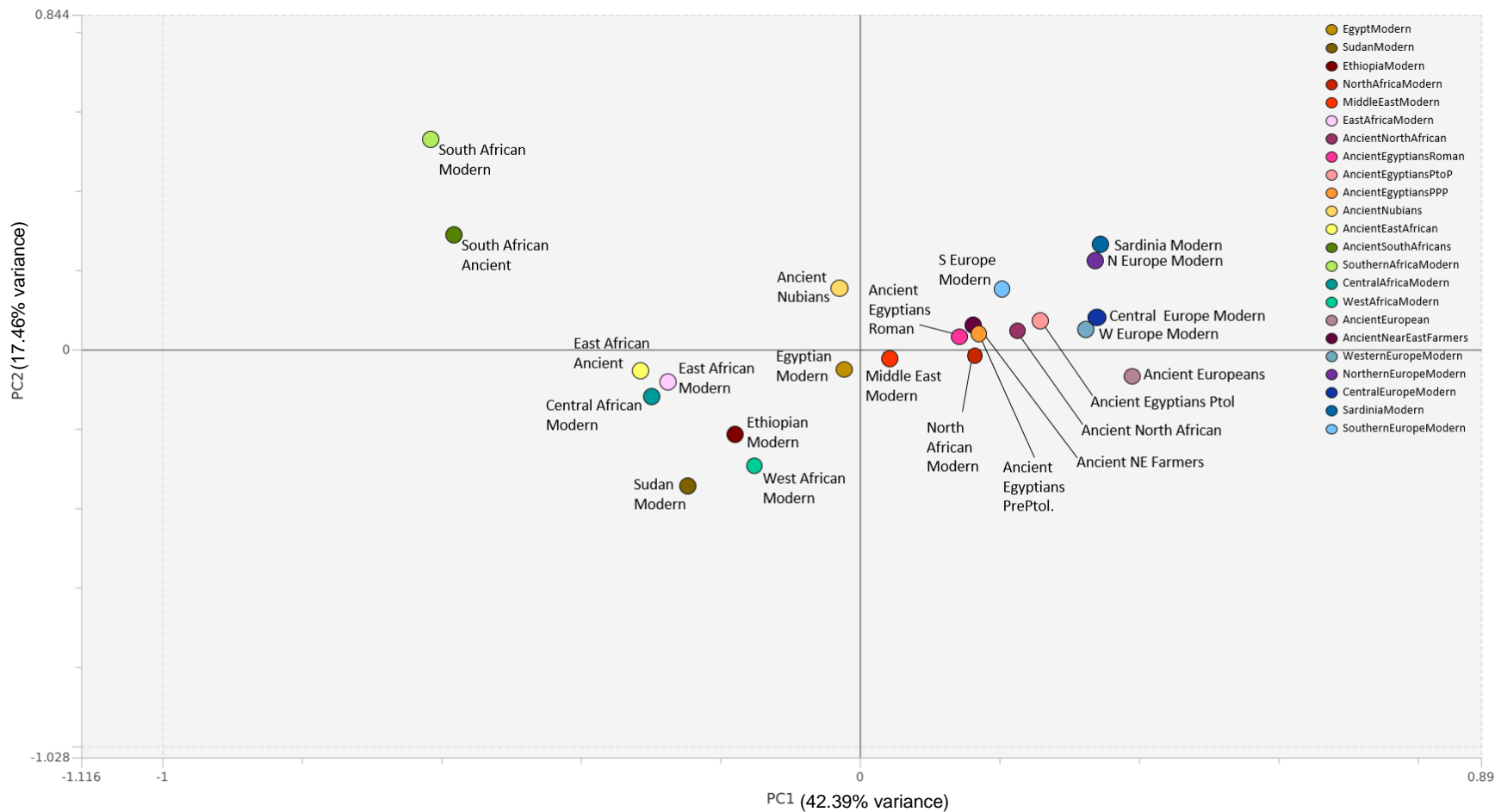
PCA is a standard tool used in genetic studies. It is a means to detect genetic structure, or any pattern in the genetic makeup of individuals or subpopulations within a population

(Chakraborty 1993). For this analysis, haplotype lineages, derived from full MT sequence data, were compared across 23 population groups. PC 1 characterized 42.39% of the variation, PC 2 characterized 17.46%, and PC 3 characterized 14.12%. Differences were observed among populations based on geography as dispersed by the first component in a south to north cline (left to right in Figure 4.16). The groups with the largest variation have the most influence on PC 1, namely South Africans and Europeans, which also were separated by the most physical distance. Populations with the highest genetic affinity cluster together. This was evident with Ancient and Modern Europeans and especially Near Easterners and Ancient Egyptians, which was expected as per Schuenemann, et al. (2017). North Africans of the Maghreb (or Northwestern Africa) also showed a close genetic signal to those populations geographically to the north. The Ancient Nubians clustered with Modern Egyptians and Middle Easterners. The Ancient Nubians and Modern Egyptians were not separated by PC 1, only by PC 2. Modern Sudanese and East Africans (modern and ancient) were separate from Ancient Nubians indicating genetic differences among these groups.

Generally, almost all African groups are on the left side of the plot, while Eurasian populations are on the right (Figure 4.16). The six Nubians have more affinity to African populations. The only exception to this divide is the Ancient Egyptians. This result is consistent with previously reported data: these Ancient Egyptian populations from the northern Fayum and temporally from three different time periods showed high affinities to modern populations in the Levant and Near East, as well as showed population continuity (Schuenemann, et al. 2017). In general, PC 2 does not separate the groups, except for the South Africans (both ancient and modern).

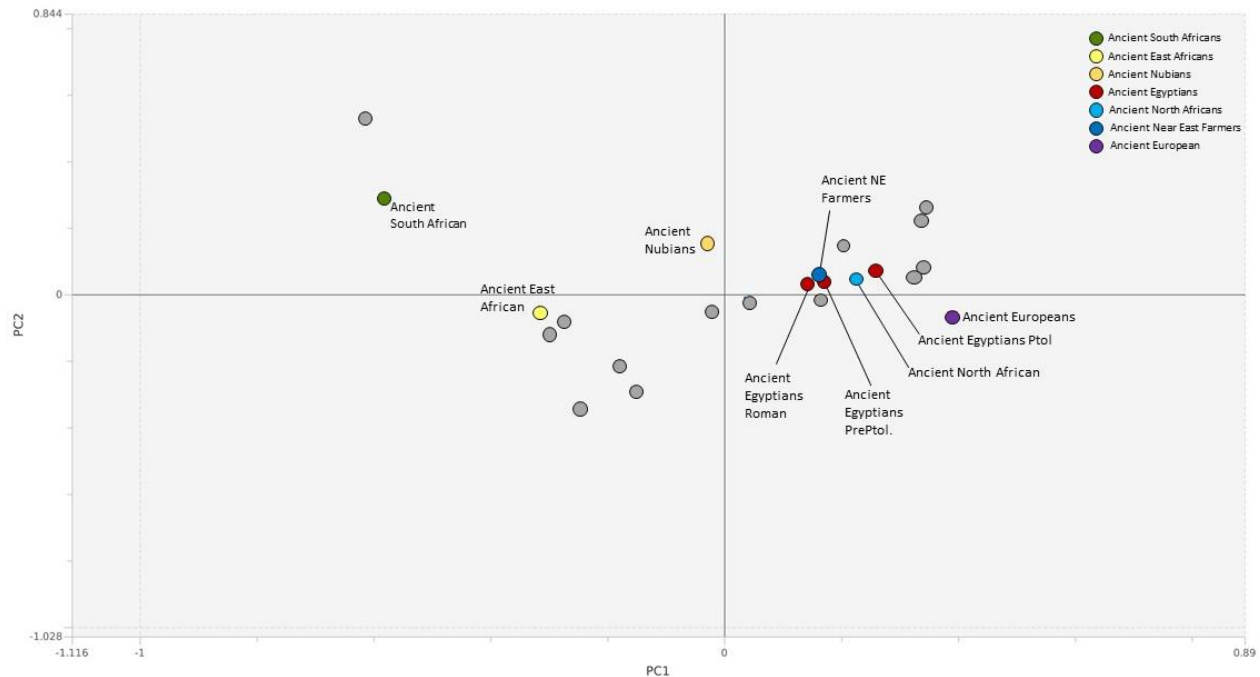
When only highlighting the ancient populations (Figure 4.17), again the role of geography was prominent and the most important driving factor for variation among these groups. While it was expected to observe the clustering of Ancient Egyptians with Near Eastern farmers and Europeans, Ancient Nubians fell between East African populations and groups centered around the Mediterranean. With considering modern populations only, Ancient Nubians showed the most affinity to Modern Egyptians and Middle Easterners, and somewhat to Southern Europeans and North Africans; in general, Mediterranean populations, rather than modern African populations. Overall the Ancient Nubians show affinity toward both African and European groups and much more so than Ancient Egyptians.

Figure 4.16. Principle Component Analysis based on haplotype frequencies, whole MT genomes.



PCA constructed in MitoBench. Legend on the right, with corresponding colors of groups listed in Table 4.1.

Figure 4.17. Principle Component Analysis based on haplotype frequencies, ancient groups only.



PCA constructed in MitoBench. Modern populations in grey to highlight only ancient populations. Legend on the right, with corresponding colors of groups listed in Table 4.1. Ancient Egyptians colored the same for simplicity. PC 1 characterizes 42.39% of the variance, PC 2 characterizes 17.46% of the variance.

Pairwise F_{ST} is a measure of population differentiation (Weir & Cockerham 1984, Holsinger & Weir 2009). Much like a percentage, values of this statistic range from 0 to 1, with zero indicating no genetic difference and one indicating complete genetic divergence. Whole MT genome data was used to examine pairwise differences of all populations listed in Table 4.2. In general, populations that were geographically close had lower pairwise F_{ST} . Values ranged from -0.015 to 0.363 (Table 4.8). (Negative values were the result of the transformation of F_{ST} values by Arlequin and likely the smaller population sizes given that the estimator requires large population sizes (Weir & Cockerham 1984)). Pairwise F_{ST} was the greatest between South Africans and modern Northern Europeans ($F_{ST} = 0.305$). The negative F_{ST} values are effectively not different from zero, we can therefore conclude that the Ancient Nubians had the closest affinity (or lowest F_{ST}) with modern Egyptians ($F_{ST} = -0.015$), with modern Ethiopians ($F_{ST} = -0.001$), and Modern East Africans ($F_{ST} = -0.011$). Following these were close affiliations with modern Central Africans ($F_{ST} = 0.0041$), modern Middle Easterners ($F_{ST} = 0.012$), and modern Western Africans ($F_{ST} = 0.013$). Slightly less similarity was shown to modern Sudanese ($F_{ST} = 0.037$) and North Africans ($F_{ST} = 0.049$) as well as ancient East Africans ($F_{ST} = 0.029$). Ancient Nubians were the least similar to Northern Europeans ($F_{ST} = 0.305$) and modern Southern

Africans ($F_{ST} = 0.363$). Overall, the values obtained from the F_{ST} analysis support the clustering shown in the PCA and show the differentiation of South African groups.

Table 4.8. F_{ST} Values for comparisons to Ancient Nubians.

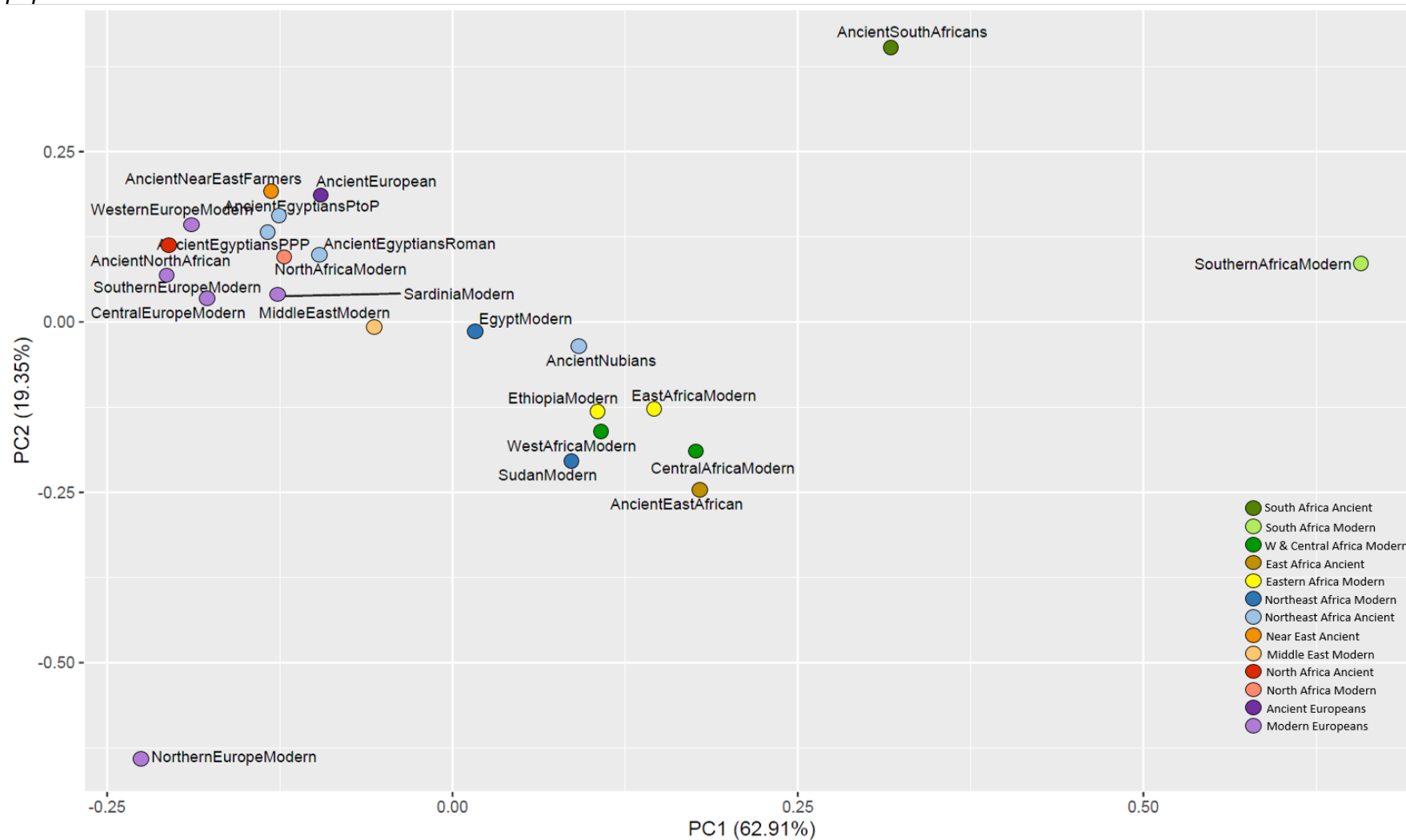
Population	F_{ST}
EgyptModern	-0.015*
EastAfricaModern	-0.011*
EthiopiaModern	-0.001*
CentralAfricaModern	0.004
MiddleEastModern	0.012
WestAfricaModern	0.013
AncientEastAfrican	0.029
SudanModern	0.037
NorthAfricaModern	0.049
AncientEgyptiansRoman	0.065
AncientEuropean	0.072
AncientEgyptiansPPP	0.087
AncientEgyptiansPtoP	0.100
WesternEuropeModern	0.102
CentralEuropeModern	0.105
AncientNorthAfrican	0.113
AncientNearEastFarmers	0.120
AncientSouthAfricans	0.127
SardiniaModern	0.151
SouthernEuropeModern	0.163
NorthernEuropeModern	0.305
SouthernAfricaModern	0.363

* Negative values were the result of the transformation of F_{ST} values by Arlequin and likely the smaller population sizes given that the estimator requires large population sizes (Weir & Cockerham 1984). Negative values were changed to “zero” for the heat map and ‘0.0001’ for the Multi-Dimensional Scaling plot.

F_{ST} values were visualized using an MDS plot (Figure 4.18). Like the PCA analysis, this dimension-reduction is a means to graphically represent the similarities (clustering) and differences (distances) captured in the F_{ST} values. Distance calculations derived from genetic variation across the entire MT genome were used for analysis. PC 1 explained 62.91% of the differences, while PC 2 characterized the next 19.35% variation. Ignoring the clear outliers, Northern Europeans and Southern Africans, two clusters were visible (Figure 4.18). One included all (other) Europeans, North Africans, Middle East or Near Easterners, and all Ancient Egyptians. The second cluster included Modern Egyptians and Africans south of North Africa (East, Central, Western) (Figure 4.18). Ancient Nubians were again between East Africans and the Egyptians. Focusing on the right cluster, these groups (modern Egyptians, Ethiopians,

Sudanese, Central, West, and East Africans, Ancient Nubians, and East Africans) vary amongst one another with Dimension 2 more so than the cluster with Eurasian populations, North Africans, and Ancient Egyptians. Within this cluster, Nubians (and Modern Egyptians) showed the most differences between Ancient East Africans and Modern Sudanese. Like the PCA plot, PC 1 served as a means to classify groups by geography, where this dimension separated African populations groups from Eurasian groups, with the exception of Modern and Ancient North Africans and Ancient Egyptians. Overall, Ancient Nubians clustered most closely with Modern Egyptians, Modern East Africans, and Modern Ethiopians.

Figure 4.18. Multi-Dimensional Scaling Plot mapping F_{ST} pairwise differences among Ancient and Modern African and Eurasian populations.



Population labels simplified to geographic region. Colors of light and dark shades correspond with these simplified regions for better visualization.

DISCUSSION

In the ancient past, northern Sudan was home to multiple powerful and dynamic Nubian kingdoms (i.e. Kermites, Kushites, Christians). We know much of this time from various fields of study including archaeological research, historical and ethnographic records, and anthropological research, but the population genomics of this time has yet to be investigated. Modern genetic data of Nubian Sudan tells two stories: possible links exist to an ancestral past with East Africa and the effects of the Arab expansion dominate the genetic profiles of modern individuals. What was the genetic landscape of Nubians before this major event? Archaeological, historical, and anthropological work has demonstrated that Nubians had a dynamic history in the Nile River Valley with notable demographic shifts – colonialism, entanglement, conquest, expansion – that likely had a quantifiable impact on their genetic structure. To explore this and begin to join these lines of evidence, paleogenomic methods were used to sample mtDNA from ancient Nubians, providing a new line of data to understand Sudan's ancient past and begin to define their biological ancestry.

ADNA was extracted from archaeological samples from Sudan dating (c14 or contextually) to before the Arab expansion. Sequence data from targeted MT genome capture was used to characterize the haplogroups of the ancient Nubians. The full mitogenomes obtained here were the first ancient Nubian genomes to date. Only one other study has published genomes of Nile River Valley individuals (Schuenemann, et al. 2017). The analyses performed here were the first to contextualize Ancient Nubians within the African and Eurasian landscape. In general, Nubians are more closely affiliated with African populations than Ancient Egyptians.

Two individuals were assigned to have African ancestry (L haplogroups) and four were assigned to non-African lineages, namely those originating in the Near East (H, N, T haplogroups). These individuals derive from varying archaeological contexts and therefore different cultural horizons in Nubian history. The individual deepest in time, the Napatan period, is likely the oldest Nubian to be sequenced yet and helps address our questions about Nubian genetic structure in the past. Individual TARP 9B originated from deep within the Nubian lands and was assigned the haplogroup L0a, which demonstrates the presence of this haplogroup during the Napatan (ca. 800-300 BCE) time period. The macrogroup L0 is the most ancient lineage of mtDNA and its subgroup L0a1 dates to roughly 25,000 years ago with a probable origin in Southeast Africa (Rito, et al. 2013, Soares, et al. 2009) (Figure 1.5). The other individual with African ancestry is GHZ 2, who was dated much later in the early Christian period

and was assigned L2. This group is a very common macrohaplogroup within Sudan, being the second most abundant following L3 (Hassan 2009). Kulubnarti individuals from ancient Lower Nubia have also been classified with this haplogroup (Sirak, et al. 2016). Both of African lineages were within the range of Sub-Saharan African variability and are extremely rare outside Africa (Salas, et al. 2004). Beyond Sudan, the macrogroup L2a likely originated in central or western regions of Africa (Silva, et al. 2015) and its subgroup L2a1, which dates to roughly 20,000 years ago, is common all over the continent (Salas, et al. 2002, Soares, et al. 2009). Generally, within the ancient Nile Valley, these two L assignments of African lineages have not been detected in Egypt (Schuenemann, et al. 2017), but have been in ancient Tanzania and Malawi (Skoglund, et al. 2017, Prendergast et al. 2019). These are overall rare, and more sampling of ancient individuals inside Africa will offer more context. In the meantime, these data build our narrative of the African component of Nubian genetic background and specifically characterize the unique background of inhabitants in this region.

The four other individuals which we obtained full mitogenomes for were assigned to lineages which have origins outside Africa (H, N, T) and demonstrate the presence of these haplogroups within the ancient Nubian genetic landscape. Individuals GHZ 5 (Christian era monk) and KWC 2 (Meroitic individual from 5th Cataract) were both assigned H2a haplogroups. The H macrogroup is the most common one in Europe and Eurasia but has Near Eastern origins with a modern distribution around the Middle East, particularly in the Caucasus region and the Arabian Peninsula (Pereira, et al. 2005, Achilli, et al. 2004, Roostalu, et al. 2007). While the H or HV lineages are common in Ancient Egypt, none have the H2a assignment. The appearance of this haplotype deep in Sudan suggests migrations from the Near East or Levant regions and it is especially plausible that one individual, GHZ 5, was buried at a monastery where people may have traveled for pilgrimages.

The other individual from Kwieka, KWC 6, was assigned to the haplogroup N1a1a3. The macrogroup N1a originated in the Near East and is common amongst Neolithic Europeans (Haak, et al. 2005). N1a is distributed throughout Eurasia and northeastern Africa, especially with Afro-Asiatic speakers (Hassan 2009). This haplogroup also originated in the Near East and is a subgroup of the R and JT lineages (Figure 1.5). This specific haplogroup was present in one Ancient Egyptian dating to around the same period and another dating to dynastic eras (Schuenemann, et al. 2017, Neukamm *in prep*). Within modern genetic context of Sudan, this haplogroup is prevalent among modern Afro-Asiatic speakers (i.e. those groups of Arab descent), while being virtually absent in Nilo-Saharan speakers (Bekanda, et al. 2015). This is also the case for the Berber 6a individual (BMC 6a) who was assigned as belonging to

haplogroup T1. This group has origins in the Near East, but more so in West Eurasia (Fernandez, et al. 2015). Although these are only two individuals, this hints at dating the presence of a Eurasian component well before the Arab expansion and reaffirms the idea that the Nile Valley was a corridor of movement in antiquity (Krings, et al. 1999, Lalueza Fox 1997). Additionally, this challenges the hypothesis that the genetic structure of Ancient Nubians resembled Nilotic groups, which have no Eurasian signatures within autosomal or mitochondrial genomes (Hollfelder, et al. 2017). However, this is but one individual cannot speak for a population and should certainly be carefully interpreted since multiple markers are in use when investigating the genetic structure of Sudan, which have their own biases and advantages. More sampling and collecting autosomal data are of the utmost importance moving forward.

All haplotypes that were classified in the Ancient Nubians were found in modern Nubians (Table 4.7), so population continuity cannot be ruled out. Specifically, the Berber 6a individual was assigned as T1; this lineage was found in all groups except those groups that represent ancestral East Africans. The TARP 9 and GHZ 2 individuals were assigned African L lineages, shared by all populations in this region, while all others were non-African. Furthermore, these two individuals were the separated by the most time, likely more than one thousand years. The haplogroup H2a was assigned to two individuals from two sites separated by both time and space. This haplotype was present in Egyptians, Libyans, Ethiopians, northern Sudanese groups, but not the Central Arab group. The N lineage haplogroup assigned to the Lower Nubian KWC 6 individual was much rarer within this context but was present in extant Nubians. This lineage was most common in the Egyptians. Moving forward, more individuals are needed to formally test continuity between past and extant populations.

When grouping these individuals as a very approximate population, F_{ST} calculations and PCA showed that Nubians were genetically close with modern Egyptians, followed by modern Middle Easterners and modern East African groups. This close affinity with Egyptians also has been demonstrated with modern Northern Sudanese genetic data and has been hypothesized to extend back in time (Babiker, et al. 2011, Krings, et al. 1999). Results presented here do not indicate population continuity, but also do not rule it out. Further testing of this hypothesis is warranted. The PCA also showed Ancient Nubians were not as closely affiliated with their descendants, but showed clear signs of gene flow during antiquity as indicated by Lalueza Fox (1997), Dobon, et al. (2015), and Babiker, et al. (2011). Overall, Nubians were characterized by a significant African component within their profile (more so than Ancient Egyptians) with enough gene flow from the Middle East and Europe to make them distinct from other African populations. These signals suggest more genetic structure than hypothesized by Hollfelder, et

al. (2017) when surveying modern Nubians in northern Sudan. The haplotype assignments, even only six, show vast differentiation from the Southern Nilotes, which were genetically isolated and hypothesized as being ancestral East African, as per Hollfelder, et al. (2017). The variety of haplogroups suggests more admixture due to the presence of non-African lineages while Southern Nilotes have none. These data are consistent with the notion Nubians have African and Mediterranean or Eurasian ancestry, which is reflected in anthropological, archaeological, and ethnographic observations and confirms this dimension of Nubian character (Armelagos & Van Gerven 2017).

The analyses of the mitogenomes reinforce the influential role geography plays in shaping the genetic landscape of Africa. The most variance captured in PC 1 differentiated African groups in a south to north cline in both dimension-reducing analyses. This suggests that geography is a sound indicator of mitochondrial structure. This finding reinforces the idea that population geneticists should consider geography when investigating genetic diversity across wide areas (Peter, et al. 2018).

Relating to the methodological specifics of this study, we performed an enrichment step in order to retrieve full ancient mitogenomes. For many individuals, initial shotgun sequencing of reads mapping to the mitochondrion were as low as zero but increased to several thousand post-enrichment. Merged consensus sequences produced deeper coverage of the mitogenome and provided subsequent haplogroup assignments with more confidence. For example, merged reads for KWC 6 assigned the haplogroup N1a1a3 with 89.62% confidence, which was higher than the separate reads, and with 2 times less N's (or no calls/data) for diagnostic loci. Based on these findings, we advocate that enrichment be implemented for all future work with Nubian samples. In addition, the use of two separate, parallel extracts with enrichment was required for full reconstruction of five out of the six genomes obtained. Each extract contributed unique sequence reads that increased the coverage of the MT genome. In other words, each extract exhibited high complexity and little to no overlap. For example, the mean coverage of the merged reads for KWC 6 was 10X and 7X for the non-bleached and bleached powder, respectively, and following merger, the coverage increased to 17X, demonstrating the uniqueness of the libraries from each extract (Table 4.3). However, it should be noted that two extracts require more starting tissue and therefore multiple extractions from the same individual should only be performed after careful consideration of the benefits. Libraries should be immortalized, especially those not enriched, to extend the use of these extracts to the fullest capacity (i.e. to be used for whole genome or SNP-enrichment assays).

Several limitations narrowed the scope of this study. First, our final sample size was small. Out of 43 individuals trialed, six individuals had full genomes for analysis (14% success rate). Furthermore, this small number of individuals does not create a homogeneous “population” since they were excavated from four different field sites with unique archaeological contexts and span up to 1,000 years in time (Figure 1.5, Table 4.4). These analyses would greatly benefit from a larger dataset with each archaeological context considered independently (e.g. Brandt, et al. 2013). Second, our analysis lacked resolution of the Sudanese mitochondrial landscape. Despite robust research projects focused on Sudanese population genetics, mitochondrial sequence data has not generated. Only one seminal dataset, Krings, et al. (1999), is available. However, it only characterizes two regions of the country (i.e. Northern Nubians and Southern Nilotes) and is limited to HVR1 sequence data. In the NGS age, trends toward larger datasets mean full mitogenomes will likely be available in the future. Fortunately, Dr. Hisham Yousif Hassan (from Hassan (2009), Bahrain Defense Force Hospital) has full mitogenome sequences for 15 known ethnic groups (used in Dobon, et al. 2011) within the country. These data will be published in the next year and will bring meaningful resolution to the mitochondrial landscape of modern Sudan for future work. Lastly, mtDNA analyses only represent the maternal landscape. Additional loci would be informative for understanding the history of paternal lineages, sex-biased gene flow, and genetic adaptation. Nevertheless, mtDNA can address cross-disciplinary questions from archaeologists and anthropologists about ancestry and migrations and should be included whenever possible.

Future directions of this work include further sampling of individuals across the Nubian landscape, possibly expanding into Lower Nubia, as well as augmenting the sample size of the populations that were successful and previously demonstrated very good preservation of sample tissue, i.e. Ghazali and Kwieka individuals. Data from the nuclear genome would be very informative for understanding Nubian paleodemography beyond the maternally inherited mtDNA. Shotgun sequencing results of the samples extracted here showed preservation of ancient nuclear DNA, even in the absence of mitochondrial DNA. This suggests that nuclear enrichment would be plausible to explore the Nubian autosomal genome. Further anthropological context of the successful individuals and their archaeological sites should also be collected. Prendergast, et al. (2019) serves as a notable publication worth emulating as it provides equal footing of archaeological context with genetic data within a manuscript.

This work demonstrated the viability of paleogenomic work using archaeological material from Middle Nile region. Even with mitogenomes from only six individuals, the dynamic ancestry of Nubia is reflected in their genetic past and begins to build the narrative centered on Nubian

genetic structure. Given the long tradition of the research in this region of the Nile Valley by other disciplines, aDNA will supplement and advance our knowledge of Nubian history. Overall, paleogenomic work offers a unique perspective to join with archaeological and historical data and can be especially helpful when these sources are sparse, contested, or unavailable.

CONCLUSION

Recent advances ancient DNA methodologies has opened the continent of Africa to the paleogenomic revolution. Mitochondrial DNA from ancient Nubian sources showed that these individuals have gene flow from the Eurasia, but have close genetic ties with Africans. This is consistent with the population interactions and demographic shifts attested to in archaeological and anthropological studies as well as historical texts. These data are the first ancient mitochondrial genomes to be reported and offer a new facet to understanding Nubian ancestry, specifically the ties to Near Eastern haplogroups but also the ancestral African ones. This blending can be further explored with more sampling and better comparative datasets built with mitochondrial DNA.

CHAPTER 5: Conclusion

This dissertation synthesized Nubian paleogenomic data with skeletal bioarchaeological evidence to understand the population history of the El-Kurru population, dating to the end of the Christian era and beginning of Arab expansion in Upper Nubia. This multidisciplinary approach included paleogenomic analyses of the ancient individuals set within an archaeological and bioarchaeological framework. Since modern genetic data does not shed light on the genetic landscape prior to the Arab expansion in Sudan and there is a lack of ancient Nubian genetic datasets for comparison, seven additional archaeological sites were sampled to define Nubian ancestry in this region. Additionally, new paleogenomic methodologies were optimized using newly or previously developed techniques because African samples are difficult to work with on account of poor DNA preservation and thermal degradation. While the ancient DNA extraction was not successful for the El-Kurru individuals, it was with individuals from other archaeological sites. These six individuals help build what we know about Nubian genetics in the ancient past and establish the viability for continued work with material from the Middle Nile region of Sudan.

With a viable method to extract aDNA, the two part approach can be implemented in various other regions of the Nile Valley, namely pairing paleogenomic data with bioarchaeological analyses of individuals and populations. Mortuary and bioarchaeological data can add a meaningful viewpoint on the daily lives and environments in which these individuals lived. As was demonstrated with the Neolithic Transition example, the genetic perspective can be very useful when in context with multiple layers of evidence. For the population from El-Kurru, a group likely at the brink of transition to Islam as it expanded to the south, their Christian religious affiliation was expressed in death with typical body treatment and grave construction. Their hardships with malnutrition, disease, and/or other stressors was recorded in their remains and told a story that despite a heavy disease burden on the younger individuals, adults were still living to an old age. Their burial practices suggested that this time of transition to Islam had not arrived, or even if it had and the inhabitants kept to their Christian identities, the health profiles as a community speak to little to no negative impact of this transition. More populations from this

area and time period would supplement this narrative and give greater insight into life during this transitional time period, in addition to successful paleogenomic analyses.

This work defined a workable protocol that should be shared with other colleagues working with African materials or those from similar arid climates. There is also room for further improvements. To build full mitochondrial genomes at 10X coverage or more, either or both pretreatments of sample powder were enough to prepare the samples for enrichment, but two separate extracts were necessary. This is an important area to improve upon to be less consuming of archaeological material. For those samples from tumuli burials which performed incredibly poorly, more trials could be conducted to obtain aDNA, as these individuals represent an important transitional time period (the Post-Meroitic, ca. 350-650 CE) in Nubian history and the skeletal remains are accompanied by extensive bioarchaeological data. This would represent another area to implement the two-part research design. However, we would generally caution restraint when sampling material for a second time as it is destructive and it is important to leave some tissue unsampled for future developments within the field. Given the blistering pace at which paleogenomics progresses, it may not take much time for improved techniques to yield robust aDNA yields from samples that yield minimal to no aDNA with current methods.

With an established methodology, an expansion of this project is achievable. Mitochondrial DNA was the first survey step and initial successes open more options for further research in this field, including autosomal DNA retrieval for more impactful comparisons with available datasets from modern Sudanese and other ancient Africans (Figure 1.8). Expansion is also possible during the laboratory phase; for example, the inclusion of automated steps during the enrichment part would make the process more high-throughput since multiple extracts are required to build the mitogenomes. Despite the small number of successful genomes obtained, the initial results, where two Nubians have African ancestry and four have non-African ancestry, supported the role of the Nile River Valley as a corridor. Compared to modern mitochondrial DNA, these Nubians are most genetically close to modern Egyptians, Middle Easterners, and East Africans. They are less affiliated to modern Sudanese, Ancient Egyptians, and Ancient East Africans. This lack of genetic closeness to the modern Sudanese may be a product of sampling, given the high diversity within Sudan which is heavily driven by geography. More informative comparative populations with provenience are required to better contextualize the results and also those concerning the closeness to modern Egyptians. Lastly, additional Nile Valley populations from Egypt and Ethiopia would increase this resolution

To address questions concerning ancestry and characterizing of the genetic make-up of Nubians before the Arab expansion, development of more homogeneous populations for each site is critical for further analyses. This would involve obtaining genetic sequences from more individuals at each site, all of which represent distinct time periods and cultural contexts. Given the vast number of collections previously excavated and those yet to be discovered, building a larger sampling base is possible and will further advance the foundational research described here. It will be especially imperative to augment those individuals who are temporally, spatially, or contextually linked (e.g. individuals from El-Zuma, El-Detti, and Tanqasi which are close in proximity and date to the same Post-Meroitic period). In general, deeper sampling will create valuable resolution for work in this area.

As we expand our knowledge of the genetics of Upper Nubia, this narrative would specifically benefit from a contribution of sample populations from Lower Nubia, or the region between modern Aswan and the 2nd Cataract. This region was significant as the buffer-zone between Upper Nubia, where the capitals of Kush, Napata and later Meroe, are located, and southern ancient Egyptians. During dynastic time periods, this region fluctuated between peaceful and forceful Egyptian occupation, often to protect the flow of trade goods (Flammini 2008). During the Roman period, this area had an ever-shifting frontier zone, fortified or not, but continued to be an interface for populations (Török 2008). Later, this region played a crucial role in keeping the Arab forces at bay beginning in the 6th century CE through to when the Arab forces took control of northern Sudan. Given this long history of interaction, the contribution of samples from this region is of great importance when mapping the genetic landscape of Nubia and widens the scope to include the greater Nile River Valley.

Appendices

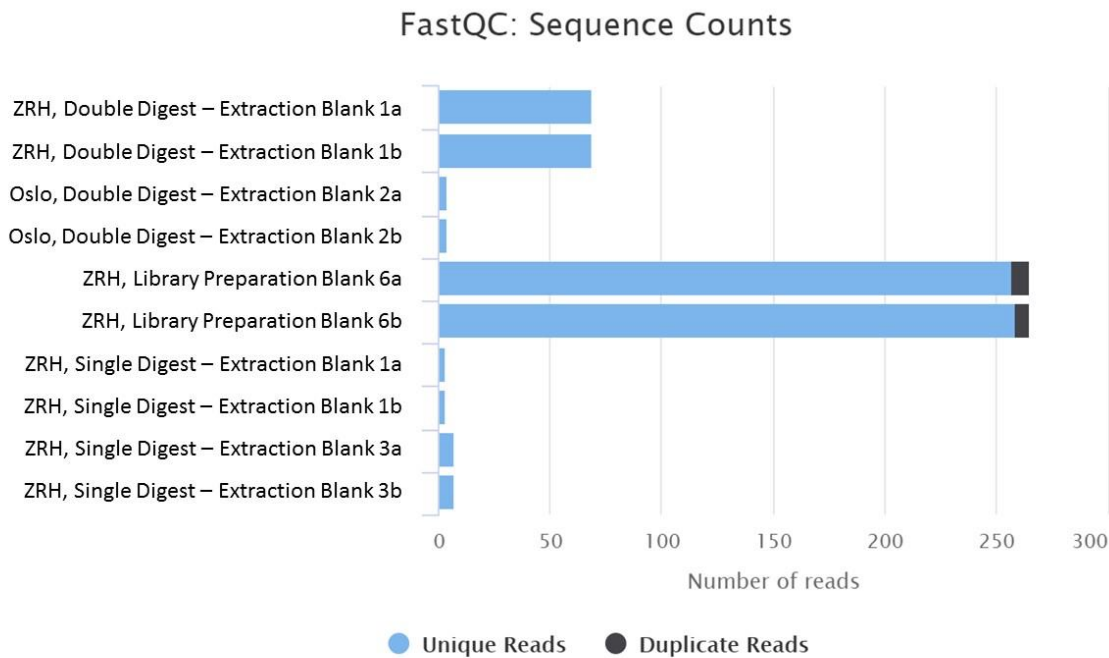
Appendix A - Supplementary information relating to methods:

1. Stainless steel mortar and pestle (or “Bone Crusher”) cleaning – after Oslo Lab protocols
 - After each use, clean each piece (mortar, pestle, sleeve) with dish detergent (crystal form for more abrasiveness) and a tooth brush to clear away bone dust
 - Rise all pieces with tap water until no bubbles remain, usually 3x
 - Place all pieces, laying flat, in a small tray or bin. It is helpful to reassemble the mortar and sleeve for bleach bath in next step
 - Cover with 2X bleach solution, making sure all used surfaces are completely covered
2. Sodium Hypochlorite solution is typically available at 14X concentration and should be diluted to 2X, i.e. 100mL 14X bleach diluted with 700mL Milli-Q water (UV irradiated)
 - Incubate for at least 15 minutes to disinfect
 - Rinse thoroughly with Milli-Q water (UV irradiated)
 - Rinse with 20% Ethanol solution and dry with lab tissues
 - UV treat for at least 10 minutes before next use

Appendix B - Analysis / MultiFastQC of negative control samples

As outlined in the methodology, negative blanks were carried through all parts of the protocol including mitochondrial enrichment and in both laboratories. In total, there were 15 blanks from all enrichment trials: three from Oslo, three from extractions via single digest method, three from extractions via double digest method, six blanks from the library preparation step. Most libraries were completely empty, while some had few reads that mapped the human reference sequence. Those with read counts ranged from 3 to 259 (Figure S1). The only sample with enough reads to observe typical damage patterns of ancient material was Library Prep Blank 6 that had an average MT coverage of 0.0057. These reads showed exactly zero percent damage suggesting no cross-contamination of the ancient samples during lab work.

Figure S1. Sequence counts histogram of Negative Blank libraries with more than zero reads.



Created with MultiQC

MultiQC Analysis (Ewels, et al. 2016).

References

- Abdallah, M. S. (2018). Preliminary report on the excavations in Kwieka cemetery (KWC) – seasons 2016 and 2018. *Sudan & Nubia*, 22, 142-149.
- Abu-Amero, K. K., Larruga, J. M., Cabrera, V. M., & González, A. M. (2008). Mitochondrial DNA structure in the Arabian Peninsula. *BMC Evolutionary Biology*, 8(1), 45.
- Achilli, A., Rengo, C., Magri, C., Battaglia, V., Olivieri, A., Scozzari, R., Cruciani, F., Zeviani, M., Briem, E., Carelli, P., Dugoujon, J., Roostalu, U., Loogväli, E., Kivislid, T., Brandelt, H., Richards, M., Villems, R., Santachiara-Benerecetti, A.S., Semino, O., & Torroni, A., (2004). The molecular dissection of mtDNA haplogroup H confirms that the Franco-Cantabrian glacial refuge was a major source for the European gene pool. *The American Journal of Human Genetics*, 75(5), 910-918.
- Adams, W. Y. (1967). Continuity and change in Nubian cultural history. *Sudan Notes and Records*, 48, 1-32.
- Adams, W. Y. (1977). *Nubia: corridor to Africa*. 1st edition. London: Allen Lane.
- Adams, W. Y. (1984). The first colonial empire: Egypt in Nubia, 3200–1200 BC. *Comparative Studies in Society and History*, 26(1), 36-71.
- Afonso, C., Alshamali, F., Pereira, J. B., Fernandes, V., Costa, M., & Pereira, L. (2008). MtDNA diversity in Sudan (East Africa). *Forensic Science International: Genetics Supplement Series*, 1(1), 257-258.
- Allentoft, M. E., Collins, M., Harker, D., Haile, J., Oskam, C. L., Hale, M. L., Campos, P.F., Samaniego, J.A., Gilbert, M.T., Willerslev, E., Zhang, G., Scofield, R.P., Holdaway, R.N., & Bruce, M. (2012). The half-life of DNA in bone: measuring decay kinetics in 158 dated fossils. *Proceedings of the Royal Society B: Biological Sciences*, 279(1748), 4724-4733.
- AlQahtani S. J. (2008). Atlas of tooth development and eruption. Barts and the London School of Medicine and Dentistry. London, Queen Mary University of London. MCLinDent.
- Ammerman, A. J., & Cavalli-Sforza, L. L. (1971). Measuring the rate of spread of early farming in Europe. *Man*, 674-688.
- Amorim, C. E. G., Vai, S., Posth, C., Modi, A., Koncz, I., Hakenbeck, S., La Rocca, M.C., Mende, B., Pohl, W., Baricco, L. P., Bedini, E., Francalacci, P., Giostra, C., Vida, T., Winger, D., von Freeden, U., Ghirotto, S., Lari, M., Barbujani, G., Krause, J., Caramelli, D., Geary, P., & Veeramah, K.R. (2018). Understanding 6th-century barbarian social organization and migration through paleogenomics. *Nature Communications*, 9(1), 3547.
- Andrews, R. M., Kubacka, I., Chinnery, P. F., Lightowlers, R. N., Turnbull, D. M., & Howell, N. (1999). Reanalysis and revision of the Cambridge reference sequence for human mitochondrial DNA. *Nature Genetics*, 23(2), 147.
- Antoine, D. (2018). Human Remains Recording Sheet. Institute for Bioarchaeology, British Museum, London.
- Armstrong, G. J. (1969). Disease in ancient Nubia. *Science*, 163(3864), 255-259.
- Armstrong, G. J., & Van Gerven, D. P. (2017). *Life and Death on the Nile: A Bioethnography of Three Ancient Nubian Communities*. Gainesville: University Press of Florida.
- Aronsen, G. P., Fehren-Schmitz, L., Krigbaum, J., Kamenov, G. D., Conlogue, G. J., Warinner, C., Ozga, A.T., Sankaranarayanan, K., Griego, A., DeLuca, D.W., Eckels, H.T., Byczkiewicz, R.K., Grgurich, T.,

- Pelletier, N.A., Brownlee, S.A., Marichal, A., Williamson, K., Tonoike, Y., & Bellatoni, N.F. (2019). "The dead shall be raised": Multidisciplinary analysis of human skeletons reveals complexity in 19th century immigrant socioeconomic history and identity in New Haven, Connecticut. *PloS one*, 14(9), e0219279.
- Aufderheide, A. C., Rodríguez-Martín, C., & Langsjoen, O. (1998). *The Cambridge encyclopedia of human paleopathology* (Vol. 478). Cambridge: Cambridge University Press.
- Babiker, H. M., Schlebusch, C. M., Hassan, H. Y., & Jakobsson, M. (2011). Genetic variation and population structure of Sudanese populations as indicated by 15 Identifier sequence-tagged repeat (STR) loci. *Investigative Genetics*, 2(1), 12.
- Baker, B. J. (2016). Biocultural investigations of ancient Nubia. In Zuckerman, M.K. & Martin, D.L. (Eds.) *New Directions in Biocultural Anthropology*, (p. 181-199). Hoboken: Wiley Blackwell.
- Baker, B. J., & Judd, M. (2012). Development of paleopathology in the Nile valley. In Buikstra, J & Roberts, C. (Eds.) *The Global History of Paleopathology*, (p. 209-34). Oxford: Oxford University Press.
- Baker, W., van den Broek, A., Camon, E., Hingamp, P., Sterk, P., Stoesser, G., & Tuli, M. A. (2000). The EMBL nucleotide sequence database. *Nucleic Acids Research*, 28(1), 19-23.
- Bamshad, M. J., Watkins, W. S., Dixon, M. E., Jorde, L. B., Rao, B. B., Naidu, J. M., Prasad, B.V., Rasanayagam, A. & Hammer, M. F. (1998). Female gene flow stratifies Hindu castes. *Nature*, 395(6703), 651-52.
- Barta, J. L., Monroe, C., & Kemp, B. M. (2013). Further evaluation of the efficacy of contamination removal from bone surfaces. *Forensic science international*, 231(1-3), 340-348.
- Basha, W. A., Chamberlain, A. T., Zaki, M. E., Kandeel, W. A., & Fares, N. H. (2016). Diet reconstruction through stable isotope analysis of ancient mummified soft tissues from Kulubnarti (Sudanese Nubia). *Journal of Archaeological Science: Reports*, 5, 71-79.
- Bashir, M. (2010). A recently discovered Meroitic cemetery at Berber, River Nile State, Sudan. Preliminary report. *Sudan & Nubia*, 14, 69-74.
- Bashir, M. (2013). A Third Season of Rescue Excavations in the Meroitic Cemetery at Berber, October 2012: Preliminary Report. *Sudan & Nubia*, 17, 90-100.
- Bashir, M. and R. David. G. (2015). The Meroitic Cemetery at Berber. *Recent Fieldwork and Discussion on Internal Chronology. Sudan & Nubia*, 19, 97-105.
- Behar, D. M., Van Oven, M., Rosset, S., Metspalu, M., Loogväli, E. L., Silva, N. M., Kivisild, T., Torroni, A., & Villems, R. (2012). A "Copernican" reassessment of the human mitochondrial DNA tree from its root. *The American Journal of Human Genetics*, 90(4), 675-684.
- Bekada, A., Arauna, L. R., Deba, T., Calafell, F., Benhamamouch, S., & Comas, D. (2015). Genetic heterogeneity in Algerian human populations. *PloS one*, 10(9), e0138453.
- Benson, D. A., Cavanaugh, M., Clark, K., Karsch-Mizrachi, I., Ostell, J., Pruitt, K. D., & Sayers, E. W. (2018). GenBank. *Nucleic Acids Research*, 46(D1), D41-D47.
- Berkovitz, B. K., Holland, G. R., & Moxham, B. J. (2017). *Oral Anatomy, Histology and Embryology E-Book*. Elsevier Health Sciences.
- Bietak, M. (1987). "The C-Group and Pan-Grave culture in Nubia." In T Hägg (Ed.) *Nubian Culture Past and Present*. Stockholm: Almqvist and Wiksell.
- Binder, M. (2014). Health and Diet in Upper Nubia through Climate and Political Change-A bioarchaeological investigation of health and living conditions at ancient Amara West between 1300 and 800BC (Doctoral dissertation, Durham University).
- Binder, M. (2019). The Role of Physical Anthropology in Nubian Archaeology. In Raue, D. (Ed.) *Handbook of Ancient Nubia* (p. 103-127). Berlin: de Gruyter.

- Boessenkool, S., Hanghøj, K., Nistelberger, H. M., Der Sarkissian, C., Gondek, A. T., Orlando, L., Barrett, J.H., & Star, B. (2017). Combining bleach and mild predigestion improves ancient DNA recovery from bones. *Molecular Ecology Resources*, 17(4), 742-751.
- Bonnet, C. (1986). *Kerma, Territoire et Metropole*, Cairo: IFAO.
- Bonnet, C. (ed.) (1990). *Kerma, Royaume de Nubie*, Geneva: Musee d'Art et d'Histoire.
- Borsch, S. (2005). *The Black Death in Egypt and England*. University of Texas Press. Retrieved from <http://www.jstor.org/stable/10.7560/706170>
- Brandstätter, A., Peterson, C.T., Irwin, J.A., Mpoke, S., Koech, D.K., Parson, W., & Parsons, T.J. (2004). Mitochondrial DNA control region sequences from Nairobi (Kenya): inferring phylogenetic parameters for the establishment of a forensic database. *International Journal of Legal Medicine*, 118:294-306.
- Brandt, G., Haak, W., Adler, C. J., Roth, C., Szécsényi-Nagy, A., Karimnia, S., Möller-Rieker, S., Meller, H., Gansleier, R., Friedrich, S., Dresely, V., Nicklisch, N., Pickrell, J., Sirocko, F., Reich, D., Cooper, A., Alt, K.W., & the Genenographic Consortium. (2013). Ancient DNA reveals key stages in the formation of central European mitochondrial genetic diversity. *Science*, 342(6155), 257.
- Brickley, M. B. (2018). Cribra orbitalia and porotic hyperostosis: A biological approach to diagnosis. *American Journal of Physical Anthropology*, 167(4), 896-902.
- Briggs, A. W., Stenzel, U., Johnson, P. L., Green, R. E., Kelso, J., Prüfer, K., Meyer, M., Krause, J., Ronan, M.T., Lachmann, M., & Pääbo, S. (2007). Patterns of damage in genomic DNA sequences from a Neandertal. *Proceedings of the National Academy of Sciences*, 104(37), 14616-14621.
- Brooks, S., & Suchey, J. M. (1990). Skeletal age determination based on the os pubis: a comparison of the Acsádi-Nemeskéri and Suchey-Brooks methods. *Human evolution*, 5(3), 227-238.
- Brothwell, D. (1967). The bio-cultural background to disease. In Brothwell, D & Sandison, A. (Eds.) *Diseases in Antiquity* (p. 45-68). Springfield: Charles C. Thomas.
- Buikstra, J. E. & Ubelaker, D.H. (1994). Standards for Data Collection from Human Skeletal Remains. Arkansas Archaeological Survey, Research Seminar Series 44. Arkansas Archaeological Survey: Fayetteville, AR.
- Buikstra, J. E. (Ed.). (2019). *Ortner's Identification of Pathological Conditions in Human Skeletal Remains*. Academic Press.
- Bushara, M., Abdalah, M.S., and Bashir, M.S. (2017). Between Napata and Meroe: a newly discovered cemetery at Enapis (TARP) in the Middle Nile Region. *Sudan & Nubia*, 21, 128-133.
- Buzon, M. R. (2006). Health of the non-elites at Tombos: Nutritional and disease stress in New Kingdom Nubia. *American Journal of Physical Anthropology: The Official Publication of the American Association of Physical Anthropologists*, 130(1), 26-37.
- Buzon, M. R. (2008). A bioarchaeological perspective on Egyptian colonialism in Nubia during the New Kingdom. *The Journal of Egyptian Archaeology*, 94(1), 165-182.
- Buzon, M. R., Smith, S. T., & Simonetti, A. (2016). Entanglement and the Formation of the Ancient Nubian Napatan State. *American Anthropologist*, 118(2), 284-300.
- Caldarini, C., Catalano, P., Gazzaniga, V., Marinozzi, S., & Zavaroni, F. (2015). The study of ancient bone remains. In *Bones* (pp. 3-38). Springer, Cham.
- Callaway, Ewen. (2017). African's genomes expose Africa's past. *Nature*, 13 July 2017, 149.
- Campos, P. F., Craig, O. E., Turner-Walker, G., Peacock, E., Willerslev, E., & Gilbert, M. T. P. (2012). DNA in ancient bone—where is it located and how should we extract it?. *Annals of Anatomy-Anatomischer Anzeiger*, 194(1), 7-16.
- Cann, R. L., Stoneking, M., & Wilson, A. C. (1987). Mitochondrial DNA and human evolution. *Nature*, 325(6099), 31-36.

- Canós-Donnay, S. (2019, February 25). The Empire of Mali. *Oxford Research Encyclopedia of African History*. Retrieved 16 Sep. 2019, from <https://oxfordre.com/africanhistory/view/10.1093/acrefore/9780190277734.001.0001/acrefore-9780190277734-e-266>
- Carlson, D. S., Armelagos, G. J., & Van Gerven, D. P. (1974). Factors influencing the etiology of cribra orbitalia in prehistoric Nubia. *Journal of Human Evolution*, 3(5), 405-410.
- Cavendish, M. 1966. The Custom of Placing Pebbles on Nubian Graves', *Sudan Notes and Records* 47, 151-156.
- Cerezo, M., Achilli, A., Olivieri, A., Perego, U. A., Gómez-Carballa, A., Brisighelli, F., Lancioni, H., Woodward, S.R., Lopez-Soto, M., Carracedo, A., Capelli, C., Torroni, A., & Salas, A. (2012). Reconstructing ancient mitochondrial DNA links between Africa and Europe. *Genome research*, 22(5), 821-826.
- Chakraborty R. (1993) Analysis of Genetic Structure of Populations: Meaning, Methods, and Implications. In Majumder P.P. (Ed.) *Human Population Genetics*. Boston: Springer.
- Chiang, C. W., Marcus, J. H., Sidore, C., Biddanda, A., Al-Asadi, H., Zoledziwska, M., Pitzalis, M., Busonero, F., Maschio, A., Pistis, G., Steri, M., Angius, A., Lohmueller, K. E., Abecasis, G. R., Schlessinger, D., Cucca, F., & Novembre, J. (2018). Genomic history of the Sardinian population. *Nature Genetics*, 50(10), 1426.
- Childe, V. G. (1968). *The Dawn of European civilization*. London: Routledge.
- Clark, J. G. D. (1965). Radiocarbon dating and the spread of farming economy. *Antiquity*, 39(153), 45-48.
- Claussen, M., Kubatzki, C., Brovkin, V., Ganopolski, A., Hoelzmann, P., & Pachur, H. J. (1999). Simulation of an abrupt change in Saharan vegetation in the mid-Holocene. *Geophysical Research Letters*, 26(14), 2037-2040.
- Clima, R., Preste, R., Calabrese, C., Diroma, M. A., Santorsola, M., Scioscia, G., Simone, D., Shen, S., Gasparre, G., & Attimonelli, M. (2016). HmtDB 2016: data update, a better performing query system and human mitochondrial DNA haplogroup predictor. *Nucleic Acids Research*, 45(D1), D698-D706.
- Close, A.E. (1995). Few and far between: Early ceramics in North Africa. In W.K. Barnett and J.W. Hoops (Eds.) *The Emergence of Pottery*, Washington, D.C.: Smithsonian.
- Cooper, A., & Poinar, H. N. (2000). Ancient DNA: do it right or not at all. *Science*, 289(5482), 1139-1139.
- Cunningham, C., Scheuer, L., & Black, S. (2016). *Developmental Juvenile Osteology*. Academic Press.
- Dabney, J., & Meyer, M. (2019). Extraction of Highly Degraded DNA from Ancient Bones and Teeth. In Shapiro, B & Holfreiter, M. (Eds.) *Ancient DNA* (pp. 25-29). New York: Humana Press.
- Dabney, J., Knapp, M., Glocke, I., Gansauge, M. T., Weihmann, A., Nickel, B., Valdiosera, C., García, N., Pääbo, S., Arsuaga, J.L., & Meyer, M. (2013). Complete mitochondrial genome sequence of a Middle Pleistocene cave bear reconstructed from ultrashort DNA fragments. *Proceedings of the National Academy of Sciences*, 110(39), 15758-15763.
- Dabney, J., Knapp, M., Glocke, I., Gansauge, M. T., Weihmann, A., Nickel, B., Valiosera, C., Garcia, I., Pääbo, S., Arsuaga, J., & Meyer, M. (2013). Complete mitochondrial genome sequence of a Middle Pleistocene cave bear reconstructed from ultrashort DNA fragments. *Proceedings of the National Academy of Sciences*, 110(39), 15758-15763.
- Damgaard, P. B., Margaryan, A., Schroeder, H., Orlando, L., Willerslev, E., & Allentoft, M. E. (2015). Improving access to endogenous DNA in ancient bones and teeth. *Scientific Reports*, 5, 11184.
- Dann, R. J., Emberling, G., et al. 2016. El Kurru 2015-16. Preliminary Report. *Sudan & Nubia*, 20, 35-49.
- deMenocal, P., Ortiz, J., Guilderson, T., Adkins, J., Sarnthein, M., Baker, L., & Yarusinsky, M. (2000). Abrupt onset and termination of the African Humid Period: rapid climate responses to gradual insolation forcing. *Quaternary Science Reviews*, 19(1-5), 347-361.

- Der Sarkissian, C., Allentoft, M. E., Ávila-Arcos, M. C., Barnett, R., Campos, P. F., Cappellini, E., Ermini, L., Fernández, R., da Fonseca, R., Ginolhac, A., Hansen, A.J., Jónsson, H., Korneliussen, T., Margaryan, A., Martin, M.D., Moreno-Mayar, J.V., Raghavan, M., Rasmussen, M., Velasco, M.S., Schroeder, H., Schubert, M., Seguin-Orlando, A., Wales, N., Gilbert, M.T., Willerslev, E., & Orlando, L. (2015). Ancient genomics. *Philosophical Transactions of the Royal Society B: Biological Sciences*, 370(1660), 20130387.
- DeSalle, R., Schierwater, B., & Hadrys, H. (2017). MtDNA: The small workhorse of evolutionary studies. *Frontiers in Bioscience*, 22, 873-887.
- Djuric, M., Milovanovic, P., Janovic, A., Draskovic, M., Djukic, K., & Milenkovic, P. (2008). Porotic lesions in immature skeletons from Stara Torina, late medieval Serbia. *International Journal of Osteoarchaeology*, 18(5), 458-475.
- Dobon, B., Hassan, H. Y., Laayouni, H., Luisi, P., Ricaño-Ponce, I., Zhernakova, A., Wijmenga, C., Tahir, H., Comas, D., Netea, M.G. & Bertranpetit, J. (2015). The genetics of East African populations: a Nilo-Saharan component in the African genetic landscape. *Scientific Reports*, 5, 9996.
- Edwards, D. N. (2004). *The Nubian Past: An Archaeology of the Sudan*. New York: Routledge.
- Edwards, D. N. (2013). Medieval and Post-Medieval States of the Nile Valley. In Mitchell, P. & Lane, P.J. (Eds.) *The Oxford Handbook of African Archaeology*.
- El Tayeb, M., Juszczak-Futkowska, K. and Czyżewska, E. (2014). El-Zuma 2011: the fourth season of excavations on the site. Preliminary report. *Polish Archaeology in the Mediterranean* 23/1, 357–374.
- El-Tayeb, M. (2007). Early Makuria Research Project. el-Zuma excavations preliminary report on the second season, 2007. *Polish archaeology in the Mediterranean*, 19, 467-479.
- El-Tayeb, M., & Czyżewska, E. (2011). Early Makuria Research Project. Excavations at ez-Zuma. The third season, Jan.–Feb. 2009. *Sudan & Nubia*, 15, 108-118.
- El-Tayeb, M., Czyżewska-Zalewska, E., Kowarska, Z., & Lenarczyk, S. (2016a). Early Makuria Research Project: interim report on the excavation at el-Detti in 2014 and 2015. In PAM (Vol. 25, pp. 403-430).
- El-Tayeb, M., Skowrońska, E., Czyżewska, E. (2016). Early Makuria Research Project. The Results of Three Seasons of Excavation at El-Zuma Cemetery, 2013, 2014 and 2015. *Sudan & Nubia* 20, 110–126.
- Emberling, G. (2012). Archaeological salvage in the Fourth Cataract, Northern Sudan (1991-2008). *Ancient Nubia: African Kingdoms on the Nile*, 71-77.
- Emberling, G. (2012). Archaeological salvage in the Fourth Cataract, Northern Sudan (1991-2008). *Ancient Nubia: African Kingdoms on the Nile*, 71-77.
- Emberling, G., Dann, R. J., et al. 2013. New Excavations at El Kurru: Beyond the Napatan Royal Cemetery. *Sudan & Nubia*, 17, 42-60.
- Emberling, G., Dann, R. J., et al. 2015. In a Royal Cemetery of Kush: Archaeological Investigations at El Kurru, Northern Sudan, 2014-15. *Sudan & Nubia*, 19, 54-70.
- Emberling, Geoff. (2011). "Nubia: Ancient Kingdoms of Africa." The Institute for the Study of the Ancient World, New York University.
- Emery, L. S., Magnaye, K. M., Bigham, A. W., Akey, J. M., & Bamshad, M. J. (2015). Estimates of continental ancestry vary widely among individuals with the same mtDNA haplogroup. *The American Journal of Human Genetics*, 96(2), 183-193.
- Ewels, P., Magnusson, M., Lundin, S., & Käller, M. (2016). MultiQC: summarize analysis results for multiple tools and samples in a single report. *Bioinformatics*, 32(19), 3047-3048.
- Excoffier, L., & Lischer, H. E. (2010). Arlequin suite ver 3.5: a new series of programs to perform population genetics analyses under Linux and Windows. *Molecular Ecology Resources*, 10(3), 564-567.
- Fadhlaoui-Zid, K., Rodríguez-Botigué, L., Naoui, N., Benammar-Elgaaied, A., Calafell, F., & Comas, D. (2011). Mitochondrial DNA structure in North Africa reveals a genetic discontinuity in the Nile Valley. *American Journal of Physical Anthropology*, 145(1), 107-117.

- Fernandes, V., Triska, P., Pereira, J. B., Alshamali, F., Rito, T., Machado, A., Fajkosova, Z., Cavadas, B., Cerny, V., Soares, P., & Richards, M. B. (2015). Genetic stratigraphy of key demographic events in Arabia. *PloS one*, 10(3), e0118625.
- Flammini, R. (2008). Ancient Core-Periphery Interactions: Lower Nubia during Middle Kingdom Egypt (ca. 2050-1640 BC). *Journal of World-Systems Research*, 14(1), 50-74.
- Fregel, R., Méndez, F. L., Bokbot, Y., Martin-Socas, D., Camalich-Massieu, M. D., Santana, J., Morales, J., Avila-Arcos, A.E., Underhill, P.A., Shapiro, B., Wojcik, G., Rasmussen, M., Soares, A.E.R., Kapp, J., Sockell, A., Rodriguez-Santos, J., Mikdad, A., Trujillo-Medros, A., Bustamante, C. (2018). Ancient genomes from North Africa evidence prehistoric migrations to the Maghreb from both the Levant and Europe. *Proceedings of the National Academy of Sciences*, 115(26), 6774-6779.
- Fregel, R., Ordóñez, A. C., Santana-Cabrera, J., Cabrera, V. M., Velasco-Vázquez, J., Alberto, V., Moreno-Benítez, M.A., Delgado-Darias, T., Rodríguez-Rodríguez, A., Hernández, J.C., Pais, J., González-Montelongo, R., Lorenzo-Salazar, J.M., Flores, C., Cruz-de-Mercadal, M.C., Álvarez-Rodríguez, N., Shapiro, B., Arnay, M., & Bustamante, C.D. (2019). Mitogenomes illuminate the origin and migration patterns of the indigenous people of the Canary Islands. *PloS one*, 14(3), e0209125.
- Fu, Q., Mittnik, A., Johnson, P. L., Bos, K., Lari, M., Bollongino, R., Sun, C., Giemsch, L., Schmitz, R., Burger, J., Ronchitelli, A.M., Martini, F., Cremonesi, R. G., Svoboda, J., Bauer, P., Caramelli, D., Castellano, S., Reich, D., & Krause, J. (2013). A revised timescale for human evolution based on ancient mitochondrial genomes. *Current Biology*, 23(7), 553-559.
- Fulton, T. L., & Shapiro, B. (2019). Setting up an ancient DNA laboratory. In Shapiro, B & Holfreiter, M. (Eds.) *Ancient DNA* (pp. 1-13). New York: Humana Press.
- Gallego Llorente, M., Jones, E. R., Eriksson, A., Siska, V., Arthur, K. W., Arthur, J. W., Curtis, M.C., Stock, J.T., Coltorti, M., Pieruccini, P., Stretton, S., Brock, F., Higham, T., Park, Y., Hofreiter, M., Bradley, D.G., Bhak, J., Pinhasi, R., & Manica, A. (2015). Ancient Ethiopian genome reveals extensive Eurasian admixture throughout the African continent. *Science*, 350(6262), 820-822.
- Gamba, C., Jones, E. R., Teasdale, M. D., McLaughlin, R. L., Gonzalez-Fortes, G., Mattiangeli, V., Domboróczki, L., Kóvári, I., Pap, I., Anders, A., Whittle, A., Dani, J., Raczky, P., Higham, T.F., Hofreiter, M., Bradley, D.G., & Pinhasi, R. (2014). Genome flux and stasis in a five millennium transect of European prehistory. *Nature Communications*, 5, 5257.
- Gatto, M. C. (2006). The Nubian A-group: A reassessment. *Archéo-Nil*, 16, 61-76.
- Giles, R. E., Blanc, H., Cann, H. M., & Wallace, D. C. (1980). Maternal inheritance of human mitochondrial DNA. *Proceedings of the National Academy of Sciences*, 77(11), 6715-6719.
- Ginolhac, A., Rasmussen, M., Gilbert, M. T. P., Willerslev, E., & Orlando, L. (2011). mapDamage: testing for damage patterns in ancient DNA sequences. *Bioinformatics*, 27(15), 2153-2155.
- Godlewski, W. (2014). Dongola Capital of early Makuria: Citadel–Rock Tombs–First Churches. *Der Antike Sudan. Mitteilungen der Sudanarchäologischen Gesellschaft zu Berlin e.V. Sonderheft*. Berlin.
- Gondek, A. T., Boessenkool, S., & Star, B. (2018). A stainless-steel mortar, pestle and sleeve design for the efficient fragmentation of ancient bone. *BioTechniques*, 64(6), 266-269.
- Goodman, A. H., & Martin, D. L. (2002). Reconstructing health profiles from skeletal remains. In Steckel, R. H. & Rose, J. C. *The Backbone of history: Health and Nutrition in the Western hemisphere* (pp. 11-60). Cambridge: Cambridge University Press.
- Goodman, A. H., & Rose, J. C. (1991). Dental enamel hypoplasias as indicators of nutritional status. *Advances in dental anthropology*, 5, 225-240.
- Goodman, A. H., Armelagos, G. J., & Rose, J. C. (1980). Enamel hypoplasias as indicators of stress in three prehistoric populations from Illinois. *Human Biology*, 52(3), 515-528.
- Goodman, A. H., Brooke Thomas, R., Swedlund, A. C., & Armelagos, G. J. (1988). Biocultural perspectives on stress in prehistoric, historical, and contemporary population research. *American Journal of Physical Anthropology*, 31(S9), 169-202.

- Green, R. E., Krause, J., Ptak, S. E., Briggs, A. W., Ronan, M. T., Simons, J. F., Du, L., Egholm, M., Rothber, J.M., Paunovic, M. & Pääbo, S. (2006). Analysis of one million base pairs of Neanderthal DNA. *Nature*, 444(7117), 330.
- Haak, W., Forster, P., Bramanti, B., Matsumura, S., Brandt, G., Tänzer, M., Villems, R., Renfrew, C., Gronenborn, D, Alt, K.W., & Burger, J. (2005). Ancient DNA from the first European farmers in 7500-year-old Neolithic sites. *Science*, 310(5750), 1016-1018.
- Hagelberg, E., Hofreiter, M., & Keyser, C. (2015). Ancient DNA: the first three decades.
- Hansen, H. B., Damgaard, P. B., Margaryan, A., Stenderup, J., Lynnerup, N., Willerslev, E., & Allentoft, M. E. (2017). Comparing ancient DNA preservation in petrous bone and tooth cementum. *PloS one*, 12(1), e0170940.
- Harris, N. J., & Tayles, N. (2012). Burial containers—A hidden aspect of mortuary practices: Archaeoethanatology at Ban Non Wat, Thailand. *Journal of Anthropological Archaeology*, 31(2), 227-239.
- Hassan Mohamed, H.Y. (2009). Genetic Patterns of Y-chromosome and Mitochondrial DNA Variation, with Implications to the Peopling of the Sudan. (Doctoral Thesis, University of Khartoum.) Retrieved from <https://www.docdroid.net/8GAlp0X/genetic-patterns-of-y-chromosome-and-mitochondrial-hassan-2009.pdf>
- Hassan, H. Y., Underhill, P. A., Cavalli-Sforza, L. L., & Ibrahim, M. E. (2008). Y-chromosome variation among Sudanese: restricted gene flow, concordance with language, geography, and history. *American Journal of Physical Anthropology*, 137(3), 316-323.
- Henneberger, K., Barlow, A., & Pajmans, J. L. (2019). Double-Stranded Library Preparation for Ancient and Other Degraded Samples. In Shapiro, B. & Hofreiter, M. (Eds.) *Ancient DNA* (pp. 65-73). New York: Humana Press.
- Herbig, A., Maixner, F., Bos, K. I., Zink, A., Krause, J., & Huson, D. H. (2016). MALT: Fast alignment and analysis of metagenomic DNA sequence data applied to the Tyrolean Iceman. *BioRxiv*, 050559.
- Hibbs, A. C., Secor, W. E., Van Gerven, D., & Armelagos, G. (2011). Irrigation and infection: the immunoepidemiology of schistosomiasis in ancient Nubia. *American Journal of Physical Anthropology*, 145(2), 290-298.
- Hillelson, S. (1930). Nubian Origins. *Sudan Notes and Records*, 13(1), 137-148.
- Hillson, S. (1996). *Dental Anthropology*. Cambridge: Cambridge University Press.
- Hintze, F. (1967). "Meroe and the Noba", *Der Antike Sudan*. Mitteilungen der Sudanarchäologischen Gesellschaft zu Berlin 10:49-55.
- Hofreiter, M., Pajmans, J. L., Goodchild, H., Speller, C. F., Barlow, A., Fortes, G. G., Thomas, J. Ludwig, A., & Collins, M. J. (2014). The future of ancient DNA: Technical advances and conceptual shifts. *BioEssays*, 37(3), 284-293.
- Hollfelder, N., Schlebusch, C. M., Günther, T., Babiker, H., Hassan, H. Y., & Jakobsson, M. (2017). Northeast African genomic variation shaped by the continuity of indigenous groups and Eurasian migrations. *PLoS Genetics*, 13(8), e1006976.
- Holsinger, K. E., & Weir, B. S. (2009). Genetics in geographically structured populations: defining, estimating and interpreting F_{ST}. *Nature Reviews Genetics*, 10(9), 639.
- Höss, M., Jaruga, P., Zastawny, T. H., Dizdaroglu, M., & Paabo, S. (1996). DNA damage and DNA sequence retrieval from ancient tissues. *Nucleic Acids Research*, 24(7), 1304-1307.
- Hummert, J. R., & Van Gerven, D. P. (1983). Skeletal growth in a medieval population from Sudanese Nubia. *American Journal of Physical Anthropology*, 60(4), 471-478.
- Hurst, C. V. (2013). Growing up in medieval Nubia: Health, disease, and death of a medieval juvenile sample from Mis Island. Ph.D. thesis. Michigan State University, Lansing.

- Irish, D., & Joel, D. (2005). Population continuity vs. discontinuity revisited: Dental affinities among late Paleolithic through Christian-era Nubians. *American Journal of Physical Anthropology*, 128(3), 520-535.
- Jackes, M. (2011). Representativeness and bias in archaeological skeletal samples. In Agarwal, S.C. & Glencross, B.A. (Eds.) *Social bioarchaeology*, (pp. 107-146). Hoboken: Blackwell Publishing Inc.
- Jesse, F. (2010). Early pottery in northern Africa—an overview. *Journal of African Archaeology*, 8(2), 219-238.
- Jónsson, H., Ginolhac, A., Schubert, M., Johnson, P. L., & Orlando, L. (2013). mapDamage2. 0: fast approximate Bayesian estimates of ancient DNA damage parameters. *Bioinformatics*, 29(13), 1682-1684.
- Judd, M. (2002). Ancient injury recidivism: an example from the Kerma period of ancient Nubia. *International Journal of Osteoarchaeology*, 12(2), 89-106.
- Judd, M.A. (2000). Trauma and interpersonal violence in ancient Nubia during the Kerma period (ca. 2500-1500 BC). Ph.D. thesis, University of Alberta, Edmonton.
- Jugert, F., Klatt, T. W., Grosskopf, B., and Hummel, S. (2018). Anthropologic and Paleogenetic Studies on Human Skeletal Remains from the Wadi Abu Dom, Sudan. In Lohwasser, A., Kerberg, T., and Auenmüller, J. (Eds.), *Bayuda Studies: Proceedings of the First International Conference on the Archaeology of the Bayuda Desert in Sudan* (pp. 231-246). Wiesbaden, Germany: Harrassowitz Verlag.
- Kaestle, F. A. (2010). Paleogenetics: Ancient DNA in Anthropology. In Larsen, L (Ed.) *A Companion to Biological Anthropology*, 427.
- Kemp, B. M., & Smith, D. G. (2005). Use of bleach to eliminate contaminating DNA from the surface of bones and teeth. *Forensic Science International*, 154(1), 53-61.
- Kendall, T. (1999). The origin of the Napatan State: El Kurru and the evidence for the royal ancestors. In S. Wenig, ed., *Studien zum antiken Sudan: Akten der 7. Internationalen Tagung für meroitische Forschungen: 2–117*. Wiesbaden
- Kircher, M., Sawyer, S., & Meyer, M. (2011). Double indexing overcomes inaccuracies in multiplex sequencing on the Illumina platform. *Nucleic acids research*, 40(1), e3-e3.
- Kivisild T, Reidla M, Metspalu E, Rosa A, Brehm A, Pennarun E, Parik J, Geberhiwot T, Usanga E, Villems R. (2004). Ethiopian Mitochondrial DNA Heritage: Tracking Gene Flow Across and Around the Gate of Tears. *American Journal of Human Genetics*, 75, 752-770.
- Klimaszewska-Drabot, E. (2008). Early Makuria Research Project: The Pottery. *Polish Archaeology in the Mediterranean*, (XVIII), 477-491.
- Korlević, P., & Meyer, M. (2019). Pretreatment: Removing DNA Contamination from Ancient Bones and Teeth Using Sodium Hypochlorite and Phosphate. In Shaprio, B. & Hofreiter, M. (Eds.) *Ancient DNA* (pp. 15-19). New York: Humana Press.
- Korlević, P., Gerber, T., Gansauge, M. T., Hajdinjak, M., Nagel, S., Aximu-Petri, A., & Meyer, M. (2015). Reducing microbial and human contamination in DNA extractions from ancient bones and teeth. *Biotechniques*, 59(2), 87-93.
- Krings, M., Halim Salem, A., Bauer, K., Geisert, H., Malek, A.K., Chaix, L., Simon, C., Welsby, D., Di Rienzo, A., Utermann, G., Sajantila, A., Pääbo, S., & Stoneking, M. (1999). mtDNA analysis of Nile valley populations: A genetic corridor or a barrier to migration? *American Journal of Human Genetics*, 64(4), 1166-1176.
- Krings, M., Stone, A., Schmitz, R. W., Krainitzki, H., Stoneking, M., & Pääbo, S. (1997). Neandertal DNA sequences and the origin of modern humans. *Cell*, 90(1), 19-30.
- Lalueza Fox, C. (1997). mtDNA analysis in ancient Nubians supports the existence of gene flow between sub-Saharan and North Africa in the Nile Valley. *Annals of Human Biology*, 24(3), 217-227.
- Larsen, C. S. (2015). *Bioarchaeology: Interpreting Behavior from the Human Skeleton*. Cambridge: Cambridge University Press.

- Larsson, A. (2014). AliView: a fast and lightweight alignment viewer and editor for large data sets. *Bioinformatics* 30(22): 3276-3278. <http://dx.doi.org/10.1093/bioinformatics/btu531>
- Lazaridis, I., Nadel, D., Rollefson, G., Merrett, D. C., Rohland, N., Mallick, S., Fernandes, D., Novak, M., Gamarra, B., Sirak, K., Connell, S., Stewardson, K., Harney, E., Fu, Q., Gonzalez-Fortes, G., Jones, E.R., Roodenberg, S.A., Lengyel, G., Bocquentin, F., Gasparian, B., Monge, J.M., Gregg, M., Eshed, V., Mizrahi, A.S., Meiklejohn, C., Gerritsen, F., Bejenaru, L., Blüher, M., Campbell, A., Cavalleri, G., Comas, D., Froguel, P., Gilbert, E., Kerr, S.M., Kovacs, P., Krause, J., McGettigan, D., Merrigan, M., Merriwether, D.A., O'Reilly, S., Richards, M.B., Semino, O., Shamoon-Pour, M., Stefanescu, G., Stumvoll, M., Tönjes, A., Torroni, A., Wilson, J.F., Yengo, L., Hovhannisyann, N.A., Patterson, N., Pinhasi, R., & Reich D. (2016). Genomic insights into the origin of farming in the ancient Near East. *Nature*, 536(7617), 419.
- Leonard, J. A. (2008). Ancient DNA applications for wildlife conservation. *Molecular Ecology*, 17(19), 4186-4196.
- Leplogeon, A. (2017). Technological variability in the Late Palaeolithic lithic industries of the Egyptian Nile Valley: The case of the Silsilian and Afian industries. *PloS one*, 12(12), e0188824.
- Lewis, M. E. (2004). Endocranial Lesions in Non - Adult Skeletons: Understanding Their Aetiology. *International Journal of Osteoarchaeology* 14:87–97.
- Lewis, M. E. (2007). *The Bioarchaeology of Children: Perspectives from Biological and Forensic Anthropology*. Cambridge: Cambridge University Press.
- Lindahl, T. (1993). Instability and decay of the primary structure of DNA. *Nature*, 362(6422), 709-715.
- Lovejoy, C. O., Meindl, R. S., Mensforth, R. P., & Barton, T. J. (1985). Multifactorial determination of skeletal age at death: a method and blind tests of its accuracy. *American Journal of Physical Anthropology*, 68(1), 1-14.
- Luo, S., Valencia, C. A., Zhang, J., Lee, N. C., Slone, J., Gui, B., Wang, X., Li, Z., Dell, S., Brown, J., Chen, S. M., Chien, Y.H., Hwu, W.L., Fan, P.C., Wong, L.J., Atwal, P.S., & Huang, T. (2018). Biparental inheritance of mitochondrial DNA in humans. *Proceedings of the National Academy of Sciences*, 115(51), 13039-13044.
- MacEachern, S. (2013). Genetics and Archaeology. In *The Oxford handbook of African Archaeology*. Oxford: Oxford University Press.
- Maricic, T., Whitten, M., & Pääbo, S. (2010). Multiplexed DNA sequence capture of mitochondrial genomes using PCR products. *PloS one*, 5(11), e14004.
- McIlvaine, B. K. (2015). Implications of reappraising the iron-deficiency anemia hypothesis. *International Journal of Osteoarchaeology*, 25(6), 997-1000.
- Menozzi, P., Piazza, A., & Cavalli-Sforza, L. (1978). Synthetic maps of human gene frequencies in Europeans. *Science*, 201(4358), 786-792.
- Mensforth, R. P., Lovejoy, C. O., Lallo, J. W., & Armelagos, G. J. (1978). Part two: the role of constitutional factors, diet, and infectious disease in the etiology of porotic hyperostosis and periosteal reactions in prehistoric infants and children. *Medical Anthropology*, 2(1), 1-59.
- Meyer, M., & Kircher, M. (2010). Illumina sequencing library preparation for highly multiplexed target capture and sequencing. *Cold Spring Harbor Protocols*, 2010(6), pdb-prot5448.
- Miquel-Feucht, M. J., Polo-Cerda, M., & Villalaín-Blanco, J. D. (1999). Anthropological and paleopathological studies of a mass execution during the war of independence in Valencia, Spain (1808-1812). *Journal of Paleopathology*, 11(3), 15-24.
- Mitchell, P. D. (2006). Child health in the crusader period inhabitants of Tel Jezreel, Israel. *Levant*, 38(1), 37-44.
- Mittler, D. M., & Van Gerven, D. P. (1994). Developmental, diachronic, and demographic analysis of cribra orbitalia in the medieval Christian populations of Kulubnarti. *American Journal of Physical Anthropology*, 93(3), 287-297.

- Mitnik, A., Wang, C. C., Svoboda, J., & Krause, J. (2016). A molecular approach to the sexing of the triple burial at the Upper Paleolithic Site of Dolní Věstonice. *PLoS one*, 11(10), e0163019.
- Morris, A. G., Heinze, A., Chan, E. K., Smith, A. B., & Hayes, V. M. (2014). First ancient mitochondrial human genome from a prepastoralist southern African. *Genome Biology and Evolution*, 6(10), 2647-2653.
- Moseley J.E. (1974). Skeletal changes in the anemias. *Seminars in Roentgenology* 9(3), 169-184.
- Mulligan, C. J., & Szathmáry, E. J. (2017). The peopling of the Americas and the origin of the Beringian occupation model. *American Journal of Physical Anthropology*, 162(3), 403-408.
- Neukamm, J., & Peltzer, A. (2009, March 9), mitobench/MitoBench: MitoBench version 1.1 beta (Version v1.1-beta). Zenodo. <http://doi.org/10.5281/zenodo.2588120>
- Nilsson Stutz, L. (2003). Embodied rituals and ritualized bodies: tracing ritual practices in Late Mesolithic burials. *Acta Archaeologica Lundensia. Series in 8*, 46.
- Noonan, J. P., Hofreiter, M., Smith, D., Priest, J. R., Rohland, N., Rabeder, G., Krause, J., Detter, J.C., Pääbo, S., & Rubin, E.M. (2005). Genomic sequencing of Pleistocene cave bears. *Science*, 309(5734), 597-599.
- Obłuski, A. (2014). Ghazali Site Presentation Project 2012 – 2014: Preliminary Results. *Der Antike Sudan*, 25, 197-204.
- Obłuski, A., Ochała, G., Bogacki, M., Małkowski, W., Maślak, S., and Zaki ed-Din, M. (2015). Ghazali 2012: preliminary report. *Polish Archaeology in the Mediterranean*, 24(1), 431-442.
- Ortner, D. J. (2003). *Identification of pathological conditions in human skeletal remains*. Academic Press.
- Pääbo, S. (1985). Molecular cloning of ancient Egyptian mummy DNA. *Nature*, 314(6012), 644.
- Pääbo, S., & Wilson, A. C. (1988). Polymerase chain reaction reveals cloning artefacts. *Nature*, 334(6181), 387.
- Palanichamy, M. G., Zhang, C. L., Mitra, B., Malyarchuk, B., Derenko, M., Chaudhuri, T. K., & Zhang, Y. P. (2010). Mitochondrial haplogroup N1a phylogeography, with implication to the origin of European farmers. *BMC evolutionary biology*, 10(1), 304.
- Peltzer, A., Jäger, G., Herbig, A., Seitz, A., Knip, C., Krause, J., & Nieselt, K. (2016). EAGER: efficient ancient genome reconstruction. *Genome Biology*, 17(1), 60. <https://github.com/apeltzer/EAGER-GUI>
- Pereira, L., Richards, M., Goios, A., Alonso, A., Albarrán, C., Garcia, O., Behar, D.M., Gölge, M., Hatina, J., Al-Gazali, L., Bradley, D.G., Macauley, V., & Amorim, A. (2005). High-resolution mtDNA evidence for the late-glacial resettlement of Europe from an Iberian refugium. *Genome research*, 15(1), 19-24.
- Peter, B. M., Petkova, D., & Novembre, J. (2018). Genetic landscapes reveal how human genetic diversity aligns with geography. *BioRxiv*, 233486.
- Phenice, T. W. (1969). A newly developed visual method of sexing the os pubis. *American Journal of Physical Anthropology*, 30(2), 297-301.
- Phillips, J. (2003): An Overview of the Ceramics. In: Żurawski, Bogdan T. (Ed.) *Survey and Excavations between Old Dongola and Ez-Zuma. Southern Dongola Reach of the Nile from Prehistory to 1820 AD based on the Fieldwork conducted in 1997-2003 by the Polish Archaeological Joint Expedition to the Middle Nile. Southern Dongola Reach Survey 1*. (pp. 387-437) Warsaw: Nubia II.
- Pickrell, J. K., & Reich, D. (2014). Toward a new history and geography of human genes informed by ancient DNA. *Trends in Genetics*, 30(9), 377-389.
- Pinhasi, R., & Bourbou, C. (2007). How representative are human skeletal assemblages for population analysis?. In Pinhasi, R. & Simon, M. (Eds.) *Advances in Human Palaeopathology* (p. 31-44). Hoboken: John Wiley & Sons, Ltd.
- Pinhasi, R., Fernandes, D. M., Sirak, K., & Cheronet, O. (2019). Isolating the human cochlea to generate bone powder for ancient DNA analysis. *Nature Protocols*, 14(4), 1194.

- Pinhasi, R., Fernandes, D., Sirak, K., Novak, M., Connell, S., Alpaslan-Roodenberg, S., Anders, A., Pietrusewsky, M., Rollefson, G., Jovanovic, M., Trinhhoang, H., Bar-Oz, G., Oxenham, M., Matsumura, H., & Hofreiter, M. (2015). Optimal ancient DNA yields from the inner ear part of the human petrous bone. *PloS one*, 10(6), e0129102.
- Poinar, H. N., Schwarz, C., Qi, J., Shapiro, B., MacPhee, R. D., Buigues, B., Tikhonov, A., Huson, D.H., Tomsho, L.P., Auch, A., Rampp, M., Miller, W., & Schuster, S.C. (2006). Metagenomics to paleogenomics: large-scale sequencing of mammoth DNA. *Science*, 311(5759), 392-394.
- Prendergast, M. E., Lipson, M., Sawchuk, E. A., Olalde, I., Ogola, C. A., Rohland, N., Sirak, K.A., Adamski, N., Bernardos, R., Broomandkhoshbacht, N., Callan, K., Culleton, B.J., Eccles, L., Harper, T.K., Lawson, A.M., Mah, M., Oppenheimer, J., Stewardson, K., Zalzal, F., Ambrose, S.H., Ayodo, G., Gates, H.L. Jr., Gidna, A.O., Katongo, M., Kwekason, A., Mabulla, A.Z.P., Mudenda, G.S., Ndiema, E.K., Nelson, C., Robertshaw, P., Kennett, D.J., Manthi, F.K., & Reich, D. (2019). Ancient DNA reveals a multistep spread of the first herders into sub-Saharan Africa. *Science*, eaaw6275.
- Renaud, G., Slon, V., Duggan, A. T., & Kelso, J. (2015). Schmutzi: estimation of contamination and endogenous mitochondrial consensus calling for ancient DNA. *Genome Biology*, 16(1), 224.
- Rinaldo, N., Zedda, N., Bramanti, B., Rosa, I., & Gualdi-Russo, E. (2019). How reliable is the assessment of Porotic Hyperostosis and Cribra Orbitalia in skeletal human remains? A methodological approach for quantitative verification by means of a new evaluation form. *Archaeological and Anthropological Sciences*, 1-11.
- Rito, T., Richards, M. B., Fernandes, V., Alshamali, F., Cerny, V., Pereira, L., & Soares, P. (2013). The first modern human dispersals across Africa. *PloS one*, 8(11), e80031.
- Roostalu, U., Kutuev, I., Loogväli, E. L., Metspalu, E., Tambets, K., Reidla, M., Khusnutdinova, E.K., Usanga, E., Kivisild, T. & Villems, R. (2006). Origin and expansion of haplogroup H, the dominant human mitochondrial DNA lineage in West Eurasia: The Near Eastern and Caucasian perspective. *Molecular Biology and Evolution*, 24(2), 436-448.
- Rowold, D. J., Luis, J. R., Terreros, M. C., & Herrera, R. J. (2007). Mitochondrial DNA gene flow indicates preferred usage of the Levant Corridor over the Horn of Africa passageway. *Journal of Human Genetics*, 52(5), 436.
- Salas, A., Richards, M., De la Fe, T., Lareu, M. V., Sobrino, B., Sánchez-Diz, P., Macauley, V., & Carracedo, Á. (2002). The making of the African mtDNA landscape. *The American Journal of Human Genetics*, 71(5), 1082-1111.
- Salas, A., Richards, M., Lareu, M. V., Scozzari, R., Coppa, A., Torroni, A., Macauley, V., & Carracedo, A. (2004). The African diaspora: mitochondrial DNA and the Atlantic slave trade. *The American Journal of Human Genetics*, 74(3), 454-465.
- Salter, S.J., Cox, M.J., Turek, E.M., Calus, T.S., Cookson, W.O., Moffatt, M.F., Turner, P., Parkhill, J., Loman, N.J. & Walker, A.W. (2014). Reagent and Laboratory contamination can critically impact sequence-based microbiome analyses. *BMC Biology* 12(1), 87.
- Schaefer, M., Black, S. M., Schaefer, M. C., & Scheuer, L. (2009). *Juvenile osteology*. London: Academic Press.
- Scheinfeldt, L. B., Soi, S., & Tishkoff, S. A. (2010). Working toward a synthesis of archaeological, linguistic, and genetic data for inferring African population history. *Proceedings of the National Academy of Sciences*, 107(Supplement 2), 8931-8938.
- Schlebusch, C. M., Malmström, H., Günther, T., Sjödin, P., Coutinho, A., Edlund, H., Munters, A.R., Visente, M., Steyn, M., Soodyall, H., Lombard, M., & Jakobsson, M. (2017). Southern African ancient genomes estimate modern human divergence to 350,000 to 260,000 years ago. *Science*, 358(6363), 652-655.
- Schroeder, H., de Barros Damgaard, P., & Allentoft, M. E. (2019). Pretreatment: Improving Endogenous Ancient DNA Yields Using a Simple Enzymatic Predigestion Step. In Shapiro, B. & Hofreiter, M. (Eds.) *Ancient DNA* (pp. 21-24). New York: Humana Press.

- Schuenemann, V. J., Peltzer, A., Welte, B., van Pelt, W. P., Molak, M., Wang, C. C., Furtwaegler, A., Urban, C., Reiter, E., Nieselt, K., Teßmann, B. Francken, M., Harvati, K., Haak, W., Schiffels, S. & Krause, J. (2017). Ancient Egyptian mummy genomes suggest an increase of Sub-Saharan African ancestry in post-Roman periods. *Nature Communications*, 8: 15694.
- Schwarz, C., Debruyne, R., Kuch, M., McNally, E., Schwarcz, H., Aubrey, A. D., Bada, J., & Poinar, H. (2009). New insights from old bones: DNA preservation and degradation in permafrost preserved mammoth remains. *Nucleic Acids Research*, 37(10), 3215-3229.
- Silva, M., Alshamali, F., Silva, P., Carrilho, C., Mandlate, F., Trovada, M. J., Černý, V. & Soares, P. (2015). 60,000 years of interactions between Central and Eastern Africa documented by major African mitochondrial haplogroup L2. *Scientific Reports*, 5, 12526.
- Sirak, K. A., Fernandes, D. M., Cheronet, O., Novak, M., Gamarra, B., Balassa, T., Bernert, Z6, Cséki A7, Dani J8, Gallina JZ9, Kocsis-Buruzs G10, Kővári I11, László O12, Pap I6, Patay R13, Petkes Z14, Szenthe G15, Szeniczey T16, Hajdu T16, Pinhasi R2,17 & Kocsis-Buruzs, G. (2017). A minimally-invasive method for sampling human petrous bones from the cranial base for ancient DNA analysis. *BioTechniques*, 62(6), 283-289.
- Sirak, K., Fernandes, D., Novak, M., Van Gerven, D., & Pinhasi, R. (2016, January). A community divided? Revealing the community genome (s) of Medieval Kulubnarti using next-generation sequencing. In IUAES Inter-Congress 2016.
- Skoglund, P., Northoff, B. H., Shunkov, M. V., Derevianko, A. P., Pääbo, S., Krause, J., & Jakobsson, M. (2014). Separating endogenous ancient DNA from modern day contamination in a Siberian Neanderthal. *Proceedings of the National Academy of Sciences*, 111(6), 2229-2234.
- Skoglund, P., Thompson, J. C., Prendergast, M. E., Mitnik, A., Sirak, K., Hajdinjak, M., Salie, T., Rohland, N., Mallick, S., Peltzer, A., Heinze, A., Olalde, I., Ferry, M., Harney, E., Michel, M., Stewardson, K., Cerezo-Román, J.I., Chiumia, C., Crowther, A., Gomani-Chindebvu, E., Gidna, A.O., Grillo, K.M., Helenius, I.T., Hellenthal, G., Helm, R., Horton, M., López, S., Mabulla, A.Z.P., Parkington, J., Shipton, C., Thomas, M.G., Tibesasa, R., Welling, M., Hayes, V.M., Kennett, D., Ramesar, R., Meyer, M., Pääbo, S., Patterson, N., Morris, A.G., Boivin, N., Pinhasi, R., Krause, J., & Reich, D. (2017). Reconstructing prehistoric African population structure. *Cell*, 171(1), 59-71.
- Skuldbøl, T., Uildriks, M., Rose, K., Philips, J., & Breidenstein, A. (2016). "The Medieval Fortification, Settlement, and Cemetery" in El-Kurru 2015-16: Preliminary Report. *Sudan & Nubia*, 20, 40-46.
- Smith, B. H. (1991). *Standards of Human Tooth Formation and Dental Age Assessment*. Wiley-Liss Inc.
- Smith, G.E., & Jones, F.W. (1910). *The Archaeological Survey of Nubia: Report for 1907–1908, volume II, Report on Human Remains*. Cairo: National Printing Department.
- Smith-Guzmán, N. E. (2015a). Cribra orbitalia in the ancient Nile Valley and its connection to malaria. *International Journal of Paleopathology*, 10, 1-12.
- Smith-Guzmán, N. E. (2015b). The skeletal manifestation of malaria: An epidemiological approach using documented skeletal collections. *American journal of physical anthropology*, 158(4), 624-635.
- Soares, P., Ermini, L., Thomson, N., Mormina, M., Rito, T., Röhl, A., Salas, A., Oppenheimer, S., Macauley, V., & Richards, M. B. (2009). Correcting for purifying selection: an improved human mitochondrial molecular clock. *The American Journal of Human Genetics*, 84(6), 740-759.
- Sokal, R. R., Oden, N. L., & Wilson, C. (1991). Genetic evidence for the spread of agriculture in Europe by demic diffusion. *Nature*, 351(6322), 143.
- Soler, A. (2012). *Life and death in a medieval Nubian farming community: the experience at Mis Island*. Ph.D. thesis. Michigan State University. Lansing.
- Spyrou, M. A., Bos, K. I., Herbig, A., & Krause, J. (2019). Ancient pathogen genomics as an emerging tool for infectious disease research. *Nature Reviews Genetics*, 20, 323-340.

- Stark, R. J., & Ciesielska, J. (2019). Vertebral infection in a male individual buried in the monastic cemetery (Cemetery 2) at Ghazali (ca. 670–1270 CE), Northern Sudan. *International Journal of Paleopathology*, 24, 34-40.
- Steinbock, R.T. (1976). *Paleopathological Diagnosis and Interpretation: Bone Diseases in Ancient Human Populations*, Charles C. Thomas, Illinois.
- Stevanovitch A, Gilles A, Bouzaid E, Kefi R, Paris F, Gayraud RP, Spadoni JL, El-Chenawi. (2003). Mitochondrial DNA Sequence diversity in a sedentary population from Egypt. *Annals of Human Genetics*, 68, 23-39.
- Stoneking, M. (2018). Mitochondrial DNA. In Trevathan, W. (Ed.) *The International Encyclopedia of Biological Anthropology*. John Wiley & Sons, Inc.
- Stuart-Macadam, P. (1989). Porotic hyperostosis: relationship between orbital and vault lesions. *American Journal of Physical Anthropology*, 80(2), 187-193.
- The Arizona Science Center. (2011, May 13). Broken Bones. ASU - Ask A Biologist. Retrieved August 8, 2019 from <https://askabiologist.asu.edu/how-bone-breaks>
- Thoma, K. H., & Goldman, H. M. (1960). *Oral pathology* (p. 1192). St. Louis: Mosby.
- Thomas, M.G., Weale, M.E., Jones, A.L., Richards, M., Smith, A., Redhead, N., Torroni, A., Scozzari, R., Gratrix, F., Tarekegn, A., Wilson, J.F., Capelli, C., Bradman, N., & Goldstein, D.B. (2002). Founding mothers of Jewish communities: geographically separated Jewish groups were independently founded by very few female ancestors. *Am J Hum Genet* 70:1411-1420.
- Tishkoff, S. A., Reed, F. A., Friedlaender, F. R., Ehret, C., Ranciaro, A., Froment, A., Hirbo, J.B., Awomoyi, A.A., Bodo, J.M., Doumbo, O., Ibrahim, M., Juma, A.J., Kotze, M.J., Lema, G., Moore, J.H., Mortensen, H., Nyambo, T.B., Omar, S.A., Powell, K., Pretorius, G.S., Smith, M.W., Thera, M.A., Wambebe, C., Weber, J.L., & Williams, S.M. (2009). The genetic structure and history of Africans and African Americans. *Science*, 324(5930), 1035-1044.
- Török, L. (2008). *Between two worlds: the frontier region between ancient Nubia and Egypt 3700 BC-500 AD*. Leiden: Brill.
- Vai, S., Sarno, S., Lari, M., Luiselli, D., Manzi, G., Gallinaro, M., Mataich, S., Hübner, A., Modi, A., Pilli, E., Tafuri, M. & Tafuri, M. A. (2019). Ancestral mitochondrial N lineage from the Neolithic 'green' Sahara. *Scientific Reports*, 9(1), 3530.
- van de Loosdrecht, M., Bouzouggar, A., Humphrey, L., Posth, C., Barton, N., Aximu-Petri, A., Nickel, B., Nagel, S., Talbi, E.H., El Hajraoui, M.A., Amzazi, S., Hublin, J.J., Pääbo, S., Schiffels, S., Meyer, M., Haak, W., Jeong, C., & Krause, J. (2018). Pleistocene North African genomes link near Eastern and sub-saharan African human populations. *Science*, 360(6388), 548-552.
- Van Gerven, D. P., Beck, R., & Hummert, J. R. (1990). Patterns of enamel hypoplasia in two medieval populations from Nubia's Batn el Hajar. *American Journal of Physical Anthropology*, 82(4), 413-420.
- Van Gerven, D. P., Sandford, M. K., & Hummert, J. R. (1981). Mortality and culture change in Nubia's Batn el Hajar. *Journal of Human Evolution*, 10(5), 395-408.
- Van Gerven, D. P., Sheridan, S. G., & Adams, W. Y. (1995). The health and nutrition of a medieval Nubian population: the impact of political and economic change. *American Anthropologist*, 97(3), 468-480.
- Vigilant, L., Stoneking, M., Harpending, H., Hawkes, K., & Wilson, A. C. (1991). African populations and the evolution of human mitochondrial DNA. *Science*, 253(5027), 1503-1507.
- Volk, A. A., & Atkinson, J. A. (2013). Infant and child death in the human environment of evolutionary adaptation. *Evolution and Human Behavior*, 34(3), 182-192.
- Waldron, H. A. (2000). The study of the human remains from Nubia: the contribution of Grafton Elliot Smith and his colleagues to palaeopathology. *Medical history*, 44(3), 363-388.

- Waldron, T. (2008). *Palaeopathology*. Cambridge: Cambridge University Press.
- Walker, P. L., Bathurst, R. R., Richman, R., Gjerdrum, T., & Andrushko, V. A. (2009). The causes of porotic hyperostosis and cribra orbitalia: A reappraisal of the iron-deficiency-anemia hypothesis. *American Journal of Physical Anthropology: The Official Publication of the American Association of Physical Anthropologists*, 139(2), 109-125.
- Walker, P. L., Dean, G., & Shapiro, P. (1991). Estimating age from tooth wear in Archaeological Populations. *Advances in Dental Anthropology*, 169-178.
- Wall, J. D., & Kim, S. K. (2007). Inconsistencies in Neanderthal genomic DNA sequences. *PLoS Genetics*, 3(10), e175.
- Weir, B. S., & Cockerham, C. C. (1984). Estimating F-statistics for the analysis of population structure. *Evolution*, 38(6), 1358-1370.
- Weissensteiner, H., Pacher, D., Kloss-Brandstätter, A., Forer, L., Specht, G., Bandelt, H. J., Kronenber, F., Salas, A. & Schönherr, S. (2016). HaploGrep 2: mitochondrial haplogroup classification in the era of high-throughput sequencing. *Nucleic Acids Research*, 44(W1), W58-W63.
- Welsby, D. 2016. Observations on the graves of the Medieval period in the SARS concession at the Fourth Cataract', in A. Łajtar, A. Obluski and I. Zych (eds), *Aegyptus et Nubia Christiana. The Włodzimierz Godlewski Jubilee Volume on the Occasion of his 70th Birthday*, 613-628.
- Welsby, D. A. (1996). *The Kingdom of Kush: The Napatan and Meroitic Empires*. London: British Museum Press.
- Welsby, D. A. (2002). *The Medieval Kingdoms of Nubia: Pagans, Christians and Muslims along the Middle Nile*. London: British Museum Press.
- Wendorf, F., Schild, R., & Schild, R. (1976). *Prehistory of the Nile Valley (Studies in Archeology)*. New York: Academic.
- Wendorf, F., Schild, R., Close, A. E., Hillman, G. C., Gautier, A., Van Neer, W., Donahue, D.J., Jull, A.J.T, & Linick, T. W. (1988). New radiocarbon dates and late Palaeolithic diet at Wadi Kubbania, Egypt. *Antiquity*, 62(235), 279-283.
- White, C. D., & Schwarcz, H. P. (1994). Temporal trends in stable isotopes for Nubian mummy tissues. *American Journal of Physical Anthropology*, 93(2), 165-187.
- White, T. D., & Folkens, P. A. (2005). *The Human Bone Manual*. New York: Elsevier.
- Wolbach, S. B., & Bessey, O. A. (1941). Vitamin A deficiency and the nervous system. *Archives of Pathology*, 32, 689-722.
- Ziesemer, K. A., Ramos-Madrigal, J., Mann, A. E., Brandt, B. W., Sankaranarayanan, K., Ozga, A. T., Hoogland, M., Hofman, C.A., Salazar-Garcia, D.C., Frohlich, B., Milner, G.R., Stone, A.C., Aldenderfer, M., Lewis, C.M., Hofman, C.L., Warinner, C., & Schroeder. (2019). The efficacy of whole human genome capture on ancient dental calculus and dentin. *American Journal of Physical Anthropology*, 168(3), 496-509.
- Zurawski, B. (2007). Where the water is crying. Survey and excavations in Shemkhiya, Dar el-Arab (Suegi el-Gharb) and Saffi Island carried out by the Polish Expedition to the Fourth Cataract in the winter of 2004/2005. Preliminary report. In Näser, C., & Lange, M. (Eds.). *Proceedings of the Second International Conference on the Archaeology of the Fourth Nile Cataract, Berlin, August 4th-6th, 2005 (Vol. 23)*. Otto Harrassowitz Verlag.